Proteomics approaches for the study of adipose tissue biology

TRIB3 and beyond

Miguel Hernandez Quiles

Colofon

Proteomics approaches for the study of adipose tissue biology

TRIB3 and beyond

Proteomics-benaderingen voor de studie van vetweefselbiologie

TRIB3 en verder

(met een samenvatting in het Nederlands)

Proefschrift

ter verkrijging van de graad van doctor aan de
Universiteit Utrecht
op gezag van de
rector magnificus, prof.dr. H.R.B.M. Kummeling,
ingevolge het besluit van het college voor promoties
in het openbaar te verdedigen op

vrijdag 26 mei 2023 des middags te 4.15 uur

door
Miguel Hernandez Quiles

geboren op 8 november 1988
te Madrid, Spanje

Promotor:
Prof. dr. B.M.T. Burgering

Copromotor:
Dr. E. Kalkhoven

Beoordelingscommissie:
Prof. dr. H.C. Korswagen
Prof. dr. S.M.A. Lens
Prof. dr. J.P.G. Sluijter (voorzitter)
Prof. dr. A.J.A. van de Sluis
Prof. dr. C.J.M. de Vries

Financial support by the Dutch Heart Foundation for the publication of this thesis is gratefully acknowledged.

Table of contents

Chapter 1

General introduction

Miguel Hernandez-Quiles[1] and Eric klakhoven[1]

[1] Center for Molecular Medicine, University Medical Center Utrecht, Utrecht University, Utrecht the Netherlands.

Adipocytes and adipose tissue

The storage of energy as lipids is a mechanism present in unicellular and multicellular organisms and is highly conserved. Prokaryotes and single cell eukaryotes have specialized intracellular organelles capable of accumulating lipid droplets and specialized cells have evolved to store lipids in more complex organisms [1, 2]. Invertebrates and vertebrates have specialized lipid-storing cells that share developmental programs, transcriptional cascades and key enzymes that are important for fat synthesis, storage and release. The specialized lipid-storing cells are known as adipocytes and they are the defining component of adipose tissue (AT).

AT is not only composed of adipocytes but also of immune cells -such as macrophages, T-regulatory cells (T-regs) and invariant natural killer cells (iNKT)-, endothelial cells and fibroblasts. AT functions can be separated in i) "classical" functions of AT, i.e. protection against cold and mechanical stress and storage and release of energy, and ii) "novel", more recently identified functions, i.e. the production and secretion of adipokines that regulate whole body metabolism [3-5]. Two main types of adipose tissue are found in mammals that differ in origin and function, white (WAT) and brown (BAT) [6, 7]. Adipocytes in BAT contain multilocular lipid droplets and high amounts of mitochondria that are used for the conversion of stored lipids into heat, in contrast with WAT, where adipocytes contain a single lipid droplet and significantly less mitochondria. The origin of WAT and BAT remain largely unexplored; WAT and BAT develop from the mesoderm germline but BAT originates from Myf5 and Pax7 positive precursor cells [8]. In fact, muscle cells and brown adipocytes share a common lineage and the dermomyotome can give rise to both cell types but not white adipocytes [9]. In addition, WAT and BAT also differ in location, as BAT is restricted to the intrascapular region in mice and the supraclavicular, neck and paravertebral regions in humans. Recently it has been shown that adipocytes holding characteristics of both brown and white are more common than previously appreciated, the so-called beige adipose tissue [10].

As mentioned above, the classical function of WAT has been traditionally centered around its ability to control energy homeostasis through the storage and release of lipids in response to systemic nutritional and metabolic needs. Dysregulation of adipose tissue due to an excessive and prolonged exposure to over-caloric diet is a hallmark in the development of obesity and obesity-associated diseases like Type II Diabetes and cancer [11]. Currently, the incidence of obesity is increasing in every country and the global incidence of type II diabetes is projected to double by 2030 reaching the remarkable number of 350 million cases [12].

Obesity is viewed as an important first step in the development of Insulin resistance and is characterized by an increase in adipose tissue size mass [13, 14]. This increase in size mass leads to an increased secretion of free fatty acids and several adipokines, like resistin and TNFa, together with reduced secretion of other adipokines, like adiponectin, ultimately resulting in a metabolic state in which muscle, liver and AT have a reduced response to insulin. White adipose tissue can increase in mass by two different ways, an increase in size of existing adipocytes, known as hypertrophy, and an increase in the number of adipocytes through the differentiation of mesenchymal stem cells into new adipocytes, a process referred to as hyperplasia [15]. The number of preadipocytes in a given depot is established early in life and is somehow stable through adulthood. Recently it has been shown however, that during prolonged caloric excess new adipocytes can emerge and can contribute to the expansion of the AT [15]. These processes can be observed after only a few days of an obesogenic diet, whereas a reduction in cell number or cell size can be appreciated within 24 hours of fasting [15, 16]. The balance between hypertrophy and hyperplasia plays a crucial role in the metabolic health of the AT. The relation between an increase in adipocyte size and systemic insulin resistance was noted more than 70 years ago [17, 18]. In addition, studies have shown that small adipocytes can counteract the effects of obesity-related metabolic complications [19], for instance an increase in small adipocytes number have a protective effect in the development of diabetes [20, 21]. The understanding of the molecular ques that govern adipocyte differentiation and function remain of capital importance in order to develop appropriate therapies that improve insulin resistance and stop the development of type 2 diabetes.

The differentiation of preadipocytes into mature adipocytes is known as adipogenesis. This process is regulated by a network of transcription factors that are tightly controlled and synchronized to coordinate the expression of hundreds of proteins responsible for establishing the mature adipocyte phenotype [22, 23]. Among these transcription factors there is one that stands out, Peroxisome Proliferator Activated Receptor gamma (PPARγ), known as the master regulator of adipogenesis. Without PPARγ, adipocyte progenitor cells are incapable of expressing any differentiated adipocyte characteristic [23]. Furthermore, expression of PPARγ in mesenchymal stem cells is sufficient to initiate the adipocyte transcriptional program that leads to the typical adipocyte phenotype [24]. The role of PPARγ in adipocytes, immune cells and its contribution to cancer will be extensively discussed in Chapter 2.

Transcription factors are proteins that activate or repress the expression of their target genes and they do so predominantly by binding the DNA. Transcription factors are activated by different means, such as ligands, post-translational modifications or interactions with specific transcriptional cofactors. They often represent the endpoint

of a cascade of events that leads to the activation of a certain cellular pathway. Adipocyte differentiation and function are controlled by a number of transcription factors that cooperate and have to be coordinated to ensure a full adipocyte phenotype [22]. In this context, proteins that regulate signal transduction from the membrane to the transcription factors are of crucial importance. These proteins modulate the signal flow into different pathways that triggers the activation of the specific genes that will lead to a fully differentiated adipocyte. Protein kinases and pseudokinases are a good example of this, and in recent years they have emerged as important regulators of AT function [25]. As will be discussed in **Chapter 4** and **chapter 5**, pseudokinases such as TRIB3 and signal transmitters such as FHL2 are important regulators of adipocyte differentiation and function.

Adipose tissue, metabolism and cancer

Many epidemiological studies highlight the role of adipose tissue in cancer: it is estimated that one fifth of all cancer deaths in the United States can be attributed to obesity [26]. It has been shown that adiposity increases the incidence of at least 13 different types cancer, including colon, breast (in post-menopausal woman), endometrium, kidney, esophagus, gastric cardia, pancreas, gallbladder and liver cancer [27]. While the correlation between adiposity and cancer incidence is already strong, the correlation between adiposity and cancer mortality is even higher: in the case of breast cancer, very obese women have a three times higher cancer death rate compared to very lean women [28]. When all the epidemiological evidence is taken together, studies have concluded that the percentage of disease that can be attributed to adiposity ranged from 56.8% in the case of endometrial cancer to 14.2% in the case of colorectal cancer in women [29]. Adiposity is responsible for 22.6% of breast cancer cases, 42.5% of kidney cancer cases and 26.9% pancreas cancer cases, illustrating the enormous number of cases that could have been prevented by maintaining a normal weight through adulthood. Since the global obesity epidemic has not shown clear signs of declining, understanding the molecular mechanisms behind the relation between adipose tissue and cancer has become a highly relevant field of research.

The mechanisms through which AT contributes to an increased cancer risk are not always clear and some of them are speculative. However, there are some clear factors that have been shown to be important. As discussed before, hypertrophic, malfunctioning adipocytes are responsible for an increase in systemic insulin levels and an altered circulating lipid profile, known as hyperinsulinemia and hyperlipidemia respectively. Chronic high levels of insulin have been associated with colon, breast and pancreas cancer [30-32]. Insulin and insulin-like growth factor 1 (IGF1) induce activation of PI3-kinase and MAP kinase pathways that regulate cellular

processes such as metabolism, cell growth or apoptosis. Overactivation of these pathways is among the most well-established mechanisms to drive cancer initiation and progression [33], providing a strong hypothesis as to how high insulin levels can contribute to the development of tumours and their proliferation. In **chapter 7** we discuss the molecular details of the interaction between TRIB3 and Akt/PKB, a downstream kinase activated by insulin and IGF1. In addition, hyperlipidemia is also associated with increase in cancer risk and mortality through a similar mechanism. Hyperlipidemia is characterized by elevated low-density lipoprotein (LDL) cholesterol and triglycerides (TG) and low high-density lipoprotein (HDL) cholesterol. This metabolic alteration in circulating lipids leads to the activation of oncogenic pathways such as Akt/mTOR and Akt/glycogen synthase kinase 3β/β-catenin [34].

Altered adipokine profile secretion is another mechanism that can contribute to cancer onset and progression [35, 36]. Low levels of adiponectin, a 30-KDa adipokine involved in the regulation of insulin sensitivity and glucose levels [37], are associated with obesity and cardiovascular diseases. Studies have shown that low levels of adiponectin are associated with increased cancer risk while high levels have protective effects [37]. Leptin, which displays high levels in obesity, is also positively correlated to increase cancer risk [38]. Adipokines have been implicated in the metabolic reprogramming that cancer cells undergo in order to increase their glucose uptake and glycolytic activity [39], known as Warburg effect, a metabolic adaptation of cancer cells that supports their high proliferative state [40, 41].

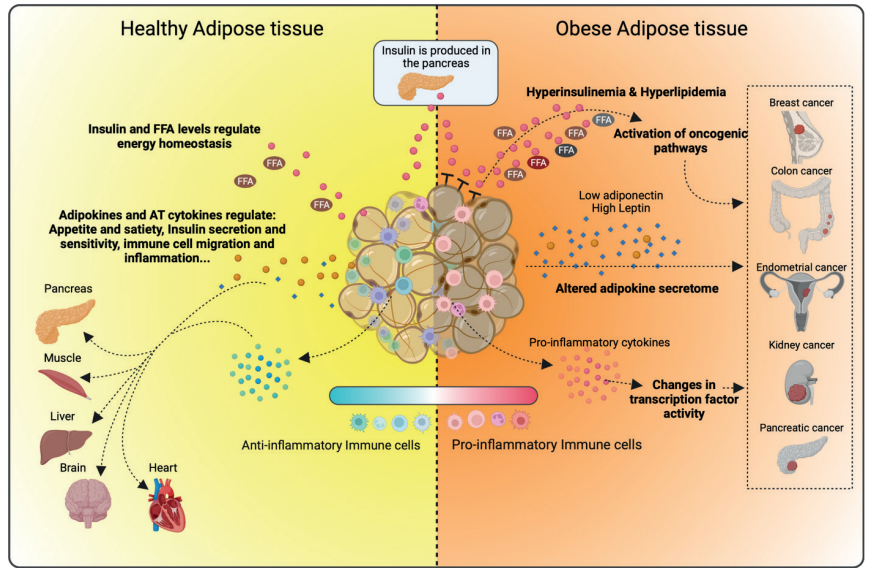

Figure 1: The role of healthy and obese AT.

Moreover, adiposity is known to influence the production and bioavailability of endogenous sex steroids hormones through several mechanism [42]. For example, AT is responsible for the expression of aromatase enzymes, and elevated levels of proinflammatory cytokines such as TNFα and IL6 increases their expression in obesity [43]. High levels of aromatases produced by breast adipose tissue led to increased estradiol concentrations that ultimate results in increased estrogen receptor (ER) activity [44]. Dysregulation of ER activity is one of the most well-known mechanisms behind breast cancer physiopathology [45]. PPARγ, which belongs to the same nuclear receptor superfamily of transcription factors as ER, has also gained attention in recent years as a tumor suppressor. Thiazolidinediones (TZDs) are PPARγ ligands that are used as insulin sensitizing drugs, which have been shown to have anti-tumor effects in several cancer types including breast and colon [46]. In **Chapter 2** we summarized the current knowledge on the different mechanism of action of PPARγ, including its overall role in cancer cells and the role of PPARγ mutations described in different cancers.

The epidemiological links between AT and cancer are various and strong, and the mechanisms described above are only some of all the different ways AT and adipocytes influence cancer initiation and progression. Some other mechanisms that are less well understood and are still under investigation include the role of adipocytes in remodeling the extracellular matrix and the crosstalk between cancer cells and the cancer-associated adipocytes [47, 48]. In this context, where AT is not just a cancer risk factor but even a more direct contributor to tumorigenesis, understanding the molecular basis of adipocyte function and malfunction is critical to design new therapies against obesity-related complications and cancer.

The importance of Pseudoenzymes in biology

As mentioned above, transcription factors and signal transduction intermediates rely heavily on post-translational modifications to carry out their function, these modifications are the result of enzymatic reactions. Enzymes are proteins that transformed substrates into products by catalyzing a chemical reaction, i.e., transferases, hydrolases or ligases.

Nearly all types of known enzyme families include pseudoenzyme homologues, proteins that are predicted to be catalytic inactive due to the lack of key catalytic domains and are conserved across all branches of life [49]. Pseudoenzymes have evolved to regulate cell biology in a catalytically-independent manner and our understanding of their molecular actions is very poor compared to their enzymatically active counterparts. Pseudoenzymes can be divided according to their mechanism of action into four mayor classes; allosteric regulators, molecular switchers, interaction platforms and enzymatic

competitors. The first class, allosteric regulators, exert their function through binding of an –often related– active enzyme. Pseudoenzymes that fall into this category retain an enzyme-like structure and they have been proposed to arise from gene duplications. Examples of these pseudoenzymes can be found in the protein kinase, phosphatase and ubiquitination fields, such as HER3/EGFR, KSR/RAF and MDM2/MDMX [50-52]. The second class of pseudoenzymes are molecular switches that can alternate between an inactive and active conformation. This change in activity can be triggered by ligands or post-translational modifications. A good example of this is Mixed lineage kinase domain-like (MLKL) pseudokinase, where phosphorylation of its activation loop by RIPK3 has been proposed to trigger a conformational change that results in the release of the N-terminal domain [53, 54]. The third class of pseudoenzymes diverge more from their catalytic active homologues as they have gained a specific function as protein interaction modules; these protein scaffolds can facilitate or inhibit protein complex formation or regulate their localization or trafficking. Tribbles are a good example of this category as they have been shown to be able to form a ternary complex between COP1 and C/EBPα promoting the ubiquitination and degradation of the latter [55]. Finally, the last category are the enzymatic competitors: these proteins act as competitors for substrate binding or complex assembly with an active enzyme regulating its enzymatic activity. An example of the first mechanism is STYX, which has been shown to bind and prevent ERK1 and ERK2 dephosphorylation and subsequent inactivation by DUSP4 [56, 57]. Most likely this group has evolved from loss of catalytic function and is highly abundant in nature.

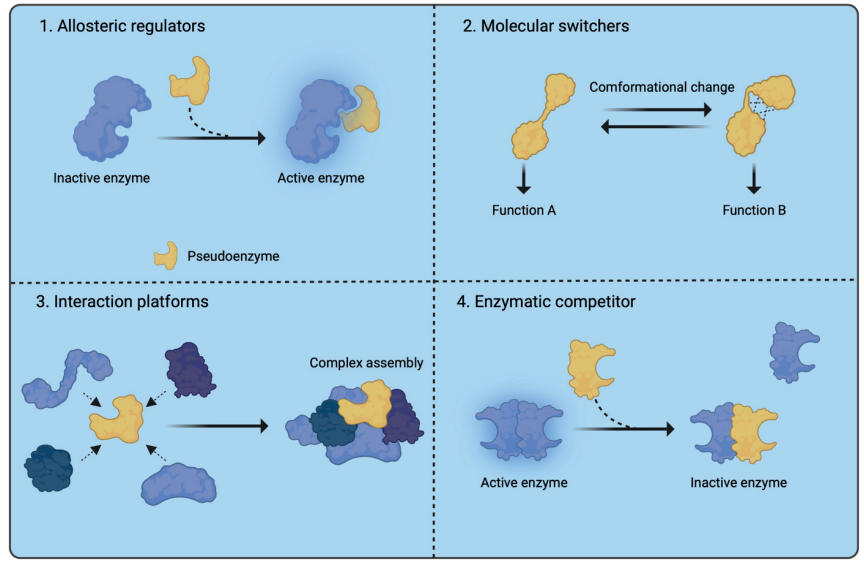

Figure 2: Different mechanism of action of pseudoenzymes.

In terms of their evolutionary trajectory, pseudoenzymes have mostly evolved from ancestral active enzymes through the loss of catalytic residues or motifs. Interestingly, the gain of these motifs does not always restore the catalytic function of the pseudoenzyme and whether a pseudoenzyme can be reverted into an active enzyme depends widely on the protein family [58]. For example, pseudophosphatases can often be converted into active enzymes by simply introducing lost catalytic residues, indicating that the phosphopeptide-binding site ability has been preserved because of its importance for the biological function of the pseudoenzyme [59]. On the other hand, pseudokinases are a family of pseudoenzymes that are rarely convertible into active kinases by reintroducing catalytic residues or small domains. This might have different explanations, as it has been noted by others that kinases have a more complex catalytic mechanism that relies vastly on conformational changes, which may explain why the introduction of the necessary catalytic motifs might not be enough to gain the lost activity [60]. Another possibility is that pseudokinases have evolved away from their catalytic counterparts and their biological function is more linked to the interaction platform that they provide in complex formation, trafficking and localization or allosteric regulators [60]. Pseudoenzymes that have evolved structurally and functionally away from the enzyme they originate from are more complex to associate to specific pathways or functions, and pseudokinases are a good example of this. Pseudokinases are often expressed temporally and spatially alongside the enzyme they are derived from, as most pseudokinases arisen from gene duplications [61]. However, the loss of evolutionary pressure on catalytic domains and specific architectures allowed them to acquire new functions, reinforcing their roles as interactions platforms [62, 63].

The study of pseudoenzyme functions is shifting away from being considered only catalytic dead enzymes and their roles as interaction platform that can regulate a plethora of signaling and metabolic processes is becoming more and more important. Mass spectrometry-based proteomic approaches provide an exceptionally well-suited way to study their function within cells in the context of protein complexes, allowing the identification of protein-protein interactions that are pivotal for understanding the role of these pseudoenzymes [64] (see Box 1).

Box 1: Mass spectrometry in molecular biology

Mass spectrometry (MS) instruments measure the mass-to-charge ratio of ionized molecules from which we can infer qualitative and quantitative information ranging from molecular structures to elemental composition. All mass spectrometers are composed of three main parts: an ion source, a mass analyzer and a detector. The ion source generates ions by transferring molecules from liquid or solid state to a gas phase. Two soft ionizing techniques are the most widely used in proteomics, Electro Spray Ionization (ESI) and Matrix Assisted Laser Desorption and Ionization (MALDI) techniques. The charged macromolecules are then separated according to their mass-to-charge ratio in the mass analyzer by using electric or magnetic fields. Mass analyzers are often used in tandem to analyzed the fragmentation pattern of the ionized biomolecules, allowing for example the identification of specific peptide sequences. Ion sources and mass analyzers can be combined, named for example MALDI/TOF (time-of-flight) or ESI-Orbitrap [65, 66]. Finally, the ions reach the detector and are recorded, and the results are then transformed to intensities as a function of mass-over-charge values in a plot known as a mass spectrum.

Complex samples can be separated using a liquid chromatography connected to the MS (LC-MS) and a series of MS spectra can be collected as the molecules elute. In a common proteomics MS setup for protein identification, an MS/MS spectrum is generated where peptides have been fragmented and analyzed so the peptide information sequence is obtained, and subsequently the MS spectrum is then used to query a protein database using an array of bioinformatic tools. In the last decade MS has become the most popular method to study all aspects of proteins as it presents clear advantages compared to other proteomics techniques, such as sensitivity, opportunities for automation and reproducibility. MS-based proteomics is widely used for the identification and quantification of proteins and to study posttranslational modifications of proteins [67].

To gain insight into the biological function of pseudoenzymes, especially pseudokinases, it is crucial to elucidate the set of proteins that are interacting with, the so-called interactome, in a given biological context. MS-based proteomics approaches are the method of choice to comprehensively identify protein-protein interactions (PPI). The popularity of this technology has led to a great number of methodologies and workflows that have been reviewed elsewhere [68]. Affinity-purification mass spectrometry (AP-MS) and proximity ligation workflows are among the most commonly used. These methods rely either on a purification step of the protein of interest or on the purification of the modified proteins in close proximity to the protein of interest, respectively. AP-MS experiments require antibodies with

high enough specificity and affinity and therefore proteins of interest are often tagged with well-defined epitopes to allow the use of high affinity, high specificity antibodies against these epitope tags. In recent years nanobodies have been introduced and have drastically reduced the disadvantages of antibody-based research, such as problems of cross-reactivity, low affinity and large size of the antibody. Nanobodies contain a single antigen-binding domain that carries a very high affinity for the target protein and minimized background binding and peptides release during sample digestion, allowing a fast and efficient purification [69, 70]. Recently there has also been improvements in proximity ligation methods, which both circumvent the need for high affinity, high specificity antibodies as well as allowing the identification of protein-protein interactions of a weak and/or transient nature. One method known as BioID relies on the high affinity of streptavidin for biotin by fusing a promiscuous biotin protein ligase to the protein of interest to biotinylate proteins in close proximity [71]. Alternatively, ascorbate peroxidase was engineered to allow labeling of close proximity proteins in the so-called APEX method [72]. In this method the protein of interest is fused to a peroxidase that upon treatment with H_2O_2 catalyze the covalent labeling of proteins in a radius of 20nm. Both methods allow for stringent enrichments and washing protocol that reduce background binding when compared to antibody-based AP-MS.

Tribbles family of pseudokinases

Protein kinases are present in all branches of life and their impact in cellular biology has long been appreciated [73]. Recently, also non-enzymatic roles have become clear, particularly their role as interaction platforms [61]. This may explain, at least in part, the amount of non-catalytic kinases and their conservation across different species. In fact, pseudokinases represent 10% of the human kinome [62]. Tribbles (TRIB) proteins represent a family of serine/threonine pseudokinases that play a key role in many metabolic and cellular pathways [74, 75]. Tribbles proteins function as signaling mediators and scaffolding proteins that regulate protein stability and activity, they exert their non-enzymatic roles through interactions with kinases, phosphatases, transcription factors and components of the ubiquitin-proteasomal system. Tribbles were first discovered in Drosophila (*trbl*) where they were found to induce proteasome-mediated degradation of slbo and String, homologues of the transcription factor C/EBPα and the phosphatase CDC25, respectively [76, 77]. In addition, Tribbles proteins have been implicated in cellular proliferation, differentiation, cell cycle and cell death [78-80].

Evolving from a common ancestor, the three mammalian TRIB proteins (TRIB1, TRIB2 and TRIB3) have a central bi-lobed pseudokinase domain that contains a DLK motif shared by most bona fide kinases, but lacks the ATP coordination site VAIK and the magnesium binding motif DFG [81]. Interestingly, instead of the canonical DFG motif found in kinases almost all Tribbles contain a S/NLE motif [82], underpinning an evolutionary selective pressure to maintain this motif in the pseudokinase domain. The central pseudokinase domain is flanked by a divergent N-terminus domain that has been proposed to mediate protein turnover and a C-terminus tail that contains binding motifs for mitogen-activated protein kinase (MAPK) and the E3 ubiquitin ligase COP1 [83-86]. Current knowledge on additional roles of the N- and C-terminal domains of Tribbles proteins is limited. In **chapter 3** we investigated additional roles of the N- and C-terminus of TRIB3 using MS-based proteomics approaches.

The 3 mammalian TRIB family members (TRIB1, -2 and -3) function as interaction platforms regulating a plethora of signaling and metabolic pathways, and all three members of the family have evolved to have largely non-redundant roles despite their high degree of homology. A good example of this is the role of Tribbles in hematopoiesis, where TRIB1 and TRIB2 are able to regulate maturation and function of myeloid and lymphoid lineages, respectively, while TRIB3 plays no role in either process [80, 87]. The interactions with protein kinase B (also known as Akt kinase) and C/EBP transcription factors are among the most well-studied partners of Tribbles, and here the roles of the individual TRIB family members are not only non-redundant but even opposing. Whereas TRIB3 has been reported to inhibit PKB phosphorylation and activation by mTOR, TRIB1 and TRIB2 have been showed to enhance PKB phosphorylation [88, 89]. In addition, different member of the C/EBP family of transcription factors have been reported bind to Tribbles proteins. Upon binding to C/EBP proteins, Tribbles proteins undergo conformational changes that disrupts intermolecular interactions between their C-terminal tail and their pseudokinase domain [82], resulting in the release of the C-terminus and exposing the binding motif for COP1. The binding of COP1 will ultimately result on the ubiquitination and subsequent degradation of the C/EBP protein bound in the first place. Although all mammalian Tribbles can interact with C/EBP proteins and COP1, the result of this ternary complex between C/EBP protein, COP1 and a TRIB member does not always result in same level of degradation of the C/EBP protein: TRIB1 has an enhanced capacity to promote the degradation of C/EBP molecules when compared to TRIB2 and -3 [55].

Furthermore, TRIB1 and -3 have been shown to play a critical role in metabolism. Shortly after the discovery of drosophila Trbl one of the human homologs, TRIB3, was linked to AKT/PKB phosphorylation in response to insulin in the liver [90]. In

fact, high Drosophila Trbl levels have been associated with decreased phospho-PKB levels in response to a high fat diet (HFD) [91], a hallmark in the development of insulin resistance. Moreover, a human TRIB3 non-synonymous polymorphism resulting in substitution of a glutamine residue with an arginine residue at position 84 (84R variant) results in a stronger inhibitory capacity of insulin-mediated PKB activation and is associated with increased risk to develop insulin resistance and T2DM [92]. In addition, TRIB3 has been shown to promote acetyl-CoA carboxylase ubiquitination and degradation by COP1 during fasting, thus affecting lipolysis and regulating lipid metabolism [86]. TRIB1 has also been extensively associated with lipid metabolism in the liver [93, 94], in mice TRIB1 over-expression in liver cells was shown to promote fatty acid oxidation and reduce triglyceride synthesis [95] and TRIB1 knock down mice showed traits of hypertriglyceridemia [96]. More recently, TRIB1 has been shown to influence hepatic lipid metabolism in humans by regulating C/EBPα posttranslational status [97]. In addition to its role in the liver, adipose TRIB1 has been reported to regulate plasma adiponectin levels [98], an important adipokine secreted by the AT that controls glucose levels and fatty acid oxidation. As we discuss in **chapter 4**, TRIB3 knock out mice show impaired adiposity without being challenged with an HFD. In addition to insulin resistance and diabetes, TRIB3 has been associated with atherosclerotic plaque rupture, β-cell dysfunction and non-alcoholic fatty liver disease (NAFLD) [99-101], underscoring the need to expand our understanding of the functions of TRIB3 in metabolic related complications.

Outline of the thesis

In this thesis, we broaden the basic knowledge on how adipose tissue in regulated and what factors contribute to adipocytes differentiation and function and also try to cross the boundary between the adipose tissue and the cancer field, to study proteins that are traditionally studied in an adipocyte context in cellular cancer models. We made extensive use of MS-based proteomics approaches in combination with other molecular biology techniques, unraveling previously unknown interactions and functions.

One of the cellular proteins traditionally studied in an adipocyte context is PPARγ, the master regulator of adipocyte differentiation and function. In **chapter 2**, we review its role and different molecular actions in adipocytes, but expand that to cancer cells and immune cells. In **chapter 3** we established an MS-based approach to study the Tribbles interactome in different cancer cells, identifying new interactors as well as unravelling the role of the N-terminal domain of TRIB3. In **Chapter 4** we use a combination of in vivo and in vitro approaches to study the role of TRIB3 in AT. We characterized the overall adipose tissue phenotype in the $Trib3^{-/-}$ mice and also describe the TRIB3 interactome in adipocytes. In **chapter 5** we used the previously described MS-based approach (Chapter 3) to study the role of FHL2 during adipogenesis, validating a new interaction and a new role for this protein in adipocytes. In **chapter 6,** we presented TRIB3 as a regulator of PPARγ expression in breast cancer cells. We showed that TRIB3 levels affect the phosphorylation status of a number of transcription factors and the levels of $H3K4me^3$ in the cell. Moreover, we speculate with the possibility that this new role of TRIB3 could be mediated through the newly discovered interaction with the MLL-WRAD complex. In **chapter 7**, we investigated the interaction between TRIB3 and AKT/PKB. We used a combination of in vitro and computational modeling to unravel a new function for the C-terminal domain of TRIB3. Finally, in **chapter 8,** we summarized our findings and discuss the future directions of our studies.

References

1. Ottaviani, E., D. Malagoli, and C. Franceschi, *The evolution of the adipose tissue: a neglected enigma.* Gen Comp Endocrinol, 2011. **174**(1): p. 1-4.
2. Driskell, R.R., et al., *Defining dermal adipose tissue.* Exp Dermatol, 2014. **23**(9): p. 629-31.
3. van Eijkeren, R.J., et al., *Endogenous lipid antigens for invariant natural killer T cells hold the reins in adipose tissue homeostasis.* Immunology, 2018. **153**(2): p. 179-189.
4. Jung, U.J. and M.S. Choi, *Obesity and its metabolic complications: the role of adipokines and the relationship between obesity, inflammation, insulin resistance, dyslipidemia and nonalcoholic fatty liver disease.* Int J Mol Sci, 2014. **15**(4): p. 6184-223.
5. Schipper, H.S., et al., *Adipose tissue-resident immune cells: key players in immunometabolism.* Trends Endocrinol Metab, 2012. **23**(8): p. 407-15.
6. Rosen, E.D. and B.M. Spiegelman, *What we talk about when we talk about fat.* Cell, 2014. **156**(1-2): p. 20-44.
7. Frontini, A. and S. Cinti, *Distribution and development of brown adipocytes in the murine and human adipose organ.* Cell Metab, 2010. **11**(4): p. 253-6.
8. Boon, M.R. and W.D. van Marken Lichtenbelt, *Brown Adipose Tissue: A Human Perspective.* Handb Exp Pharmacol, 2016. **233**: p. 301-19.
9. Enerback, S., *The origins of brown adipose tissue.* N Engl J Med, 2009. **360**(19): p. 2021-3.
10. Wang, W. and P. Seale, *Control of brown and beige fat development.* Nat Rev Mol Cell Biol, 2016. **17**(11): p. 691-702.
11. Clee, S.M. and A.D. Attie, *The genetic landscape of type 2 diabetes in mice.* Endocr Rev, 2007. **28**(1): p. 48-83.
12. Hogan, P., et al., *Economic costs of diabetes in the US in 2002.* Diabetes Care, 2003. **26**(3): p. 917-32.
13. Czech, M.P., *Insulin action and resistance in obesity and type 2 diabetes.* Nat Med, 2017. **23**(7): p. 804-814.
14. Unger, R.H. and P.E. Scherer, *Gluttony, sloth and the metabolic syndrome: a roadmap to lipotoxicity.* Trends Endocrinol Metab, 2010. **21**(6): p. 345-52.
15. Jeffery, E., et al., *Rapid depot-specific activation of adipocyte precursor cells at the onset of obesity.* Nat Cell Biol, 2015. **17**(4): p. 376-85.
16. Kleemann, R., et al., *Time-resolved and tissue-specific systems analysis of the pathogenesis of insulin resistance.* PLoS One, 2010. **5**(1): p. e8817.
17. Salans, L.B., J.L. Knittle, and J. Hirsch, *The role of adipose cell size and adipose tissue insulin sensitivity in the carbohydrate intolerance of human obesity.* J Clin Invest, 1968. **47**(1): p. 153-65.
18. Krotkiewski, M., et al., *Impact of obesity on metabolism in men and women. Importance of regional adipose tissue distribution.* J Clin Invest, 1983. **72**(3): p. 1150-62.
19. McLaughlin, T., et al., *Enhanced proportion of small adipose cells in insulin-resistant vs insulin-sensitive obese individuals implicates impaired adipogenesis.* Diabetologia, 2007. **50**(8): p. 1707-15.
20. Lonn, M., et al., *Adipocyte size predicts incidence of type 2 diabetes in women.* FASEB J, 2010. **24**(1): p. 326-31.
21. Yang, J., et al., *The size of large adipose cells is a predictor of insulin resistance in first-degree relatives of type 2 diabetic patients.* Obesity (Silver Spring), 2012. **20**(5): p. 932-8.
22. Farmer, S.R., *Transcriptional control of adipocyte formation.* Cell Metab, 2006. **4**(4): p. 263-73.
23. Rosen, E.D., et al., *C/EBPalpha induces adipogenesis through PPARgamma: a unified pathway.* Genes Dev, 2002. **16**(1): p. 22-6.
24. Rosen, E.D., et al., *PPAR gamma is required for the differentiation of adipose tissue in vivo and in vitro.* Mol Cell, 1999. **4**(4): p. 611-7.
25. Ahmad, B., et al., *Molecular Mechanisms of Adipogenesis: The Anti-adipogenic Role of AMP-Activated Protein Kinase.* Front Mol Biosci, 2020. **7**: p. 76.
26. Calle, E.E., et al., *Overweight, obesity, and mortality from cancer in a prospectively studied cohort of U.S. adults.* N Engl J Med, 2003. **348**(17): p. 1625-38.
27. Steele, C.B., et al., *Vital Signs: Trends in Incidence of Cancers Associated with Overweight and Obesity - United States, 2005-2014.* MMWR Morb Mortal Wkly Rep, 2017. **66**(39): p. 1052-1058.
28. Petrelli, J.M., et al., *Body mass index, height, and postmenopausal breast cancer mortality in a prospective cohort of US women.* Cancer Causes Control, 2002. **13**(4): p. 325-32.
29. Calle, E.E. and R. Kaaks, *Overweight, obesity and cancer: epidemiological evidence and proposed mechanisms.* Nat Rev Cancer, 2004. **4**(8): p. 579-91.
30. McKeown-Eyssen, G., *Epidemiology of colorectal cancer revisited: are serum triglycerides and/or plasma glucose associated with risk?* Cancer Epidemiol Biomarkers Prev, 1994. **3**(8): p. 687-95.
31. Kaaks, R., *Nutrition, hormones, and breast cancer: is insulin the missing link?* Cancer Causes Control, 1996. **7**(6): p. 605-25.
32. Weiderpass, E., et al., *Occurrence, trends and environment etiology of pancreatic cancer.* Scand J Work Environ Health, 1998. **24**(3): p. 165-74.
33. Tao, Y., et al., *Mechanisms of disease: signaling of the insulin-like growth factor 1 receptor pathway--therapeutic perspectives in cancer.* Nat Clin Pract Oncol, 2007. **4**(10): p. 591-602.
34. Samuel, S.M., et al., *Challenges and perspectives in the treatment of diabetes associated breast cancer.* Cancer Treat Rev, 2018. **70**: p. 98-111.
35. Guaita-Esteruelas, S., et al., *Exogenous FABP4 increases breast cancer cell proliferation and activates the expression of fatty acid transport proteins.* Mol Carcinog, 2017. **56**(1): p. 208-217.
36. Hu, M.B., et al., *High-fat diet-induced adipokine and cytokine alterations promote the progression of prostate cancer in vivo and in vitro.* Oncol Lett, 2018. **15**(2): p. 1607-1615.
37. Parida, S., S. Siddharth, and D. Sharma, *Adiponectin, Obesity, and Cancer: Clash of the Bigwigs in Health and Disease.* Int J Mol Sci, 2019. **20**(10).
38. Peng, C., et al., *Leptin stimulates the epithelialmesenchymal transition and proangiogenic capability of cholangiocarcinoma cells through the miR122/PKM2 axis.* Int J Oncol, 2019. **55**(1): p. 298-308.
39. Pham, D.V. and P.H. Park, *Tumor Metabolic Reprogramming by Adipokines as a Critical Driver of Obesity-Associated Cancer Progression.* Int J Mol Sci, 2021. **22**(3).
40. Liberti, M.V. and J.W. Locasale, *The Warburg Effect: How Does it Benefit Cancer Cells?* Trends Biochem Sci, 2016. **41**(3): p. 211-218.

41. DeBerardinis, R.J. and N.S. Chandel, *We need to talk about the Warburg effect.* Nat Metab, 2020. **2**(2): p. 127-129.
42. Park, J., et al., *Obesity and cancer--mechanisms underlying tumour progression and recurrence.* Nat Rev Endocrinol, 2014. **10**(8): p. 455-465.
43. Bulun, S.E., et al., *Aromatase, breast cancer and obesity: a complex interaction.* Trends Endocrinol Metab, 2012. **23**(2): p. 83-9.
44. Mukhopadhyay, K.D., et al., *Aromatase expression increases the survival and malignancy of estrogen receptor positive breast cancer cells.* PLoS One, 2015. **10**(4): p. e0121136.
45. Liang, J. and Y. Shang, *Estrogen and cancer.* Annu Rev Physiol, 2013. **75**: p. 225-40.
46. Hernandez-Quiles, M., M.F. Broekema, and E. Kalkhoven, *PPARgamma in Metabolism, Immunity, and Cancer: Unified and Diverse Mechanisms of Action.* Front Endocrinol (Lausanne), 2021. **12**: p. 624112.
47. Zhao, C., et al., *Cancer-associated adipocytes: emerging supporters in breast cancer.* J Exp Clin Cancer Res, 2020. **39**(1): p. 156.
48. Kim, D.S. and P.E. Scherer, *Obesity, Diabetes, and Increased Cancer Progression.* Diabetes Metab J, 2021. **45**(6): p. 799-812.
49. Murphy, J.M., H. Farhan, and P.A. Eyers, *Bio-Zombie: the rise of pseudoenzymes in biology.* Biochem Soc Trans, 2017. **45**(2): p. 537-544.
50. Littlefield, P., et al., *Structural analysis of the EGFR/HER3 heterodimer reveals the molecular basis for activating HER3 mutations.* Sci Signal, 2014. **7**(354): p. ra114.
51. Rajakulendran, T., et al., *A dimerization-dependent mechanism drives RAF catalytic activation.* Nature, 2009. **461**(7263): p. 542-5.
52. Linke, K., et al., *Structure of the MDM2/MDMX RING domain heterodimer reveals dimerization is required for their ubiquitylation in trans.* Cell Death Differ, 2008. **15**(5): p. 841-8.
53. Murphy, J.M., et al., *The pseudokinase MLKL mediates necroptosis via a molecular switch mechanism.* Immunity, 2013. **39**(3): p. 443-53.
54. Hildebrand, J.M., et al., *Activation of the pseudokinase MLKL unleashes the four-helix bundle domain to induce membrane localization and necroptotic cell death.* Proc Natl Acad Sci U S A, 2014. **111**(42): p. 15072-7.
55. Murphy, J.M., et al., *Molecular Mechanism of CCAAT-Enhancer Binding Protein Recruitment by the TRIB1 Pseudokinase.* Structure, 2015. **23**(11): p. 2111-21.
56. Kidger, A.M., et al., *Dual-specificity phosphatase 5 controls the localized inhibition, propagation, and transforming potential of ERK signaling.* Proc Natl Acad Sci U S A, 2017. **114**(3): p. E317-E326.
57. Reiterer, V., et al., *Pseudophosphatase STYX modulates cell-fate decisions and cell migration by spatiotemporal regulation of ERK1/2.* Proc Natl Acad Sci U S A, 2013. **110**(31): p. E2934-43.
58. Eyers, P.A. and J.M. Murphy, *The evolving world of pseudoenzymes: proteins, prejudice and zombies.* BMC Biol, 2016. **14**(1): p. 98.
59. Murphy, J.M., et al., *A robust methodology to subclassify pseudokinases based on their nucleotide-binding properties.* Biochem J, 2014. **457**(2): p. 323-34.

60. Mace, P.D. and J.M. Murphy, *There's more to death than life: Noncatalytic functions in kinase and pseudokinase signaling.* J Biol Chem, 2021. **296**: p. 100705.
61. Jacobsen, A.V. and J.M. Murphy, *The secret life of kinases: insights into non-catalytic signalling functions from pseudokinases.* Biochem Soc Trans, 2017. **45**(3): p. 665-681.
62. Pils, B. and J. Schultz, *Inactive enzyme-homologues find new function in regulatory processes.* J Mol Biol, 2004. **340**(3): p. 399-404.
63. Todd, A.E., C.A. Orengo, and J.M. Thornton, *Sequence and structural differences between enzyme and nonenzyme homologs.* Structure, 2002. **10**(10): p. 1435-51.
64. Smits, A.H. and M. Vermeulen, *Characterizing Protein-Protein Interactions Using Mass Spectrometry: Challenges and Opportunities.* Trends Biotechnol, 2016. **34**(10): p. 825-834.
65. Fenn, J.B., et al., *Electrospray ionization for mass spectrometry of large biomolecules.* Science, 1989. **246**(4926): p. 64-71.
66. Hu, Q., et al., *The Orbitrap: a new mass spectrometer.* J Mass Spectrom, 2005. **40**(4): p. 430-43.
67. Zhang, Q., et al., *Epitope mapping of a 95 kDa antigen in complex with antibody by solution-phase amide backbone hydrogen/deuterium exchange monitored by Fourier transform ion cyclotron resonance mass spectrometry.* Anal Chem, 2011. **83**(18): p. 7129-36.
68. Vermeulen, M., N.C. Hubner, and M. Mann, *High confidence determination of specific protein-protein interactions using quantitative mass spectrometry.* Curr Opin Biotechnol, 2008. **19**(4): p. 331-7.
69. Rothbauer, U., et al., *Targeting and tracing antigens in live cells with fluorescent nanobodies.* Nat Methods, 2006. **3**(11): p. 887-9.
70. Rothbauer, U., et al., *A versatile nanotrap for biochemical and functional studies with fluorescent fusion proteins.* Mol Cell Proteomics, 2008. **7**(2): p. 282-9.
71. Roux, K.J., et al., *A promiscuous biotin ligase fusion protein identifies proximal and interacting proteins in mammalian cells.* J Cell Biol, 2012. **196**(6): p. 801-10.
72. Rhee, H.W., et al., *Proteomic mapping of mitochondria in living cells via spatially restricted enzymatic tagging.* Science, 2013. **339**(6125): p. 1328-1331.
73. Fabbro, D., S.W. Cowan-Jacob, and H. Moebitz, *Ten things you should know about protein kinases: IUPHAR Review 14.* Br J Pharmacol, 2015. **172**(11): p. 2675-700.
74. Kiss-Toth, E., G. Velasco, and W.S. Pear, *Tribbles at the cross-roads.* Biochem Soc Trans, 2015. **43**(5): p. 1049-50.
75. Richmond, L. and K. Keeshan, *Pseudokinases: a tribble-edged sword.* FEBS J, 2020. **287**(19): p. 4170-4182.
76. Rorth, P., K. Szabo, and G. Texido, *The level of C/EBP protein is critical for cell migration during Drosophila oogenesis and is tightly controlled by regulated degradation.* Mol Cell, 2000. **6**(1): p. 23-30.
77. Mata, J., et al., *Tribbles coordinates mitosis and morphogenesis in Drosophila by regulating string/CDC25 proteolysis.* Cell, 2000. **101**(5): p. 511-22.
78. Zareen, N., S.C. Biswas, and L.A. Greene, *A feed-forward loop involving Trib3, Akt and FoxO mediates death of NGF-deprived neurons.* Cell Death Differ, 2013. **20**(12): p. 1719-30.
79. Hong, B., et al., *TRIB3 Promotes the Proliferation and Invasion of Renal Cell Carcinoma Cells via Activating MAPK Signaling Pathway.* Int J Biol Sci, 2019. **15**(3): p. 587-597.

80. Keeshan, K., et al., *Tribbles homolog 2 inactivates C/EBPalpha and causes acute myelogenous leukemia.* Cancer Cell, 2006. **10**(5): p. 401-11.
81. Eyers, P.A., K. Keeshan, and N. Kannan, *Tribbles in the 21st Century: The Evolving Roles of Tribbles Pseudokinases in Biology and Disease.* Trends Cell Biol, 2017. **27**(4): p. 284-298.
82. Jamieson, S.A., et al., *Substrate binding allosterically relieves autoinhibition of the pseudokinase TRIB1.* Sci Signal, 2018. **11**(549).
83. Yokoyama, T., et al., *Trib1 links the MEK1/ERK pathway in myeloid leukemogenesis.* Blood, 2010. **116**(15): p. 2768-75.
84. Guan, H., et al., *Competition between members of the tribbles pseudokinase protein family shapes their interactions with mitogen activated protein kinase pathways.* Sci Rep, 2016. **6**: p. 32667.
85. Dedhia, P.H., et al., *Differential ability of Tribbles family members to promote degradation of C/EBPalpha and induce acute myelogenous leukemia.* Blood, 2010. **116**(8): p. 1321-8.
86. Qi, L., et al., *TRB3 links the E3 ubiquitin ligase COP1 to lipid metabolism.* Science, 2006. **312**(5781): p. 1763-6.
87. Salome, M., L. Hopcroft, and K. Keeshan, *Inverse and correlative relationships between TRIBBLES genes indicate non-redundant functions during normal and malignant hemopoiesis.* Exp Hematol, 2018. **66**: p. 63-78 e13.
88. Hill, R., et al., *TRIB2 as a biomarker for diagnosis and progression of melanoma.* Carcinogenesis, 2015. **36**(4): p. 469-77.
89. Yu, J.M., et al., *TRIB3 supports breast cancer stemness by suppressing FOXO1 degradation and enhancing SOX2 transcription.* Nat Commun, 2019. **10**(1): p. 5720.
90. Du, K., et al., *TRB3: a tribbles homolog that inhibits Akt/PKB activation by insulin in liver.* Science, 2003. **300**(5625): p. 1574-7.
91. Hong, S.H., et al., *High fat diet-induced TGF-beta/Gbb signaling provokes insulin resistance through the tribbles expression.* Sci Rep, 2016. **6**: p. 30265.
92. Gong, H.P., et al., *TRIB3 functional Q84R polymorphism is a risk factor for metabolic syndrome and carotid atherosclerosis.* Diabetes Care, 2009. **32**(7): p. 1311-3.
93. Soubeyrand, S., et al., *Role of Tribbles Pseudokinase 1 (TRIB1) in human hepatocyte metabolism.* Biochim Biophys Acta, 2016. **1862**(2): p. 223-32.
94. Iwamoto, S., et al., *The role of TRIB1 in lipid metabolism; from genetics to pathways.* Biochem Soc Trans, 2015. **43**(5): p. 1063-8.
95. Ishizuka, Y., et al., *TRIB1 downregulates hepatic lipogenesis and glycogenesis via multiple molecular interactions.* J Mol Endocrinol, 2014. **52**(2): p. 145-58.
96. Burkhardt, R., et al., *Trib1 is a lipid- and myocardial infarction-associated gene that regulates hepatic lipogenesis and VLDL production in mice.* J Clin Invest, 2010. **120**(12): p. 4410-4.
97. Bauer, R.C., et al., *Tribbles-1 regulates hepatic lipogenesis through posttranscriptional regulation of C/EBPalpha.* J Clin Invest, 2015. **125**(10): p. 3809-18.
98. Ha, E.E., et al., *Adipocyte-specific tribbles pseudokinase 1 regulates plasma adiponectin and plasma lipids in mice.* Mol Metab, 2021. **56**: p. 101412.

99. Wang, Z.H., et al., *Silence of TRIB3 suppresses atherosclerosis and stabilizes plaques in diabetic ApoE-/-/LDL receptor-/- mice.* Diabetes, 2012. **61**(2): p. 463-73.
100. Qian, B., et al., *TRIB3 [corrected] is implicated in glucotoxicity- and endoplasmic reticulum-stress-induced [corrected] beta-cell apoptosis.* J Endocrinol, 2008. **199**(3): p. 407-16.
101. Geng, T., et al., *Fatty acids differentially regulate insulin resistance through endoplasm reticulum stress-mediated induction of tribbles homologue 3: a potential link between dietary fat composition and the pathophysiological outcomes of obesity.* Diabetologia, 2013. **56**(9): p. 2078-87.

Chapter 2

PPARgamma in metabolism, immunity and cancer: unified and diverse mechanisms of action

Miguel Hernandez-Quiles[1#], Marjoleine F. Broekema[1,2#], and Eric Kalkhoven[1]

[1] Center for Molecular Medicine, University Medical Center Utrecht, Utrecht University, Utrecht, the Netherlands.

[2] Present address: Department of Clinical genetics, Amsterdam UMC, Vrije Universiteit Amsterdam, Amsterdam, The Netherlands.

[#] Authors contributed equally

*Correspondence: Dr. Eric Kalkhoven e.kalkhoven@umcutrecht.nl

Frontiers in endocrinology, 12, 624112. https://doi.org/10.3389/fendo.2021.624112

Abstract

The proliferator-activated receptor γ (PPARγ), a member of the nuclear receptor superfamily, is one of the most extensively studied ligand-inducible transcription factors. Since its identification in the early 1990's, PPARγ is best known for its critical role in adipocyte differentiation, maintenance, and function. Emerging evidence indicates that PPARγ is also important for the maturation and function of various immune system-related cell types, such as monocytes/macrophages, dendritic cells, and lymphocytes. Furthermore, PPARγ controls cell proliferation in various other tissues and organs, including colon, breast, prostate, and bladder, and dysregulated of PPARγ signaling is linked to tumour development in these organs. Recent studies have shed new light on PPARγ (dys)function in these three biological settings, showing unified and diverse mechanisms of action. Classical transactivation - where PPARγ activates genes upon binding to PPAR response elements as a heterodimer with RXRα - is important in all 3 settings, as underscored by natural loss-of-function mutations in FPLD3 and loss- and gain-of-function mutations in tumours. Transrepression-where PPARγ alters gene expression independent of DNA binding - is particularly relevant in immune cells. Interestingly, gene translocations resulting in fusion of PPARγ with other gene products, which are unique to specific carcinomas, present a third mode of action, as they potentially alter PPARγ's target gene profile. Improved understanding of the molecular mechanism underlying PPARγ activity in the complex regulatory networks in metabolism, cancer, and inflammation may help to define novel potential therapeutic strategies for prevention and treatment of obesity, diabetes, or cancer.

Introduction: PPARG

General modes of action

Since its discovery in the early 1990's by Tontonoz *et al.* (1), the nuclear receptor PPARγ, encoded by the *PPARG* gene on chromosome 3p25.2 in humans (Figure 1A) (2), has been recognized as the master regulator of adipose tissue biology. The human *PPARG* gene, encompassing 9 exons, generates four PPARG splice variants (PPARG1-4) encoding for two protein isoforms via differential promoter usage and alternative splicing (Figure 1B) (3). The mRNAs PPARG1, PPARG3, and PPARG4 all give rise to the PPARγ1 isoform. PPARγ1 is a 477 amino acid protein that is broadly expressed with relative high levels in the adipose tissue, liver, colon, heart, various epithelial cell types and skeletal muscle. In addition, PPARγ1 is expressed in numerous cells of the immune system, including monocytes/macrophages, dendritic cells, and T lymphocytes. The PPARG2 mRNA transcript translates into the PPARγ2 isoform. PPARγ2, containing an additional 28 amino acids in its NH2-terminus, is almost exclusively expressed in adipose tissue. This isoform is also expressed in urothelial cells (4,5), which are highly specialized transitional epithelial cells that line the organs of the urinary system, including the bladder, and in regulatory T cells (Tregs) and other T cell populations, albeit that total PPARγ expression is low in non-Tregs (6). Recently, a third and fourth PPARγ protein isoform, denoted as PPARγ1Δ5, and PPARγ2Δ5, respectively, have been reported (Figure 1B) (7). PPARγ2Δ5 is endogenously expressed in adipose tissue and lacks the entire ligand binding domain (LBD) due to physiological exon 5 skipping (7). The endogenous expression PPARγΔ5 positively correlates with body mass index (BMI) in overweight or obese and type 2 diabetic patients. The naturally occurring PPARγΔ5 isoforms impair the adipogenic potential of adipocyte precursor cells by dominant-negative inhibition of PPARγ, which possibly contributes to adipose tissue dysfunction in obesity (7).

PPARγ is a representative member of the nuclear receptor (NR) superfamily. To date, 48 NRs have been identified in human. NRs regulate various critical aspects in development, physiology, reproduction, and homeostasis. NRs are multi-domain ligand-inducible transcription factors that share a structural homology to a varying extent (8). Alike other NRs, PPARγ contains an autonomous transactivation domain 1 (AF-1) in the unstructured N-terminus (Figure 2). The AF-1 domain is implicated in the constitutive ligand-independent activation of PPARγ target genes. Juxtaposed to the AF-1 domains is the DNA binding domain (DBD) that contains two zinc fingers required for DNA binding. The DBD connected to the ligand binding domain (LBD) via a flexible hinge region. In the case of PPARγ, this hinge region physically interacts with the DNA (9). The ligand binding domain (LBD) is situated in the C-terminus.

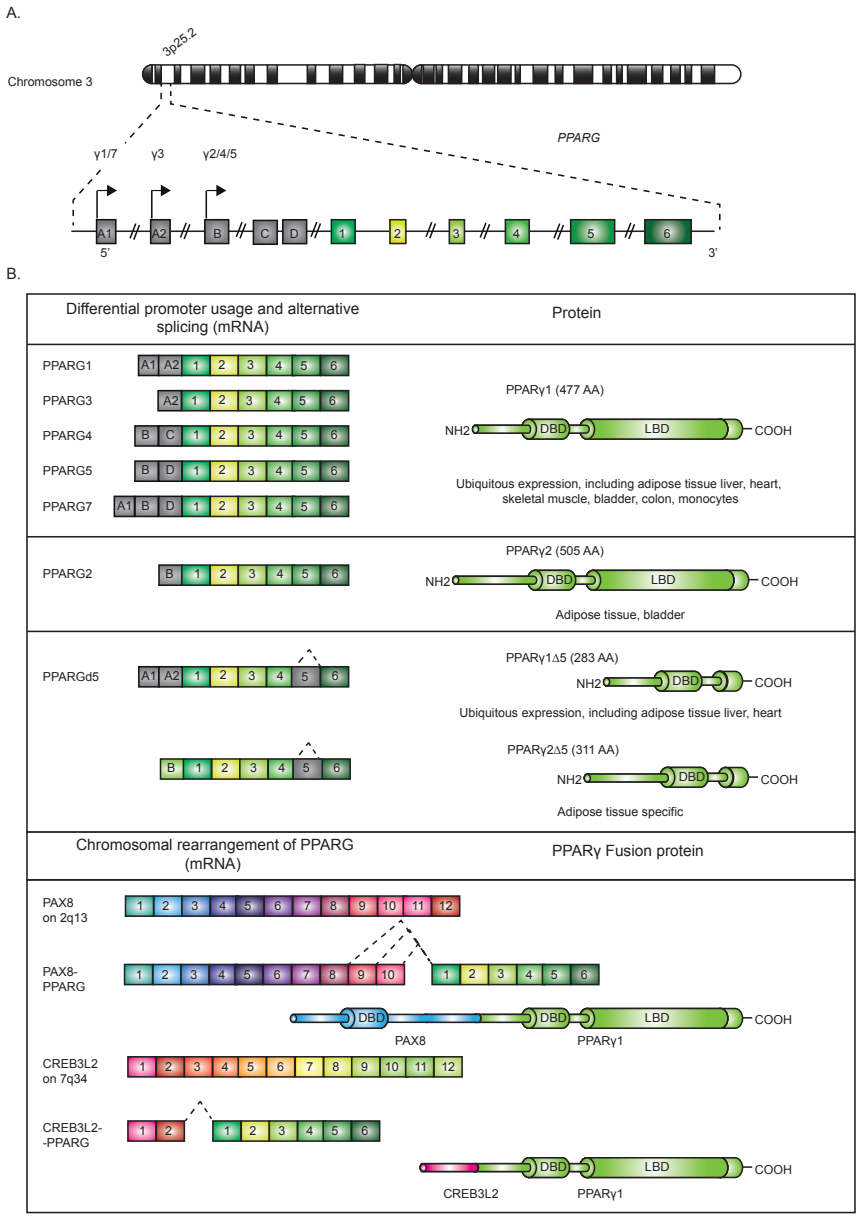

Figure 1. Genomic Map of the PPARG Gene On Chromosome 3p25 And Structure of PPARγ Isoforms. **A.** The gene *PPARG* is situated on chromosome 3p25. The gene encompassed 9 exons (exon A1-2, exon B-D, and exons 1-6). **B.** Alternative promoter and mRNA splicing give rise to several PPARγ mRNA and protein isoforms. The mRNAs PPARG1, -3, and -4 translate into PPARγ1 (477 amino acids; AA). mRNA PPARG2 gives rise to PPARγ2 (505 AA). A third and fourth PPARγ protein isoform, denoted as PPARγ1Δ5 and PPARγ2Δ5, have been reported. These isoforms lack the ligand binding domain (LBD), which is due to alternative splicing. Chromosomal rearrangement of PPARγ leading to PAX8/PPARγ and CREB3L2/PPARγ fusion proteins, contains functional DBDs of both proteins, have been described in carcinogenesis.

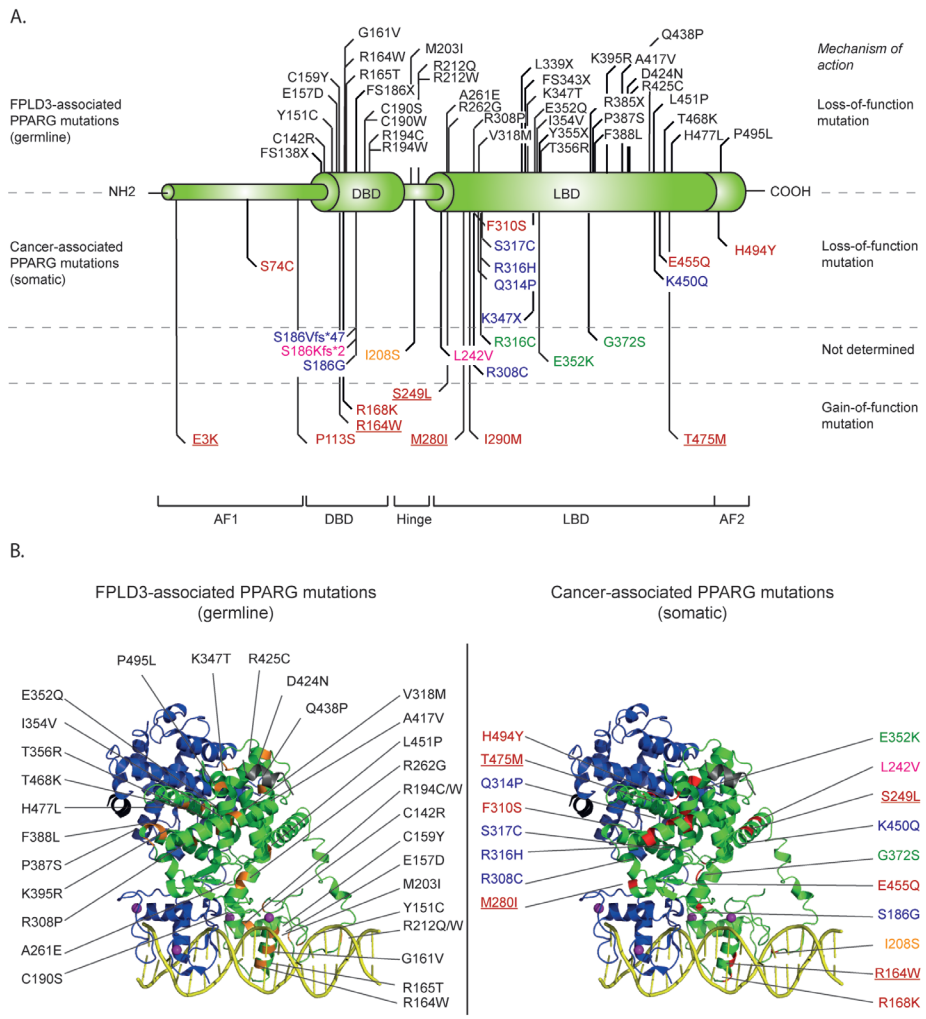

Figure 2. Overview of identified natural *PPARG* mutations implicated in FPLD3 and cancer. **A)** Schematic representation of the distinct domains of PPARγ. Mutations indicated above the PPARγ structure are mutations are germline loss-of-function mutation, implicated in FPLD3. Mutations depicted below the PPARγ structure are somatic loss-of-function or gain-of-function mutations identified in different cancer types. Mutations have been identified in tissue form digestive tract (colon, stomach, oesophagus, and pancreas; indicated in blue), melanoma (green), breast cancer (pink), prostate cancer (yellow), and bladder cancer (red). Some bladder cancer-associated PPARγ mutations (underscored in figure) have also been identified in other types of cancer, including lung cancer (E3K), kidney cancer (R164W), endometrium cancer (S249L), melanoma (M280I), and diffuse glioma (T465M) respectively. **B)** FPLD3 (orange) and cancer associated mutations (red) indicated in 3D representation. PPARγ (green) was crystalized in complex with RXRa (blue) on DNA (yellow) with Rosiglitazone, 9-cis retinoic acid and NCOA2 peptide (grey).

The LBD is a complicated structure that is arranged in a conserved three-layered α-helical sandwich containing 12 α-helices and four β-strand elements (8). The LBD overlaps with the ligand-dependent transactivation domain 2 (AF-2). The LBD is a key domain for transactivation of PPARγ target genes as it is implicated in ligand binding, heterodimerization with binding partner retinoid X receptor alpha (RXRα) and interactions with transcriptional co-regulators.

PPARγ exerts its gene regulatory potential via transactivation and transrepression (Figure 3). Transactivation involves a mechanism by which PPARγ binds as a heterodimer complex with RXRα to PPAR response elements (PPREs) (10). PPREs consist of a hexameric repeat (AGGTCA) spaced by one or two nucleotides (referred to as DR1 and DR2 elements) (11), which are situated in promoter and enhancer regions of PPARγ target genes (12). Noteworthy, enhancers may not only loop to the nearest promoters, but can also increase transcription of their target genes via looping to promoters at greater genomic distances.

In the last decade genome-wide binding profiles of PPARγ have been mapped in different cell types, including adipocytes and macrophages (13–17). These binding profiles have not only indicated that PPARγ binds to thousands of sites in the genome, of which many binding sites are located far from proximal promoters, but also that the PPARγ binding is highly context-dependent as binding sites differ between cell types and even between adipocytes from different anatomical locations (13–17). The context-dependency of PPARγ binding is at least in part mediated by cooperative binding to the chromatin with other adipogenic transcription factors, such as C/EBPα, followed by cooperative recruitment of coactivators (15).

Transcriptional control of the target genes by PPARγ furthermore depend on multiprotein coregulatory complexes that are recruited to the PPREs (18). In basal conditions, *i.e.* in absence of ligand, PPARγ/RXRα favours stable interactions with corepressor complexes, containing NCoR or SMRT, which recruit chromatin-modifying enzymes such as histone deacetylases that make the chromatin inaccessible to binding of transcription factors or resistant to their actions and thereby actively repress transcription (Figure 3A). Upon ligand binding, the PPARγ/RXRα heterodimer undergoes a conformational change that promotes corepressor release and recruitment of coactivators, like SRC1 and CBP. Coactivators enhance PPARγ transactivation by facilitating acetylation of the histone tails, making the chromatin less restrictive, and assembly of general transcriptional machinery. Next to the 'classical' transactivation mechanism described above, PPARγ can also negatively regulate gene expression by a mechanism referred to as ligand-dependent

transrepression (Figure 3B). This mechanism involves antagonizing the NF-κB and AP-1 pro-inflammatory signalling pathways, and has been mostly described in immune cells (19–23). In this case PPARγ does not bind to DNA itself, and several studies indicate that PPARγ transrepresses genes as a monomer, i.e. independent of RXRα (23). While various mechanisms have been postulated for transrepression by different NRs (24–26), the most detailed mechanism proposed for PPARγ involves inhibition of co-repressor degradation. Pascual et al. (2005) showed that clearance of NCoR/SMRT-HDAC3 complexes by proteosomal degradation from various AP1- and NFkB -regulated promoters (e.g IL-8, Mmp12 and iNOS) upon activation is prevented in the presence of liganded, monomeric PPARγ.

Interestingly, the transrepression mechanism described above involves a specific post-translational modification, SUMOylation of lysine 365. In fact, to adequately processes external signals and adapt to relevant gene expression programs PPARγ activity is regulated by several, probably interconnected, post-translational modifications, including phosphorylation, acetylation and the aforementioned SUMOylation (reviewed in (27)). Depending on cellular context and the kinases involved, phosphorylation of PPARγ S112 can either impair or increase PPARγ activity (28). Phosphorylation of PPARγ S273 by Cdk5 does not affect its adipogenic capacity, but affects many PPARγ target genes that have been shown to be dysregulated in obesity (29). In addition, acetylation of K268 and K293 correlates with the phosphorylation status of S273 and favours lipid storage and cell proliferation (30). Selective adipocyte deletion of the deacetylase Sirt1 that deacetylates PPARγ K268 and K293 leads to dephosphorylation of S273 and improve metabolic functions (31).

Alike other NRs, PPARγ governs nutrient- and hormone-mediated responses. Despite intensive efforts, it is not clear whether PPARγ is *in vivo* activated by a specific, high-affinity, endogenous ligand. PPARγ LBD crystal structures reveal a large ligand binding pocket (LBP), which not only allows for promiscuous binding of ligands with lower affinity, but also allows ligands to occupy the canonical LBP in different conformations (32). Indeed, the activity of PPARγ can be modulated by a variety of natural compounds, including polyunsaturated fatty acids (33), eicosanoids (34,35), and oxidized lipid components (discussed below) (36), suggesting that PPARγ functions as a general lipid or nutrient sensor (33). However, the physiological relevance of these compounds is not exactly clear. Endogenous ligands not only bind with low affinity for PPARγ, also the physiological concentrations in mammalian cells are often insufficient to function as a physiological ligand (37). Alternatively, the physiological activation of PPARγ could be the resultant of combined effects

of multiple ligands that simultaneously bind with different affinities to distinct subregions in the LBP (38), thereby inducing different PPARγ conformations with potential different biological outcomes (38).

PPARγ is the cognate receptor for thiazolidinediones (TZDs), a class of anti-hyperglycaemic drugs, including rosiglitazone and pioglitazone (39). TZDs stimulate adipogenesis (39) and cause a metabolically beneficial shift in lipid repartitioning from storage in visceral to subcutaneous adipose tissue depots as well as from ectopic storage in non-AT organs (*e.g.* liver muscle) to AT (40–42). TZDs and endogenous ligands have overlapping binding sites in the LBP, which potentially allows for binding competition to the same site. TZDs occupy the canonical LBP of PPARγ and by interacting with residues in helices 3, 5, 6, and 7 and the β-sheet, stabilizes the dynamics of helix 12 and the AF2 surface (43,44).

Whereas TZDs are commonly referred to as full classical PPARγ agonists, TZDs have a separate biochemical activity: inhibition of the Cdk5-mediated phosphorylation of PPARγ at serine residue 273 (29). Phosphorylation of PPARγ S273 requires a physical interaction between CDK5 and PPARγ (45). The transcriptional corepressor NCoR is an adaptor protein for the physical interaction between CDK5 and PPARγ. Upon rosiglitazone the interaction between NCoR and PPARγ is reduced, which leads to i) derepression of PPARγ and activation of the PPARγ transcriptional program and ii) attenuation of the psychical interaction between CDK5 and PPARγ and subsequent reduced phosphorylation of S273 (45). Interestingly, MRL24 that displays poor agonistic activity but robust anti-diabetic activity in mice (46), was also very effective in inhibiting the Cdk5-mediated phosphorylation (47). This suggests that new classes of antidiabetic drugs that i) bind with high affinity to PPARγ, ii) specifically target the Cdk5-mediated phosphorylation of S273, and iii) completely lack the classical transcriptional agonism, hold promise for treatment of T2DM. The PPARγ ligand SR1664 was essentially displayed no transcriptional activity and was very effective in blocking the Cdk5-mediated phosphorylation (48). In obese mice, SR1664 displayed strong antidiabetic effects without adverse effects (48). However, unfavorable pharmacokinetic properties of SR1664 preclude its administration in human (48). Therefore, SR1664 should rather be considered as a proof-of-principle.

In addition to binding in the canonical LBP, a recent structure-function study shows that some PPARγ ligands denoted as noncanonical agonist ligands (NALs), like the aforementioned compound MRL24, and SR1664, can also bind to an alternate site of PPARγ (49). TZDs, including rosiglitazone and pioglitazone display less prominent alternate site functional effects (49). The alternate binding of PPARγ

ligands can occur when the canonical LBP is occupied by the covalent antagonists or endogenous ligands. Although the exact mechanisms are not clear, alternate site binding stabilizes the AF2 surface, most likely indirectly via stabilization of helix 3. Furthermore, coregulator-binding assays indicate that alternate site binding has an impact on coregulator interactions, transactivation, and target gene expression (49). The identification of the alternate binding site has three important implications. Firstly, compounds that block phosphorylation of S273 with little transactivation might be complicated by alternate site binding if this site *in vivo* contributes to classical PPARγ agonism. Secondly, it needs to be defined whether some of the supposed PPARγ-independent effects of TZDs could in fact be mediated by the alternate site binding. Lastly, allosteric modulators that target the alternate site might be particularly relevant for obese individuals in which the probability that canonical LBP is occupied by oxidized fatty acids due to increased bioavailability of endogenous ligands is increased (49).

PPARγ in adipose tissue

White, beige, and brown adipocytes have been identified in mammals. Although these three type of adipocytes rise from different precursors and differ significantly in their morphology and function, the cells all go through a well-orchestrated differentiation process to become mature and fully functional (50). During the various stages of the adipocyte lifespan, PPARγ is a well-established key player. Recently a fourth type of adipocyte, denoted as pink adipocytes, has been described in in mammary glands of pregnant mice (51). During pregnancy, lactation, and post-lactation subcutaneous white adipocytes in murine mammary gland undergo a transdifferentiation process ending in milk-producing epithelial glandular cells that contain abundant cytoplasmic lipid droplets to meet the nutritional needs of the pups. (51,52). As the number of studies in pink adipocytes is limited so far, we will focus in this review on the role of PPARγ in white, brown, and beige adipocytes. In these cells PPARγ exerts its essential functions primarily via 'classical' transactivation of target genes.

White adipocytes

White adipose tissue (WAT) is the most abundant adipose tissue in the human body (53). Mature white adipocytes are unilocular cells composed of a large lipid droplet occupying ~95% of the cellular volume. Depending on the size of the lipid droplet, the cell size varies from 20-200 μM (54). The *in vivo* regulation of adipocyte development, including the stem cell commitment towards white adipocytes, is poorly understood. Adipocyte-lineage tracing, which so far can only be performed in mice, indicate that white adipocytes can be derived from both $Myf5^-$ and $Myf5^+$ precursor cells (55).

The Myf5-lineage distribution in adipose tissue is dynamic and can be affected by ageing and diet. The Myf5^{-} and Myf5^{+} white adipocytes can compensate for each other during development, reflecting adipose tissue plasticity (55). In mice, depot-dependent variations were observed among the degree of plasticity (55). Although it remains to be defined whether this concept also applies to human adipocytes, a heterogeneity in adipocyte origins may explain the heterogeneity in adipose tissue depot function and contribute to adipose tissue patterning variations in the human population (55). After stem cell commitment towards white adipocyte lineage, the expression and activation of PPARγ is both sufficient and crucial to initiate the adipogenic differentiation program and maintain adipocyte phenotype, integrity, and function, based on a large set of different genetic mouse models (56). PPARγ primarily regulates the expression of genes implicated in adipocyte differentiation and adipocyte maintenance. In addition, PPARγ governs the expression genes involved in various processes in lipid and glucose metabolism including lipogenesis (e.g. *LPL, ANGTPL4, CIDEC*), fatty acid transport (e.g. *FABP4*), and gluconeogenesis (e.g. *PEPCK, GYK, AQP7*).

The importance of PPARγ for white adipose tissue biology in humans is underscored in patients suffering from familial partial lipodystrophy subtype 3 (FPLD3), a rare autosomal dominant inherited condition caused by loss-of-function mutations in the *PPARG* gene (reviewed in (27)). Patients with FPLD3 lack subcutaneous adipose tissue in the extremities and gluteal region combined with lipohypertrophy in the face, neck, and trunk, and suffer from multiple metabolic complications including type 2 diabetes mellitus (T2DM). Since the first report of a germline loss-of-function mutation in *PPARG* in patients with FPLD3 (57) an increasing number of FPLD3-associated mutations in *PPARG* has been identified (reviewed in (27)). The FPLD3-associated PPARγ mutations are mainly situated in either the DBD or LBD (Figure 2). Mutations in the DBD interfere in efficient DNA binding. Mutations affecting the LBD -which are scattered over the whole LBD based crystal structures (Figure 2)- often cause multiple molecular defects by impairing heterodimerization with RXRα, ligand- and/or cofactor binding (18).

Taken together, genetic mouse models together with the FPLD3-associated PPARγ mutations indicate that PPARγ plays a key role in white AT differentiation, function and maintenance. The dominant mode of action in this biological setting appears to be 'classical' transactivation: the majority of genes regulated by PPARγ in white adipocytes rely on direct DNA binding, and FPLD3-associated PPARγ mutations do not alter transrepression, although this is not studied frequently (58).

Brown adipocytes

Brown adipose tissue (BAT) emerged approximately 150 million years ago in mammals (59). BAT is unique for endothermic placental mammals and makes it possible to maintain a body temperature that is higher than the ambient temperature by producing heat independently of shivering and locomotor activity. This process is also referred to as non-shivering thermogenesis (59). BAT is richly innervated and vascularized and is composed of brown adipocytes (~ 40 μM in size) that contain multilocular lipid droplets and a large number of mitochondria (54). BAT derives its brown colour from the conspicuous iron-rich mitochondrial mass. BAT uniquely expresses the gene *UCP1*, which encodes for uncoupling protein 1 (UCP1), located in the inner mitochondrial membrane. When activated, UCP1 mediates non-shivering thermogenesis by uncoupling of the oxidative phosphorylation from ATP synthesis, thereby provoking 1) dissipation of chemical energy in the form of heat and 2) stimulating high levels of fatty acid oxidation (60).

BAT is present in dedicated depots. In rodents BAT is abundantly present throughout life. In human adults, BAT is located mainly cervical/axillary, perirenal/adrenal, and in the mediastinum along large blood vessels, trachea and surrounding the intercostal arteries (61). In new-born infants, BAT is also situated between the shoulder blades as a thin kite-shaped layer (60). Although BAT depots regress with increasing age and can become even indistinguishable from WAT, healthy adults retain metabolically active BAT (62–64). For instance, positron emission tomography (PET) Computer Tomography (CT) in human indicated that BAT-mediated thermogenesis is activated and increases in size by cold exposure (62–64). This process is also known as BAT recruitment. Depending on the size of the BAT depots, thermogenesis can account for up to approximately 15% of the total daily energy expenditure (65). Therefore, increasing energy expenditure by activation of BAT has been suggested as a therapeutic strategy for treating obesity (66).

Mice studies indicate that PPARγ functions is a master regulator in BAT (67). BAT-specific PPARγ knock out mice showed reduced wet weight of BAT, smaller brown adipocytes and smaller lipid droplets when compare to wild type animals. However, there was no difference in total body weight or body composition (68). Furthermore, it was also shown that loss of PPARγ inhibited the ability of brown adipocytes to respond to β -adrenergic stimulus in *in vitro* cultures (68). An increase in non-shivering thermogenesis was observed in mice treated with TZDs (69,70), and *in vitro* studies showed that activation of PPARγ in brown adipocytes leads to increase in adipogenesis and increase in lipid metabolism (71). Additional studies pointed at PPARγ as crucial regulator of UCP1 expression and BAT function (72). Specific BAT

PPARγ target genes have been described (FABP3 and GYK), and particularly the de-acetylation of K268 and K293 of PPARγ by SIRT1 have been linked to BAT (73). De-acetylation of these residues is required for the recruitment of Prdm16, an essential cofactor in BAT (74). Moreover PGC1a, one of the most well-known regulators of BAT, has also been identified as a cofactor of PPARγ in BAT (75).

Collectively, PPARγ plays a key role in BAT differentiation and function, which most likely relies on 'classical' transactivation, although transrepression cannot be excluded given the limited number of studies. BAT-specific molecular mechanisms, which may be different from WAT, could involve for example specific transcriptional cofactors (76), but details remain to be fully elucidated.

Beige adipocytes

Mammals possess a second type of thermogenic adipocytes: beige adipocytes, also denoted as "brite" (brown-like in white) adipocytes (77). Beige adipocytes are inducible thermogenic cells that are sporadically located in white adipose tissue depots (77). Beige adipocytes share many morphological and biochemical features with brown adipocytes (Figure 1) (60). Alike brown adipocytes, beige adipocytes contain multiple small lipid droplets and a large number of mitochondria that express UCP1. Recruitment of beige adipocytes, referred to as 'browning' or 'beigeing/beiging' of white adipose tissue, is induced in response to environmental conditions, including chronic cold exposure, exercise, long-term treatment with PPARγ agonists or β3-adrenergic receptor agonists, cancer cachexia, and tissue injury (78). It is currently unknown whether beige adipocytes arise through transdifferentiation from pre-existing white adipocytes or by *de novo* adipogenesis from a precursor cell pool, or both (79).

Although, the exact mechanism by which PPARγ agonists induce browning of white adipocytes is not exactly known, PPARγ agonist require full agonism to activate the browning fat program. The effect is at least in part mediated by PRDM16, a factor that as described above is essential in the development of classical brown fat (80). Therefore, it is likely that in beige adipocytes, alike brown adipocytes, 'classical' transactivation by PPARγ is an important mechanism of action.

PPARγ in immune cells

Even though PPARγ is the master regulator of adipocyte differentiation and function (81), already in one of the first publications showed high PPARγ expression in mouse spleen (82) suggesting a role for PPARγ in immune cells. In fact, PPARγ is expressed in a variety of immune cells and its role and importance have been investigated during the last twenty years (83–85). Although PPARγ expression have been described in several types of immune cells we will focus on monocyte/macrophages and dendritic cells as part of the innate immune system, and T cells of the adaptative immune system.

As described above for adipocytes, PPARγ plays a role in determining the cellular phenotype by regulating differentiation (adipogenesis) and function (e.g. lipid metabolism and secretome) by directly activating the transcription of so-called PPARγ target genes. Similar molecular mechanisms are in place in immune cells, and also here PPARγ can deterimine cellular phenotype: amongst others, PPARγ 1) regulates macrophage differentiation, 2) regulates classical/alternative macrophage activation ('polarization'), 3) controls lipid metabolism in multiple immune cell types, and 4) plays an immune-modulatory role. PPARγ function in immune cells could also be categorized according to its mechanism of action, with the regulation of lipid metabolism and the ability to induce differentiation of immune cells more linked to 'classical' transactivation, while the transrepression activity of PPARγ is more important in its immunomodulatory role and both mechanisms are involved in macrophage activation.

Transactivation by PPARγ in immune cells

PPARγ can directly activate the transcription of target genes in immune cells through direct DNA binding, similar to its activity in adipocytes described above. As mentioned earlier, the genomic locations where PPARγ binds and the target genes partly overlap between for example adipocytes and macrophages, but cell-type specific regulation may depend on cooperation with other transcription factors like PU.1 and STAT6 (86,87).

PPARγ expression is highly induced during monocyte to macrophage differentiation (88–90), and although initial studies using embryonic stem cells suggested that PPARγ is dispensable in this process (91), more recent studies have demonstrated that PPARγ is essential for the differentiation of fetal monocytes into alveolar macrophages (92). In mature macrophages, PPARγ was found to cooperate with *PU1* specifically on monocyte-unique target genes (86), reminiscent of the interplay between PPARγ and C/EBPa in adipocytes mentioned earlier. PPARγ is also expressed in several dendritic cell (DC) subtypes and is also highly upregulated in monocyte-derived DC differentiation (93,94). Although the importance of PPARγ in immune cell differentiation is evident, little is known about the exact function of the receptor in these differentiation processes. Better models are required as well as studying the contribution of PPARγ in a more cell-type specific way.

Next to macrophage differentiation, PPARγ is also an important regulator in macrophage polarization, where PPARγ activation drives the alternative M2 macrophage phenotype (95–97). Alternatively activated macrophages (M2 phenotype) can be induced by IL-4, IL-10 and IL-13 and are characterized by the expression of several genes including Arg1 and Mgl1/CD301a, CD-204 and mannose receptor/CD163 and IL-10 and transforming growth factor beta (TGF-β). Some of these, including Arg1 and Mgl1 (98), are direct PPARγ target genes. Furthermore, PPARγ expression is induced by IL-4/STAT6 signaling as well as IL-13 (99), and STAT6 functions as a 'facilitator' of PPARγ signaling, all supporting the idea that PPARγ is crucial for the anti-inflammatory M2 phenotype in macrophages. It was recently found that PPARγ contributes to maintain a chromatin structure that facilitates the binding of STAT6 and polymerase II upon repeated IL-4 treatments. PPARγ recruits the coactivator P300 and RAD21 to the DNA and thus reinforcing a M2-like phenotype in macrophages (100), is worth mention that this function of PPARγ is independent of ligand binding.

Next to macrophage and DC differentiation and macrophage polarization, PPARγ can also directly regulate lipid metabolism in immune cells (91,96,101–103), reminiscent of its role in white and brown adipocytes. In monocytes, macrophages and dendritic cells, PPARγ directly regulates the expression of genes involve in lipid transport and metabolism such as the class B scavenger receptor *CD36* (104), *FABP4, LXRA and PGAR* (90) . The use of PPARγ ligands in these cells has shown that the expression of these genes is upregulated upon treatment and downregulated when treated with PPARγ antagonists (105). The CD36 protein is also involved in macrophage uptake of oxLDL, but at the same time PPARγ directly activates an LXR-ABCA1 pathway for cholesterol efflux (102). In DCs PPARγ also plays a key role in lipid homeostasis by directly regulating many 'known suspects' (106) but it also regulates another aspect of lipid homeostasis, lipid antigen presentation. Activation of PPARγ gives higher expression of CD1d, a molecule involved in the presentation of lipid antigens to T-cells, resulting in a DC subtype with increased potential to activate iNKT cells (105,107,108). These findings indicate that PPARγ has a functional role in the modulation of the immune response through DCs beyond regulation of more classical lipid metabolism pathways.

Changes in the lipid microenvironment can trigger different DC functions that regulate the immune response (109). PPARγ classical transactivation role bridges the lipid microenvironment and the DC function by activating genes involve in lipid transport, metabolism and presentation.

The classical role of PPARγ as a gene activator has also been studied in T-cells and again relates to lipid metabolism (84,85). T-cells can be subdivided into cytotoxic T-cells, T-helper and regulatory T cells (Treg), and the T-helper cells can be further classified depending on the phenotype into Th1, Th2 and Th17; less well characterized are Th9 and Th22 subsets. Regardless of the subtype of T-cell, activation of PPARγ is linked to an activation of genes related to lipid metabolism (CD36 and FABPs) indicating the importance of PPARγ in this process. Special mention deserves the visceral adipose tissue resident regulatory T-cells (VAT Tregs), in which PPARγ has been implicated in its function and development (110). VAT Tregs represents a unique subtype of cells in which the expression of PPARγ positively correlates with the expression of chemokines and chemokines receptors (Ccr2, Cxcl3, Cxcr6) that regulates leukocyte migration and infiltration, lipid metabolism genes and IL10. Interestingly the PPARγ1 and PPARγ2 isoforms induce the same genes upon activation in VAT Tregs (mainly related to lipid metabolism) but differ in the genes that they downregulate (110), the latter happening most likely through the mechanism of transrepression.

Transrepression by PPARγ in immune cells

The role of PPARγ as an immune-modulator, and in particular a repressor of inflammation, has been studied in most detail in macrophages and T cells (19–22,97). Although the transrepression activity of PPARγ is probably not exclusive to immune cells, this immunomodulatory role is a good example of the importance of this specific mechanism of action of PPARγ.

In macrophages it has been shown that activation of PPARγ using TZDs suppresses the production of pro-inflammatory cytokine, such as TNFα, IL-1B and IL-6 (19,97) and the expression of other genes involved in inflammation, including iNOS and MMP9, in a dose-dependent manner. As described above, inhibition of the transcription factors NFkB and AP-1 is the most widely studied mechanism, but other mechanisms are also possible (23). Similarly, in DCs PPARγ ligands downregulate chemokines and receptors (IL-12, CD80, CXCL10, RANTES) that recruit Th1 lymphocytes (105,107). In addition, PPARγ activation in DC may impair the migration of these cells to the lymph nodes, and this might be partially due to inhibition of CCR7 by PPARγ (107,111).

The role of transrepression by PPARγ in T-cells has been the object of intensive discussion during the last two decades (84,85,112), as this mechanism of action was implicated in seemingly conflicting biological proccesses. Initial studies suggested that PPARγ had an inhibitory effect on T-cell proliferation (113), and that the underlying mechanism involved transrepression of the IL2 gene: activated PPARγ was shown to bind to nuclear factor of activated T cells (NFAT) and repress its activity

and binding to the IL-2 promotor (113,114). Besides T-cell proliferation, PPARγ-mediated transrepression was reported as a repressor of excessive Th1 response, by on the one hand inhibiting production of the Th1 cytokine and antigen-specific proliferation and on the other hand controlling Th2 sensitivity to IL-33 (115,116). In fact, Cunard and colleagues showed that PPARγ binds to the IFNγ promoter and is able to repress its expression when T-cell were treated with PPARγ ligands, and that IFNγ expression was enhanced when cells were treated with PPARγ antagonist GW9662 (117). The underlying mechanism was proposed to be inhibition of AP-1 activity, similar to the transrepression mechanism in macrophages. However, while these studies suggest a pro-Th2 role for PPARγ mediated transrepression, PPARγ was also reported to be involved in the downregulation of well-known Th2 cytokines like IL-4, IL-5 and IL-13, again through interaction with NFAT (118). All together these studies indicate that the role of PPARγ in the modulation of the Th2 response in T-cells remain unclear and further research is needed to fully elucidate its function. Finally, PPARγ-mediated repression is important for Th17 differentiation, as lack of PPARγ leads to increased Th17 differentiation while activation of PPARγ was shown to have inhibitory effects(22). PPARγ recruits NCoR and SMRT to the *Rorc* promoter, thereby inhibiting IL-17a expression, and blocks IL-6 signaling by inhibiting the DNA binding activity of STAT3 (20,21).

In summary, transrepression by PPARγ – where it counteracts other transcription factors like NFkB, AP-1, NFAT and STAT3- may be a major molecular mechanism that drives the functional phenotype(s) and secretory output of macrophages, dendritic cells and T-cells. Findings in T-cells appear sometimes conflicting, which makes it difficult to assign a clear pro-Th1 or pro-Th2 role to PPARγ activation. It also indicates that the use of ligands in these cells might 'hide' some of the PPARγ functions and more subtle approaches, such as the use of cels harbouring specific PPARγ mutations or selective PPARγ modulators, must be used in order to fully elucidated PPARγ role in immune cells, taking the complex interactions between immune cell population into account.

PPARγ in cancer

Cancer is driven by the acquisition of genome instability. The cancer genome landscape contains an enormous diverse repertoire of amplifications, deletions, inversions, translocations, point mutations, loss of heterozygosity, and epigenetic changes that collectively result in tumorigenesis. The role of PPARγ in tumorigenesis is controversial. A large body of evidence suggests that PPARγ functions as a tumor suppressor, as activation of the PPARγ/RXRα signaling pathway in different types of cancer, including colon (119), lung (120,121), pancreatic (122), prostate (123),

and breast (124,125) cancers, leads to inhibition of cell growth, decreased tumor invasiveness, and reduced production of proinflammatory cytokines. In addition, treatment with TZDs was shown to increase sensitivity to chemotherapy through downregulation of Metallothionein genes (126) and/or endotrophin (127), which may be linked to ligand-mediated prevention of S273 phosphorylation (128).

Furthermore, in lung cancer cells a tumor suppressive function of PPARγ was contributed metabolic reprogramming (129), an essential biochemical adaptation required for cancer viability that is considered to be a crucial emerging hallmark of cancer (130). In contrast, a protumorigenic role for PPARγ has been suggested in a variety of cancers as well (5,131,132). Here, we will discuss several loss-of-function and gain-of-function mechanisms by which PPARγ can be implicated in tumor initiation and progression in several major cancers. In addition, we will address the yet partly undefined role of PPARγ fusion proteins in cancer.

Transactivation by PPARγ

Loss-of-function mutations

As discussed above, the PPARγ1 isoform is highly expressed in colon epithelial cells. The role of PPARγ in the development of normal colon epithelium and colorectal cancers is not completely understood and seems to be dual. The growth and differentiation of many colorectal cancers can be considerably inhibited upon ligand activation of PPARγ1 (119). This finding suggests that PPARγ functions as a tumor suppressor during colorectal carcinogenesis. In line with this, somatic *PPARG* mutations have been reported in ~8% of sporadic colorectal cancers (Figure 2) Genetic and epigenetic phenomena due to genetic alterations in other genes, like *RAS*, can further decrease PPARγ function in colon cancer. Activating mutations in *RAS* for example can result in hyperactivation of ERK1/2 and JNK pathways and ultimately impair PPARγ activity (27). Whereas all FPLD3-associated *PPARG* mutations that have been reported to date lead to mutant proteins that show a consistent and profound impairment in the transcriptional activity of PPARγ, the functional effects of colon cancer-associated *PPARG* mutations vary considerably (133). So far, six unique somatic *PPARG* mutations in colorectal cancers have been reported (134,135). A side-by-side analysis of these colon-cancer associated mutants with some FPLD3-associated PPARγ mutants, shows that the colon-cancer associated mutants do not consistently display profound intra- and/or intermolecular defects (133). Moreover, while the abovementioned studies suggest that PPARγ functions as a tumor suppressor during colorectal carcinogenesis, it should be noted that other studies suggest that PPARγ activation increases the risk of developing colorectal cancer.

Ligand-activation of PPARγ in *min* mice, an animal model for familial adenomatous polyposis due to mutations in the *APC* gene, results in a considerably greater number of polyps in the colon (131). Follow-up studies are clearly needed to reconcile these apparently conflicting findings and assign a clear role to PPARγ in colon cancer.

In basal bladder tumors four non-recurrent loss-of-function PPARγ mutations (S74C, F310S, E455Q, and H494Y, Figure 2) have been identified (136). All four PPARγ mutants display significantly reduced transcriptional activities. Biochemical and biophysical analysis of amino acid residues F310 and H494, situated in helix 3 and 12 respectively, indicated that both residues are essential for proper stabilization of helix 12. F310S and H494Y favor an inactive conformation, impairing both a proper release of corepressors and recruitment of coactivators (136). Basal tumors rely on EGFR signaling for growth (137). Interestingly, in basal cell lines the overexpression of wildtype but not H494Y, downregulates EGFR signaling.

Although the cancer-related PPARγ mutants -which are mainly scattered through the LBD (Figure 2)- may display variable and more subtle, *i.e.* context-dependent, intra- and/or intermolecular defects than the FPLD3-associated PPARγ, the cancer-related PPARγ mutants (Figure 2) are impaired in their ability to exert 'classical' transactivation.

Gain-of-function mutations

In addition to its well-established role as master regulator in adipocyte biology, PPARγ has also been shown to be involved in the terminal differentiation of urothelium (4), a layer of specialized epithelial cells lining the lower urinary tract. However, little is known about its function in the bladder and in the pathogenesis of bladder cancer. In 12-17% of the muscle-invasive bladder carcinomas (MIBC) and in 10% of the non-muscle-invasive bladder carcinomas, *PPARγ* focal amplifications leading to PPARγ overexpression, have been reported, suggesting a role for PPARγ in the initiation and maintenance of bladder cancer. MIBC are biologically heterogeneous and can further be grouped into basal and luminal subtypes (138). PPARγ has a protumorigenic role in luminal MIBCS, as the loss of PPARγ expression impairs the bladder cancer cell viability (139). These luminal tumors maintain molecular urothelial differentiation, even in the loss of morphological differentiation (140). This molecular differentiation depends on PPARγ (140).

In approximately 5% of the MIBCs and the luminal subgroup of MIBCs hotspot mutations of RXRα (S427F/Y) has been identified. These RXRα mutations rely on the introduction of an aromatic amino acid residue that enhances the ligand-independent activation of PPARγ (141). Tumors harbouring RXR S427F/Y display enhanced expression of genes implicated in adipogenesis and lipid metabolism,

including *ACOX1, ACSL1, ACSL5,* and *FABP4* (142). In addition, the RXRα hotspot mutations stimulate the proliferation of urothelial organoids, render bladder tumor cell growth PPARγ-dependent, and favour tumor evasion by the immune system.

Recently, seven recurrent driver gain-of-function PPARγ mutations have been identified in luminal bladder tumors (E3K, S249L, M280I, K164W, T475M) (5). The mutations occur throughout the protein, affecting the N-terminus, DNA-binding domain, and ligand-binding domain (Figure 2). One recurrent mutation (E3K) was specific to the PPARγ isoform as it was situated in the N-terminal end. Functional analysis indicates that five mutations promote the transcriptional activity of PPARγ, which renders PPARγ-dependence to the cells. The three recurrent LBD-mutations promote, in absence of PPARγ ligands, the adoption of the active conformation of PPARγ by stabilizing helix 12 and induce recruitment of co-activators. Interestingly, four of the seven recurrent PPARγ mutations have also been identified in other types of cancer, including lung cancer, kidney cancer, cutaneous melanoma, and diffuse glioma (Figure 2) (5). Furthermore, other recurrent mutations that have not been identified in bladder cancer, have been identified in other types of cancer, including melanoma and prostate cancer (Figure 2) (5). Surprisingly, one of these recurrent PPARγ mutations, which are yet functionally uncharacterized, results in the same amino acid changes as FPLD3-associated loss-of-function PPARγ mutations (e.g. R164W and E352Q/K). This may indicate that a potential loss-of-function or gain-of-function effect is context dependent.

Although, not all recently identified gain-of-function PPARγ mutants have extensively been characterized and even affect different domains in the protein, at least some of the mutants have implications for 'classical' transactivation of PPARγ target genes in bladder cancer.

Somatic PPARγ fusion proteins in cancer

Besides the loss- and gain-of-function mechanisms described above, a third way in which PPARγ may be involved in carcinogenesis is represented by PPARG gene fusions observed in follicular thyroid carcinomas (FTCs). The t(2;3)(q13;p25) chromosomal translocation results in a *PAX8/PPARG* fusion gene that is detected in approximately 35% of FTCs and in a subset of follicular variant of papillary thyroid carcinomas (143). This chromosomal rearrangement is occasionally present in follicular adenomas as well (144). The gene paired-box gene 8 (*PAX8*) encodes for a member of the paired box (PAX) family of transcription factors and is a critical regulator in physiological thyroid development (145). In addition, PAX8 promotes the thyroid progenitor survival en in the mature thyroid it drives the expression thyroid specific genes, including genes encoding for thyroglobin and thyroid peroxidase

(146,147). The endogenous expression of *PPARG* in the thyroid is extremely low and it remains to be defined whether PPARγ has a physiological function in the thyroid (148). The translocation t(2;3)(q13;p25) results in a fusion transcript, driven by the *PAX8* promoter, wherein most of the coding sequence of PAX8 is fused in - frame to the entire coding sequence of PPARγ1 (149). The PAX8-PPARγ fusion protein (PPFP) contains functional DBDs of both the PAX8 and PPARγ (150). *In vitro* and *in vivo* evidence indicates that the PAX8-PPARγ fusion protein can function as an oncoprotein i) by acting as a negative inhibitor of tumor suppressor PPARγ or as ii) a novel transcriptional factor with proto-oncogene activity. Nevertheless, the expression of *PAX8-PPARG* in FTCs does not affect prognosis (151).

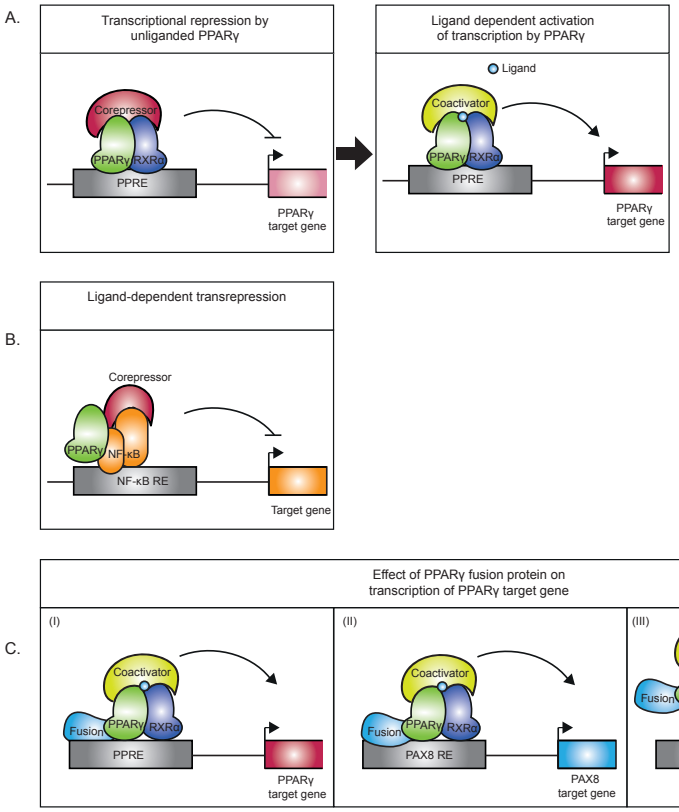

Figure 3. Mechanisms of action exerted by the PPARγ/RXRα heterodimer. A. Transcriptional repression by unliganded PPARγ. Upon ligand binding the PPARγ/RXRα heterodimer undergoes a conformational change that promotes corepressor release and recruitment of coactivators, initiating transcription. **B.** Ligand-dependent transrepression by antagonizing the NF-κB (and AP-1, not indicated) pro-inflammatory signalling pathways. This effect does not require DNA binding by the PPARγ. C. The mode of action performed by PPARγ-fusion proteins in carcinogenesis is not completely understood. (I) altered expression of PPARγ target genes, (II) altered expression of PAX8 target genes (III) PPARγ fusion protein may act as a negative inhibitor of tumor suppression by inhibiting PPARγ target gene expression.

A second chromosomal translocation, t(3;7)(p25;q34) resulting in a *CREB3L2/PPARG* fusion gene, is a low incidence fusion mutation that is found in <3% of the FTCs (152). The gene cAMP Responsive Element Binding Protein 3 Like 2 (*CREB1L2*) encodes for a member of the bZIP transcription factor family. The CREB3L2/PPARγ fusion protein consists of amino acids 1 to 106 of wildtype CREB3L2, a new glutamic acid at position 107 juxtaposed to the all 477 amino acids of wildtype PPARγ1 (152). The CREB3L2/PPARγ fusion protein stimulates cell growth of transduced primary thyroid cells by inducing proliferation (152). The fusion protein seems to be unresponsive to thiazolidinediones. In addition, CREB3L2/PPARγ interferes in the CRE-related transcription as overexpression of CREB3L2/PPARγ inhibits the transcription of native cAMP-responsive genes in normal thyroid cells (152). The impaired ability to stimulate transcription is consistent with the loss of CREB3L2 bZIP domain, implicated in dimerization and DNA binding, in the CREB3L2/PPARγ fusion protein (152). The oncogenic activities of the CREB3L2/PPARγ fusion protein are most likely (at least in part) due to 1) disruption one functional CREB3L2 allele and 2) inhibition of cAMP responsive genes by interfering in CREB3L2 DNA-binding (152).

Taken together, the PPARγ fusion proteins display a third mode of PPARγ action, as they potentially alter the target gene profile of both parent proteins in the chimeric protein (Figure 3C) and will target multiple signaling pathways implicated in cancer.

Since the identification of the *PPARG* gene in the early 1990s the role of PPARγ in cancer has extensively been studied in many different human cancer cells and animal models. However, the biological significance of PPARγ in cancer development and progression is far from completely understood and for some cancers appears to be even inconsistent and contradicting. At best, the overall conclusion from these studies is that the context, *e.g.* specific tumour type, tumour stage, tumour microenvironment, determines the exact role and function of PPARγ in human cancer. Therefore, cell-culture studies are limited in representing the complex gene-gene and gene-environment molecular interactions that are implicated in cancer onset and progression.

Future perspectives

For many years PPARγ was referred to mainly as the master regulator of adipocyte function, and although its expression in the immune system was already described in early research, its actual role in these cells only became apparent later (figure 4). Nowadays the immunomodulatory role of PPARγ in several immune cells is well-established as described in this review. While PPARγ clearly functions in gene transactivation in both adipocytes and immune cells, gene repression by PPARγ has

been predominantly investigated in immune cells. PPARγ has also emerged as a factor involved in cancer onset and progression of several cancer types in recent years. Also in this case transactivation mechanisms are clearly relevant, underscored by both loss-of-function and gain-of-function mutations. It should be noted however that no single unifying role for PPARγ in human cancer emerges, and that transrepression has not always been studied specifically. Finally, gene fusions with other gene products (PAX8, CREB3L2) as reported in specific carcinoma presents a third way in which PPARγ regulates gene expression, resulting in either altered target gene sets and/or loss of activation.

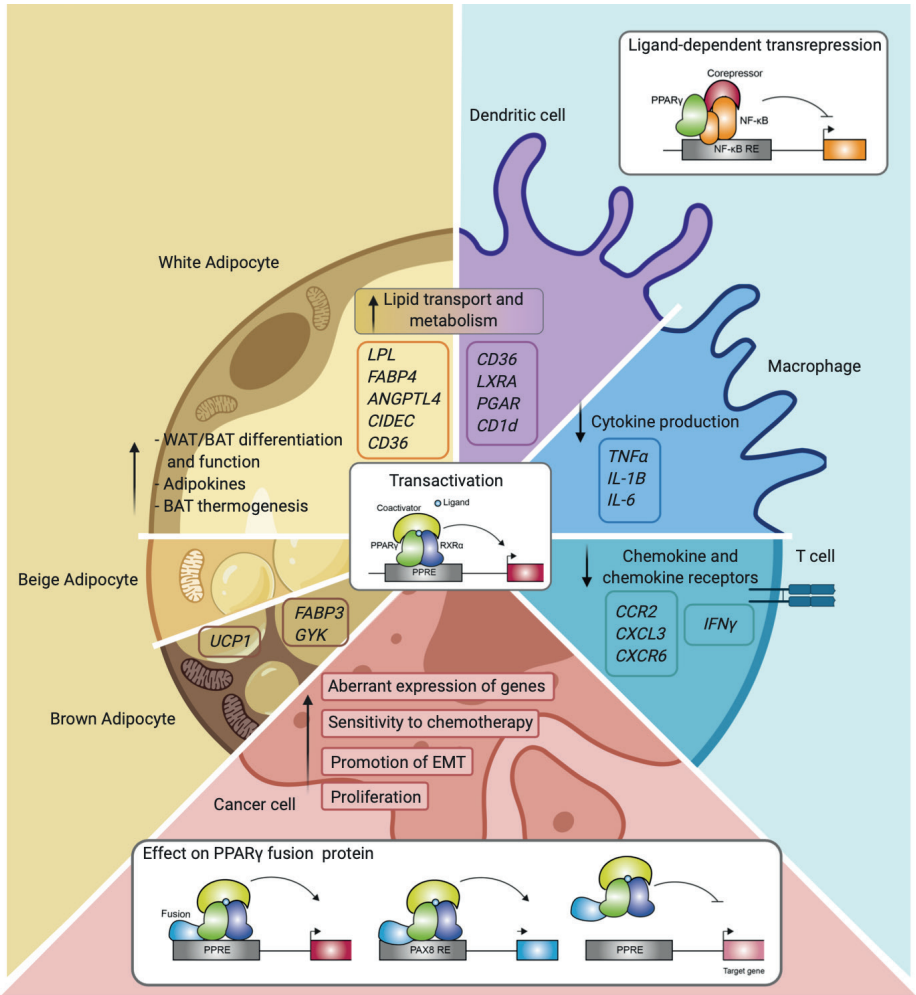

Figure 4. Overview of PPARγ function and mechanisms in the different cell types. Schematic representation of PPARγ in adipocytes (white, beige and brown adipocytes), immune cells (macrophages, dendritic cells and T-cells) and cancer cells. Indicated are different cellular processes and mechanisms of action in which PPARγ is involved.

It is well known that PPARγ is the molecular target for TZDs, these drugs have been widely used for the treatment of hyperglycemia and T2DM. TZDs stimulate the expression of genes implicated in lipid uptake and storage (153) and consequently the levels of ectopically stored and circulating lipids are decreased. In addition, TZDs also increase the expression of adiponectin, which contributes to enhance insulin sensitivity of the liver, and improves hepatic steatosis (153). Given its central role in adipocyte biology and energy homeostasis, there is a clear rationale behind therapeutically targeting PPARγ and improving insulin sensitivity. However, the use of TZDs is curtailed due to serious side-effects (review in (154)). Although some side-effects, such as troglitazone-associated hepatotoxicity and rosiglitazone-associated myocardial infarction have been solved (155), others are still present. These common side-effects include weight gain, fluid retention and osteoporosis. These unwanted side-effects are due to the ubiquitous expression of PPARγ1 in combination with the full agonism characteristics of TZDs. As indicated earlier, new generations of ligands, referred to as noncanonical agonist ligands (NALs) and selective PPARγ modulators (SPPARMs), hold promise in that respect. In fact, very recently is has been shown how selective modulators of PPARγ can improve liver histology without affecting body weight in biopsy-confirmed mouse model of nonalcoholic steatohepatitis (NASH) (156).

Similar to being a potential drug target in metabolism, PPARγ could represent a therapeutic target for a variety of cancers because of its ability to be selectively activated through its LBD. As indicated above, various parameters including tumour type and genetic background must be taken into account, as PPARγ displays oncogenic and tumour suppressor roles. Nonetheless, targeting PPARγ in the cancer context can be effective. In pancreatic ductal adenocarcinoma for example, the fourth most frequent cause in cancer-related deaths, PPARγ ligands have shown promising results *in vitro* and *in vivo* increasing apoptosis and reducing tumor growth respectively (157,158).

While we have described above that PPARγ is expressed in multiple cancer cell types, and PPARγ ligands can affect cancer cell function and behaviour (e.g. proliferartion, sensitivity to chemotherapy), some of the anti-cancer effects may actually occur indirectly through adipocytes surrounding the tumour or distal adipose tissue. PPARγ plays a crucial role in AT, and as it has been shown before, AT influences cancer initiation and progression through several mechanisms (159). Is estimated that obesity contributes to up to 20% of cancer-related deaths. Obesity is associated with increased risk of cancer development (ei: colorectal, post-menopausal breast and kidney among others) but the association with poor prognosis is even stronger for some of these cancer types. Obese AT is characterized by a chronic low-grade inflammation that leads to dysfunctional adipocytes, metabolic dysregulation and secretion of

pro-inflammatory cytokines are some of the factors that have been correlated with increased risk of cancer death. A clear example of this is the adipokine endotrophin (160), a cleavage product of the collagen VIa3 chain. Endotrophin has been shown to promote tumor growth by enhancing the ability of breast cancer cells to undergo epithelial to mesenchymal transition (EMT) in mice and humans (161). Interestingly, TZDs have been shown to decrease levels of endotrophin in obese patients (162).

A second exciting option to consider when considering the use of PPARγ ligands in cancer treatment is the role of the receptor in epithelial to mesenchymal transition (EMT). Epithelial cells that undergo EMT in the primary tumor acquire crucial features that increase their invasiveness, migratory phenotype and resistance to apoptosis that are essential for the development of metastasis (163). Transdifferentiation of breast cancer epithelial cells undergoing EMT into post-mitotic adipocytes cells using TZDs and MEK inhibitors have been shown to be a promising therapeutic approach to repress primary tumor invasion and metastasis formation (164). The ability of PPARγ to drive or inhibit EMT might be subjected to the specific cell type from which the tumor arises however, as for example different studies in lung cancer cells have shown PPARγ ligands to inhibit and promote EMT (165). More research is needed to study the implication of PPARγ in EMT to fully determine its role and if it can be a real cancer treatment option.

PPARγ plays a pivotal role in the crossroad between obesity, immunity and cancer. Understanding the common and unique molecular mechanism underlying the function of PPARγ in these situations will allow the development of new therapies. In order to do so, some challenges have to be overcome; achieving a selective modulation of PPARγ and a cell-specific delivery of these modulators are two of them. In order to maximize the beneficial effects of targeting PPARγ the key might be that PPARγ has to be targeted in one specific cell type, and not indiscriminately throughout the whole body. The use of nanoparticles coupled to biological ligands that binds to specific membrane receptors for drug delivery is a technique that is been study for cancer treatment and it could have a bright future in the nuclear receptor field if its proven successful. Given the different and complex roles of PPARγ in metabolism, immunity and cancer, which rely on overlapping and diverse mechsmisms of action, cell-specific delivery of PPARγ ligands, especially noncanonical agonist ligands (NALs) and selective PPARγ modulators (SPPARMs), represent a promising field of study for future research.

Acknowledgements

MHQ was funded by the European Training Networks Project (H2020-MSCA-ITN-308 2016 721532).

References

1. Tontonoz P, Hu E, Graves RA, Budavari AI, Spiegelman BM. mPPAR gamma 2: tissue-specific regulator of an adipocyte enhancer. Genes Dev. 1994 May;8(10):1224–34.
2. Greene ME, Blumberg B, McBride OW, Yi HF, Kronquist K, Kwan K, et al. Isolation of the human peroxisome proliferator activated receptor gamma cDNA: expression in hematopoietic cells and chromosomal mapping. Gene Expr. 1995;4(4–5):281–99.
3. Fajas L, Auboeuf D, Raspé E, Schoonjans K, Lefebvre A-M, Saladin R, et al. The Organization, Promoter Analysis, and Expression of the Human PPARγ Gene. J Biol Chem . 1997 Jul;272(30):18779–89.
4. Varley CL, Stahlschmidt J, Lee W-C, Holder J, Diggle C, Selby PJ, et al. Role of PPAR γ and EGFR signalling in the urothelial terminal differentiation programme. J Cell Sci. 2004 Apr;117(10):2029 LP – 2036.
5. Rochel N, Krucker C, Coutos-Thévenot L, Osz J, Zhang R, Guyon E, et al. Recurrent activating mutations of PPARγ associated with luminal bladder tumors. Nat Commun. 2019;10(1):253.
6. Cipolletta D, Feuerer M, Li A, Kamei N, Lee J, Shoelson SE, et al. PPAR-γ is a major driver of the accumulation and phenotype of adipose tissue Treg cells. Nature. 2012 Jun;486(7404):549–53.
7. Aprile M, Cataldi S, Ambrosio MR, D'Esposito V, Lim K, Dietrich A, et al. PPARγΔ5, a Naturally Occurring Dominant-Negative Splice Isoform, Impairs PPARγ Function and Adipocyte Differentiation. Cell Rep [Internet]. 2018 Nov;25(6):1577--1592.e6. Available from: https://doi.org/10.1016/j.celrep.2018.10.035
8. Rastinejad F, Huang P, Chandra V, Khorasanizadeh S. Understanding nuclear receptor form and function using structural biology. J Mol Endocrinol . 2013 Dec;51(3):T1–21.
9. Chandra V, Huang P, Hamuro Y, Raghuram S, Wang Y, Burris TP, et al. Structure of the intact PPAR-γ–RXR-α nuclear receptor complex on DNA. Nature. 2008 Oct;456:350.
10. Tontonoz P, Graves RA, Budavari AI, Erdjument-Bromage H, Lui M, Hu E, et al. Adipocyte-specific transcription factor ARF6 is a heterodimeric complex of two nuclear hormone receptors, PPARγ and RXRa. Nucleic Acids Res. 1994 Jan;22(25):5628–34.
11. Dreyer C, Krey G, Keller H, Givel F, Helftenbein G, Wahli W. Control of the peroxisomal β-oxidation pathway by a novel family of nuclear hormone receptors. Cell. 1992;68(5):879–87.
12. Lefterova MI, Haakonsson AK, Lazar MA, Mandrup S. PPARγ and the global map of adipogenesis and beyond. Trends Endocrinol Metab. 2014;25(6):293–302.
13. Nielsen R, Grøntved L, Stunnenberg HG, Mandrup S. Peroxisome proliferator-activated receptor subtype- and cell-type-specific activation of genomic target genes upon adenoviral transgene delivery. Mol Cell Biol. 2006 Aug;26(15):5698–714.
14. Nielsen R, Pedersen TAÅ, Hagenbeek D, Moulos P, Siersbaek R, Megens E, et al. Genome-wide profiling of PPARγ:RXR and RNA polymerase II occupancy reveals temporal activation of distinct metabolic pathways and changes in RXR dimer composition during adipogenesis. Genes Dev. 2008 Nov;22(21):2953–67.

15. Madsen MS, Siersbæk R, Boergesen M, Nielsen R, Mandrup S. Peroxisome Proliferator-Activated Receptor γ and C/EBPα Synergistically Activate Key Metabolic Adipocyte Genes by Assisted Loading. Mol Cell Biol. 2014 Mar;34(6):939–54.
16. Siersbaek MS, Loft A, Aagaard MM, Nielsen R, Schmidt SF, Petrovic N, et al. Genome-Wide Profiling of Peroxisome Proliferator-Activated Receptor γ in Primary Epididymal, Inguinal, and Brown Adipocytes Reveals Depot-Selective Binding Correlated with Gene Expression. Mol Cell Biol . 2012 Sep;32(17):3452–63.
17. Lefterova MI, Steger DJ, Zhuo D, Qatanani M, Mullican SE, Tuteja G, et al. Cell-Specific Determinants of Peroxisome Proliferator-Activated Receptor γ Function in Adipocytes and Macrophages Cell-Specific Determinants of Peroxisome Proliferator-Activated Receptor ∥ Function in Adipocytes and Macrophages §. Mol Cell Biol. 2010;30(9):2078–89.
18. Jeninga EH, Gurnell M, Kalkhoven E. Functional implications of genetic variation in human PPARγ. Trends Endocrinol Metab. 2009;20(8):380–7.
19. Welch JS, Ricote M, Akiyama TE, Gonzalez FJ, Glass CK. PPARγ and PPARδ negatively regulate specific subsets of lipopolysaccharide and IFN-γ target genes in macrophages. Proc Natl Acad Sci U S A. 2003;
20. Li B, Reynolds JM, Stout RD, Bernlohr DA, Suttles J. Regulation of Th17 Differentiation by Epidermal Fatty Acid-Binding Protein. J Immunol. 2009;
21. Wang LH, Yang XY, Zhang X, Huang J, Hou J, Li J, et al. Transcriptional Inactivation of STAT3 by PPARγ Suppresses IL-6-Responsive Multiple Myeloma Cells. Immunity. 2004;
22. Klotz L, Burgdorf S, Dani I, Saijo K, Flossdorf J, Hucke S, et al. The nuclear receptor PPARγ selectively inhibits Th17 differentiation in a T cell-intrinsic fashion and suppresses CNS autoimmunity. J Exp Med. 2009;
23. Ricote M, Glass CK. PPARs and molecular mechanisms of transrepression. Biochimica et Biophysica Acta - Molecular and Cell Biology of Lipids. 2007.
24. Chinenov Y, Gupte R, Rogatsky I. Nuclear receptors in inflammation control: repression by GR and beyond. Mol Cell Endocrinol. 2013 Nov;380(1–2):55–64.
25. Pascual G, Glass CK. Nuclear receptors versus inflammation: mechanisms of transrepression. Trends Endocrinol Metab [Internet]. 2006 Oct 1;17(8):321–7. Available from: https://doi.org/10.1016/j.tem.2006.08.005
26. Hollman DAA, Milona A, van Erpecum KJ, van Mil SWC. Anti-inflammatory and metabolic actions of FXR: Insights into molecular mechanisms. Biochim Biophys Acta - Mol Cell Biol Lipids [Internet]. 2012;1821(11):1443–52. Available from: http://www.sciencedirect.com/science/article/pii/S1388198112001382
27. Broekema MF, Savage DB, Monajemi H, Kalkhoven E. Gene-gene and gene-environment interactions in lipodystrophy: Lessons learned from natural PPARγ mutants. Biochim Biophys Acta - Mol Cell Biol Lipids. 2019;1864(5):715–32.
28. van Beekum O, Fleskens V, Kalkhoven E. Posttranslational modifications of PPAR-gamma: fine-tuning the metabolic master regulator. Obesity (Silver Spring). 2009 Mar;17(2):213–9.

29. Choi JH, Banks AS, Estall JL, Kajimura S, Bostrom P, Laznik D, et al. Anti-diabetic drugs inhibit obesity-linked phosphorylation of PPARgamma by Cdk5. Nature. 2010;466(7305):451–6.
30. Qiang L, Wang L, Kon N, Zhao W, Lee S, Zhang Y, et al. Brown Remodeling of White Adipose Tissue by SirT1-Dependent Deacetylation of Pparγ. Cell. 2012 Aug;150(3):620–32.
31. Mayoral R, Osborn O, McNelis J, Johnson AM, Oh DY, Izquierdo CL, et al. Adipocyte SIRT1 knockout promotes PPARγ activity, adipogenesis and insulin sensitivity in chronic-HFD and obesity. Mol Metab [Internet]. 2015;4(5):378–91. Available from: http://www.ncbi.nlm.nih.gov/pmc/articles/PMC4421024/
32. Nolte RT, Wisely GB, Westin S, Cobb JE, Lambert MH, Kurokawa R, et al. Ligand binding and co-activator assembly of the peroxisome proliferator-activated receptor-gamma. Nature. 1998;395(6698):137–43.
33. Kliewer SA, Sundseth SS, Jones SA, Brown PJ, Wisely GB, Koble CS, et al. Fatty acids and eicosanoids regulate gene expression through direct interactions with peroxisome proliferator-activated receptors α and γ. Proc Natl Acad Sci. 1997 Apr;94(9):4318 LP – 4323.
34. Forman BM, Tontonoz P, Chen J, Brun RP, Spiegelman BM, Evans RM. 15-Deoxy-Δ12,14-Prostaglandin J2 is a ligand for the adipocyte determination factor PPARγ. Cell. 1995;83(5):803–12.
35. Kliewer SA, Lenhard JM, Willson TM, Patel I, Morris DC, Lehmann JM. A prostaglandin J2 metabolite binds peroxisome proliferator-activated receptor γ and promotes adipocyte differentiation. Cell. 1995 Dec;83(5):813–9.
36. Nagy L, Tontonoz P, Alvarez JGA, Chen H, Evans RM. Oxidized LDL Regulates Macrophage Gene Expression through Ligand Activation of PPARγ. Cell. 1998;93(2):229–40.
37. Bell-Parikh LC, Ide T, Lawson JA, McNamara P, Reilly M, FitzGerald GA. Biosynthesis of 15-deoxy-Δ12,14-PGJ2 and the ligation of PPARγ. J Clin Invest. 2003 Sep;112(6):945–55.
38. Balint BL, Nagy L. Selective Modulators of PPAR Activity as New Therapeutic Tools in Metabolic Diseases. Vol. 6, Endocrine, Metabolic & Immune Disorders - Drug Targets. 2006. p. 33–43.
39. Lehmann JM, Moore LB, Smith-Oliver TA, Wilkison WO, Willson TM, Kliewer SA. An Antidiabetic Thiazolidinedione Is a High Affinity Ligand for Peroxisome Proliferator-activated Receptor γ (PPARγ). J Biol Chem [Internet]. 1995 Jun 2;270(22):12953–6. Available from: http://www.jbc.org/content/270/22/12953.abstract
40. Kelly IE, Han TS, Walsh K, Lean ME. Effects of a thiazolidinedione compound on body fat and fat distribution of patients with type 2 diabetes. Diabetes Care. 1999 Feb;22(2):288 LP – 293.
41. Nakamura T, Funahashi T, Yamashita S, Nishida M, Nishida Y, Takahashi M, et al. Thiazolidinedione derivative improves fat distribution and multiple risk factors in subjects with visceral fat accumulation—double-blind placebo-controlled trial. Diabetes Res Clin Pract. 2001;54(3):181–90.
42. Akazawa S, Sun F, Ito M, Kawasaki E, Eguchi K. Efficacy of troglitazone on body fat distribution in type 2 diabetes. Diabetes Care. 2000 Aug;23(8):1067 LP – 1071.
43. Kroker AJ, Bruning JB. Review of the Structural and Dynamic Mechanisms of PPARγ Partial Agonism. PPAR Res. 2015 Sep;2015:816856.

44. Kojetin DJ, Burris TP. Small Molecule Modulation of Nuclear Receptor Conformational Dynamics: Implications for Function and Drug Discovery. Mol Pharmacol. 2013 Jan;83(1):1 LP – 8.
45. Li P, Fan W, Xu J, Lu M, Yamamoto H, Auwerx J, et al. Adipocyte NCoR Knockout Decreases PPARγ Phosphorylation and Enhances PPARγ Activity and Insulin Sensitivity. Cell. 2011;147(4):815–26.
46. Acton JJ, Black RM, Jones AB, Moller DE, Colwell L, Doebber TW, et al. Benzoyl 2-methyl indoles as selective PPARγ modulators. Bioorg Med Chem Lett. 2005;15(2):357–62.
47. Choi JH, Banks AS, Estall JL, Kajimura S, Bostrom P, Laznik D, et al. Anti-diabetic drugs inhibit obesity-linked phosphorylation of PPARgamma by Cdk5. Nature [Internet]. 2010;466(7305):451–6. Available from: http://www.ncbi.nlm.nih.gov/pubmed/20651683
48. Choi JH, Banks AS, Kamenecka TM, Busby SA, Chalmers MJ, Kumar N, et al. Antidiabetic actions of a non-agonist PPARγ ligand blocking Cdk5-mediated phosphorylation. Nature. 2011 Sep;477:477.
49. Hughes TS, Giri PK, de Vera IMS, Marciano DP, Kuruvilla DS, Shin Y, et al. An alternate binding site for PPARγ ligands. Nat Commun. 2014 Apr;5:3571.
50. Rosen ED, Spiegelman BM. What we talk about when we talk about fat. Cell. 2014;156(1–2):20–44.
51. Morroni M, Giordano A, Zingaretti MC, Boiani R, De Matteis R, Kahn BB, et al. Reversible transdifferentiation of secretory epithelial cells into adipocytes in the mammary gland. Proc Natl Acad Sci U S A. 2004 Nov;101(48):16801 LP – 16806.
52. Cinti S. Pink Adipocytes. Trends Endocrinol Metab. 2018;29(9):651–66.
53. Hausman DB, DiGirolamo M, Bartness TJ, Hausman GJ, Martin RJ. The biology of white adipocyte proliferation. Obes Rev. 2001 Nov;2(4):239–54.
54. Cedikova M, Kripnerová M, Dvorakova J, Pitule P, Grundmanova M, Babuska V, et al. Mitochondria in White, Brown, and Beige Adipocytes. Stem Cells Int. 2016/03/17. 2016;2016:6067349.
55. Sanchez-Gurmaches J, Guertin DA. Adipocytes arise from multiple lineages that are heterogeneously and dynamically distributed. Nat Commun. 2014 Jun;5:4099.
56. Rosen ED, Hsu C-H, Wang X, Sakai S, Freeman MW, Gonzalez FJ, et al. C/EBPα induces adipogenesis through PPARγ: a unified pathway. Genes Dev . 2002 Jan;16(1):22–6.
57. Barroso I, Gurnell M, Crowley VEF, Agostini M, Schwabe JW, Soos MA, et al. Dominant negative mutations in human PPAR gamma associated with severe insulin resistance, diabetes mellitus and hypertension. Nature. 1999;402(December):880–3.
58. Jeninga EH, van Beekum O, van Dijk ADJ, Hamers N, Hendriks-Stegeman BI, Bonvin AMJJ, et al. Impaired peroxisome proliferator-activated receptor gamma function through mutation of a conserved salt bridge (R425C) in familial partial lipodystrophy. Mol Endocrinol [Internet]. 2007;21(5):1049–65. Available from: http://www.ncbi.nlm.nih.gov/pubmed/17312272
59. Enerbäck S. Human Brown Adipose Tissue. Cell Metab. 2010;11(4):248–52.
60. Enerback S. Brown adipose tissue in humans. Int J Obes. 2010;34:S43–6.
61. Enerbäck S. Human Brown Adipose Tissue. Cell Metab [Internet]. 2010;11(4):248–52. Available from: http://www.sciencedirect.com/science/article/pii/S1550413110000781
62. van Marken Lichtenbelt WD, Vanhommerig JW, Smulders NM, Drossaerts JMAFL, Kemerink GJ, Bouvy ND, et al. Cold-Activated Brown Adipose Tissue in Healthy Men. N Engl J Med. 2009 Apr;360(15):1500–8.

63. Virtanen KA, Lidell ME, Orava J, Heglind M, Westergren R, Niemi T, et al. Functional Brown Adipose Tissue in Healthy Adults. N Engl J Med. 2009 Apr;360(15):1518–25.
64. Cypess AM, Lehman S, Williams G, Tal I, Rodman D, Goldfine AB, et al. Identification and Importance of Brown Adipose Tissue in Adult Humans. N Engl J Med. 2009 Apr;360(15):1509–17.
65. van Marken Lichtenbelt WD, Schrauwen P. Implications of nonshivering thermogenesis for energy balance regulation in humans. Am J Physiol Integr Comp Physiol. 2011 Apr;301(2):R285–96.
66. Li Z, de Jonge WJ, Wang Y, Rensen PCN, Kooijman S. Electrical Neurostimulation Promotes Brown Adipose Tissue Thermogenesis. Front Endocrinol (Lausanne). 2020;11:567545.
67. Nedergaard J, Petrovic N, Lindgren EM, Jacobsson A, Cannon B. PPARγ in the control of brown adipocyte differentiation. In: Biochimica et Biophysica Acta - Molecular Basis of Disease. 2005.
68. Lasar D, Rosenwald M, Kiehlmann E, Balaz M, Tall B, Opitz L, et al. Peroxisome Proliferator Activated Receptor Gamma Controls Mature Brown Adipocyte Inducibility through Glycerol Kinase. Cell Rep. 2018;
69. Thurlby PL, Wilson S, Arch JRS. Ciglitazone is not itself thermogenic but increases the potential for thermogenesis in lean mice. Biosci Rep. 1987;
70. Mercer SW, Trayhurn P. Effects of ciglitazone on insulin resistance and thermogenic responsiveness to acute cold in brown adipose tissue of genetically obese (ob/ob) mice. FEBS Lett. 1986;
71. Tai TAC, Jennermann C, Brown KK, Oliver BB, MacGinnitie MA, Wilkison WO, et al. Activation of the nuclear receptor peroxisome proliferator-activated receptor γ promotes brown adipocyte differentiation. J Biol Chem. 1996;
72. Rosen ED, Walkey CJ, Puigserver P, Spiegelman BM. Transcriptional regulation of adipogenesis. Genes and Development. 2000.
73. Mayoral R, Osborn O, McNelis J, Johnson AM, Oh DY, Izquierdo CL, et al. Adipocyte SIRT1 knockout promotes PPARγ activity, adipogenesis and insulin sensitivity in chronic-HFD and obesity. Mol Metab. 2015;
74. Seale P, Kajimura S, Yang W, Chin S, Rohas LM, Uldry M, et al. Transcriptional Control of Brown Fat Determination by PRDM16. Cell Metab. 2007;
75. Koppen A, Kalkhoven E. Brown vs white adipocytes: The PPARγ coregulator story. FEBS Letters. 2010.
76. Koppen A, Kalkhoven E. Brown vs white adipocytes: The PPAR?? coregulator story. FEBS Lett. 2010;584(15):3250–9.
77. Wu J, Boström P, Sparks LM, Ye L, Choi JH, Giang A-H, et al. Beige Adipocytes Are a Distinct Type of Thermogenic Fat Cell in Mouse and Human. Cell. 2012 Jul;150(2):366–76.
78. Ikeda K, Maretich P, Kajimura S. The Common and Distinct Features of Brown and Beige Adipocytes. Trends Endocrinol Metab. 2018;29(3):191–200.
79. Giralt M, Villarroya F. White, Brown, Beige/Brite: Different Adipose Cells for Different Functions? Endocrinology. 2013 Sep;154(9):2992–3000.
80. Ohno H, Shinoda K, Spiegelman BM, Kajimura S. PPARγ agonists induce a white-to-brown fat conversion through stabilization of PRDM16 protein. Cell Metab [Internet]. 2012;15(3):395–404. Available from: http://dx.doi.org/10.1016/j.cmet.2012.01.019

81. Tontonoz P, Spiegelman BM. Fat and beyond: The diverse biology of PPARγ. Annual Review of Biochemistry. 2008.
82. Kliewer SA, Forman BM, Blumberg B, Ong ES, Borgmeyer U, Mangelsdorf DJ, et al. Differential expression and activation of a family of murine peroxisome proliferator-activated receptors. Proc Natl Acad Sci U S A. 1994;
83. Széles L, Töröcsik D, Nagy L. PPARγ in immunity and inflammation: cell types and diseases. Biochimica et Biophysica Acta - Molecular and Cell Biology of Lipids. 2007.
84. Choi JM, Bothwell ALM. The nuclear receptor PPARs as important regulators of T-cell functions and autoimmune diseases. Molecules and Cells. 2012.
85. Le Menn G, Neels JG. Regulation of immune cell function by PPARs and the connection with metabolic and neurodegenerative diseases. International Journal of Molecular Sciences. 2018.
86. Lefterova MI, Steger DJ, Zhuo D, Qatanani M, Mullican SE, Tuteja G, et al. Cell-Specific Determinants of Peroxisome Proliferator-Activated Receptor γ Function in Adipocytes and Macrophages. Mol Cell Biol. 2010;
87. Szanto A, Balint BL, Nagy ZS, Barta E, Dezso B, Pap A, et al. STAT6 transcription factor is a facilitator of the nuclear receptor PPARγ-regulated gene expression in macrophages and dendritic cells. Immunity. 2010;
88. Ricote M, Huang J, Fajas L, Li A, Welch J, Najib J, et al. Expression of the peroxisome proliferator-activated receptor γ (PPARγ) in human atherosclerosis and regulation in macrophages by colony stimulating factors and oxidized low density lipoprotein. Proc Natl Acad Sci U S A. 1998;
89. Moore KJ, Rosen ED, Fitzgerald ML, Randow F, Andersson LP, Altshuler D, et al. The role of PPAR-γ in macrophage differentiation and cholesterol uptake. Nat Med. 2001;
90. Tontonoz P, Nagy L, JG A, VA T, RM E. PPAR gamma promotes monocyte/macrophage differentiation and uptake of oxidized LDL. PPARg promotes monocyte/macrophage differentiation and uptake of oxidized LDL. 2002.
91. Chawla A, Barak Y, Nagy L, Liao D, Tontonoz P, Evans RM. PPAR-γ dependent and independent effects on macrophage-gene expression in lipid metabolism and inflammation. Nat Med. 2001;
92. Schneider C, Nobs SP, Kurrer M, Rehrauer H, Thiele C, Kopf M. Induction of the nuclear receptor PPAR-γ 3 by the cytokine GM-CSF is critical for the differentiation of fetal monocytes into alveolar macrophages. Nat Immunol. 2014;
93. Gosset P, Charbonnier AS, Delerive P, Fontaine J, Staels B, Pestel J, et al. Peroxisome proliferator-activated receptor γ activators affect the maturation of human monocyte-derived dendritic cells. Eur J Immunol. 2001;
94. Le Naour F, Hohenkirk L, Grolleau A, Misek DE, Lescure P, Geiger JD, et al. Profiling Changes in Gene Expression during Differentiation and Maturation of Monocyte-derived Dendritic Cells Using Both Oligonucleotide Microarrays and Proteomics. J Biol Chem. 2001;
95. Bouhlel MA, Derudas B, Rigamonti E, Dièvart R, Brozek J, Haulon S, et al. PPARγ Activation Primes Human Monocytes into Alternative M2 Macrophages with Anti-inflammatory Properties. Cell Metab. 2007;

96. Odegaard JI, Ricardo-Gonzalez RR, Goforth MH, Morel CR, Subramanian V, Mukundan L, et al. Macrophage-specific PPARγ controls alternative activation and improves insulin resistance. Nature. 2007;
97. Jiang C, Ting AT, Seed B. PPAR-γ agonists inhibit production of monocyte inflammatory cytokines. Nature. 1998;
98. Gallardo-Soler A, Gómez-Nieto C, Campo ML, Marathe C, Tontonoz P, Castrillo A, et al. Arginase I induction by modified lipoproteins in macrophages: A peroxisome proliferator-activated receptor-γ/δ-mediated effect that links lipid metabolism and immunity. Mol Endocrinol. 2008;
99. Huang JT, Welch JS, Ricote M, Binder CJ, Willson TM, Kelly C, et al. Interleukin-4-dependent production of PPAR-γ ligands in macrophages by 12/15-lipoxygenase. Nature. 1999;
100. Daniel B, Nagy G, Czimmerer Z, Horvath A, Hammers DW, Cuaranta-Monroy I, et al. The Nuclear Receptor PPARγ Controls Progressive Macrophage Polarization as a Ligand-Insensitive Epigenomic Ratchet of Transcriptional Memory. Immunity. 2018;
101. Nagy L, Tontonoz P, Alvarez JGA, Chen H, Evans RM. Oxidized LDL regulates macrophage gene expression through ligand activation of PPARγ. Cell. 1998;
102. Chawla A, Boisvert WA, Lee CH, Laffitte BA, Barak Y, Joseph SB, et al. A PPARγ-LXR-ABCA1 pathway in macrophages is involved in cholesterol efflux and atherogenesis. Mol Cell. 2001;
103. Chinetti G, Lestavel S, Bocher V, Remaley AT, Neve B, Torra IP, et al. PPAR-α and PPAR-γ activators induce cholesterol removal from human macrophage foam cells through stimulation of the ABCA1 pathway. Nat Med. 2001;
104. Albert ML, Pearce SFA, Francisco LM, Sauter B, Roy P, Silverstein RL, et al. Immature dendritic cells phagocytose apoptotic cells via αvβ5 and CD36, and cross-present antigens to cytotoxic T lymphocytes. J Exp Med. 1998;
105. Szatmari I, Gogolak P, Im JS, Dezso B, Rajnavolgyi E, Nagy L. Activation of PPARγ specifies a dendritic cell subtype capable of enhanced induction of iNKT cell expansion. Immunity. 2004;
106. Szatmari I, Töröcsik D, Agostini M, Nagy T, Gurnell M, Barta E, et al. PPARγ regulates the function of human dendritic cells primarily by altering lipid metabolism. Blood. 2007;
107. Nencioni A, Grünebach F, Zobywlaski A, Denzlinger C, Brugger W, Brossart P. Dendritic Cell Immunogenicity Is Regulated by Peroxisome Proliferator-Activated Receptor γ. J Immunol. 2002;
108. Szatmari I, Pap A, Rühl R, Ma JX, Illarionov PA, Besra GS, et al. PPARγ controls CD1d expression by turning on retinoic acid synthesis in developing human dendritic cells. J Exp Med. 2006;
109. Cuaranta-Monroy I, Kiss M, Simandi Z, Nagy L. Genomewide effects of peroxisome proliferator-activated receptor gamma in macrophages and dendritic cells - Revealing complexity through systems biology. Eur J Clin Invest. 2015;
110. Cipolletta D, Feuerer M, Li A, Kamei N, Lee J, Shoelson SE, et al. PPAR-γ is a major driver of the accumulation and phenotype of adipose tissue T reg cells. Nature. 2012;
111. Angeli V, Hammad H, Staels B, Capron M, Lambrecht BN, Trottein F. Peroxisome Proliferator-Activated Receptor γ Inhibits the Migration of Dendritic Cells: Consequences for the Immune Response. J Immunol. 2003;

112. Park B V., Pan F. The role of nuclear receptors in regulation of Th17/Treg biology and its implications for diseases. Cellular and Molecular Immunology. 2015.
113. Yang XY, Wang LH, Chen T, Hodge DR, Resau JH, DaSilva L, et al. Activation of human T lymphocytes is inhibited by peroxisome proliferator-activated receptor γ (PPARγ) agonists. PPARγ co-association with transcription factor NFAT. J Biol Chem. 2000;
114. Clark RB, Bishop-Bailey D, Estrada-Hernandez T, Hla T, Puddington L, Padula SJ. The Nuclear Receptor PPARγ and Immunoregulation: PPARγ Mediates Inhibition of Helper T Cell Responses. J Immunol. 2000;
115. Hontecillas R, Bassaganya-Riera J. Peroxisome Proliferator-Activated Receptor γ Is Required for Regulatory CD4 + T Cell-Mediated Protection against Colitis . J Immunol. 2007;
116. Nobs SP, Natali S, Pohlmeier L, Okreglicka K, Schneider C, Kurrer M, et al. PPARγ in dendritic cells and T cells drives pathogenic type-2 effector responses in lung inflammation. J Exp Med. 2017;
117. Cunard R, Eto Y, Muljadi JT, Glass CK, Kelly CJ, Ricote M. Repression of IFN-γ Expression by Peroxisome Proliferator-Activated Receptor γ. J Immunol. 2004;
118. Chung SW, Kang BY, Kim TS. Inhibition of Interleukin-4 Production in CD4+ T Cells by Peroxisome Proliferator-Activated Receptor-γ (PPAR-γ) Ligands: Involvement of Physical Association between PPAR-γ and the Nuclear Factor of Activated T Cells Transcription Factor. Mol Pharmacol. 2003;
119. Sarraf P, Mueller E, Jones D, King FJ, DeAngelo DJ, Partridge JB, et al. Differentiation and reversal of malignant changes in colon cancer through PPARγ. Nat Med. 1998;4(9):1046–52.
120. Tsubouchi Y, Sano H, Kawahito Y, Mukai S, Yamada R, Kohno M, et al. Inhibition of human lung cancer cell growth by the peroxisome proliferator-activated receptor-gamma agonists through induction of apoptosis. Biochem Biophys Res Commun. 2000 Apr;270(2):400—405.
121. Bren-Mattison Y, Van Putten V, Chan D, Winn R, Geraci MW, Nemenoff RA. Peroxisome proliferator-activated receptor-gamma (PPAR(gamma)) inhibits tumorigenesis by reversing the undifferentiated phenotype of metastatic non-small-cell lung cancer cells (NSCLC). Oncogene. 2005;24(8):1412—1422.
122. Motomura W, Okumura T, Takahashi N, Obara T, Kohgo Y. Activation of peroxisome proliferator-activated receptor gamma by troglitazone inhibits cell growth through the increase of p27KiP1 in human. Pancreatic carcinoma cells. Cancer Res. 2000 Oct;60(19):5558–64.
123. Kubota T, Koshizuka K, Williamson EA, Asou H, Said JW, Holden S, et al. Ligand for Peroxisome Proliferator-activated Receptor γ (Troglitazone) Has Potent Antitumor Effect against Human Prostate Cancer Both in Vitro and in Vivo Cancer Res. 1998 Aug;58(15):3344 LP – 3352.
124. Bonofiglio D, Cione E, Qi H, Pingitore A, Perri M, Catalano S, et al. Combined low doses of PPARgamma and RXR ligands trigger an intrinsic apoptotic pathway in human breast cancer cells. Am J Pathol. 2009/07/30. 2009 Sep;175(3):1270–80.
125. Mueller E, Sarraf P, Tontonoz P, Evans RM, Martin KJ, Zhang M, et al. Terminal Differentiation of Human Breast Cancer through PPARγ. Mol Cell. 1998;1(3):465–70.
126. Girnun GD, Naseri E, Vafai SB, Qu L, Szwaya JD, Bronson R, et al. Synergy between PPARγ Ligands and Platinum-Based Drugs in Cancer. Cancer Cell. 2007;

127. Park J, Morley TS, Scherer PE. Inhibition of endotrophin, a cleavage product of collagen VI, confers cisplatin sensitivity to tumours. EMBO Mol Med. 2013;
128. Khandekar MJ, Banks AS, Laznik-Bogoslavski D, White JP, Choi JH, Kazak L, et al. Noncanonical agonist PPARγ ligands modulate the response to DNA damage and sensitize cancer cells to cytotoxic chemotherapy. Proc Natl Acad Sci U S A. 2018;
129. Phan ANH, Vo VTA, Hua TNM, Kim MK, Jo SY, Choi JW, et al. PPARγ sumoylation-mediated lipid accumulation in lung cancer. Oncotarget. 2017;
130. Hanahan D, Weinberg RA. Hallmarks of cancer: The next generation. Cell. 2011.
131. Saez E, Tontonoz P, Nelson MC, Alvarez JGA, U TM, Baird SM, et al. Activators of the nuclear receptor PPARγ enhance colon polyp formation . Nat Med. 1998;4(9):1058–61.
132. Lefebvre AM, Chen I, Desreumaux P, Najib J, Fruchart JC, Geboes K, et al. Activation of the peroxisome proliferator-activated receptor gamma promotes the development of colon tumors in C57BL/6J-APCMin/+ mice. Nat Med. 1998 Sep;4(9):1053—1057.
133. Broekema MF, Massink MPG, Donato C, de Ligt J, Schaarschmidt J, Borgman A, et al. Natural helix 9 mutants of PPARγ differently affect its transcriptional activity. Mol Metab. 2018;
134. Sarraf P, Mueller E, Smith WM, Wright HM, Kum JB, Aaltonen L a, et al. Loss-of-function mutations in PPAR gamma associated with human colon cancer. Mol Cell. 1999;3:799–804.
135. Gupta RA, Sarraf P, Mueller E, Brockman JA, Prusakiewicz JJ, Eng C, et al. Peroxisome proliferator-activated receptor γ-mediated differentiation: A mutation in colon cancer cells reveals divergent and cell type-specific mechanisms. J Biol Chem. 2003;278(25):22669–77.
136. Coutos-Thévenot L, Beji S, Neyret-Kahn H, Pippo Q, Fontugne J, Osz J, et al. PPARγ is a tumor suppressor in basal bladder tumors offering new potential therapeutic opportunities. bioRxiv. 2019 Jan;868190.
137. Rebouissou S, Bernard-Pierrot I, de Reyniès A, Lepage M-L, Krucker C, Chapeaublanc E, et al. EGFR as a potential therapeutic target for a subset of muscle-invasive bladder cancers presenting a basal-like phenotype. Sci Transl Med. 2014 Jul;6(244):244ra91 LP-244ra91.
138. Choi W, Porten S, Kim S, Willis D, Plimack ER, Hoffman-Censits J, et al. Identification of distinct basal and luminal subtypes of muscle-invasive bladder cancer with different sensitivities to frontline chemotherapy. Cancer Cell. 2014 Feb;25(2):152–65.
139. Biton A, Bernard-Pierrot I, Lou Y, Krucker C, Chapeaublanc E, Rubio-Pérez C, et al. Independent Component Analysis Uncovers the Landscape of the Bladder Tumor Transcriptome and Reveals Insights into Luminal and Basal Subtypes. Cell Rep. 2014 Nov;9(4):1235–45.
140. Biton A, Bernard-Pierrot I, Lou Y, Krucker C, Chapeaublanc E, Rubio-Pérez C, et al. Independent Component Analysis Uncovers the Landscape of the Bladder Tumor Transcriptome and Reveals Insights into Luminal and Basal Subtypes. Cell Rep [Internet]. 2014 Nov 20;9(4):1235–45. Available from: https://doi.org/10.1016/j.celrep.2014.10.035
141. Halstead AM, Kapadia CD, Bolzenius J, Chu CE, Schriefer A, Wartman LD, et al. Bladder-cancer-associated mutations in RXRA activate peroxisome proliferator-activated receptors to drive urothelial proliferation. Levine RL, editor. Elife. 2017;6:e30862.

142. Weinstein JN, Akbani R, Broom BM, Wang W, Verhaak RGW, McConkey D, et al. Comprehensive molecular characterization of urothelial bladder carcinoma. Nature. 2014;507(7492):315–22.
143. Kroll TG, Sarraf P, Pecciarini L, Chen C-J, Mueller E, Spiegelman BM, et al. Detection of the PAX8-PPAR gamma fusion oncogene in both follicular thyroid carcinomas and adenomas. Science (80-). 2000 Aug;289(5483):1357 LP – 1360.
144. Cheung L, Messina M, Gill A, Clarkson A, Learoyd D, Delbridge L, et al. Detection of the PAX8-PPARγ Fusion Oncogene in Both Follicular Thyroid Carcinomas and Adenomas. J Clin Endocrinol Metab. 2003 Jan;88(1):354–7.
145. Pasca di Magliano M, Di Lauro R, Zannini M. Pax8 has a key role in thyroid cell differentiation. Proc Natl Acad Sci [Internet]. 2000 Nov 21;97(24):13144 LP – 13149. Available from: http://www.pnas.org/content/97/24/13144.abstract
146. Macchia PE, Lapi P, Krude H, Pirro MT, Missero C, Chiovato L, et al. PAX8 mutations associated with congenital hypothyroidism caused by thyroid dysgenesis. Nat Genet. 1998;19(1):83–6.
147. Pasca di Magliano M, Di Lauro R, Zannini M. Pax8 has a key role in thyroid cell differentiation. Proc Natl Acad Sci. 2000 Nov;97(24):13144 LP – 13149.
148. Karger S, Berger K, Eszlinger M, Tannapfel A, Dralle H, Paschke R, et al. Evaluation of Peroxisome Proliferator-Activated Receptor-γ Expression in Benign and Malignant Thyroid Pathologies. Thyroid. 2005 Sep;15(9):997–1003.
149. Raman P, Koenig RJ. Pax-8–PPAR-γ fusion protein in thyroid carcinoma. Nat Rev Endocrinol. 2014;10(10):616–23.
150. Zhang Y, Yu J, Grachtchouk V, Qin T, Lumeng C, Sartor M, et al. Genomic binding of PAX8-PPARG fusion protein regulates cancer-related pathways and alters the immune landscape of thyroid cancer. Oncotarget. 2017 Apr;5(0):5761–73.
151. Boos LA, Dettmer M, Schmitt A, Rudolph T, Steinert H, Moch H, et al. Diagnostic and prognostic implications of the PAX8–PPARγ translocation in thyroid carcinomas—a TMA-based study of 226 cases. Histopathology. 2013 Aug;63(2):234–41.
152. Lui W-O, Zeng L, Rehrmann V, Deshpande S, Tretiakova M, Kaplan EL, et al. CREB3L2-PPARγ Fusion Mutation Identifies a Thyroid Signaling Pathway Regulated by Intramembrane Proteolysis. Cancer Res. 2008 Sep;68(17):7156 LP – 7164.
153. Yki-Järvinen H. Thiazolidinediones. N Engl J Med [Internet]. 2004 Sep;351(11):1106–18. Available from: https://doi.org/10.1056/NEJMra041001
154. Soccio RE, Chen ER, Lazar MA. Thiazolidinediones and the promise of insulin sensitization in type 2 diabetes. Cell Metab [Internet]. 2014;20(4):573–91. Available from: http://dx.doi.org/10.1016/j.cmet.2014.08.005
155. FDA Drug Safety Communication: FDA eliminates the Risk Evaluation and Mitigation Strategy (REMS) for rosiglitazone-containing diabetes medicines [Internet]. [cited 2019 Jun 10]. Available from: https://www.fda.gov/drugs/drug-safety-and-availability/fda-drug-safety-communication-fda-eliminates-risk-evaluation-and-mitigation-strategy-rems

156. Perakakis N, Joshi A, Peradze N, Stefanakis K, Li G, Feigh M, et al. The Selective Peroxisome Proliferator-Activated Receptor Gamma Modulator CHS-131 Improves Liver Histopathology and Metabolism in a Mouse Model of Obesity and Nonalcoholic Steatohepatitis. Hepatol Commun. 2020;
157. Ninomiya I, Yamazaki K, Oyama K, Hayashi H, Tajima H, Kitagawa H, et al. Pioglitazone inhibits the proliferation and metastasis of human pancreatic cancer cells. Oncol Lett. 2014;
158. Ceni E, Mello T, Tarocchi M, Crabb DW, Caldini A, Invernizzi P, et al. Antidiabetic thiazolidinediones induce ductal differentiation but not apoptosis in pancreatic cancer cells. World J Gastroenterol. 2005;
159. Quail DF, Dannenberg AJ. The obese adipose tissue microenvironment in cancer development and progression. Nature Reviews Endocrinology. 2019.
160. Bu D, Crewe C, Kusminski CM, Gordillo R, Ghaben AL, Kim M, et al. Human endotrophin as a driver of malignant tumor growth. JCI Insight. 2019;
161. Park J, Scherer PE. Adipocyte-derived endotrophin promotes malignant tumor progression. J Clin Invest. 2012;
162. Sun K, Park J, Kim M, Scherer PE. Endotrophin, a multifaceted player in metabolic dysregulation and cancer progression, is a predictive biomarker for the response to PPARγ agonist treatment. Diabetologia. 2017.
163. Dongre A, Weinberg RA. New insights into the mechanisms of epithelial–mesenchymal transition and implications for cancer. Nature Reviews Molecular Cell Biology. 2019.
164. Ishay-Ronen D, Diepenbruck M, Kalathur RKR, Sugiyama N, Tiede S, Ivanek R, et al. Gain Fat—Lose Metastasis: Converting Invasive Breast Cancer Cells into Adipocytes Inhibits Cancer Metastasis. Cancer Cell. 2019;
165. Reka AK, Kurapati H, Narala VR, Bommer G, Chen J, Standiford TJ, et al. Peroxisome proliferator-activated receptor-g activation inhibits tumor metastasis by antagonizing smad3-mediated epithelial-mesenchymal transition. Mol Cancer Ther. 2010;

Chapter 3

Comprehensive profiling of mammalian Tribbles interactomes implicates TRIB3 in gene repression

Miguel Hernández-Quiles[1], Rosalie Baak[1], Anouska Borgman[1], Suzanne den Haan[1], Paula Sobrevals Alcaraz[3], Robert van Es[3], Endre Kiss-Toth[2], Harmjan Vos[3], Eric Kalkhoven[1, 4, *]

[1] Center for Molecular Medicine, University Medical Center Utrecht, Utrecht University, Utrecht the Netherlands.

[2] Department of Infection, Immunity and Cardiovascular Disease, Medical School, University of Sheffield, Sheffield, United Kingdom.

[3] Oncode Institute and Molecular Cancer Research, Center for Molecular Medicine, University Medical Center, Utrecht, The Nederlands.

[4] A list of members and affiliations appears in the Supplementary Note.

[*] Correspondence: e.kalkhoven@umcutrecht.nl; Tel: +31-88-7554258.

Simple Summary: Tribbles proteins play various roles in cancer initiation and progression. However, still little is known about their molecular actions. Here we developed a Mass Spectrometry based approach to study the Tribbles interactomes, allowing us to discover new interactors and functions that might help to understand their behavior better. Our proteomics data highlight the ability of TRIB3 to interact with transcription regulatory proteins and point to a new role in gene repression. Systematic analyses like these will help to evaluate the potential of Tribbles proteins as biomarkers for disease diagnosis and prognosis.

Abstract: The 3 human Tribbles (TRIB) pseudokinases have been implicated in a plethora of signaling and metabolic processes linked to cancer initiation and progression and can potentially be used as biomarkers of disease and prognosis. While their modes of action reported so far center around protein-protein interactions, comprehensive profiling of TRIB interactomes has not been reported yet. Here we developed a robust mass spectrometry (MS)-based proteomics approach to characterize Tribbles interactomes and report a comprehensive assessment and comparison of TRIB1, -2 and -3 interactomes as well as domain-specific interactions for TRIB3. Interestingly, TRIB3, which is predominantly localized in the nucleus, interacts with multiple transcriptional regulators, including proteins involved in gene repression. Indeed, we found that TRIB3 repressed gene transcription when tethered to DNA in breast cancer cells. Taken together, our comprehensive proteomic assessment reveals previously unknown interacting partners and functions of Tribbles proteins that expand our understanding of this family of proteins. In addition, our findings show that MS-based proteomics provides a powerful tool to unravel novel pseudokinase biology.

Keywords: Keywords: Tribbles; Proteomics; Interactome; Breast cancer

1. INTRODUCTION

Kinases regulate a plethora of cellular processes and changes in their enzymatic activity are intimately linked to human diseases, hence the large research field studying the basic biology of kinases and their potential as therapeutic targets [1,2]. In addition to the 518 kinases, the human genome also encodes ~60 pseudokinases, proteins that resemble serine/threonine and tyrosine protein kinases but lack several amino acids critical for enzymatic activity [3,4]. The human pseudokinase family includes the three members of the Tribbles (TRIB) family - TRIB1, TRIB2 and TRIB3- that share a high degree of homology as well as a similar domain composition [5,6]. They can be divided into three major domains: an N-terminal domain associated with protein stability and subcellular localization [7,8], a well-conserved centrally located pseudokinase domain and a C-terminal domain where the binding motifs of MAPK and COP1 are found [9,10]. A fourth, more distally related protein called STK40 shares important similarities in terms of function and structure [11,12].

Tribbles proteins have been implicated in multiple critical signaling and metabolic processes and alterations in their expression and/or activity is linked to various human diseases [13]. While lacking intrinsic enzymatic activity, Tribbles proteins exert their biological roles predominantly via binding to other proteins, including kinases, phosphatases, transcription factors and components of the ubiquitin-proteosome system [14–16]. This diverse range of interactors explains at least in part the difficulties to associate a TRIB family member with a single specific cellular pathway or role. In addition, it should be noted that different and even contradictory observations have been made regarding the subcellular localization of Tribbles proteins, suggesting their localization and thereby function depends on cellular context and conditions [17,18]

In recent years many studies have pointed to Tribbles proteins as important modulators of cancer initiation and progression [19–22]. Therefore, Tribbles proteins hold potential as biomarkers of disease diagnosis and prognosis as well as pharmaceutical targets for a number of cancers [23]. For example, TRIB1 upregulation is significantly associated with metastasis and poor prognosis in prostate cancer [24], it has been shown that TRIB1 mediates radioresistance in glioma cells by a HDAC1 dependent pathway [25] and high levels of TRIB1 are associated with poor breast cancer survival through the regulation of PI3K-NFκB pathway [26]. TRIB2 has been shown to contribute to tumorigenesis in lung cancer through the downregulation of C/EBPα [27] and TRIB2 direct interaction with AKT has been shown to be an important mechanism that contributes to resistance to anti-cancer drug therapy [28].

Finally, TRIB3 has been shown to support breast and colorectal cancer stemness through the interaction with AKT and beta-catenin respectively [29,30]. These examples illustrate that the different Tribbles family members can all play a regulatory role in cancer initiation and progression, but their contribution may be tumor type specific. Furthermore, these examples also add to anecdotal evidence that critical interacting proteins may differ between Tribbles family members and to previous reports that the affinity of distinct TRIB proteins to the same binding partner may differ [31]. We hypothesize therefore that particular Tribbles functions are dictated by its interactome –the specific set of proteins a tribble family member is interacting within a given biological setting– and improving our understanding of how these interactions take place will help to define the roles of Tribbles proteins in each context. To date, comprehensive Tribbles interactomes have not been reported.

Mass spectrometry (MS)-based proteomics approaches have been widely used in recent decades to study and identify protein-protein interactions (PPIs)[32]. Affinity-purification mass spectrometry (AP-MS) is used for purification of a protein (endogenous or tagged) and its interacting partners from a cell lysate [32]. This technique relies on the affinity of an antibody (or nanobody) for a protein and is followed by MS analysis [32]. We have previously used this approach successfully to identify the interactomes of various intracellular proteins [33–35].

In this study we have developed a robust AP-MS approach to characterize the TRIB1, -2 and -3 interactomes. In addition, we have investigated the contribution of the different domains of TRIB3 to its interactome. Finally, we have generated an inducible system to evaluate the similarities and differences between TRIB1 and -3 interactomes in breast cancer cells as a first proof-of-principle study showing that comprehensive profiling of interactomes can improve our understanding of Tribbles' role in cancer onset and progression.

2. MATERIALS AND METHODS

2.1. MATERIALS

Primary antibodies anti-turboGFP (Origene, #TA150041), anti-Gal4DBD (Santa Cruz, sc-510) and anti-tubulin (Sigma Aldrich, T9026) were used. Secondary antibodies anti-mouse-HRP (Dako, P0260) and anti-rabbit-HRP (Thermofisher, #31460) were used. GFP-Trap and tGFP-Trap Agarose beads (Chromotek) were used for Immunoprecipitation. Doxycycline (Sigma Aldrich, D9891).

2.2. CELL CULTURE

Human HEK293T embryonic kidney cell line (ATCC CRL-3216) and human MCF7 breast cancer cells (ATCC HTB-22) were maintained in DMEM 4.5 g/L d-glucose supplemented with 10% fetal bovine serum and 1% penicillin and streptomycin. Cells were incubated in 5% CO2 incubator at 37°C and 95% humidity. To generate cells stably overexpressing TRIB1 or -3, MCF7 cells were transduced with third-generation lentiviral constructs using supernatants from HEK293T cells transfected with lentiviral packaging plasmids. HEK293T cells were transfected using X-treme gene 9 DNA transfection reagents (Roche) according to manufactures protocol.

2.3. PLASMIDS

TRIB3 and TRIB1 expression plasmids were kindly provided by Dr. Endre Kiss-Toth. Pcw57.1 lentiviral construct was provided by Dr. S.W.C. van Mil (UMC Utrecht, Utrecht, the Netherlands). Deletions of the N- and C-terminal region of TRIB3 were generated using Quickchange mutagenesis kit (Stratagene). Successful mutagenesis was verified by Sanger sequence analysis. The reporter construct 5xGAL4-TK-Luc-pGL3 has been described previously [36]. The pCDNA-Gal4DBD-TRIB3, was generated by cloning TRIB3 BamH1/Xba1 fragment from TRIB3 expression plasmid into the respective sites of pCDNA-Gal4DBD as described before [37]. pCDNA-Gal4DBD-TRIB3-ΔN-terminal (amino acids 69 to 358) and pCDNA-Gal4DBD-TRIB-ΔC-terminal (amino acids 1 to 316) were generated using Quickchange mutagenesis kit (Stratagene).

2.4. LUCIFERASE REPORTER ASSAYS

HEK-293T and MCF7 cells were transfected using Xtreme gene 9 DNA transfection reagent (Roche) in 24-well plate format; 100 ng pCDNA3.1-Gal4DBD-TRIB3WT and mutants, 1 μg of pGL3 reporter and 2 ng of TK-Renilla luciferase were used for the experiments. After 48h cells were lysed and firefly and Renilla luciferase were measured with Dual-Luciferase Reporter Assay System (Promega) in a TriStar2 LB942 Multimode Reader (Berthold Technologies). Results are expressed in Relative Luciferase Units; the results are average of three independent experiments. Student's t-test were used. Statistical significance was defined as a p value of $p < 0.05$.

2.5. WESTERN BLOT ANALYSIS

Western blotting was performed as described before [37] In short, cells were grown in 6-well format or 10 cm dishes. After induction with 2 μg/ml doxycycline for 24h, cells were washed with ice cold PBS twice and scraped in ice cold lysis buffer (150

mM NaCl, 1% NP40, 0.5% sodium DOC, 0.1 % SDS, 25 mM Tris pH 7.4) supplemented with protease inhibitors. After incubation on ice for 20', samples were centrifuged at maximum speed for 10' at 4°C and supernatants were collected. Protein concentrations were measured, samples were supplemented with Laemmli Sample Buffer (LSB) and incubated at 95°C for 5' before use. Samples were separated by SDS-PAGE and then transferred to PVDF membrane. Blocking was performed in 5% milk in TBS-T for 45'. Incubation with primary antibody was done overnight at 4°C and secondary for 1h at room temperature. Membranes were treated with ECL Western blot solution and protein expression was detected using LAS4000 Image Quant.

2.6. IMMUNOPRECIPITATION

HEK293T cells were seeded in 15 cm dishes and transfected when the cells were approximately at 80% confluency. 48h after transfection cells were washed in ice cold PBS twice and then scrapped in 2mL of lysis buffer (50 mM Tris 8.0 pH, 1mM EDTA pH 8.0, 0.1% NP40, 250 mM NaCl, 10% Glycerol). Samples were incubated on ice for 20' and then spin down at max speed for 10' at 4°C, supernatant was collected. GFP-Trap beads (Chromotek) were equilibrated according to manufactures protocol and incubated with supernatant from previous step for 2h at 4°C. Then beads were collected by spinning down the samples at 2500g for 5' at 4°C. Beads were washed two times with lysis buffer and one final time in PBS before been transfer to a low-binding Eppendorf tube. Finally, the beads were spun down and dried using a Pasteur pipette. MCF7 cells were induced with 2 μg/mL doxycycline for 24h before lysis and incubation with turboGFP-Trap beads (Chromotek) as described above.

2.7. CONFOCAL MICROSCOPY:

Cells were grown in μ-Slide 8 well glass bottom chambers (Ibidi) and treated with 2 μg/mL doxycycline for 24h. Cells were incubated with DAPI (Vectashield) for 10 minutes to stain nuclei. Images were obtained using LSM880 Zeiss Microscope.

2.8. MASS SPECTROMETRY:

The precipitated proteins were denatured and alkylated in 50 µl 8 M Urea, 1 M ammonium bicarbonate containing 10 mM tris (2-carboxyethyl) phosphine hydrochloride and 40 mM 2-chloro-acetamide. After 4 fold further dilution with 1M ammonium bicarbonate and digestion with trypsin (250 ng/200 µl), peptides were separated from the sepharose beads and desalted with homemade C-18 stage tips (3 M, St Paul, MN). Peptides were eluted with 80% ACN and, after evaporation of the solvent in the speedvac, redissolved in buffer A (0,1% formic acid). After separation on a 30 cm pico-tip column (75 µm ID, New Objective) in-house packed with C-18 material (1.9 µm aquapur gold, dr. Maisch) using a 140 minute gradient (7% to 80% ACN, 0.1% FA), delivered by an easy-nLC 1000 (Thermo), peptides were electro-sprayed directly into a Orbitrap Fusion Tribrid Mass Spectrometer (Thermo Scientific). The MS was run in DDA mode with a cycle time of 1 second, in which the full scan (400-1500 mass range) was performed at a resolution of 240,000. Ions reaching an intensity threshold of 10.000, were isolated by the quadrupole and fragmented with a HCD collision energy of 30%.

The obtained raw data was analyzed with MaxQuant [version 1.6.3.4], using the Uniprot fasta file (UP000005640) of Homo sapiens (taxonomy ID: 9606), extracted at 21/01/2021. Minimum and maximum peptide lengths of 7 and 25 amino acids respectively, with Oxidation on Methionine and Acetylation on Protein N-term as variable modifications and Carbamidomethyl on Cysteine as fixed modification. Peptide and protein false discovery rates were set to 1%.

To determine proteins of interest, we performed a differential enrichment analysis on the generated Maxquant output. First, we generated unique names for the genes associated to multiple proteins to be able to match them. Second, we filtered for proteins that were identified in at least three out of four of the replicates of one condition. Then, we background corrected and normalized the data by variance stabilizing transformation; shifting and scaling the proteins intensities by sample group. We used a left-shifted Gaussian distribution to impute for missingness since our data presented a pattern of missingness not at random (MNAR). Finally, we performed a differential enrichment analysis to identify those proteins that were over-enriched and selected those with at least 2.5 Fold Change and adjusted p-value ≤ 0.05. The adjusted p-value was calculated using Benjamin-Hochberg procedure. The program used for the analyses was R [version 4.0.4] through R-Studio [version 1.5.64]. The mass spectrometry proteomics data have been deposited to the ProteomeXchange Consortium via the PRIDE partner repository (http://www.ebi.ac.uk/pride). Dataset identifiers will be provided during review.

3. RESULTS

3.1. ANALYSIS OF TRIB1, TRIB2 AND TRIB3 INTERACTOMES IN HEK293T CELLS USING AP-MS

To better understand the distinct role of each Tribbles family member as well as their

redundancies, we developed a method to robustly identify Tribbles interactomes. We transiently overexpressed TRIB1, TRIB2 and TRIB3 as GFP-fusion proteins in HEK293T cells and performed AP-MS experiments. We used nanobodies against GFP to purify Tribbles proteins and their interacting partners that allowed us to reduce background binding and minimize the amount of peptides released during on-bead digestion [38]. After purification we used liquid chromatography-tandem mass spectrometry (LC-MS) to characterize Tribbles interactomes (Figure 1A).

Among the different interactors that were found we could detect known binding partners of TRIB1, TRIB2 and TRIB3 as well as interactors that have not yet been reported. The results are described in Tables 1, 2 and 3. As reported before [9,39], all Tribbles family members were able to physically interact with the E3 ubiquitin degradation complex formed by the ubiquitin E3 ligase COP1 and the adaptors proteins DET1 and DDB1. Confirm the specificity of our methodology, we mutated the COP1 binding motif (Figure 1A) and thus specifically depleted the interactome from COP1 and DET1 (Figure 1B and 1D). TRIB1 and TRIB2 were found to interact with TRIB1 and the Tribbles-related pseudokinase STK40, suggesting that Tribbles proteins can form homo- and heterodimers in mammalian cells, as has been shown for the Drosophila Tribbles homologue Trbl [40] and for the mammalian versions in protein complementation assays (PCA; unpublished observations). Other previously described interaction partners that were detected included Activating transcription Factor 4 (ATF4) [41]. While not previously described as binding partners, the mTOR regulatory subunits RICTOR and RAPTOR were also detected in the TRIB2 interactome (Figure 1C). Previous studies have shown however that TRIB2 regulates mTOR signaling [42,43]. Interactions that have not been described earlier included the interaction between TRIB3 and the mitochondrial transporters TIM-TOM complex, a complex found in the mitochondrial membrane that transport proteins into the inner membrane of the mitochondria [44]. In addition, whilst the interaction between TRIB proteins and the E3 ubiquitin ligase COP1 is well-established [9,45], TRIB1 and TRIB3 showed interaction with another family of E3 ubiquitin ligases, that includes STIP1 and STUB1. Among the most enriched interactors of TRIB2 were SKT and BDH2, two interaction partners newly identified here that are involved in the development of different tissues and an enzyme involved in metabolism, respectively [46,47]. In summary, the identification of known interactors of Tribbles validates our experimental approach and provides support for the newly discovered binding partners.

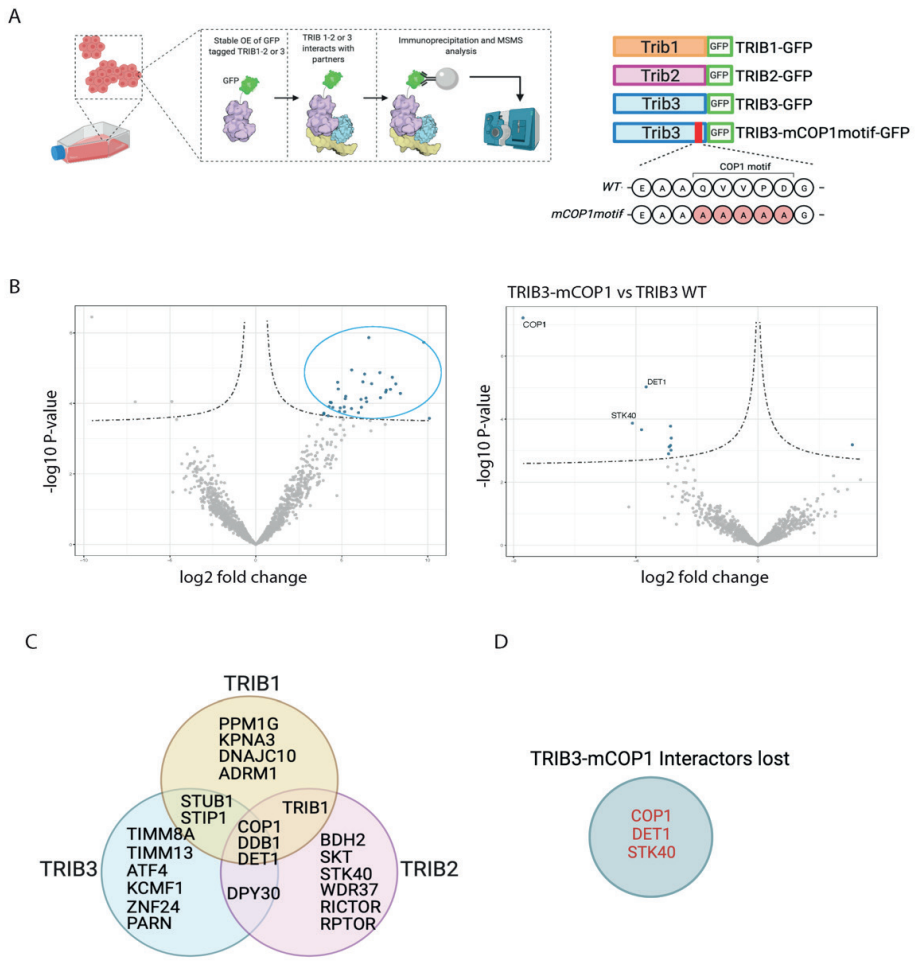

Figure 1. TRIB1, -2 and -3 interactomes in HEK293T cells. (A) Schematic representation of workflow followed for AP-MS experiments. **(B)** Volcano plots showing TRIB3 interactors compare to GFP control and TRIB3-mCOP1 interactors compared to WT TRIB3 in HEK293T cells. **(C)** Venn diagram of common and unique interactors between Tribbles family members.

Table 1. Top 25 TRIB1 interacting partners in HEK293T cells based on p-value.

Gene name	-Log (p-value)	Adjusted p-value	Log2 Fold Change*	Full name
DNAJC10	6.4354	6.18E-05	7.300	DnaJ Heat Shock Protein Family Member C10
DDB1	5.8200	0.04	4.678	Damage Specific DNA Binding Protein 1
TRIB1	5.7117	8.17E-7	2.567	Tribbles Pseudokinase 1
PPM1G	5.2926	0.02	6.113	Protein Phosphatase Mg2+ Dependent 1G
PSMA1	5.2130	5.29E-05	4.699	Proteosome 20S subunit Alpha 1
PSMA2	5.0433	0.0002	3.443	Proteosome 20S subunit Alpha 2
PSMD4	5.0242	0.0004	3.112	Proteasome 26S Subunit Ubiquitin receptor 4
HDAC6	4.9461	0.03	4.223	Histone Deacetylase 6
PSMC6	4.5066	3.12E-05	4.667	Proteosome 26S subunit ATPase 6
ADRM1	4.4064	0.0004	5.600	26S Proteosome Ubiquitin Receptor
PSMC2	4.3112	4.68E-05	2.554	Proteosome 26S subunit ATPase 2
PSMB6	4.1668	0.006	6.433	Proteosome 20S subunit Beta 7
STIP1	3.9432	0.01	4.001	Stress induced Phosphoprotein 1
PSMB2	3.9126	1.70E-05	3.333	Proteosome 20S subunit Beta 2
STUB1	3.8218	0.05	5.677	STIP1 Homology and U-Box Containing Protein 1
PSMC1	3.7980	9.63E-06	3.655	Proteosome 20S subunit Beta 7
HSPH1	3.6860	0.004	5.911	Heat Shock Protein Family H Member 1
KPNA4	3.6243	0.001	3.770	Karyopherin Subunit Alpha 4
DET1	3.5614	5.29E-5	3.190	DET 1 Partner of COP1 E3 Ubiquitin Ligase
HSPA4L	3.4984	0.003	4.675	Heat Shock Protein Family A Member 4 Like
RFWD2	3.3768	0.0004	9.453	COP1 E3 Ubiquitin Ligase
PSMA5	3.3478	0.0004	2.724	Proteosome 20S subunit Alpha 5
HSPA4	3.0482	1.30E-05	5.119	Heat Shock Protein A Memeber 4
PSMA7	3.0482	0.003	3.880	Proteosome 20S subunit Alpha 7
KPNA3	2.7785	0.001	4.654	Karyopherin Subunit Alpha 3

* Log 2 fold change calculated using mean intensity of TRIB1 condition compared to GFP.

Table 2. Top 25 TRIB22 interacting partners in HEK293T cells based on p-value.

Gene name	-Log (p-value)	Adjusted p-value	Log2 Fold Change*	Full name
TRIB1	5.771	2.76E-05	12.364	Tribbles Pseudokinase 1
USP11	5.541	0.001	4.356	Ubiquitin Specific Peptidase 11
ISCA1	5.391	0.0002	6.115	IRON-Sulfur Cluster Assembly 1
BDH2	4.951	3.90E-06	8.657	3-Hydroxybutyrate Dehtdrogenase 2
ZKSCAN1	4.945	0.0001	6.503	Zinc Finger with KRAB and SCAN Domains 1
DET1	4.885	3.4E-05	7.812	DET 1 Partner of COP1 E3 Ubiquitin Ligase
DDB1	4.523	0.001	4.456	Damage Specific DNA Binding Protein 1
AIFM1	4.274	3.27E-05	4.898	Apoptosis inducing Factor Mitochondrial Associated 1
FECH	4.262	2.76E-05	5.878	Ferrochelatase
WDR37	4.007	0.001	7.058	WD Repeat Domain 37
KIAA1217	3.789	0.001	9.837	Sickle tail Protein Homolog
KCTD21	3.751	0.002	3.573	BTB/POZ Domain-Containing Protein KCTD21
CDC42EP1	3.686	0.0003	3.082	CDC42 Effector Protein 1
MLF2	3.471	0.0003	4.887	Myeloid Leukemia factor 1
STK40	3.231	0.0001	7.644	Serine/Threonine Kinase 40
RAB3GAP1	3.218	0.0002	3.543	RAB3 GTPase Activating Protein Catalytic Subunit 1
EMD	3.153	0.01	4.316	Emerin
RFWD2	3.034	0.002	10.620	COP1 E3 Ubiquitin Ligase
RPTOR	2.864	0.002	2.346	Regulatory Associated Protein of MTOR Complex 1
FKBP4	2.841	0.01	4.293	FKBP Prolyl Isomerase 4
SRCIN1	2.762	0.0004	4.617	SRC Kinase Signaling Inhibitor 1
PKP2	2.646	0.0004	4.004	Plakophilin 2
TBC1D4	2.634	0.001	2.375	TBC1 Domain Family Member 4
HAUS8	2.163	0.002	3.115	HAUS Augmin Like COmplex Subunit 8
RICTOR	1.999	0.001	2.706	RPTOR Independent Companion of MTOR Complex 2

*Log 2 fold change calculated using mean intensity of TRIB2 condition compared to GFP.

Table 3. Top 25 TRIB3 interacting partners in HEK293T cells based on p-value.

Gene name	-Log (p-value)	Adjusted p-value	Log2 Fold Change*	Full name
TIMM13	7.1286	0.0002	12.187	Translocase of Inner Mitochondrial Membrane 13
TRIM37	6.9472	0.006	6.961	Tripartite Motif Containing 37
DDB1	6.2442	0.005	5.187	Damage Specific DNA Binding Protein 1
KCMF1	5.7442	0.007	5.885	Potassium Channel Modulatory Factor 1
ATF4	5.7130	0.01	1.345	Activating Transcription factor 4
STUB1	5.4533	0.03	5.972	STIP1 Homology and U-Box Containing Protein 1
MLLT11	5.0745	0.002	6.917	MLLT11 Transcription factor 7 Cofactor
RFWD2	5.0033	0.0006	2.489	COP1 E3 Ubiquitin Ligase
PARN	4.9405	0.01	7.321	Poly(A)-Specific Ribonuclease
PRKD2	4.6601	0.001	7.015	Protein kinase D2
PASK	4.6442	0.005	8.091	PAS Domain Containing Serine/Threonine Kinase
DPY30	4.3027	0.04	5.462	Dpy-30 Histone Methyltranferase Complex
DET1	4.1258	0.04	5.134	DET 1 Partner of COP1 E3 Ubiquitin Ligase
ZNF24	4.0712	0.001	4.125	Zinc Finger Protein 24
EP300	3.9599	0.01	6.900	E1A Binding Protein P300
STIP1	3.9000	0.020.	3.582	Stress induced Phosphoprotein 1
KANK2	3.7899	0.16	6.740	KN Motif Ankyrin Repeat Domains 2
RBBP8	3.7371	0.019	7.875	RB Binding Protein 8
ZNF507	3.6606	0.006	7.112	Zinc Finger Protein 507
PPP6C	3.5073	0.03	7.964	Protein Phosphatase 6 Catalytic Subunit
WDR62	3.5072	0.006	7.074	WD Repeat Domain 62
PPP6R3	3.4224	0.003	7.112	Protein Phosphatase 6 regulatory Subunit 3
AKAP8L	2.7110	0.0005	8.183	A-Kinase Anchoring Protein 8 Like
ZNF655	2.6525	0.01	6.810	Zinc Finger Protein 655
TIMM8A	2.6021	3.48E-05	12.262	Translocase of Inner Mitochondrial Membrane 8A

*Log 2 fold change calculated using mean intensity of TRIB3 condition compared to GFP.

3.2. CONTRIBUTION OF THE DIFFERENT DOMAINS TO THE TRIB3 INTERACTOME

Tribbles proteins contain three distinct domains with the central psuedokinase domain being the most conserved: the amino acid sequence of human TRIB1/2 and 3 shows a 55% similarity in the pseudokinase domain, but for example the C-terminal domains of TRIB3 and TRIB1 are only 9% similar (Supplementary Figure 1). This low similarity in the N- and C-terminal domains suggest that each holds unique functions and may help to develop TRIB-targeting drugs with low cross-reactivity, but these domains have not been studied intensively.

The N- and C-terminal domains of TRIB3 are unstructured domains for which a 3D conformation cannot be predicted based on the amino acid sequence, as shown in Figure 2A [7]. In order to understand the contribution of the different domains of TRIB3 (N- and C-terminus and pseudokinase domain) to its interactome and to gain an insight into how these interactions take place we generated TRIB3 mutants lacking the N-terminal domain (amino acids 1-69, TRIB3-ΔN-terminal) and the C-terminal domain (amino acids 316-358, TRIB3-ΔC-terminal) and performed an AP-MS experiments as described above (Figure 2B). A summary of top 25 interactions of the C-terminal and N-terminal domains is shown in Table 4. In agreement with previous studies [45], the interaction with COP1 and DET1 requires the presence of the C-terminal domain, as binding is lost with the TRIB3-ΔC mutant (Figure 2C). Moreover, novel proteins related to the ubiquitin degradation system were also found binding to the C-terminal domain of TRIB3, such as UBR2, a E3 ubiquitin-protein ligase that control cell growth via mTOR signaling [48]. These findings confirm the concept that the C-terminal domain is required for TRIB3 to act as a degradation platform. In addition to the E3 ubiquitin ligases we also identified USP16, a deubiquitinating enzyme that plays an important role in mitosis [49], suggesting a role for TRIB3 in this process as well. In addition, STK40 and DOCK11 were also found to interact through the C-terminal domain of TRIB3. This reinforces the notion that Tribbles proteins and the Tribbles-like protein STK40 can form homo/hetero dimers mentioned above. DOCK11 is a guanine nucleotide-exchange factor that activates CDC42 and RAC1 [50]; the biological relevance of this interaction remains to be established.

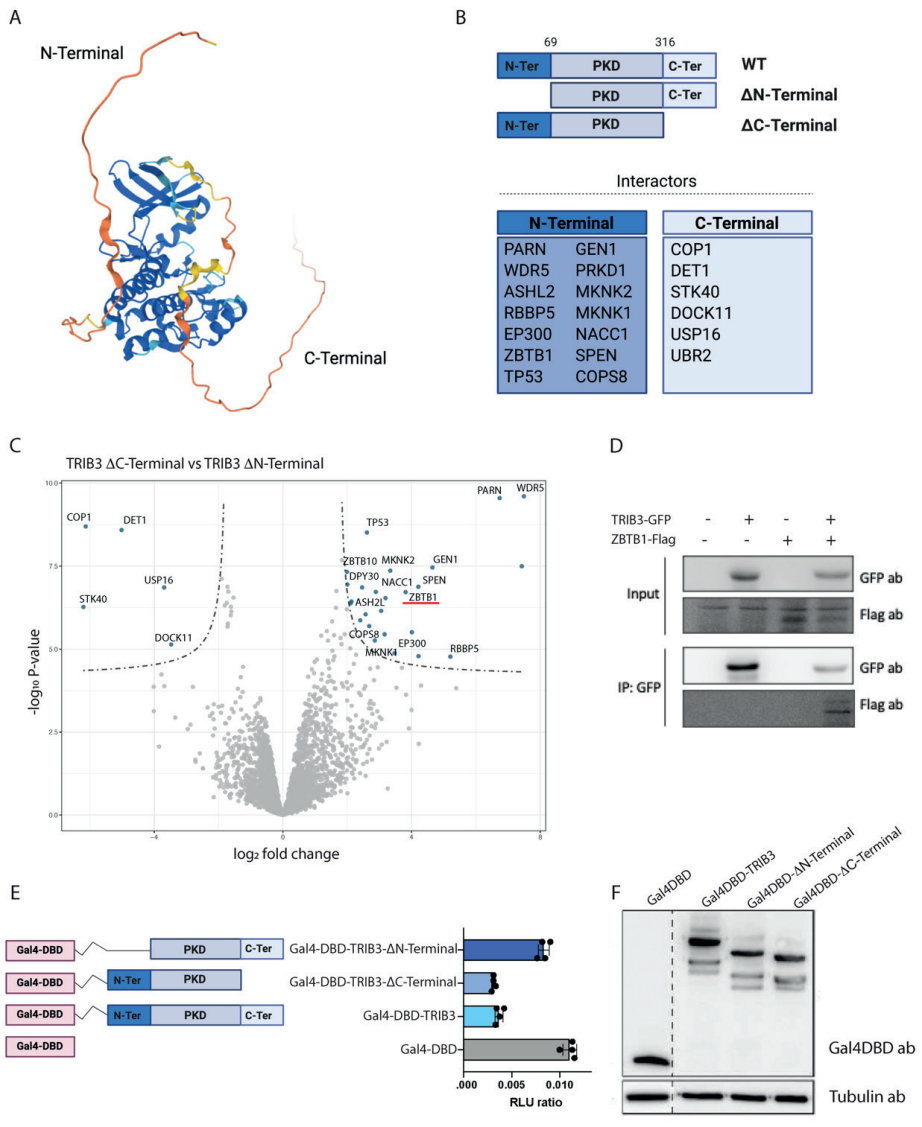

Figure 2. Contribution of TRIB3 domains to its interactome and function. (A) Human TRIB3 structure prediction by AlphaFold. Color represent pLDDT score (blue: very high confidence, light blue: confident, yellow: low and orange: very low or unstructured). (B) Schematic representation of TRIB3 mutants and specific interactors lost when the indicated domain was removed. (C) Volcano plot showing interaction of the N-terminal and C-terminal domains of TRIB3 in HEK293T cells. (D) Co-immunoprecipitation assay of TRIB3-GFP and ZBTB1-Flag in HEK293T cells. (E) Gal4 reporter assay of Gal4-DBD, Gal4-TRIB3, Gal4-TRIB3-ΔN-terminal and Gal4-TRIB3-ΔC-terminal in Hek293T cells. Data is normalized using Renilla luciferase. (F) Western blot using Gal4DBD and tubulin antibodies showing similar expression of the constructs used for the Gal4 reporter assay.

The N-terminal domain of TRIB3 contains a nuclear localization signal sequence that directs TRIB3 towards the nucleus and a PEST domain that might affect TRIB3 stability. Interactors that were lost when deleting the N-terminus included several transcription factors and regulators, which are mainly found in the nucleus, such as ZBTB1, p300, and SPEN (Figure 2C). The interaction between TRIB3 and ZBTB1 was confirmed by co-immunoprecipitation assays (Figure 2D). In addition, we found all the subunits of the WRAD complex (WDR5, DPY30, ASH2L and RbBP5) binding to the N-terminus of TRIB3. The WRAD complex is crucial for SET1 histone methyl transferases to catalyze histone 3 lysine 4 methylation [51]. The interactions between TRIB3 and WRAD complex components was also confirmed by co-immunoprecipitation experiments (to be published elsewhere).

Interestingly we also found the interaction with Serine/Threonine Protein Kinase D1 (PRKD1), and the MAPK interacting Serine/Threonine Kinase 1 and 2 (MKNK1 and MKNK2) suggesting that the regulation of Mitogen-activated protein kinase (MAPK) signaling happens not only through the C-terminal [10] and pseudokinase domains [31] as reported earlier but also through the N-terminal domain. It is also worth to mention the interactions with TP53 and COPS8. TP53, the so called "guardian of the genome", is the most common tumor suppressor that is found mutated across all cancer types [52], regulates the cell cycle as well as apoptosis of damaged cells. COPS8 is a component of the COP9 signalosome that is involved in the phosphorylation of p53 [53].

Taken together, these data indicate that TRIB3 is a putative important transcriptional regulator and this role is carried out mainly through the N-terminal domain. In contrast, the C-terminal domain of TRIB3 is required for the interaction with components of the ubiquitin system and for the formation of homo/hetero dimers.

3.3. TRIB3 FUNCTION AS A TRANSCRIPTIONAL REPRESSOR

While our data revealed and interaction between the N-terminus of TRIB3 and for example SET1 histone methyl transferase complexes and p300, which are associated with transcriptional activation [51,54], the same TRIB3 domain also interacted with various proteins that are involved in transcriptional repression, such as ZBTB1 and SPEN [55,56]. In addition, TRIM28 (also known as KAP-1 or TIF1β) and SETDB1, proteins that may form a repressor complex with ZBTB1 [57,58] (were also detected (adjusted p-value ≤ 0.05. Data not shown).

Table 4. Top binding partners of TRIB3 ΔN- and ΔC-Terminal domains based on p-value.

Gene name	-Log (p-value)	Adjusted p-value	Log2 Fold Change*	Full name
TRIB3-DC-Terminal Binding partners				
RFWD2	4.4826	4.54E-06	5.943	COP1 E3 Ubiquitin Ligase
STK40	3.1119	0.0002	6.370	Serine/Threonine Kinase 40
DOCK11	3.7967	0.004	3.498	Dedicator of Cytokinases 11
DET1	3.8995	1.02E-05	4.667	DET 1 Partner of COP1 E3 Ubiquitin Ligase
USP16	2.5863	0.01	3.822	Ubiquitin Specific Peptidase 16
UBR2	3.1640	0.001	2.610	Ubiquitin Protein Ligase E3 Component N-Recognin 2
DDI2	1.8154	0.02	1.811	DNA Damage 1 Homolog 2
TRIB3-DN-Terminal Binding partners				
MKNK2	6.0395	0.007	3.525	MAPK Interacting Serine/Threonine Kinase 2
WDR5	5.7443	4.38E-07	7.841	WD Repeat Domain 5
COPS8	5.6291	0.01	3.123	COP9 Signalosome Subunit 8
TP53	5.3723	3.16E-06	2.800	Tumor Protein P53
PARN	5.0650	4.38E-07	6.298	Poly(A)-Specific Ribonuclease
GEN1	4.8329	1.35E-05	4.438	Gen1 Holliday Junction 5′ Flap Endonuclease
SPEN	3.8986	3.87E-06	4.154	SPEN Family Transcriptional Repressor
ZNFP24	3.8823	0.0001	1.719	Zinc Finger Protein 91
NACC1	3.7582	3.08E-05	2.193	Nucleus Accumbens Associated 1
ZBTB1	3.5994	8.91E-05	4.004	Zinc Finger And BTB Domain 1
SETD2	3.5315	0.002	1.627	SET Domain 2 Histone Lysine Methyltranferase
DPY30	3.4148	5.56E-05	2.296	Dpy-30 Histone Methyltranferase Complex Subunit
RBBP5	3.2480	0.0009	4.471	RB Binding Protein 5
MYC	2.6206	0.01	2.233	MYC Proto-Oncogene
EP300	2.5832	0.005	4.017	E1A Binding Protein P300
MKNK1	2.5381	0.05	3.411	MAPK Interacting Serine/Threonine Kinase 1
ASH2L	2.4872	0.001	5.577	Set1/Ash2 Histone Methyltranferase Complex Subunit
AKAP1	2.2902	0.005	2.712	A-Kinase Anchoring Protein 1
PRKD1	1.7714	0.03	4.106	Protein kinase D1
NFAT4	3.936	0.008	2.464	Nuclear Factor of Activated T Cells 3

*Absolute Log 2 fold change calculated using mean intensity of ΔN-Terminal condition compared to ΔC-Terminal condition.

To assess the effect of TRIB3 on transcription, we fused TRIB3 to the DNA binding domain of Gal4 (Gal4DBD) and tested the transcriptional activity of the fusion protein on a reporter plasmid with high basal activity(5xGal4-TK-Luc)[59]. As shown in Figure 2E, TRIB3 had a repressive effect when compared to the Gal4DBD alone, similar to for example GalDBD fusions of ZBTB1 and TRIM28 [60,61]. This TRIB3-mediated repression was mostly lost when the N-terminus was deleted, but the TRIB3 ΔC-terminal mutant retained repressor activity (Figure 2E). These results are in line with the mass spectrometry data described above where we found a high number of transcriptional repressors are able to bind through the N-terminal of TRIB3. Gal4DBD fusion proteins were expressed at similar levels, excluding the possibility that differences in activity were due to expression differences (Figure 2F). We conclude therefore that the N-terminus of TRIB3 harbours repressive activity when tethered to the DNA, which may be due to repressor proteins, such as ZBTB1 (and its associated proteins TRIM28 and SETDB1) and SPEN binding specifically to this region of the protein. Furthermore, while the N-terminus of Tribbles has the ability to recruit both transcriptional activators (e.g., MLL complex) and repressors (e.g., ZBTB1 and SPEN), the balance appears to be in favor of transcriptional repression, at least in this experimental setting.

3.4. COMPARISON OF TRIB1 AND TRIB3 INTERACTOMES IN MCF7 CELLS

Having developed a robust AP-MS workflow to identify interaction partners of Tribbles proteins, we wished to address the different roles of TRIB1 and TRIB3 in breast cancer where high levels of both proteins have been reported to be associated with poor prognosis and lower survival rates [26,62,63]. For this we generated inducible TRIB1-tGFP and TRIB3-tGFP stable cell lines in the breast cancer cell line MCF7, a model for luminal A breast cancer, allowing immediate short-term overexpression of TRIB1 and -3 as well as control over the amount of protein being overexpressed. A summary of the constructs used and the workflow followed to identify interacting proteins is depicted in Figure 3A. Expression of TRIB1-tGFP, TRIB3-tGFP and -tGFP was observed by Western blot after 24h treatment with doxycycline and no expression was observed in untreated cells (Figure 3B). TRIB3 was predominantly -but not exclusively- localized in the nucleus as determined by confocal microscopy (Figure 3C). In contrast to the predominant nuclear localization of TRIB1 in HEK293T cells ([18] data not shown) TRIB1 was mainly localized in the cytoplasm in MCF7 cells (Fig. 3C), supporting the view that subcellular localization of Tribbles depends on cellular context and conditions [17].

Importantly, long-term overexpression of TRIB3 was recently linked to increased proliferation in MCF7 cells [63], which potentially confounds interactome profiles,

but no significant effects on cell proliferation were observed within the 24h timeframe of our experiments (data not shown). A summary of top 20 interactors for TRIB1 and TRIB3 (Figure 3D) is listed in Table 5. Interactors common to both TRIB1 and TRIB3 included COP1 and CDKN1A. The first one is a common interactor of all Tribbles family members that has been widely studied and was also detected in the current study in HEK293T cells (Figure 1), and the second one is a cyclin-dependent kinase inhibitor that is tightly controlled by TP53 [64]. CDKN1A mediates G1 cell cycle arrest in response to a variety of external stimulus. Given the fact that Tribbles were originally described as a cell cycle regulators in Drosophila [65], this might be another mechanism by which these proteins regulate proliferation. In addition, both TRIB1 and TRIB3 also interacted with Fatty Acid Synthetase (FASN), an enzyme that catalyzes the synthesis of palmitate from acetyl-CoA and malonyl-CoA. FASN overactivity has been implicated in cancer onset and progression in many cancers [66]. Interestingly, FASN has also been shown to be a transcriptional target for TRIB1 [67]. Among the specific TRIB1 interactors Histone Deacetylase 6 (HDAC6) stands out. HDAC6, which is mostly cytoplasmatic, has been implicated in cancer and metastasis formation in breast cancer [68]. As described above for HEK293T cells, TRIB3 interacted with a number of transcription factors that mostly are associated with transcriptional repression. The interaction with ZBTB1 was also detected in MCF7 cells among other zinc finger proteins (ZNF746, ZNF12, ZNF24) (Fig 3E), many of which are related to transcriptional repression [69]. In fact, ZBTB1 has been recently associated with resistance to tamoxifen and aerobic glycolysis in breast cancer cells [70]. Both resistance to drug treatment and glucose metabolism are major cellular pathways in which TRIB3 has been implicated before [71,72]; future studies are needed to establish whether the TRIB3-ZBTB1 interaction plays a role in these pathways. Similar to HEK293T cells, the interaction between TRIB3 and the TIM-TOM complex was also detected in MCF7 cells, suggesting a mitochondrial pool and function for this protein. To further validate the role of TRIB3 as a transcriptional repressor we tested the Gal4DBD-TRIB3 fusion protein as described above for HEK293T cells, and also detected reduced transcriptional activity in these MCF7 breast cancer cells (Figure 3F). These findings indicate that our AP-MSMS approach provides a powerful tool to unravel novel pseudokinase biology, that is not limited to a single cell system.

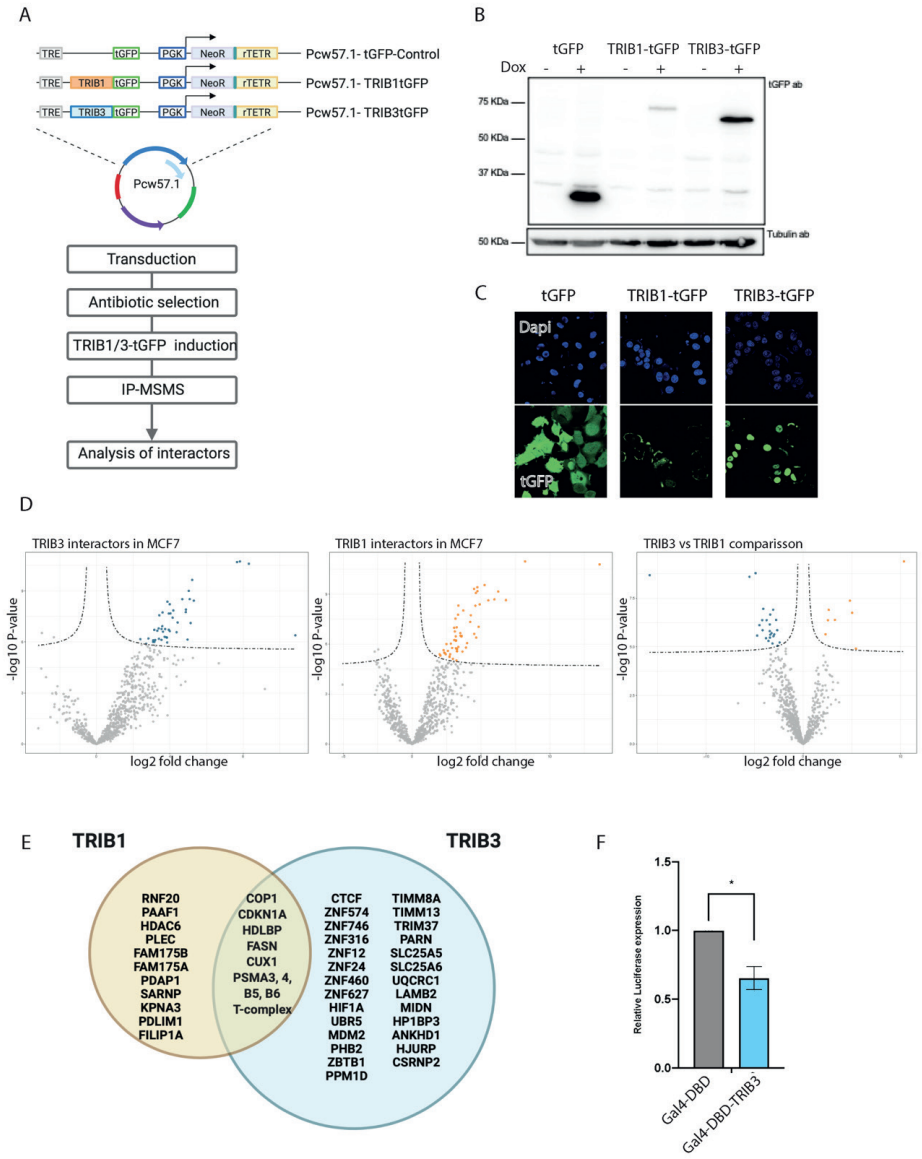

Figure 3. TRIB1 and TRIB3 interactors in MCF7 cells. (A) Schematic representation of inducible constructs and workflow of the AP-MS experiments followed in MCF7 cells. **(B)** Western blot using t-GFP antibody sowing inducible expression of TRIB1-tGFP and TRIB3-tGFP upon doxycycline treatment and Tubulin expression as loading control. **(C)** Confocal images showing tGFP, TRIB1-tGFP and TRIB3-tGFP localization upon doxycycline induction. **(D)** Volcano plots of TRIB1 and TRIB3 interactors compared to tGFP control in MCF7 cells and volcano plot showing the comparison between TRIB1 and TRIB3 interactome in these cells. **(E)** Venn diagram of similar and different interactors between TRIB1 and TRIB3 in MCF7 cells detected in the AP-MSMS experiments.

Table 5. Top 20 TRIB1 and TRIB3 Binding partners in MCF7 cells based on p-value.

Gene name	-Log (p-value)	Adjusted p-value	Log2 Fold Change	Full name
TRIB1 binding partners in MCF7				
PFN1	6.8434	0.007	2.550	Profilin 1
CDKN1A	6.7563	0.0002	2.315	Cyclin Dependent Kinase Inhibitor 1A
CCT5	6.0523	0.0002	2.083	T-complex protein 1 subunit epsilon
PDAP1	6.0427	0.006	2.151	PDGFA Associated Protein 1
PRKDC	5.8532	0.0001	2.508	DNA-dependent protein kinase catalytic subunit
ERH	5.8170	4.16E-05	3.553	ERH MRNA Splicing and Mitosis Factor
RFWD2	5.5455	1.08E-08	6.240	COP1 E3 Ubiquitin Ligase
RNF40	5.3754	7.73E-06	3.083	E3 ubiquitin-protein ligase BRE1B
FASN	5.3652	0.01	1.708	Fatty Acid Synthase
MTHFD1	5.0852	4.23E-05	2.525	C-1-tetrahydrofolate synthase
STIP1	4.9889	2.89E-05	3.699	Stress-induced-phosphoprotein 1
DNAJB1	4.9816	2.18E-07	5.567	DnaJ Heat Shock Protein Family Member B1
STK40	4.9431	5.94E-06	5.105	Serine/threonine Kinase 40
PLEC	4.3460	0.0006	3.183	Plectin
HDAC6	4.1498	0.01	2.356	Histone Deacetylase 6
PAAF1	3.9612	0.008	2.609	Proteosomal ATPase Associated Factor 1
EDF1	3.8339	1.82E-05	3.326	Endothelial Differentiation Related Factor 1
CUX1	3.7878	0.003	2.122	Cut like Homeobox 1
PRDX2	3.7664	0.01	3.741	Peroxiredoxin 2
CEBPB	2.9757	0.01	1.223	CCAAT Enhancer Binding Protein Beta
TRIB3 binding partners in MCF7				
CDKN1A	7.7691	0.0001	2.752	Cyclin Dependent Kinase Inhibitor 1A
TRIM37	7.6337	0.01	3.405	Tripartie Motif Containing 37
ZNF217	7.5252	2.35E-06	2.732	Zinc Finger Protein 217
TRIB1	6.5117	0.001	2.966	Tribbles Pseudokinase 1
HIF1A	6.4611	0.0001	2.139	Hypoxia Inducible factor 1 Subunit Alpha
PPM1D	6.4143	0.006	2.567	Protein Phosphatase Mg Dependent 1D
ZBTB1	6.0395	0.01	1.828	Zinc Finger And BTB Domain 1
CEBPB	5.7224	0.0001	2.463	CCAAT/enhancer-binding protein beta
WDR5	5.7100	0.001	2.372	WD repeat-containing protein 5
ZNF627	5.3262	0.003	2.866	Zinc Finger Protein 627
ZNF460	5.1982	0.002	1.775	Zinc Finger Protein 460
DNAJB1	5.1152	2.35E-06	4.064	DnaJ homolog subfamily B member 1
PARN	4.9613	2.48E-05	3.301	Poly(A)-specific Ribonuclease
RFWD2	4.9105	5.62E-07	3.904	COP1 E3 Ubiquitin Ligase
FASN	4.6569	0.05	1.709	Fatty Acid Synthase
TIMM13	3.8986	1.92E-05	2.370	Translocase of Inner Mitochondrial Membrane 13
ZNF12	3.7582	0.01	2.602	Zinc Finger Protein 12
KDM3B	3.5315	0.05	2.185	Lysine-specific demethylase 3B
DPY30	3.3126	0.001	2.089	Dpy-30 Histone Methyltranferase Complex
TP53	2.3725	0.0001	2.372	Cellular tumor antigen p53

*Absolute Log 2 fold change calculated using mean intensity of TRIB3 condition compared to TRIB1 condition.

4. DISCUSSION

Pseudokinases such as the 3 human TRIB proteins hold promise as biomarkers in cancer, but their molecular functions are still incompletely understood. Here we reported a systematic characterization of TRIB1, -2 and -3 interactomes in HEK 293T cells to provide a better understanding of the differences and redundancies in Tribbles function. In addition, our mass spectrometry-based approach revealed the importance of the intrinsically disordered N-Terminal domain of TRIB3 in the interaction with transcriptional regulatory proteins. We showed that TRIB3 is associated with transcriptional repression and that this role is mostly carried by the N-Terminal of TRIB3. Moreover, we discover new interactors of TRIB1 and -3 in breast cancer cells that might help to understand the role of these proteins in cancer pathophysiology.

The study of the function of pseudoenzymes presents obvious difficulties in comparison with their enzymatically active counter partners, as no catalytic product can be measured as a read-out of their activity. Most of these pseudoenzymes rely on protein-protein interactions (PPI) to exert their function and several mass spectrometry-based techniques can be used for the identification of interactors such as proximity ligation or crosslinking mass spectrometry, all with particular advantages and disadvantages [32]. Our data shows how powerful is the use of AP-MS approaches for the discovery of new interactors and the study of pseudoenzyme function. Modern mass spectrometers have a tremendous sensitivity that allows them to detect the smallest contaminant and therefore a quantitative filter must be introduced to differentiate between genuine interactors and background noise. These quantitative filters can be introduced in the form of isotopes or in the form of algorithms for label-free quantification, an example of the last one is the Intensity-based absolute quantification (iBAQ) used in this study that allow us to determine protein abundance. Taken together shows that quantitative MS-based proteomics is the most powerful method to identify PPI and study pseudoenzyme function to date.

Through AP-MS we confirmed previously reported Tribbles interacting proteins and identified novel partners. As demonstrated before, we show that all 3 human tribbles family members can interact with the E3 ubiquitin ligase COP1. However, it seems that TRIB1 function is more dominated by the interaction with COP1, and that explains the high amount of proteasomal regulatory proteins as well as the low abundance of other interactors. TRIB2 and -3 also interact with COP1 but next to that many other interactors not related to proteasomal degradation were detected. This also seems the case when we compare the interactomes of TRIB1

and -3 in breast cancer cells. Moreover, TRIB1 protein expression was lower when compared to TRIB3 upon induction with doxycycline (Figure 3B), and thus could be reverted when proteasomal degradation was inhibited (data not shown) indicating that the lower amount of TRIB1 protein was the result of proteasomal degradation and was not due to different response to doxycycline induction. TRIB1 subcellular localization appeared to be mostly cytoplasmatic in comparison with TRIB3 that showed predominant nuclear localization, this can also explain the difference in protein stability and interactomes. In addition, our data also demonstrates some interactions that had been suggested in literature before but not experimentally demonstrated, such as the interaction with p53 or the interaction with CDKN1 [73,74]. These interactions might be related to the ability of Tribbles to regulate the cell cycle and therefore the implications in carcer are potentially very important. Both of these proteins are among the most commonly found mutated across all cancer types [75,76]. These interactions, together with others described above, might suggest a role of Tribbles in DNA damage. Furthermore, whether for example the TRIB3-CDKN1 interaction contributes to increased proliferation observed upon long-term overexpression of TRIB3 in MCF7 cells [63] remains to be established.

Finally, we report many novel interacting proteins that interact with one or more Tribbles family members. Amongst the cellular proteins with well-established functions is the metabolic enzyme FASN. Interestingly, FASN is a major regulator of neoplastic lipogenesis and is commonly found overexpressed in many cancers [66], is a metabolic oncogene that has been suggested as an attractive target for cancer therapy [77] and given the ability of TRIB1 and -3 to mark proteins for proteasomal degradation this interaction represent a promising therapeutic approach for breast cancer. The class of well-characterized TRIB3 interacting proteins also includes the transcriptional repressors ZBTB1 and SPEN, which may be responsible for the transcriptional repression observed when TRIB3 is tethered to the DNA. The ability of tribbles to regulate the function of transcription factors has been reported before [29–31], however the role as a transcriptional repressor has not been shown before. While novel Tribbles interacting proteins with well-characterized functions may present immediate new entries for future research, interacting proteins with poorly understood functions such as the zinc finger proteins found interacting with TRIB3, obviously will need more characterization before their value – be it therapeutic or more fundamental – can be assessed. It should be noted that the protein kinase AKT/PKB, a previously described interaction partner of TRIB3 [14], was detected in the TRIB1 interactome but was not a dominant hit in the TRIB3 interactomes in either HEK293T or MCF7 cells. Furthermore, when we compared the TRIB3 interactomes between the genetic variants R84 and Q84 –harboring an arginine and glutamine

residue at position 84, respectively – no significant differences in interactomes were found (data not shown). The R variant was reported to be a more potent inhibitor of insulin signaling through stronger AKT binding when tested in hepatocytes [78]. Together these findings support the view that TRIB interactomes may harbor a uniform component (overlap between for example HEK293T cells and MCF7 cells) as well as a flexible component which depends on cell type (em. .g. hepatocyte vs HEK293T cells vs MCF7 breast cancer cells) or cellular status (e.g. proliferative status, metabolic status). Analyzing and comparing TRIB interactomes in more cell types and under different conditions is therefore an important future direction.

In summary, we have shown new interactions that might be very relevant for cancer therapy and could situate Tribbles as therapeutic targets in breast cancer and we have shown how powerful and useful is the study of tribbles function through MS-based proteomics approaches.

5. CONCLUSIONS

We have used a MS-based approach to find new interactors of Tribbles proteins that might serve as starting point for future research. We have shown to ability of TRIB3 to function as a transcriptional repressor as we looked at the similarities and differences between TRIB1 and -3 in breast cancer cells, finding new interactors that might help to understand better the function of these proteins in breast cancer pathology.

Supplementary Materials: The following are available online at www.mdpi.com/xxx/s1, Figure S1: title, Table S1: title, Video S1: title.

Author Contributions: Conceptualization, MHQ, EKT, HV, EK; Methodology, MHQ, RB, AB, SdH, PSA, RvE, HV; Validation, MHQ, RB, AB, SdH, PSA; Formal analysis, MHQ, RB, AB, SdH, PSA,; ; Investigation, MHQ, RB, AB, SdH, PSA, RvE, EKT, HV, EK; Data curation, PSA, HV; Writing –original draft preparation, MHQ; Writing –review and editing, MHQ, EKT, HV, EK; Supervision, EKT, HV, EK; Visualisation, MHQ, PSA; Funding acquisition, EKT, EK. All authors have read and agreed to the published version of the manuscript.

Funding: This study was supported by a grants from the European Union's Horizon 2020 Marie Skłodowska-Curie Innovative Training Network, TRAIN (project no. 721532) and a combined Diabetes Breakthrough grant from the Dutch Diabetes Research Foundation and the Netherlands Organisation for Health Research and Development (ZonMW; project no. 459001006).

Institutional Review Board Statement: Not applicable

Informed Consent Statement: Any research article describing a study involving humans should contain this statement. Please add "Informed consent was obtained from all subjects involved in the study." OR "Patient consent was waived due to REASON (please provide a detailed justification)." OR "Not applicable." for studies not involving humans. You might also choose to exclude this statement if the study did not involve humans.

Written informed consent for publication must be obtained from participating patients who can be identified (including by the patients themselves). Please state "Written informed consent has been obtained from the patient(s) to publish this paper" if applicable.

Data Availability Statement: In this section, please provide details regarding where data supporting reported results can be found, including links to publicly archived datasets analyzed or generated during the study. Please refer to suggested Data Availability Statements in section "MDPI Research Data Policies" at https://www.mdpi.com/ethics. You might choose to exclude this statement if the study did not report any data.

Acknowledgments: We thank Dr. S.W.C van Mil for plasmids. We also thank members of the Marie Skłodowska-Curie Innovative Training Network TRAIN (see Supplementary information) and Dr. A.C.O. Vertegaal (LUMC) and members of the Kalkhoven and van Mil laboratories (both UMC Utrecht) for helpful discussions.

Conflicts of Interest: The authors declare no conflict of interest

References

1. D, F.; SW, C.-J.; H, M. Ten things you should know about protein kinases: IUPHAR Review 14. *Br. J. Pharmacol.* **2015**, *172*, 2675–2700, doi:10.1111/BPH.13096.
2. Cohen, P.; Cross, D.; Jänne, P.A. Kinase drug discovery 20 years after imatinib: progress and future directions. *Nat. Rev. Drug Discov. 2021 207* **2021**, *20*, 551–569, doi:10.1038/s41573-021-00195-4.
3. DP, B.; DM, F.; PA, E. Pseudokinases: update on their functions and evaluation as new drug targets. *Future Med. Chem.* **2017**, *9*, 245–265, doi:10.4155/FMC-2016-0207.
4. Richmond, L.; Keeshan, K. Pseudokinases: a tribble-edged sword. *FEBS J.* **2020**, *287*, 4170–4182, doi:10.1111/FEBS.15096.
5. Eyers, P.A.; Keeshan, K.; Kannan, N. Tribbles in the 21st Century: The Evolving Roles of Tribbles Pseudokinases in Biology and Disease. *Trends Cell Biol.* **2017**, *27*, 284–298, doi:10.1016/J.TCB.2016.11.002.
6. E, K.-T.; G, V.; WS, P. Tribbles at the cross-roads…. *Biochem. Soc. Trans.* **2015**, *43*, 1049–1050, doi:10.1042/BST20150122.
7. S, S.; A, M.; P, L.; R, M. TRIB1 Is Regulated Post-Transcriptionally by Proteasomal and Non-Proteasomal Pathways. *PLoS One* **2016**, *11*, doi:10.1371/JOURNAL.PONE.0152346.
8. J, W.; Y, Z.; W, W.; Y, Q.; L, M.; W, X.; Y, Y.; Q, P.; F, S. Impaired phosphorylation and ubiquitination by p70 S6 kinase (p70S6K) and Smad ubiquitination regulatory factor 1 (Smurf1) promote tribbles homolog 2 (TRIB2) stability and carcinogenic property in liver cancer. *J. Biol. Chem.* **2013**, *288*, 33667–33681, doi:10.1074/JBC.M113.503292.
9. JM, M.; Y, N.; SA, J.; W, D.; IS, L.; PD, M. Molecular Mechanism of CCAAT-Enhancer Binding Protein Recruitment by the TRIB1 Pseudokinase. *Structure* **2015**, *23*, 2111–2121, doi:10.1016/J.STR.2015.08.017.
10. T, Y.; Y, K.; Y, Y.; T, T.; S, M.; T, N. Trib1 links the MEK1/ERK pathway in myeloid leukemogenesis. *Blood* **2010**, *116*, 2768–2775, doi:10.1182/BLOOD-2009-10-246264.
11. Durzynska, I.; Xu, X.; Adelmant, G.; Ficarro, S.B.; Marto, J.A.; Sliz, P.; Uljon, S.; Blacklow, S.C. STK40 Is a Pseudokinase that Binds the E3 Ubiquitin Ligase COP1. *Structure* **2017**, *25*, 287–294, doi:10.1016/J.STR.2016.12.008.
12. Yu, H.; He, K.; Wang, L.; Hu, J.; Gu, J.; Zhou, C.; Lu, R.; Jin, Y. Stk40 represses adipogenesis through translational control of CCAAT/enhancer-binding proteins. *J. Cell Sci.* **2015**, *128*, 2881–2890, doi:10.1242/JCS.170282.
13. Yokoyama, T.; Nakamura, T. Tribbles in disease: Signaling pathways important for cellular function and neoplastic transformation. *Cancer Sci.* **2011**, *102*, 1115–1122, doi:10.1111/J.1349-7006.2011.01914.X.
14. R, D.; Z, S.; L, P.; LL, D. Drosophila tribbles antagonizes insulin signaling-mediated growth and metabolism via interactions with Akt kinase. *PLoS One* **2014**, *9*, doi:10.1371/JOURNAL.PONE.0109530.
15. D, X.; X, Z.; Y, Z.; J, Z.; J, L.; L, K.; H, Z. Tribbles homolog 2 promotes hepatic fibrosis and hepatocarcinogenesis through phosphatase 1A-Mediated stabilization of yes-associated protein. *Liver Int.* **2021**, *41*, 1131–1147, doi:10.1111/LIV.14782.

16. Ferreira, B.I.; Santos, B.; Link, W.; De Sousa-Coelho, A.L. Tribbles pseudokinases in colorectal cancer. *Cancers (Basel)*. **2021**, *13*, doi:10.3390/CANCERS13112825.
17. Dobens, L.L.; Bouyain, S. Developmental roles of tribbles protein family members. *Dev. Dyn.* **2012**, *241*, 1239–1248, doi:10.1002/DVDY.23822.
18. Kung, J.E.; Jura, N. The pseudokinase TRIB 1 toggles an intramolecular switch to regulate COP 1 nuclear export . *EMBO J.* **2019**, doi:10.15252/embj.201899708.
19. JJ, Y.; DD, Z.; XX, Y.; B, C.; FW, T.; J, W.; K, L.; S, S.; C, Z.; XX, L.; et al. TRIB3-EGFR interaction promotes lung cancer progression and defines a therapeutic target. *Nat. Commun.* **2020**, *11*, doi:10.1038/S41467-020-17385-0.
20. Shahrouzi, P.; Astobiza, I.; Cortazar, A.R.; Torrano, V.; Macchia, A.; Flores, J.M.; Niespolo, C.; Mendizabal, I.; Caloto, R.; Ercilla, A.; et al. Genomic and Functional Regulation of TRIB1 Contributes to Prostate Cancer Pathogenesis. *Cancers (Basel)*. **2020**, *12*, 2593, doi:10.3390/CANCERS12092593.
21. Kim, T.; Johnston, J.; Felipe, F.J.C.; Hamby, S.; Castillo-Lluva, S.; Consortium, T.C.; Goodall, A.H.; Velasco, G.; Ocana, A.; Muthana, M.; et al. TRIB1 regulates tumour growth via controlling tumour-associated macrophage phenotypes and is associated with breast cancer survival and treatment response. *bioRxiv* **2021**, 2021.06.07.446596, doi:10.1101/2021.06.07.446596.
22. Stefanovska, B.; André, F.; Fromigué, O. Tribbles Pseudokinase 3 Regulation and Contribution to Cancer. *Cancers 2021, Vol. 13, Page 1822* **2021**, *13*, 1822, doi:10.3390/CANCERS13081822.
23. J, A.-C.; M, G.; M, M.; K, R.; Y, F.; W, G.; C, B.; E, D.; T, Q.; P, T.; et al. Tribbles-1 as a novel biomarker of chronic antibody-mediated rejection. *J. Am. Soc. Nephrol.* **2008**, *19*, 1116–1127, doi:10.1681/ASN.2007101056.
24. ZY, L.; YQ, H.; YQ, Z.; ZD, H.; HC, H.; XH, L.; X, F.; QS, D.; C, C.; JH, C.; et al. MicroRNA-224 inhibits progression of human prostate cancer by downregulating TRIB1. *Int. J. cancer* **2014**, *135*, 541–550, doi:10.1002/IJC.28707.
25. B, T.; W, W.; Q, Z.; Y, S.; Y, C.; F, W.; X, W.; G, Q.; X, L.; F, T.; et al. Inhibition of tribbles protein-1 attenuates radioresistance in human glioma cells. *Sci. Rep.* **2015**, *5*, doi:10.1038/SREP15961.
26. Gendelman, R.; Xing, H.; Mirzoeva, O.K.; Sarde, P.; Curtis, C.; Feiler, H.S.; McDonagh, P.; Gray, J.W.; Khalil, I.; Korn, W.M. Bayesian network inference modeling identifies TRIB1 as a novel regulator of cell-cycle progression and survival in cancer cells. *Cancer Res.* **2017**, *77*, 1575–1585, doi:10.1158/0008-5472.CAN-16-0512.
27. KB, G.; TA, S.; S, H.; RJ, S.; JR, W.; J, Z.; S, A.; DG, T.; EC, P.; VA, R. Overexpression of TRIB2 in human lung cancers contributes to tumorigenesis through downregulation of C/EBPα. *Oncogene* **2011**, *30*, 3328–3335, doi:10.1038/ONC.2011.57.
28. Hill, R.; Kalathur, R.K.R.; Colaço, L.; Brandão, R.; Ugurel, S.; Futschik, M.; Link, W. TRIB2 as a biomarker for diagnosis and progression of melanoma. *Carcinogenesis* **2015**, *36*, 469–477, doi:10.1093/CARCIN/BGV002.
29. Yu, J. mei; Sun, W.; Wang, Z. he; Liang, X.; Hua, F.; Li, K.; Lv, X. xi; Zhang, X. wei; Liu, Y. ying; Yu, J. jiao; et al. TRIB3 supports breast cancer stemness by suppressing FOXO1 degradation and enhancing SOX2 transcription. *Nat. Commun.* **2019**, *10*, doi:10.1038/S41467-019-13700-6.

30. Hua, F.; Shang, S.; Yang, Y. wei; Zhang, H. zeng; Xu, T. lei; Yu, J. jiao; Zhou, D. dan; Cui, B.; Li, K.; Lv, X. xi; et al. TRIB3 Interacts With β-Catenin and TCF4 to Increase Stem Cell Features of Colorectal Cancer Stem Cells and Tumorigenesis. *Gastroenterology* **2019**, *156*, 708-721.e15, doi:10.1053/J.GASTRO.2018.10.031.
31. Guan, H.; Shuaib, A.; Leon, D.D. De; Angyal, A.; Salazar, M.; Velasco, G.; Holcombe, M.; Dower, S.K.; Kiss-Toth, E. Competition between members of the tribbles pseudokinase protein family shapes their interactions with mitogen activated protein kinase pathways. *Sci. Reports 2016 61* **2016**, *6*, 1–12, doi:10.1038/srep32667.
32. AH, S.; M, V. Characterizing Protein-Protein Interactions Using Mass Spectrometry: Challenges and Opportunities. *Trends Biotechnol.* **2016**, *34*, 825–834, doi:10.1016/J.TIBTECH.2016.02.014.
33. V, M.; A, M.; HR, V.; BM, B.; SW, van M. Quantitative liver proteomics identifies FGF19 targets that couple metabolism and proliferation. *PLoS One* **2017**, *12*, doi:10.1371/JOURNAL.PONE.0171185.
34. R, Y.; HR, V.; RM, van E.; J, C.; BM, B.; B, W.; A, de B. Chk1 and 14-3-3 proteins inhibit atypical E2Fs to prevent a permanent cell cycle arrest. *EMBO J.* **2018**, *37*, doi:10.15252/EMBJ.201797877.
35. R, van N.; AH, S.; P, P.; PW, J.; M, V.; HT, T. Quantitative dissection and stoichiometry determination of the human SET1/MLL histone methyltransferase complexes. *Mol. Cell. Biol.* **2013**, *33*, 2067–2077, doi:10.1128/MCB.01742-12.
36. E, K.; H, T.; A, H.; CP, V.; A, Z. The PHD type zinc finger is an integral part of the CBP acetyltransferase domain. *Mol. Cell. Biol.* **2002**, *22*, 1961–1970, doi:10.1128/MCB.22.7.1961-1970.2002.
37. EH, J.; O, van B.; AD, van D.; N, H.; BI, H.-S.; AM, B.; R, B.; E, K. Impaired peroxisome proliferator-activated receptor gamma function through mutation of a conserved salt bridge (R425C) in familial partial lipodystrophy. *Mol. Endocrinol.* **2007**, *21*, 1049–1065, doi:10.1210/ME.2006-0485.
38. Baymaz, H.I.; Spruijt, C.G.; Vermeulen, M. Identifying Nuclear Protein–Protein Interactions Using GFP Affinity Purification and SILAC-Based Quantitative Mass Spectrometry. *Methods Mol. Biol.* **2014**, *1188*, 207–226, doi:10.1007/978-1-4939-1142-4_15.
39. Y, Y.; JA, S.; S, K.; G, G.; G, S.; J, Y.; T, I.; Y, S.; V, R.; S, K.; et al. Arabidopsis COP10 forms a complex with DDB1 and DET1 in vivo and enhances the activity of ubiquitin conjugating enzymes. *Genes Dev.* **2004**, *18*, 2172–2181, doi:10.1101/GAD.1229504.
40. KG, G.; JF, R.; B, Z.; J, M.; P, V.; N, V.; C, B.; C, W.; DY, R.; O, C.; et al. A protein complex network of Drosophila melanogaster. *Cell* **2011**, *147*, 690–703, doi:10.1016/J.CELL.2011.08.047.
41. C, J.; C, D.; AC, M.; L, P.; Y, C.; C, C.; R, L.; P, L.; A, B.; P, F. TRB3 inhibits the transcriptional activation of stress-regulated genes by a negative feedback on the ATF4 pathway. *J. Biol. Chem.* **2007**, *282*, 15851–15861, doi:10.1074/JBC.M611723200.
42. Mayoral-Varo, V.; Jiménez, L.; Link, W. The critical role of trib2 in cancer and therapy resistance. *Cancers (Basel)*. **2021**, *13*, doi:10.3390/CANCERS13112701.
43. Hill, R.; Madureira, P.A.; Ferreira, B.; Baptista, I.; Machado, S.; Colaço, L.; dos Santos, M.; Liu, N.; Dopazo, A.; Ugurel, S.; et al. TRIB2 confers resistance to anti-cancer therapy by activating the serine/threonine protein kinase AKT. *Nat. Commun. 2017 81* **2017**, *8*, 1–9, doi:10.1038/ncomms14687.

44. Bauer, M.F.; Hofmann, S.; Neupert, W.; Brunner, M. Protein translocation into mitochondria: the role of TIM complexes. *Trends Cell Biol.* **2000**, *10*, 25–31, doi:10.1016/S0962-8924(99)01684-0.
45. Jamieson, S.A.; Ruan, Z.; Burgess, A.E.; Curry, J.R.; McMillan, H.D.; Brewster, J.L.; Dunbier, A.K.; Axtman, A.D.; Kannan, N.; Mace, P.D. Substrate binding allosterically relieves autoinhibition of the pseudokinase TRIB1. *Sci. Signal.* **2018**, *11*, doi:10.1126/SCISIGNAL.AAU0597.
46. N, A.D.; N, W.; S, Z.; Z, W.; RD, B.; J, Z.; C, R.; M, H.; J, S.; K, N.; et al. KIAA1217: A novel candidate gene associated with isolated and syndromic vertebral malformations. *Am. J. Med. Genet. A* **2020**, *182*, 1664–1672, doi:10.1002/AJMG.A.61607.
47. Davuluri, G.; Song, P.; Liu, Z.; Wald, D.; Sakaguchi, T.F.; Green, M.R.; Devireddy, L. Inactivation of 3-hydroxybutyrate dehydrogenase 2 delays zebrafish erythroid maturation by conferring premature mitophagy. *Proc. Natl. Acad. Sci. U. S. A.* **2016**, *113*, E1460–E1469, doi:10.1073/PNAS.1600077113.
48. Kume, K.; Iizumi, Y.; Shimada, M.; Ito, Y.; Kishi, T.; Yamaguchi, Y.; Handa, H. Role of N-end rule ubiquitin ligases UBR1 and UBR2 in regulating the leucine-mTOR signaling pathway. *Genes to Cells* **2010**, *15*, 339–349, doi:10.1111/J.1365-2443.2010.01385.X.
49. X, Z.; X, G.; X, Z.; G, J.; Y, W.; Q, C.; Q, J.; J, L.; C, Z. Usp16 regulates kinetochore localization of Plk1 to promote proper chromosome alignment in mitosis. *J. Cell Biol.* **2015**, *210*, 727–735, doi:10.1083/JCB.201502044.
50. Q, L.; W, Y.; D, B.; Q, F.; RA, C. Identification of a DOCK180-related guanine nucleotide exchange factor that is capable of mediating a positive feedback activation of Cdc42. *J. Biol. Chem.* **2006**, *281*, 35253–35262, doi:10.1074/JBC.M606248200.
51. A, A.; S, T. Diverse roles of WDR5-RbBP5-ASH2L-DPY30 (WRAD) complex in the functions of the SET1 histone methyltransferase family. *J. Biosci.* **2017**, *42*, 155–159, doi:10.1007/S12038-017-9666-9.
52. S, S.; MP, K.; JC, B. Uncovering the role of p53 splice variants in human malignancy: a clinical perspective. *Onco. Targets. Ther.* **2013**, *7*, 57–67, doi:10.2147/OTT.S53876.
53. Bech-Otschir, D.; Kraft, R.; Huang, X.; Henklein, P.; Kapelari, B.; Pollmann, C.; Dubiel, W. COP9 signalosome-specific phosphorylation targets p53 to degradation by the ubiquitin system. *EMBO J.* **2001**, *20*, 1630, doi:10.1093/EMBOJ/20.7.1630.
54. Kalkhoven, E. CBP and p300: HATs for different occasions. *Biochem. Pharmacol.* **2004**, *68*, 1145–1155, doi:10.1016/J.BCP.2004.03.045.
55. Ariyoshi, M.; Schwabe, J.W.R. A conserved structural motif reveals the essential transcriptional repression function of Spen proteins and their role in developmental signaling. *Genes Dev.* **2003**, *17*, 1909, doi:10.1101/GAD.266203.
56. Q, L.; F, Y.; M, W.; B, Z.; H, C.; W, W.; L, J.; Q, L.; JC, W. Novel human BTB/POZ domain-containing zinc finger protein ZBTB1 inhibits transcriptional activities of CRE. *Mol. Cell. Biochem.* **2011**, *357*, 405–414, doi:10.1007/S11010-011-0911-5.
57. Serra, R.W.; Fang, M.; Park, S.M.; Hutchinson, L.; Green, M.R. A KRAS-directed transcriptional silencing pathway that mediates the CpG island methylator phenotype. *Elife* **2014**, *3*, doi:10.7554/ELIFE.02313.

58. Kim, H.; Dejsuphong, D.; Adelmant, G.; Ceccaldi, R.; Yang, K.; Marto, J.A.; D'Andrea, A.D. Transcriptional repressor ZBTB1 promotes chromatin remodeling and translesion DNA synthesis. *Mol. Cell* **2014**, *54*, 107–118, doi:10.1016/J.MOLCEL.2014.02.017.
59. Kalkhoven, E.; Teunissen, H.; Houweling, A.; Verrijzer, C.P.; Zantema, A. The PHD type zinc finger is an integral part of the CBP acetyltransferase domain. *Mol. Cell. Biol.* **2002**, *22*, 1961–1970, doi:10.1128/MCB.22.7.1961-1970.2002.
60. Matic, I.; Schimmel, J.; Hendriks, I.A.; van Santen, M.A.; van de Rijke, F.; van Dam, H.; Gnad, F.; Mann, M.; Vertegaal, A.C.O. Site-specific identification of SUMO-2 targets in cells reveals an inverted SUMOylation motif and a hydrophobic cluster SUMOylation motif. *Mol. Cell* **2010**, *39*, 641–652, doi:10.1016/J.MOLCEL.2010.07.026.
61. Moosmann, P.; Georgiev, O.; Le Douarin, B.; Bourquin, J.P.; Schaffner, W. Transcriptional repression by RING finger protein TIF1 beta that interacts with the KRAB repressor domain of KOX1. *Nucleic Acids Res.* **1996**, *24*, 4859–4867, doi:10.1093/NAR/24.24.4859.
62. M, W.; J, B.; B, S.; ID, N.; HW, van L.; JA, R.; MA, V.; JJ, H.; KM, R.; FC, S.; et al. Tribbles homolog 3 denotes a poor prognosis in breast cancer and is involved in hypoxia response. *Breast Cancer Res.* **2011**, *13*, doi:10.1186/BCR2934.
63. Orea-Soufi, A.; Castillo-Lluva, S.; Salvador-Tormo, N.; Martín-Cabrera, P.; Recuero, S.; Gabicagogeascoa, E.; Moreno-valladares, M.; Mendiburu-Eliçabe, M.; Blanco-Gómez, A.; Ramos-Pittol, J.M.; et al. The Pseudokinase TRIB3 Negatively Regulates the HER2 Receptor Pathway and Is a Biomarker of Good Prognosis in Luminal Breast Cancer. *Cancers (Basel).* **2021**, *13*, doi:10.3390/CANCERS13215307.
64. King, K.L.; Cidlowski, J.A. CELL CYCLE REGULATION AND APOPTOSIS1. *http://dx.doi.org/10.1146/annurev.physiol.60.1.601* **2003**, *60*, 601–617, doi:10.1146/ANNUREV.PHYSIOL.60.1.601.
65. Mata, J.; Curado, S.; Ephrussi, A.; Rorth, P. Tribbles Coordinates Mitosis and Morphogenesis in Drosophila by Regulating String/CDC25 Proteolysis. *Cell* **2000**, *101*, 511–522, doi:10.1016/S0092-8674(00)80861-2.
66. Flavin, R.; Peluso, S.; Nguyen, P.L.; Loda, M. Fatty acid synthase as a potential therapeutic target in cancer. *Future Oncol.* **2010**, *6*, 551, doi:10.2217/FON.10.11.
67. RC, B.; M, S.; DM, C.; J, C.; MA, S.; BO, Y.; DJ, S.; DJ, R. Tribbles-1 regulates hepatic lipogenesis through posttranscriptional regulation of C/EBPα. *J. Clin. Invest.* **2015**, *125*, 3809–3818, doi:10.1172/JCI77095.
68. Sakamoto, K.M.; Aldana-Masangkay, G.I. The role of HDAC6 in cancer. *J. Biomed. Biotechnol.* **2011**, *2011*, doi:10.1155/2011/875824.
69. Lupo, A.; Cesaro, E.; Montano, G.; Zurlo, D.; Izzo, P.; Costanzo, P. KRAB-Zinc Finger Proteins: A Repressor Family Displaying Multiple Biological Functions. *Curr. Genomics* **2013**, *14*, 268, doi:10.2174/1389202911314999000 2.
70. P, Z.; Y, Y.; K, Q.; L, L.; C, Z.; X, F.; X, Z.; H, C.; Q, L.; S, C.; et al. A novel tumor suppressor ZBTB1 regulates tamoxifen resistance and aerobic glycolysis through suppressing HER2 expression in breast cancer. *J. Biol. Chem.* **2020**, *295*, 14140–14152, doi:10.1074/JBC.RA119.010759.

71. Zhou, S.; Liu, S.; Lin, C.; Li, Y.; Ye, L.; Wu, X.; Jian, Y.; Dai, Y.; Ouyang, Y.; Zhao, L.; et al. TRIB3 confers radiotherapy resistance in esophageal squamous cell carcinoma by stabilizing TAZ. *Oncogene 2020 3918* **2020**, *39*, 3710–3725, doi:10.1038/s41388-020-1245-0.
72. Liu, J.; Zhang, W.; Chuang, G.C.; Hill, H.S.; Tian, L.; Fu, Y.; Moellering, D.R.; Garvey, W.T. Role of TRIB3 in regulation of insulin sensitivity and nutrient metabolism during short-term fasting and nutrient excess. *Am. J. Physiol. - Endocrinol. Metab.* **2012**, *303*, E908, doi:10.1152/AJPENDO.00663.2011.
73. K, L.; F, W.; WB, C.; XX, L.; F, H.; B, C.; JJ, Y.; XW, Z.; S, S.; SS, L.; et al. TRIB3 Promotes APL Progression through Stabilization of the Oncoprotein PML-RARα and Inhibition of p53-Mediated Senescence. *Cancer Cell* **2017**, *31*, 697-710.e7, doi:10.1016/J.CCELL.2017.04.006.
74. Corcoran, C.A.; Luo, X.; He, Q.; Jiang, C.; Huang, Y.; Sheikh, M.S. Genotoxic and endoplasmic reticulum stresses differentially regulate TRB3 expression. *Cancer Biol. Ther.* **2005**, *4*, 1063–1067, doi:10.4161/CBT.4.10.2205.
75. Kandoth, C.; McLellan, M.D.; Vandin, F.; Ye, K.; Niu, B.; Lu, C.; Xie, M.; Zhang, Q.; McMichael, J.F.; Wyczalkowski, M.A.; et al. Mutational landscape and significance across 12 major cancer types. *Nat. 2013 5027471* **2013**, *502*, 333–339, doi:10.1038/nature12634.
76. Abbas, T.; Dutta, A. p21 in cancer: intricate networks and multiple activities. *Nat. Rev. Cancer* **2009**, *9*, 400, doi:10.1038/NRC2657.
77. Fhu, C.W.; Ali, A. Fatty Acid Synthase: An Emerging Target in Cancer. *Molecules* **2020**, *25*, doi:10.3390/MOLECULES25173935.
78. S, P.; ML, H.; E, F.; F, T.; E, M.; S, D.C.; S, B.; V, T.; M, C.; R, L.; et al. The functional Q84R polymorphism of mammalian Tribbles homolog TRB3 is associated with insulin resistance and related cardiovascular risk in Caucasians from Italy. *Diabetes* **2005**, *54*, 2807–2811, doi:10.2337/DIABETES.54.9.2807.

SUPPLEMENTARY NOTE

Supplementary Figure 1

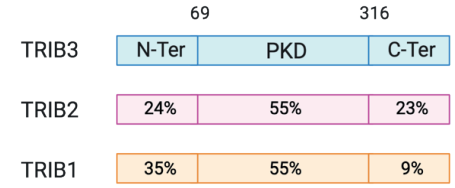

Supplementary Figure 1: Comparison of human TRIB1/2 and 3 protein sequence using Clustal Omega software.

Supplementary Figure 2

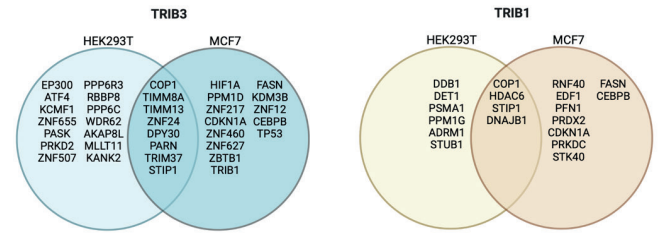

Supplementary Figure 2: Comparison of TRIB1 and TRIB3 interactors in HEK293T and MCF7 cells.

Velasco	Guillermo	Instituto de Investigacion Santaria, Hospital Clinico SanCarlos
Villacanas Perez	Oscar	MindtheByte Ltd
Wilson	Heather	The University of Sheffield

Chapter 4

The pseudokinase TRIB3 regulates adipose tissue homeostasis and adipocyte function

Miguel Hernández-Quiles[1]*, Laura Martinez Campesino[2]*, Imogen Morris[1], Zabran Ilyas[2], Paula Sobrevals Alcaraz[3], Ákos Varga[4], János Varga[4], Robert van Es[3], Harmjan Vos[3], Heather L. Wilson[2], Endre Kiss-Toth[2] and Eric Kalkhoven[1#]

[1] Center for Molecular Medicine, University Medical Center Utrecht, Utrecht University, 3584 CG Utrecht, The Netherlands.

[2] Department of Infection, Immunity and Cardiovascular Disease, Medical School, University of Sheffield, Sheffield S10 2TN, UK.

[3] Oncode Institute and Molecular Cancer Research, Center for Molecular Medicine, University Medical Center Utrecht, Utrecht University, 3584 CG Utrecht, The Netherlands.

[4] Department of Dermatology and Allergology, University of Szeged, H-6720 Szeged, Hungary.

[#] Corresponding author. Center for Molecular Medicine, University Medical Center Utrecht, Utrecht University, Utrecht, the Netherlands. E-mail: e.kalkhoven@umcutrecht.nl (E. Kalkhoven).

Abstract

Objective: *In vivo* studies in humans and mice have implicated the pseudokinase Tribbles 3 (TRIB3) in various aspects of energy metabolism. In addition, cell-based studies indicate a role for TRIB3 in adipocyte differentiation and function, but it is unclear if and how these cellular functions translate into overall metabolic health.

Methods: We investigated the metabolic phenotype of whole-body *Trib3* knockout mice, with a focus on adipocyte and adipose tissue functions. In addition, we combined lipidomics, transcriptomics, interactomics and phosphoproteomics analyses to elucidate cell-intrinsic functions of TRIB3 in (pre)adipocytes.

Results: While *Trib3* knockout mice display increased adiposity, their insulin sensitivity remains unaltered. *Trib3*^{KO} adipocytes are smaller and display higher PCNA levels, which point to i) altered proliferation-differentiation balance, ii) impaired expansion after cell division, or iii) an altered balance between lipid storage and release, or a combination thereof. Lipidome analyses indicate involvement in the latter 2 processes, as triglyceride storage is reduced and membrane composition, which can restrain cellular expansion, is altered. Integrated interactome, phosphoproteome and transcriptome analyses support a role for TRIB3 in all three cellular processes through multiple cellular pathways, including MAPK/ERK, PKA signaling and TCF7L2/beta catenin-mediated gene expression.

Conclusions: Rather than pointing to a single cellular pathway being affected, our findings support TRIB3 playing multiple distinct regulatory roles, in the cytoplasm, nucleus and mitochondria, in intertwined pathways in (pre)adipocytes, ultimately controlling adipose tissue homeostasis.

Keywords: Tribbles; adipocyte; omics analyses; Metabolism

1. Introduction

The prevalence of obesity and its related comorbidities have tripled since 1990 and the global incidence of type II diabetes is projected to reach 350 million cases by 2030 [1]. Obesity is a chronic, multifactorial disease, developed through the interaction between genetics and environmental factors, such as nutrition, physical activity and cultural influences [2-4]. The World Health Organization (WHO) defines obesity as an unhealthy state characterized by excessive and abnormal adiposity, this adipose alteration represents the first step into the development of chronic inflammation and insulin resistance that results in metabolic dysfunction [5]. Adipose tissue (AT) is responsible for the storage and release of free fatty acids in response to different metabolic needs as well as the regulation of whole-body metabolism through the production and secretion of adipose-specific chemokines [6, 7]. Adipocyte differentiation and function are tightly controlled by a set of pro- and anti-adipogenic factors; such as peroxisome proliferator- activated receptor y and CCAAT/enhancer binding proteins as pro-adipogenic factors [8] and Wnt signaling as anti-adipogenic factor [9, 10]. Prolonged and excessive exposure to a high caloric diet together with a sedentary lifestyle result in an increase in adipocyte number and size. These hypertrophic adipocytes become dysfunctional leading to a reduction in insulin sensitivity and overall metabolic health [11, 12]. In this context, understanding the mechanisms that govern adipocyte function and expandability is crucial for the development of new targeted therapies to improve insulin resistance and adipose metabolic health.

TRIB3 is a member of the Tribbles family of serine/threonine pseudokinases that functions as a protein scaffold, regulating a plethora of metabolic and cellular functions (reviewed in [13-15]). Tribbles act as interaction platforms promoting and inhibiting post-translational modification, such as ubiquitination and phosphorylation, or affecting protein-protein interactions [16], preventing or enhancing specific interactions, particularly relevant is the ability of TRIB3 to promote Wnt signaling by stabilizing the interaction between β-Catenin and TCF4 [17]. Thus, Tribbles have been shown to play a critical role in pathways that control cellular differentiation, lipid metabolism and immune cell activation among others [18-20]. Previous *in vivo* studies have pointed to TRIB3 as a critical regulator of glucose tolerance and insulin sensitivity [21-24], and *in vitro* studies have suggested a role for TRIB3 in adipocyte differentiation and function by regulating C/EBPβ [25] and Peroxisome Proliferator Activator Receptor y (PPARy) transcriptional activity [26]. Yet, the role of TRIB3 in adipocytes is far from being understood. In this study, we used a full body knock-out mice model and state-of-the-art mass spectrometry-

based proteomics approaches to determine the functional importance of TRIB3 in adipose tissue as well as assessing whether TRIB3 could be the target for future therapeutic approaches to improve insulin sensitivity and adipose tissue health. We found that TRIB3 ablation impairs adipocyte expandability and lipid profile, resulting in an increased adipose tissue mass composed of smaller adipocytes. In addition, we found that TRIB3 functions as an intermediate between molecules that regulate different signaling cascades in response to external stimulus. Our study presents TRIB3 as a critical signaling mediator that regulates AT expansion and homeostasis.

2. Materials and methods

2.1 Mice experiments licensing, husbandry and care

All experiments were performed in accordance with UK legislation under the Animals (Scientific Procedures) Act 1986. The University of Sheffield Project Review Committee approved all animal experiments which were carried out under the UK Home Office Project License 70/7992 held by Professor S.E. Francis, and Personal License to L. Martinez Campesino ID645D5F9. Mice were kept in an optimal and controlled environment to reduce mouse stress. Mice were subjected to 12 hours light/12 hours dark cycle, at 22oC with 40-60% of humidity. Their diet consisted of a standard chow (Harlan, 18% protein rodent diet) and it was unrestricted.

2.2 Mouse strains and genotyping

Full body *Trib3* knock out mice (*Trib3*KO) strain was developed using the gene-trap system. The gene trap vector targeted the first intron of the *Trib3* gene. The vector contained two expression cassettes, the first one encoded for the splice acceptor site and the b- Galactosidase and neomycin fusion protein, while the second cassette encoded for a diagnostic marker and the splice donor site. In this way, heterozygous mice (*Trib3*HET) [B6;129S5-*Trib*3Gt(OST324148)Lex/Ieg)] were generated and backcrossed with C57/BL6 mice for ten generations. New heterozygous animals were inter-crossed to finally obtain *Trib3*KO embryos. Genomic DNA isolated from mouse ear clips was amplified by PCR (Table 1) using specific primers for the *Trib3* WT and KO alleles (Table 2). Samples with a DNA ladder were run in a 2% (w/v) agarose gel, and the results were qualitatively analyzed using a trans-illuminator with EtBr/UV filter as shown in (Supplementary Figure 1). All the genotyping process was performed by the Genomics Core facility. Mice were weighed and culled via pharmacological overdose of 0.2ml sodium pentobarbital (200mg/ml) applied into the peritoneal cavity and cervical dislocation was performed as death confirmation. For mice used to assess atherosclerotic lesions or when blood was required, cervical dislocation was avoided, and cardiac puncture was performed following pentobarbital injection and prior breath cessation. Following loss of pedal reflex, the blood was collected into a heparinized syringe injected to the heart through the chest wall. Body as well as tissue weights were recorded.

Table 1. PCR conditions for genotyping

Process	Temperature	Time
Polymerase activation	95°C	5 min
Amplification 40x	95°C	30 sec
	65°C	30 sec
	72°C	30 sec
Inactivation	72°C	5 min

Table 2. Mouse *Trib3* primer sequences used for genotyping

Genotype	Primer sequence	Product size
WT	5'-CCGCGACGAATGAAAGGTTTA-3'	483 bp
	5'-AGACTCCGAGAGCTGCTCAGTTAGG-3'	
KO	5'-CCGCGACGAATGAAAGGTTTA-3'	381 bp
	5'-AAATGGCGTTACTTAAGCTAGCTTGC-3'	

2.3 Magnetic resonance imaging

15-week-old chow-fed male and female *Trib3*KO and *Trib3*WT mice (N=5 per group) were subjected to magnetic resonance imaging (MRI). Images were obtained using a 9.4 Tesla, Bruker Avance III MRI scanner (Bruker Biospin MRI GmbH, Ettlingen, Germany) with a 25mm 1H volume coil. Each mouse was placed in the center of the coil aligned with the abdomen and with the hips oriented at the top of the image. Structural MRI scans were performed using an MSME spin echo sequence (FOV 3.0x3.0 cm, 512x512 matrix, TE/TR 16ms/1000ms). A stack of contiguous slices of 1mm thick were taken for each mouse (35±1 slice per mouse in total) and processed using Bruker paravision 5.1 software. The slice package of MRI images was segmented and analyzed in FIJI/ImageJ. To align the fat measurements in the histograms, the location of the hips was used as standardized reference point. Intensity and threshold adjustment were performed for fat identification. Total adipose tissue, as well as subcutaneous (inguinal and dorsolumbar) and visceral (epididymal, mesenteric and perirenal) depots were distinguished based on their location.

2.4 Lipid profiling

Plasma was separated from isolated blood by centrifugation (1500xg for 5 min at room temperature) and immediately stored at -80oC. For analysis, 150µl of plasma was sent to the Department of Clinical Chemistry at the Royal Hallamshire Hospital (Sheffield Teaching Hospitals) to assess a full lipid profile measuring: total cholesterol, low (LDL) and high (HDL) density lipoproteins, triglycerides and glucose, using a Roche Cobas 8000 modular analyser series.

2.5 Glucose tolerance test (GTT) and insulin tolerance test (ITT)

Mice were fed on chow diet for at least 8 weeks and then fasted overnight. Fasting mice were weighted and blood was collected from the tail. A 20% glucose solution was prepared and filtered through 0.2 µm filter. For GTT, 2 mg of glucose were administrated per g of body weight and blood was collected at 0, 30, 60, 90 and 120 min after glucose challenge by tail sampling method. For ITT, mice were faster for at least 2h and then weighted. Then 0.75 mU insulin per gram of body weight was injected intraperitoneally. Using an insulin syringe. Blood glucose was measured at 0, 20, 40, and 60 minutes after injection.

2.6 Semi targeted lipidomics

shScramble and shTRIB3 3T3-L1 cells were differentiated in 6-well plates and once differentiated, cells were washed with 300µL of ice-cold PBS solution three times. 500µL of dry-ice cold methanol/water mix (80%/20%,v/v) was added and cells and scraped from the well. Cells were then collected and stored on dry ice or at at -80°C until lipidomic analysis.

2.7 Lipidomics

A volume of 50 µL homogenized cells was subjected to Liquid-Liquid extraction (LLE). The sample was vortex-mixed with methanol-methyl-tert-butylether (containing one internal standard per lipid class and an amount of antioxidant – BHT - to prevent lipid oxidation) after which an amount of water was added to induce phase separation. After incubation, the sample was centrifuged and the organic top layer containing all lipids was transferred to a clean sample vial. This lipid fraction was dried in a vacuum concentrator. Prior to analysis the lipid residue was dissolved in acetonitrile, thoroughly vortex mixed and transferred to an injection vial. LC-MS/MS sample analysis was conducted on an Ultimate 3000 UHPLC with LTQ-Orbitrap XL high resolution mass spectrometry detection. For chromatographic separation an Acquity BEH C18 column (2.1x100 mm, 1.7 µm) positioned in a 60°C column oven was used. Upon injection of 5 µL sample a 10 min gradient was started (total runtime 20 min per sample). Sample analysis was conducted in both positive mode and negative mode. Generated data were submitted to MZMine for alignment and data analysis. Raw data was uploaded and normalized via Metaboanalist 5.0. Principal component analysis (PCA) analysis and heat map generation was also performed via Metaboanalist 5.0 software [27]. Enrichment analysis of normalized lipidomic data, using 'ranking mode', was performed via LIONweb [28].

2.8 Stromal vascular cell fraction of adipose tissue and pre-adipocyte culture

Adipose tissue from *Trib3*KO and *Trib3*WT was dissected, minced and digested using a collagenase buffer (HBBS medium (Gibco), 2% (v/v) BSA (Sigma) and 1.4 mg/ml collagenase type II (Sigma)) to facilitate the dissociation between adipocytes and stromal vascular cells (SVC). To separate and discard adipocytes from SVCs, the digested tissue was filtered and centrifuged, and the supernatant containing adipocytes was removed. The cell pellet corresponding to the SVC fraction was then incubated with red blood cell (RBC) lysis buffer, neutralized and centrifuged again. The resulting cell pellet containing SVCs was further used for preadipocyte culture. The isolated SVC fraction from the AT digestion was cultured in complete DMEM media, changing media every 2 days. When 90% of confluency was reached, the cells were treated with differentiation media, consisting of complete DMEM media supplemented with 1µg/ml of Insulin (Sigma), 2.5µM Dexamethasone (Sigma) and 0.5µM 3-Isobutyl-1-methylxanthin (IBMX) (Sigma). After 48h, media was removed, and the cells were washed with PBS and fresh differentiation media was added for another 48h. After that time, cells were maintained with complete media supplemented with 1µg/ml of Insulin (Sigma) only for 7 days, until complete differentiation.

2.9 RNA extraction and reverse transcription (RT)-qPCR

Total RNA was isolated from pre-adipocytes and mature adipocytes was performed by using the RNeasy lipid tissue mini kit (Qiagen) following manufacturer's protocol. cDNA was synthesized using the Precision nanoScriptTM 2 RT kit (Primer design) according to manufacturer's instructions. Quantitative PCR was carried out using Precision PLUS SYBR-Green master mix (Primer design) in a Bio-Rad i-Cycler machine. Specific primers were designed with NCBI BLAST and all assays were performed in triplicate and normalized to the expression levels of CYCLO as a suitable house-keeping gene. Fold changes compared to the house-keeping genes were calculated using Ct method. Amplification and melting curves were checked for each reaction to ensure specific single products were amplified with >90% efficiency.

2.10 RNA sequencing and bioinformatic analyses

RNA was isolated from differentiated adipocytes from *Trib3*WT and *Trib3*KO mice (N=5, per group) using the RNeasy lipid tissue mini kit (Qiagen) according to manufacturer's instructions. Samples were then sent to Novogene Co. Ltd (https://en.novogene.com) and used for messenger RNA sequencing. RNA samples were assessed using nanodrop for preliminary quantitation, agarose gel electrophoresis to test degradation and contamination and Agilent 2100 to assess RNA integrity and final quantitation. For cDNA library construction, mRNA was enriched using oligo(dT) beads, randomly fragmented following cDNA synthesis. Then cDNA libraries were assessed for quality control and qualified libraries were used for sequencing using Illumina sequencers (NovaSeq platform). The obtained raw data files were analyzed and quality controls on the fastq files, principal component analysis and differentially expressed gene analysis was performed. Data was analyzed using Ingenuity Pathway Analysis software (IPA, Qiagen). Data will be deposited in the NCBI GEO database and accession number will be provided upon submission of the manuscript.

2.11 Tissue sections and staining

Tissue sections were dewaxed in xylene, rehydrated in graded alcohols (100%-75% v/v) and rinsed in water following incubation in Gills hematoxylin solution for 5 min. The slides were then rinsed in running water, submerged in Scott's Tap-Water for 30 seconds and rinsed in water again. Eosin-phloxine was used for counter-staining following water rinse and dehydration in graded alcohols and xylene. Slides were then mounted with coverslips using DPX mounting solution (Sigma-Aldrich, UK). Images to assess tissue morphology were taken using a brightfield microscope (Nikon Eclipse E6000) at 10x and 20x magnification. Three fields of view per tissue per mouse were captured and analyzed using Image J software. Adiposoft software [29] was used to asses adipocyte area.

2.12 Cell culture

The immortalized murine-derived brown pre-adipocyte cell line (IBA) [30, 31] were cultured in high-glucose (4.5 g/L d-glucose) DMEM medium (Life technologies, Carlsbad, CA) supplemented with 10% bovine serum and 1% penicillin and streptomycin. Cells were incubated in 5% CO_2 incubator at 37°C and 95% humidity. Generation of inducible TRIB3- tGFP IBA cells was done using third-generation lentiviral constructs using supernatants form HEK293T (ATCC CRL-3216, Manassas, VA, USA) cells transfected with lentiviral packaging plasmids. HEK293T cells were transfected using X-treme gene 9 DNA transfection reagent (Roche) following manufacturer's instructions.

2.13 Western blot analysis

Western blotting was performed as described before [32]. In short, after induction with doxycycline cells were lysed in iced-cold lysis buffer (150 mM NaCl, 1% NP40, 0.5% sodium DOC, 0.1% SDS, 25 mM Tris pH7.4 and supplemented with protease inhibitors). Protein concentrations were measured and samples were supplemented with Laemmli sample Buffer (LSB). Samples were run in SDS-PAGE gels and transfer to PVDF membranes. Blocking was performed in 5% milk in TBS-T for 45 minutes at room temperature. ECL western blot solution was used to detect protein expression using a LAS4000 Image Quant.

2.14 Immunoprecipitation

Immunoprecipitation was performed as described previously [33] using turboGFP-Trap beads (Chromotek) after 24/48h induction with doxycycline.

2.15 Mass spectrometry

Mass spectrometry methodology was extensively described previously [33] In short, precipitated proteins were digested with trypsin (250 ng/µL) and peptides were separated from beads using a C-18 stage tip (3M, St Paul, MN, USA). After separation peptides were electro-sprayed directly into an Orbitrap Fusion Tribrid Mass Spectrometer (Thermo Scientific). The MS was run in DDA mode with one cycle per second. Full scan (400-1500 mass range) at a resolution of 240,000 Ions was performed reaching an intensity threshold of 10,000. Ions were isolated by the quadrupole and fragmented with an HCD collision energy of 30%. The obtained data was analyzed with MaxQuant [Version 1.6.3.4] using the Uniprot fasta file (UP000000589) of Mus musculus (Taxonomy ID: 10090).

2.16 Phosphoproteomics

Enrichment of phospho-peptides for SILAC labeling, MCF7 TRIB3-KD cells or scramble control cells were cultured in high-glucose (10% dialyzed FBS (BioWest)) DMEM (Thermo) lacking lysine and arginine supplemented with Lys-0/Arg-0 or Lys-8/Arg-10 (Silantes). Cells were lysed in 8 M Urea, 1M Ammonium-BiCarbonate (ABC) containing 10 mM Tris(2- carboxyethyl)phosphine hydrochloride (TCEP) and 40mM 2-chloro-acetamide supplemented with protease inhibitors (Roche, complete EDTA-free) and 1% (v/v) phosphatase inhibitor cocktails 2 and 3 (Sigma, Cat. No. P5726 and Cat. No. P0044). After ultra-sonication, Heavy and light cell lysates were mixed 1:1 and proteins (20mg total) were over-night in solution digested with trypsin (1:50) (Worthington). Peptides were desalted using SepPack columns (Waters) and eluted in 80% acetonitrile (ACN). To enrich for phospho-peptides, 200 mg Calcium Titanium Oxide (CaTiO3) powder (Alfa Aesar, 325 mesh) was equilibrated 3 times with binding solution (6% Acetic acid in 50% ACN pH=1

with HCl) after which the phospho-peptides were allowed to bind at 40 ˚C for 10 minutes on a shaker. After 6 times centrifugation and washing, phospho-peptides were eluted twice with 200µl 5% NH3. The peptides were dried using a SpeedVac and the dissolved in buffer A (0.1% FA) before loading on in-house made C18 stage-tips and divided with high PH elution into three fractions (100mM NH3/FA PH=10 in 5%, 10% or 50% ACN).

2.17 Data analysis

Raw files were analyzed with the Maxquant software version 1.6.3.4 (Cox and Mann, 2008) with phosphorylation of serine, threonine and tyrosine as well as oxidation of methionine set as variable modifications, and carbamidomethylation of cysteine set as fixed modification. The Human protein database of Uniprot (January 2019) was searched with both the peptide as well as the protein false discovery rate set to 1%. The SILAC quantification algorithm was used in combination with the 'match between runs' tool (option set at two minutes). Peptides were filtered for reverse hits and standard contaminants. Forward and Reverse ratios were plotted in R (www.r-project.org). The mass spectrometry proteomics data will be deposited to the ProteomeXchange Consortium via the PRIDE partner repository (http://www.ebi.ac.uk/pride) upon manuscript submission.

3. Results

3.1 TRIB3 expression is increased in hypertrophic adipocytes and its expression correlates with different metabolic traits

First, we used publicly available databases to assess the expression of TRIB3 in adipose tissue (AT). We found that TRIB3 is highly expressed in human AT, and in particular in the adipocyte fraction (Figure 1A). In addition, we found that TRIB3 expression is elevated in AT of individuals with obesity compared to lean individuals (Figure 1B). Furthermore, TRIB3 expression is elevated in fully mature adipocytes (day 21) compared to undifferentiated adipose tissue-derived stromal stem cells (ASCs) and early differentiation state (day 7) (Figure 1C). In addition, we used a well-characterized mouse hybrid panel [34] to assess whether adipose specific TRIB3 expression correlates with any phenotypic trait [35]. We found that TRIB3 expression in AT positively correlates with leptin levels and negatively with weight and non-abdominal fat (Supplementary figure 2). Altogether, these data point to TRIB3 as a potential regulator of adipose tissue function(s) and metabolic health.

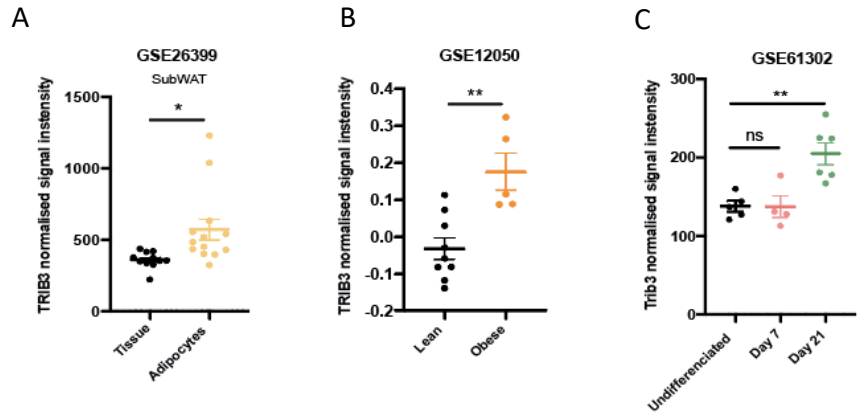

Figure 1. (A) TRIB3 expression in human subcutaneous adipose tissue (GSE26399). **(B)** TRIB3 expression is higher in obese individuals compare to lean (GSE12050). **(C)** TRIB3 expression in ASCs (GSE61302).

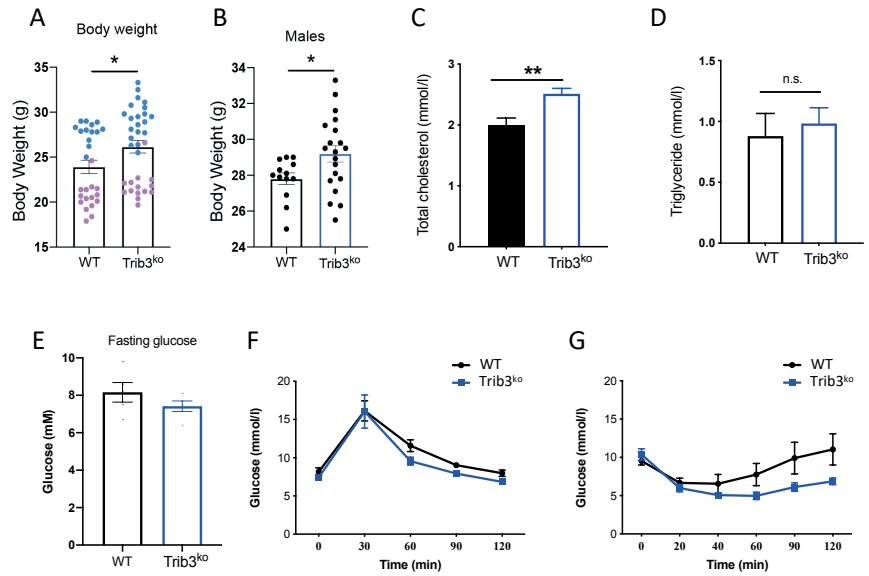

Figure 2. *Trib3*^{KO} mice show increased body weight and altered cholesterol and glucose homeostasis. **(A)** Body weight of 15-week-old males and females from *Trib3*^{KO} and WT mice. **(B)** Body weight of 15-week-old *Trib3*^{KO} and WT male mice. **(C)** Cholesterol levels in plasma from *Trib3*^{KO} male mice compared to wildtype littermates. **(D)** Plasma Triglyceride levels in *Trib3*^{KO} male mice compared to wildtype littermates. **(E)** Measured of fasting glucose levels in *Trib3*^{KO} male mice compared to wildtype littermates. **(F)** Glucose tolerance test. **(G)** Insulin tolerance test. Unpaired T-test (*p ≤ 0.05. **p ≤ 0.01. ***p ≤ 0.001. ****p ≤ 0.0001, N.S = not significant).

3.2 *Trib3*^{KO} mice show increased body weight, altered cholesterol and glucose homeostasis

To investigate the role of TRIB3 in AT we analyzed this tissue in *Trib3* full body knockout mice (*Trib3*^{KO}). Fifteen-week-old chow-fed *Trib3*^{KO} mice had increased body weight (26.16 ± 0.71 g) compared to wild-type littermates (*Trib3*^{WT}) (23.92 ± 0.74 g) (Figure 2A). When stratified by sex, only males had an increased body weight compared to wild-type littermates (Figure 2B), hence the focus on male mice for the rest of the study. *Trib3*^{KO} mice showed a significant increase in plasma total cholesterol (Fig. 2C) but not in plasma triglycerides (Figure 2D) or fasting glucose levels (Figure 2E). In addition, glucose tolerance test (GTT) indicated no difference in glucose clearance in *Trib3*^{KO} mice compared to wild type animals (Fig. 2F). Next, we performed an insulin tolerance test to assess insulin sensitivity in these animals and observed that *Trib3*^{KO} mice recover circulating glucose levels similar to the wild-type littermates after the insulin bolus (Figure 2G). Taken together, *Trib3*^{KO} mice display increased body weight and cholesterol levels that were not accompanied by altered plasma triglyceride levels or overt insulin resistance.

3.3 Adipose tissue mass and adipocyte size is affected in the *Trib3*^{KO} mice

To gain insight into the potential anatomical reasons for the observed difference in body weight in male *Trib3*^{KO} *vs. Trib3*^{WT} mice we performed magnetic resonance imaging (MRI) to assess body fat composition. Image slices were aligned at the hip level and the total adipose area per slide was quantified, shown as white area within the image (Supplementary figure 3). The total fat volume per mouse showed a trend toward increased adiposity (Figure 3A), which was significant when fat depots were analyzed separately. In fact, we found that the difference in body weight is mainly due to an increase in the inguinal fat depot (subcutaneous white adipose tissue, subWAT; Fig. 3B) and a moderate increase in epididymal WAT (visceral white adipose tissue, visWAT; Fig. 3C). This difference in adiposity was also accompanied by a change in adipocyte size. Quantifications from H&E staining of sections from inguinal and epididymal fat depots (Fig. 3D) confirmed that *Trib3* deletion results in significantly smaller adipocytes in the subWAT with a shifted frequency distribution towards smaller cell size (Figure 3E). Similar differences albeit less pronounced were found in visWAT (Figure 3F). Furthermore, the expression of Proliferating Cell Nuclear antigen (PCNA), a well-known marker of proliferating cells [36], was increased in the subWAT of *Trib3*^{KO} mice when compared to wild type littermates at the mRNA and protein level (Figure 3G). Together these data suggest that TRIB3 plays a role in adipose tissue expansion and remodeling, with the strongest effects in subWAT where the absence of TRIB3 increases adipocyte proliferation and/or constrains cell size.

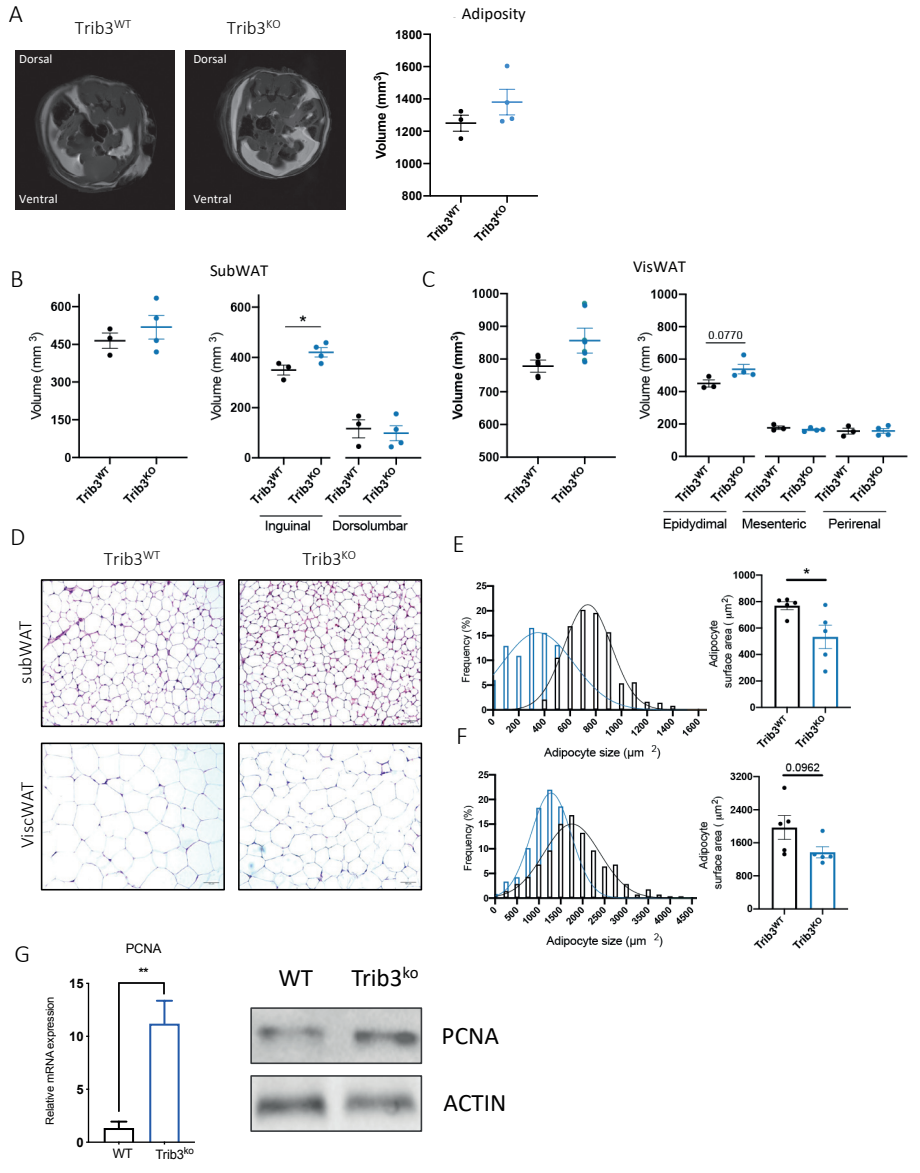

Figure 3. *Trib3*^{KO} mice display increased body weight and adiposity with smaller adipocytes. **(A)** Representative MRI cross-sectional images showing the fat distribution at the abdominal region and total adipose quantification. **(B)** Quantitative analysis of the total volume and the individual depot volumes of the subcutaneous **(B)** and visceral **(C)** adipose tissue by MRI. **(D)** Representative hematoxylin & eosin (H&E) stained subcutaneous (inguinal) and visceral (epidydimal) adipose tissue sections. Scale bar, 50 µm. Quantification of the mean adipocyte surface area and frequency distribution of adipocyte size of the H&E sections from the subcutaneous **(E)** and visceral **(F)** described depots. Graphs are presented as Mean ± SEM, unpaired student's T test, *p<0.05. **(G)** PCNA expression and protein levels in subWAT.

3.4 TRIB3 regulates the overall lipid profile of adipocytes

The reduced adipocyte size observed upon *in vivo Trib*3 ablation (Figure 3) could have different causes, including impaired expansion after cell division, an altered balance between lipid storage and release, or a combination thereof. To investigate these possibilities and exclude communication with other cell types and/or organs we generated mouse 3T3-L1 (pre)adipocytes with stable shRNA-mediated knockdown (KD) of *Trib3* (Supplementary Figure 4). First, we measured intracellular TG levels. Mature *Trib3* KD adipocytes displayed lower intracellular TG levels (Figure 4A), suggesting that *Trib3* is required to maintain a proper balance between lipid storage and release. To obtain a deeper understanding of the role of *Trib3* in lipid handling, we performed semi-targeted lipidomics, which allows in-depth total lipidome profiling by using lipid class standards to define the individual species within that class. *Trib3* KD in mature 3T3-L1 adipocytes resulted in changes in the lipid profile of these cells as shown by initial principal component analysis (PCA), where the lipidome in KD cells clusters separately from control counterparts (Figure 4B). The reduction of *Trib3* levels had broad and significant effects on the cellular lipid profile (Figure 4C). Amongst others, some membrane components were elevated (phosphatidylethanolamines (PE), phosphatidylglycerols (PG), ceramides (Cer), and phosphatidylinositol (PI)) whilst others were reduced (phosphatidylserine (PS), phosphatidylcholine (PC)), suggesting altered membrane composition and thereby potentially altered expandability. We further analyzed these data using LIONweb, an online ontology enrichment tool specifically designed to associate lipid species to biological features and functions [28]. Several processes and lipid classes linked to membrane functions were enriched (e.g. 'Glycerophosphoethanolamines' and 'Very high lateral diffusion' respectively); Figure 4C). Interestingly, the LIONweb category 'Mitochondrion' was also enriched, suggesting a yet unidentified role of TRIB3 in biology (see Discussion). In summary, the reduction of *Trib3* levels alters the balance between lipid storage and release, and potentially also their expandability through altered lipid composition of membrane components, which together may present cell-autonomous mechanisms contributing to the smaller adipocyte size observed in *Trib3*^{KO} mice (Fig. 3).

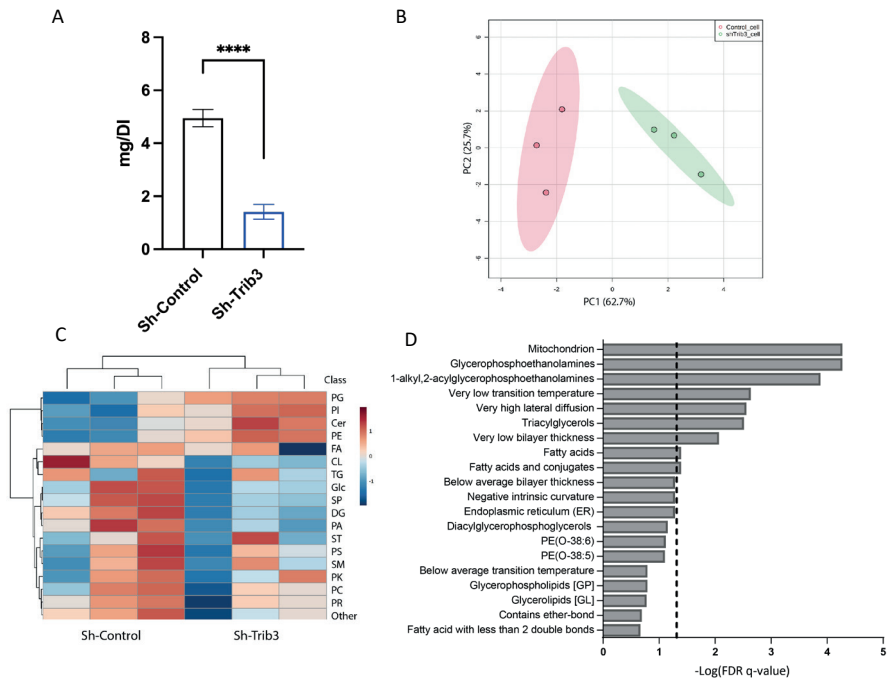

Figure 4. Knockdown of *Trib3* in 3T3-L1 adipocytes alters lipid profiles. (A) TG content of scrambled and *Trib3* shRNA KD 3T3-L1 adipocytes. **(B)** Principal component analysis of Sh-*Trib3* and Sh-Control lipidome. **(C)** Semitargeted lipidomics analysis identifies 577 lipid species total. Heat map of average lipid class abundance highlight *Trib3*'s total adipose lipid profile alteration. **(D)** LIONweb enrichment analysis of semi-targeted lipidomic data ranking mode showing the top 20 enrichment hits, black line designating threshold for significance.

3.5 Integrated omics identifies multiple TRIB3-dependent pathways regulating lipid handling and proliferation-differentiation in (pre)adipocytes

To identify cellular pathways that may underly the effects of *Trib3* ablation on the lipidome (Fig. 4), ultimately resulting in altered adiposity and reduced adipocyte size *in vivo* (Fig. 3), we employed a combination of omics approaches, including interactome, phosphoproteome and transcriptome analyses. We first analyzed the TRIB3 interactome, employing our previously developed mass spectrometry-based approach [33]. We generated inducible TRIB3-tGFP cell lines in mouse IBA (pre)adipocytes, an accessible and versatile model to study adipocyte biology [31], and induced TRIB3-tGFP expression with doxycycline for 24h at day 0 and day 6 of

adipocyte differentiation (Figure 5A); differentiation was monitored by expression of Fabp4 (Figure 5B). Subsequently, we identified TRIB3 interacting proteins by immunoprecipitating TRIB3-tGFP with a nanobody against tGFP coupled to agarose beads, followed by mass spectrometry analyses of the immunoprecipitated proteins. Among the interactors found at day 0, two serine/threonine protein kinases stand out: the Serine/Threonine kinase 1 (AKT1), a previously reported TRIB3 interacting protein that regulates –amongst others– insulin signaling [37], and MAPK6/ERK3, an atypical MAP kinase that is member of the extracellular-regulated kinases. Other interacting proteins included proteins involved in RNA binding and processing (DHX16, CCDC124 and UTP3) and microtubule associated proteins such as CCDC66 and GPHN. Interestingly, we found mitochondrial importer proteins of the TIMM/TOMM complex that we have previously identified as TRIB3 interacting proteins in cancer cells [33] and USP30, a deubiquitylation enzyme involved in mitochondrial fusion [38]. Similar to the interacting proteins identified prior to differentiation, we found that TRIB3 interacts with ERK/MAPK pathway proteins in mature adipocytes, such as TAOK1, MAPK6, PRKD2 and SIPA1L2, confirming the regulatory role of TRIB3 on ERK/MAPK signaling and described by us and others in multiple cellular contexts [39- 41]. In addition, we found the same mitochondrial transporters (TIMM13, TIMM8A1 and TIMM8B) together with two other mitochondrial proteins (STOML2 and NDUFB10). In contrast with the interacting proteins detected at day 0, at day 6 we found a high number of proteins that can be linked to transcriptional regulation such as NACC1, ASHL2, ETV6 and CTNNB1/m-catenin. NACC1 and ETV6 are associated with transcriptional repression and have been linked with ovarian cancer progression [42, 43] and leukemia [44] respectively, nad neither has been reported as an interactor of TRIB3 before. In contrast, ASHL2 and CTNNB1/m-catenin have been previously described as TRIB3 interactors. ASHL2 is a member of the WRAD complex, responsible for histone-3 lysine-4 methylation in mammalian cells, and we and others have previously reported the interaction between TRIB3 and subunits of the MLL- WRAD complex [33, 45, 46]. Previous studies have also reported the interaction between TRIB3 and m-catenin, showing that TRIB3 promotes Wnt signaling by interacting with CTNNB1/m-catenin and TCF4 and enhancing their transcriptional activity [17, 47, 48]. In adipocytes, Wnt signaling regulates the balance between proliferation and differentiation, promoting pre-adipocyte proliferation whilst inhibiting terminal differentiation into mature adipocytes [10, 49]. Taken together, the (pre)adipocyte TRIB3 interactome spans many different protein classes (e.g. kinases and transcriptional regulators) as well as cellular localizations (e.g. cytoplasm, nucleus and mitochondria), which may directly or indirectly link to proliferation, cell size and lipid storage and release.

Since interactome analyses may be limited by the strength and stability of the interactions, we complemented the TRIB3 interactome studies with TRIB3-dependent phosphoproteome analyses. While TRIB3 is not able to phosphorylate target proteins due to the lack of the metal binding motif in the kinase domain, it can interact with canonical kinases and regulate their function [50], as also observed here (Figure 5). We again used the inducible TRIB3-tGFP IBA cells described above and subjected these to SILAC-based quantitative proteomics. Cells were maintained in media containing heavy or light amino acids (lysine and arginine) for 5 passages and incorporation of labeled amino acids was assessed prior to the beginning of the experiment (data not shown). TRIB3-tGFP lines were induced with doxycycline for 24h on differentiated IBA cells, and then the phospho-proteome of induced vs uninduced differentiated TRIB3-tGFP cells was compared together with the reverse experiment (Figure 6 A). Among the top 15 canonical pathways that were found, dysregulated mTOR and insulin receptor signaling was the most significant (Figure 6B), in line with the interactome data (Figure 5) and previous studies [37, 51]. In addition, pathways that control whole-body energy balance were found to be dysregulated, including the ERK/MAPK and AMPK and PKA pathways. AMPK (AMP-activated protein kinase) inhibits fatty acid and cholesterol synthesis in adipocytes upon low levels of nutrients [52]. On the other hand, PKA is a major regulator of mitochondrial biogenesis and lipolysis, enhancing browning of WAT and the release of fatty acids from the lipid droplets by phosphorylation of lipases and perilipin [53, 54]. Moreover, the induction of TRIB3 affects the G2/M DNA damage checkpoint and ATM signaling, which, together with the result from the previous section where p53 was found as an interacting partner of TRIB3, situates the pseudokinase as a pivotal regulator of the cell cycle in adipocytes. Analysis of the upstream regulators reveals kinases and other protein complexes that are altered by TRIB3 in adipocytes (Figure 6C). Among the most significant upregulated are EGF, AKT1, GH1 and MAPK1, it is also worth mentioning the downregulation of p53, PTEN and PTPN11 according to the Z-score generated. We also find several transcription factors that have changed their phosphorylation status upon TRIB3 induction, including ATF4, ATF7 and STAT3. These results indicate that TRIB3 is able to regulate adipocyte function, modulating the activation of mTOR, insulin signaling and ERK/MAPK pathways, resulting in changes in transcription factor activation that drive adipocyte function. Finally, we analyzed the effect of *Trib3* depletion on adipocyte gene expression. The stromal vascular fraction (SVF) from subcutaneous and visceral WAT depots from $Trib3^{KO}$ and $Trib3^{WT}$ male mice was isolated, expanded and differentiated into mature adipocytes as shown before [55](Figure 7A). Adipocyte differentiation was evaluated by mRNA expression of markers such as *Pparγ, Lpl*, *Fabp4 and Adipoq* (encoding adiponectin). We found that *Trib3* deficient cells displayed significantly higher levels of *Pparγ*

and *Fabp*4 when compared to WT cells, while *Adipoq* and *Lpl* showed a strong but not significant trend of upregulation in the *Trib*3 deficient cells (Figure 7B). When the same markers were assessed in *ex-vivo* differentiated SVF from visceral WAT similar trends were observed albeit to a lesser extent (Supplementary Figure 5), in line with the stronger effect of *Trib3* ablation on subcutaneous AT volume and adipocyte size compared to vWAT (Figure 3 B-F).To gain a more comprehensive insight into *Trib3*-dependent changes in adipocyte transcriptional programmes, transcriptome analyses of ex vivo differentiated adipocytes from subcutaneous WAT of *Trib3*^{KO} and *Trib3*^{WT} mice were performed. Pathway analysis of differentially expressed genes (Ingenuity Pathway Analysis (Qiagen)) was performed and revealed 41 altered canonical pathways and 64 diseases and functions significantly affected by *Trib3* deficiency (Supplementary Table 1). The top altered canonical pathways in *Trib3*^{KO} adipocytes include downregulated pathways involved in lipid homeostasis (TAG degradation and PKA signaling) in line with our lipidome, interactome and phosphoproteome data (Figures 4-6). Among all the molecules that were found significantly dysregulated (p-value < 0.05) 'transcription regulator' was the most frequent molecule type identified (Figure 7D). Within this category, the top activated molecule was TCF7L2 while HOXA10 was the most inhibited (Figure 4D). TCF7L2 (also known as TFC4) is the endpoint of the Wnt/- Catenin signaling cascade which has been implicated in adipocyte differentiation and function [56, 57] as well as the Wnt/-Catenin pathway being associated with TRIB3 in multiple other cell types [17, 47, 48]. The homeobox transcription factor HOXA10 has also been implicated in adipocyte differentiation and function [58].

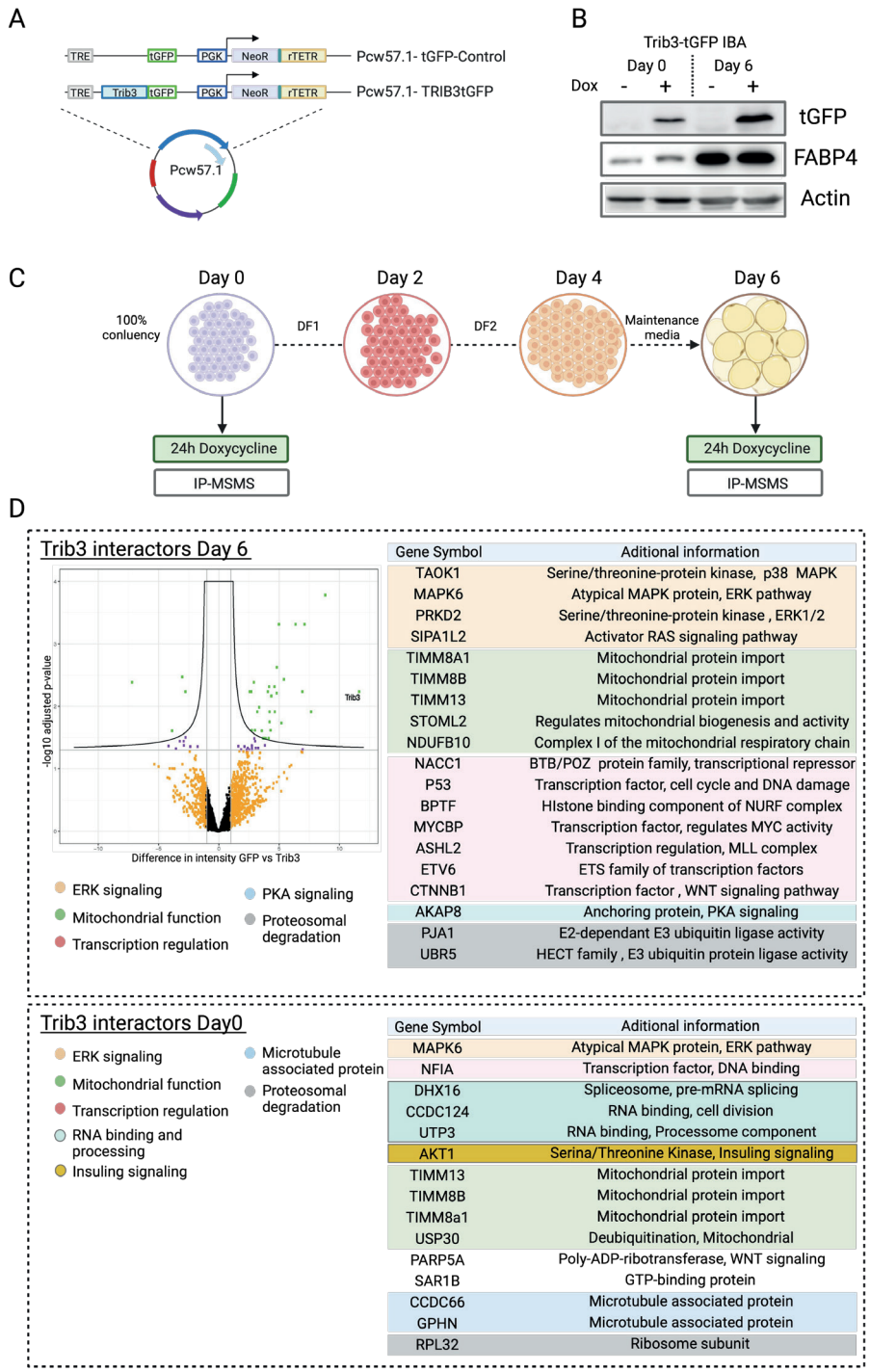

> Figure 5. Trib3 interacting proteins in (pre)adipocytes. (A) Doxycycline inducible constructs used to generate TRIB3-tGFP and tGFP control cell lines in IBA cells. **(B)** Western blots showing induction of TRIB3-tGFP only upon doxycycline induction, FABP4 as adipocyte differentiation marker and actin as loading control. **(C)** Schematic representation of adipocyte differentiation. **(D)** Table of TRIB3 interacting protrins in Undifferetaietd (Day 0) and differentiated (Day 6) IBA (pre)adipocytes.

Taken together, our integrated omics approaches indicate that i) TRIB3 can interact with a large set of proteins in adipocytes, including various kinases, such as AKT and MAPK6, and transcriptional regulators, such as CTNNB1//-catenin, ii) TRIB3 can directly or indirectly alter signaling pathways in adipocytes, such as mTOR, MAPK and PKA signaling, iii) depletion of *Trib3* affects the adipocyte transcriptome, with dominant effects on the transcription factors TCF7L2 and HOXA10. Rather than pointing to a single cellular pathway being affected, these findings support TRIB3 playing multiple roles, both in the cytoplasm and the nucleus and potentially also in mitochondria, in intertwined pathways, ultimately contributing to an optimal balance in proliferation vs. differentiation capacity, and proper lipid storage. As a consequence, ablation of *Trib3* affects the proliferation-differentiation balance and net lipid storage in *Trib3* full body knockout mice adipose tissue.

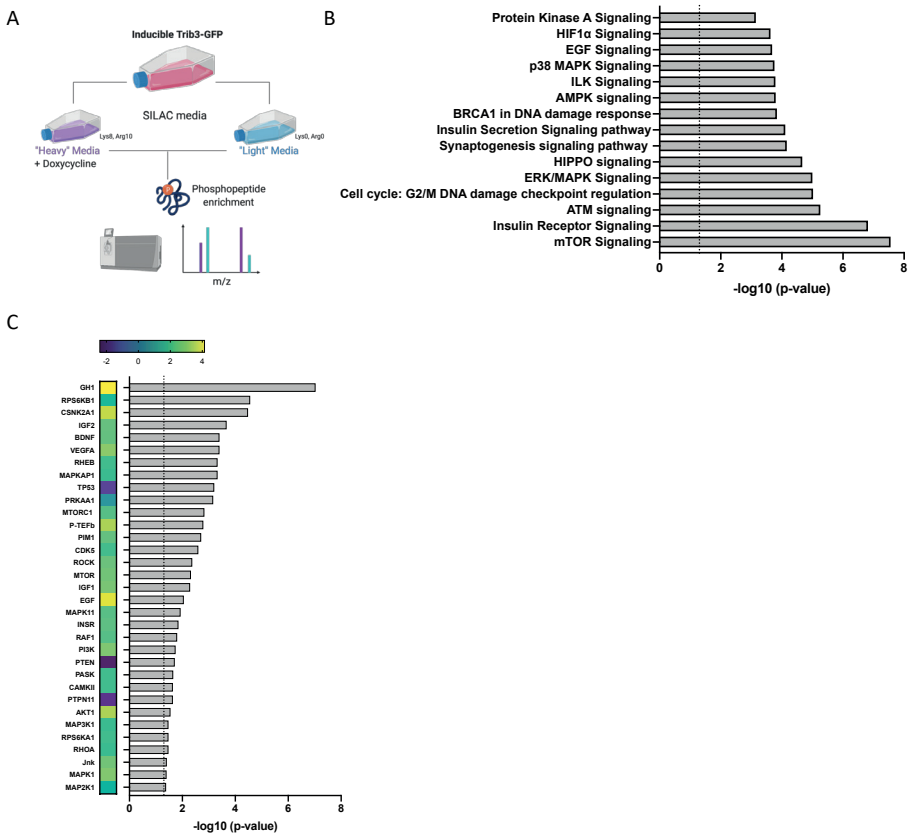

Figure 6. TRIB3 induction alters mTOR and MAPK signaling and affects adipocyte cell cycle progression. (A) Schematic representation of TRIB3-tGFP IBA cells in heavy and light SILAC media. **(B)** Top 15 altered canonical pathways of phospho-peptides found up or downregulated. **(C)** Altered upstream kinases, protein complexes and enzymes according to Ingenuity pathway analysis (Quiagen).

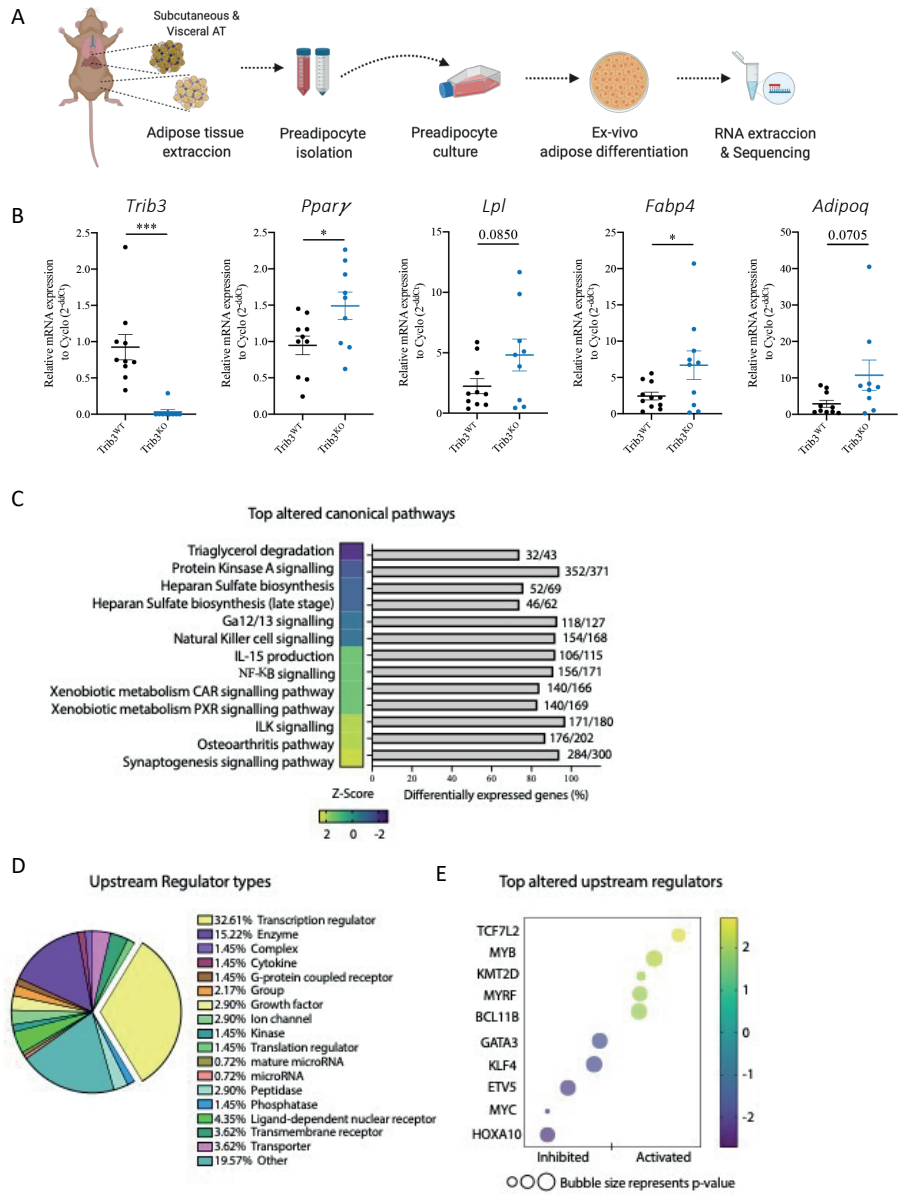

Figure 7. RNA sequencing of *ex-vivo* differentiated adipocytes reveals differences in gene expression profiles between *Trib3*^{KO} adipocytes and wild type. (A) Schematic representation of preadipocyte isolation and ex-vivo differentiation. (**B)** Expression of *Trib3*, *Pparγ*, *Lpl*, *Fabp4* and *Adipoq* in ex-vivo differentiated adipocytes. **(C)** Top altered canonical pathways found dysregulated in the RNAseq of the ex-vivo differentiated subWAT of the Trib3^{ko} mice compared to WT littermates. **(D)** Upstream regulators analysis of RNA-seq dataset using Ingenuity pathway analysis (Qiagen). **(E)** Top altered upstream regulators indicating p-value and activation Z-score.

Discussion

In vivo studies in humans and mice have indicated that the pseudokinase TRIB3 regulates energy metabolism [59, 60], and cell-based studies suggest a role in adipocytes [26], but it was unknown if these observations are causally linked. We found that whole-body ablation of *Trib3* in mice results in adipose tissue expansion while insulin sensitivity was maintained. We detected more and smaller adipocytes in the KO animals, a phenotype that has frequently been associated with insulin sensitivity [61-63]. Using a combination of lipodome, interactome, phosphoproteome and transcriptome analyses, we found a multifaceted role for TRIB3 in proliferation, TG storage and cellular expansion, potentially regulated through multiple cellular pathways, including for example MAPK/ERK and PKA signaling and TCF7L2/beta catenin-mediated gene expression. In support of these various molecular roles, TRIB3 has been reported to be localized in the cytoplasm and the nucleus [39], and to interact with a large set of cellular proteins in various biological settings [17, 64]. Interestingly, the TRIB3 interactome in adipocytes reported here as well as the interactomes in MCF7 breast cancer cells and HEK297T cells, we reported earlier [33], all suggest a potential role for TRIB3 in mitochondria, which will be the focus of future studies.

Our combined interactome and phosphoproteome analyses indicate that TRIB3 functions as an integrator of signaling pathways in adipocytes, being able to regulate kinases downstream of membrane receptors, such as AKT1, mTOR or ERK3, and transcription factors such as CTNNB1 or ASH2L that drive transcription of key factors of adipose biology. Regarding the interactions with kinases and proteins that regulate kinases, TRIB3 seems to regulate their substrate specificity skewing these kinases in certain directions. The effect of TRIB3 on transcription factor activity is also complex. TRIB3 has been shown to interact and modulate the activity of a number of transcription factors [17, 65], and can repress transcription through recruitment of repressor proteins like ZBTB1 [33] or interference with recruitment of transcriptional activators like the MLL complex [66]. In agreement with other studies [17] we describe an interaction between TRIB3 and CTNNB1/-catenin (Fig. 5) and also report upregulation of TCF7L2-mediated transcription upon ablation of *Trib3* (Figure 7E). Together, these findings suggest that TRIB3 may negatively regulate Wnt signaling in adipocytes, for example through recruiting aforementioned repressor proteins or preventing CTNNB1//-catenin from entering the nucleus. Such a model, in which reduction of TRIB3 stimulates Wnt signaling requires additional experimental studies, especially since Wnt activity impairs adipogenesis [10, 49] and TRIB3 has been described as a positive regulator of Wnt signaling in various cancer types [17, 47, 48].

Smaller adipocytes, as observed here in *Trib3* KO mice, have been associated with insulin sensitivity [61-63], and in fact, numerous therapeutic approaches have been used in the past to increase adipocyte proliferation in order to increase the number of small adipocytes [67]. While this suggests that targeting TRIB3 in adipocytes for degradation may represent a rational therapeutic approach, it should be noted that drug targeting of Tribbles and specifically TRIB3 represents a chimera, as discussed elsewhere [15, 68, 69]. Furthermore, it should be noted that adipocyte-specific targeting of TRIB3 may be required and that the role of TRIB3 in for example AT resident immune cells, which can also affect adipocyte size and functionality [70], has not been addressed directly yet. While the current study supports the view that TRIB3 is a critical regulator of adipocyte proliferation, homeostasis and function, future studies are clearly needed to address its therapeutic potential.

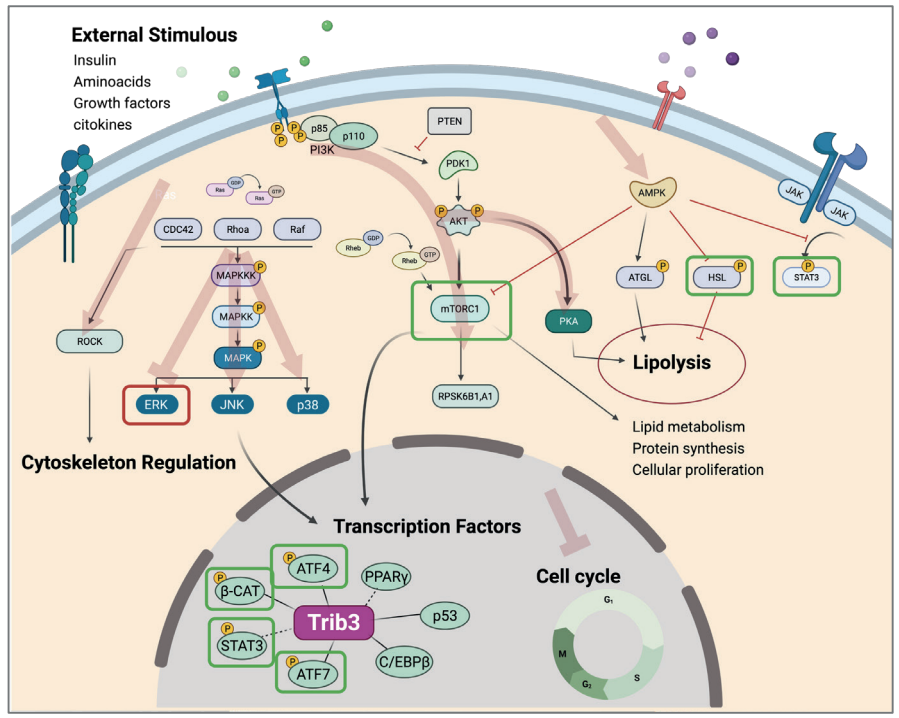

Figure 8: Schematic representation of effects of TRIB3 overexpression in adipocytes.

Author contribution statement: MHQ, LMP, IM, ZI, PSA, RE and HV performed the experiments, data-analysis, and wrote the manuscript; AV and JV performed patient inclusion and detailed clinical assessment. HLW, EKT and EK designed and supervised the study. All authors reviewed the manuscript.

Acknowledgements: This study was supported by grants from the European Union's Horizon 2020 Marie Skłodowska-Curie Innovative Training Network, TRAIN (project No. 721532) and a combined Diabetes Breakthrough grant from the Dutch Diabetes Research Foundation and The Netherlands Organisation for Health Research and Development (ZonMW; project No. 459001006). We thank Dr. Balázs Bende and Prof. Dr. Lajos Kemény for their support with the recruitment of the volunteers and the organization of the human study. We also thank members of the Marie Skłodowska-Curie Innovative Training Network TRAIN and members of the Kalkhoven and van Mil laboratories (both UMC Utrecht) for helpful discussions. Figures were created using BioRender.com.

Conflict of interest: The authors report no conflicts of interest in this work

References

1. Hogan, P., et al., *Economic costs of diabetes in the US in 2002*. Diabetes Care, 2003. **26**(3): p. 917-32.
2. Melmer, A., P. Kempf, and M. Laimer, *The Role of Physical Exercise in Obesity and Diabetes*. Praxis (Bern 1994), 2018. **107**(17-18): p. 971-976.
3. Czech, M.P., *Insulin action and resistance in obesity and type 2 diabetes.* Nat Med, 2017. **23**(7): p. 804-814.
4. Jung, U.J. and M.S. Choi, *Obesity and its metabolic complications: the role of adipokines and the relationship between obesity, inflammation, insulin resistance, dyslipidemia and nonalcoholic fatty liver disease.* Int J Mol Sci, 2014. **15**(4): p. 6184- 223.
5. Guilherme, A., et al., *Adipocyte dysfunctions linking obesity to insulin resistance and type 2 diabetes.* Nat Rev Mol Cell Biol, 2008. **9**(5): p. 367-77.
6. Zwick, R.K., et al., *Anatomical, Physiological, and Functional Diversity of Adipose Tissue.* Cell Metab, 2018. **27**(1): p. 68-83.
7. van Eijkeren, R.J., et al., *Endogenous lipid antigens for invariant natural killer T cells hold the reins in adipose tissue homeostasis*. Immunology, 2018. **153**(2): p. 179-189.
8. Moseti, D., A. Regassa, and W.K. Kim, *Molecular Regulation of Adipogenesis and Potential Anti-Adipogenic Bioactive Molecules*. Int J Mol Sci, 2016. **17**(1).
9. Bagchi, D.P., et al., *Wnt/beta-catenin signaling regulates adipose tissue lipogenesis and adipocyte-specific loss is rigorously defended by neighboring stromal-vascular cells.* Mol Metab, 2020. **42**: p. 101078.
10. Prestwich, T.C. and O.A. Macdougald, *Wnt/beta-catenin signaling in adipogenesis and metabolism.* Curr Opin Cell Biol, 2007. **19**(6): p. 612-7.
11. Chouchani, E.T. and S. Kajimura, *Metabolic adaptation and maladaptation in adipose tissue.* Nat Metab, 2019. **1**(2): p. 189-200.
12. Schenk, S., M. Saberi, and J.M. Olefsky, *Insulin sensitivity: modulation by nutrients and inflammation.* J Clin Invest, 2008. **118**(9): p. 2992-3002.
13. Kiss-Toth, E., G. Velasco, and W.S. Pear, *Tribbles at the cross-roads.* Biochem Soc Trans, 2015. **43**(5): p. 1049-50.
14. Richmond, L. and K. Keeshan, *Pseudokinases: a tribble-edged sword.* FEBS J, 2020. **287**(19): p. 4170-4182.
15. Eyers, P.A., K. Keeshan, and N. Kannan, *Tribbles in the 21st Century: The Evolving Roles of Tribbles Pseudokinases in Biology and Disease.* Trends Cell Biol, 2017. **27**(4): p. 284- 298.
16. Murphy, J.M., et al., *Molecular Mechanism of CCAAT-Enhancer Binding Protein Recruitment by the TRIB1 Pseudokinase.* Structure, 2015. **23**(11): p. 2111-21.
17. Hua, F., et al., *TRIB3 Interacts With beta-Catenin and TCF4 to Increase Stem Cell Features of Colorectal Cancer Stem Cells and Tumorigenesis.* Gastroenterology, 2019. **156**(3): p. 708-721 e15.
18. Qi, L., et al., *TRB3 links the E3 ubiquitin ligase COP1 to lipid metabolism.* Science, 2006. **312**(5781): p. 1763-6.

19. Niespolo, C., et al., *Tribbles-1 Expression and Its Function to Control Inflammatory Cytokines, Including Interleukin-8 Levels are Regulated by miRNAs in Macrophages and Prostate Cancer Cells.* Front Immunol, 2020. **11**: p. 574046.
20. Bauer, R.C., et al., *Tribbles-1 regulates hepatic lipogenesis through posttranscriptional regulation of C/EBPalpha.* J Clin Invest, 2015. **125**(10): p. 3809-18.
21. Kwon, M., et al., *Skeletal Muscle Tissue Trib3 Links Obesity with Insulin Resistance by Autophagic Degradation of AKT2.* Cell Physiol Biochem, 2018. **48**(4): p. 1543-1555.
22. Zhang, W., et al., *Skeletal Muscle TRIB3 Mediates Glucose Toxicity in Diabetes and High- Fat Diet-Induced Insulin Resistance.* Diabetes, 2016. **65**(8): p. 2380-91.
23. Prudente, S., et al., *TRIB3 R84 variant affects glucose homeostasis by altering the interplay between insulin sensitivity and secretion.* Diabetologia, 2010. **53**(7): p. 1354- 61.
24. Lee, S.K., et al., *TRIB3 Is Highly Expressed in the Adipose Tissue of Obese Patients and Is Associated With Insulin Resistance.* J Clin Endocrinol Metab, 2022. **107**(3): p. e1057- e1073.
25. Bezy, O., et al., *TRB3 blocks adipocyte differentiation through the inhibition of C/EBPbeta transcriptional activity.* Mol Cell Biol, 2007. **27**(19): p. 6818-31.
26. Takahashi, Y., et al., *TRB3 suppresses adipocyte differentiation by negatively regulating PPARgamma transcriptional activity.* J Lipid Res, 2008. **49**(4): p. 880-92.
27. Xia, J., et al., *MetaboAnalyst: a web server for metabolomic data analysis and interpretation.* Nucleic Acids Res, 2009. **37**(Web Server issue): p. W652-60.
28. Molenaar, M.R., et al., *LION/web: a web-based ontology enrichment tool for lipidomic data analysis.* Gigascience, 2019. **8**(6).
29. Galarraga, M., et al., *Adiposoft: automated software for the analysis of white adipose tissue cellularity in histological sections.* J Lipid Res, 2012. **53**(12): p. 2791-6.
30. Klein, J., et al., *Novel adipocyte lines from brown fat: a model system for the study of differentiation, energy metabolism, and insulin action.* Bioessays, 2002. **24**(4): p. 382- 8.
31. Chen, W., et al., *ZFP30 promotes adipogenesis through the KAP1-mediated activation of a retrotransposon-derived Pparg2 enhancer.* Nat Commun, 2019. **10**(1): p. 1809.
32. Jeninga, E.H., et al., *Impaired peroxisome proliferator-activated receptor gamma function through mutation of a conserved salt bridge (R425C) in familial partial lipodystrophy.* Mol Endocrinol, 2007. **21**(5): p. 1049-65.
33. Hernandez-Quiles, M., et al., *Comprehensive Profiling of Mammalian Tribbles Interactomes Implicates TRIB3 in Gene Repression.* Cancers (Basel), 2021. **13**(24).
34. Wang, S., et al., *Genetic and genomic analysis of a fat mass trait with complex inheritance reveals marked sex specificity.* PLoS Genet, 2006. **2**(2): p. e15.
35. Wu, C.C., et al., *GeneNetwork: an interactive tool for reconstruction of genetic networks using microarray data.* Bioinformatics, 2004. **20**(18): p. 3691-3.
36. Kelman, Z., *PCNA: structure, functions and interactions.* Oncogene, 1997. **14**(6): p. 629-40.
37. Du, K., et al., *TRB3: a tribbles homolog that inhibits Akt/PKB activation by insulin in liver.* Science, 2003. **300**(5625): p. 1574-7.

38. Nakamura, N. and S. Hirose, *Regulation of mitochondrial morphology by USP30, a deubiquitinating enzyme present in the mitochondrial outer membrane.* Mol Biol Cell, 2008. **19**(5): p. 1903-11.
39. Mondal, D., A. Mathur, and P.K. Chandra, *Tripping on TRIB3 at the junction of health, metabolic dysfunction and cancer.* Biochimie, 2016. **124**: p. 34-52.
40. Hong, B., et al., *TRIB3 Promotes the Proliferation and Invasion of Renal Cell Carcinoma Cells via Activating MAPK Signaling Pathway.* Int J Biol Sci, 2019. **15**(3): p. 587-597.
41. Guan, H., et al., *Competition between members of the tribbles pseudokinase protein family shapes their interactions with mitogen activated protein kinase pathways.* Sci Rep, 2016. **6**: p. 32667.
42. Shih Ie, M., et al., *Amplification of the ch19p13.2 NACC1 locus in ovarian high-grade serous carcinoma.* Mod Pathol, 2011. **24**(5): p. 638-45.
43. Wang, J., et al., *A protein interaction network for pluripotency of embryonic stem cells.* Nature, 2006. **444**(7117): p. 364-8.
44. Hock, H. and A. Shimamura, *ETV6 in hematopoiesis and leukemia predisposition.* Semin Hematol, 2017. **54**(2): p. 98-104.
45. van Nuland, R., et al., *Quantitative dissection and stoichiometry determination of the human SET1/MLL histone methyltransferase complexes.* Mol Cell Biol, 2013. **33**(10): p. 2067-77.
46. Hernández-Quiles, M., et al., *TRIB3 Modulates PPARγ-Mediated Growth Inhibition by Interfering with the MLL Complex in Breast Cancer Cells.* International Journal of Molecular Sciences, 2022. **23**(18): p. 10535.
47. Zhang, X., et al., *TRIB3 promotes lung cancer progression by activating beta-catenin signaling.* Eur J Pharmacol, 2019. **863**: p. 172697.
48. Lu, Y., et al., *TRIB3 confers glioma cell stemness via interacting with beta-catenin.* Environ Toxicol, 2020. **35**(6): p. 697-706.
49. de Winter, T.J.J. and R. Nusse, *Running Against the Wnt: How Wnt/beta-Catenin Suppresses Adipogenesis.* Front Cell Dev Biol, 2021. **9**: p. 627429.
50. Izrailit, J., et al., *High throughput kinase inhibitor screens reveal TRB3 and MAPK- ERK/TGFbeta pathways as fundamental Notch regulators in breast cancer.* Proc Natl Acad Sci U S A, 2013. **110**(5): p. 1714-9.
51. Salazar, M., et al., *TRIB3 suppresses tumorigenesis by controlling mTORC2/AKT/FOXO signaling.* Mol Cell Oncol, 2015. **2**(3): p. e980134.
52. Bijland, S., S.J. Mancini, and I.P. Salt, *Role of AMP-activated protein kinase in adipose tissue metabolism and inflammation.* Clin Sci (Lond), 2013. **124**(8): p. 491-507.
53. Wicksteed, B. and L.M. Dickson, *PKA Differentially Regulates Adipose Depots to Control Energy Expenditure.* Endocrinology, 2017. **158**(3): p. 464-466.
54. Yehuda-Shnaidman, E., et al., *Acute stimulation of white adipocyte respiration by PKA- induced lipolysis.* Diabetes, 2010. **59**(10): p. 2474-83.
55. Siersbaek, M.S., et al., *Genome-wide profiling of peroxisome proliferator-activated receptor gamma in primary epididymal, inguinal, and brown adipocytes reveals depot- selective binding correlated with gene expression.* Mol Cell Biol, 2012. **32**(17): p. 3452- 63.

56. Bagchi, D.P. and O.A. MacDougald, *Wnt Signaling: From Mesenchymal Cell Fate to Lipogenesis and Other Mature Adipocyte Functions.* Diabetes, 2021. **70**(7): p. 1419- 1430.
57. Chen, X., et al., *The Diabetes Gene and Wnt Pathway Effector TCF7L2 Regulates Adipocyte Development and Function.* Diabetes, 2018. **67**(4): p. 554-568.
58. Karastergiou, K., et al., *Distinct developmental signatures of human abdominal and gluteal subcutaneous adipose tissue depots.* J Clin Endocrinol Metab, 2013. **98**(1): p. 362-71.
59. Liu, J., et al., *Role of TRIB3 in regulation of insulin sensitivity and nutrient metabolism during short-term fasting and nutrient excess.* Am J Physiol Endocrinol Metab, 2012. **303**(7): p. E908-16.
60. Liu, J., et al., *Mammalian Tribbles homolog 3 impairs insulin action in skeletal muscle: role in glucose-induced insulin resistance.* Am J Physiol Endocrinol Metab, 2010. **298**(3): p. E565-76.
61. McLaughlin, T., et al., *Enhanced proportion of small adipose cells in insulin-resistant vs insulin-sensitive obese individuals implicates impaired adipogenesis.* Diabetologia, 2007. **50**(8): p. 1707-15.
62. Yang, J., et al., *The size of large adipose cells is a predictor of insulin resistance in first- degree relatives of type 2 diabetic patients.* Obesity (Silver Spring), 2012. **20**(5): p. 932- 8.
63. Laforest, S., et al., *Adipocyte size as a determinant of metabolic disease and adipose tissue dysfunction.* Crit Rev Clin Lab Sci, 2015. **52**(6): p. 301-13.
64. Yu, J.J., et al., *TRIB3-EGFR interaction promotes lung cancer progression and defines a therapeutic target.* Nat Commun, 2020. **11**(1): p. 3660.
65. Ord, T., et al., *Pharmacological or TRIB3-Mediated Suppression of ATF4 Transcriptional Activity Promotes Hepatoma Cell Resistance to Proteasome Inhibitor Bortezomib.* Cancers (Basel), 2021. **13**(10).
66. Hernandez-Quiles, M., et al., *TRIB3 Modulates PPARgamma-Mediated Growth Inhibition by Interfering with the MLL Complex in Breast Cancer Cells.* Int J Mol Sci, 2022. **23**(18).
67. Boden, G., et al., *Effect of thiazolidinediones on glucose and fatty acid metabolism in patients with type 2 diabetes.* Metabolism, 2003. **52**(6): p. 753-9.
68. Jamieson, S.A., et al., *Substrate binding allosterically relieves autoinhibition of the pseudokinase TRIB1.* Sci Signal, 2018. **11**(549).
69. Eyers, P.A. and J.M. Murphy, *The evolving world of pseudoenzymes: proteins, prejudice and zombies.* BMC Biol, 2016. **14**(1): p. 98.
70. van Eijkeren, R.J., et al., *Cytokine Output of Adipocyte-iNKT Cell Interplay Is Skewed by a Lipid-Rich Microenvironment.* Front Endocrinol (Lausanne), 2020. **11**: p. 479.

Supplementary figures

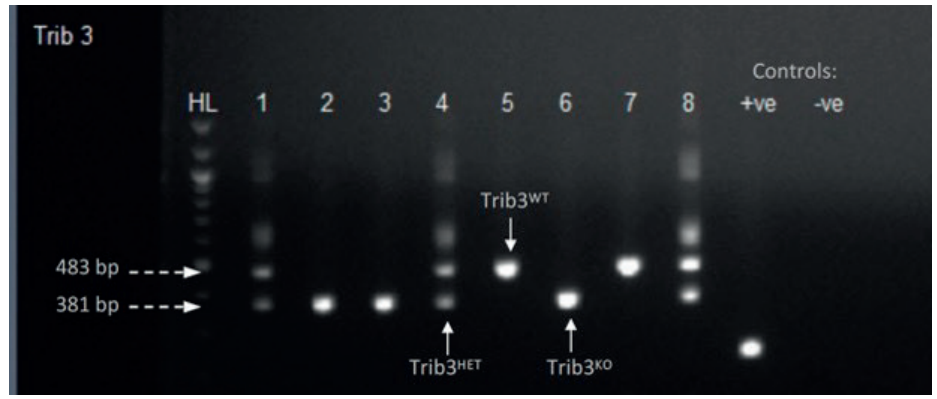

Suppl. Figure 1. Trib3 genotyping results. Result example to assess the genotype of mice from the *Trib3*KO strain. As it is shown, a single band at 381bp corresponds to the mutant allele (*Trib3* with the gene-trap vector inserted – *Trib3*KO), while the band at 483bp corresponds to the *Trib3*WT allele. The presence of both bands indicates heterozygosis (*Trib3*HET). The gel also includes positive and negative controls to ensure the reliability of the PCR.

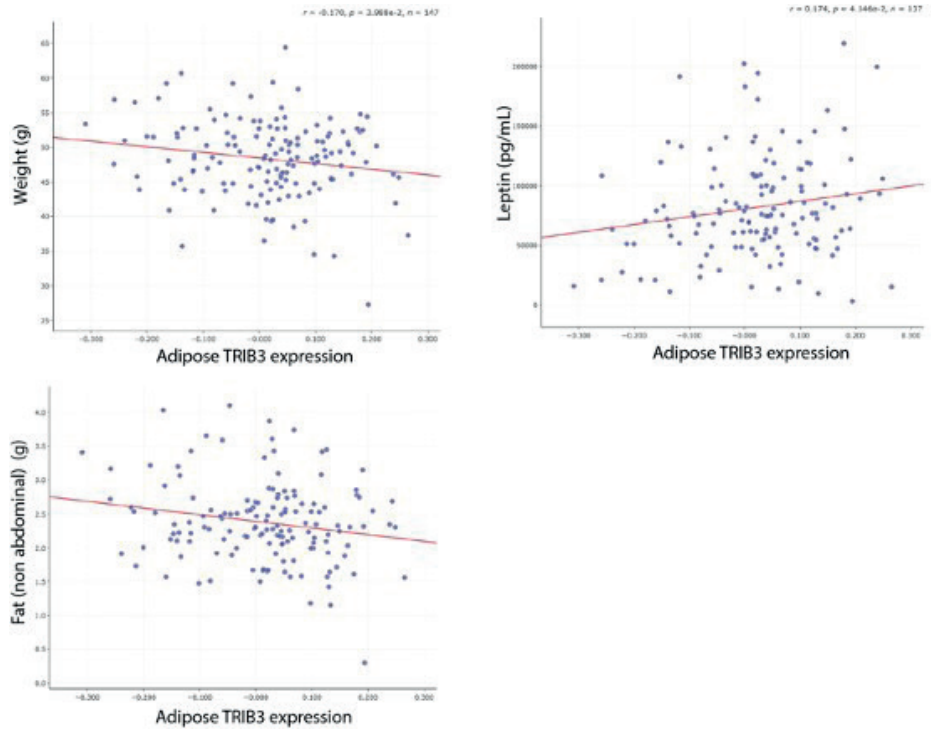

Suppl. Figure 2. correlations between TRIB3 expression in mouse white adipose tissue (WAT) and bodyweight, leptin levels and non-abdominal fat from an F2 intercross study (BHF2 population).

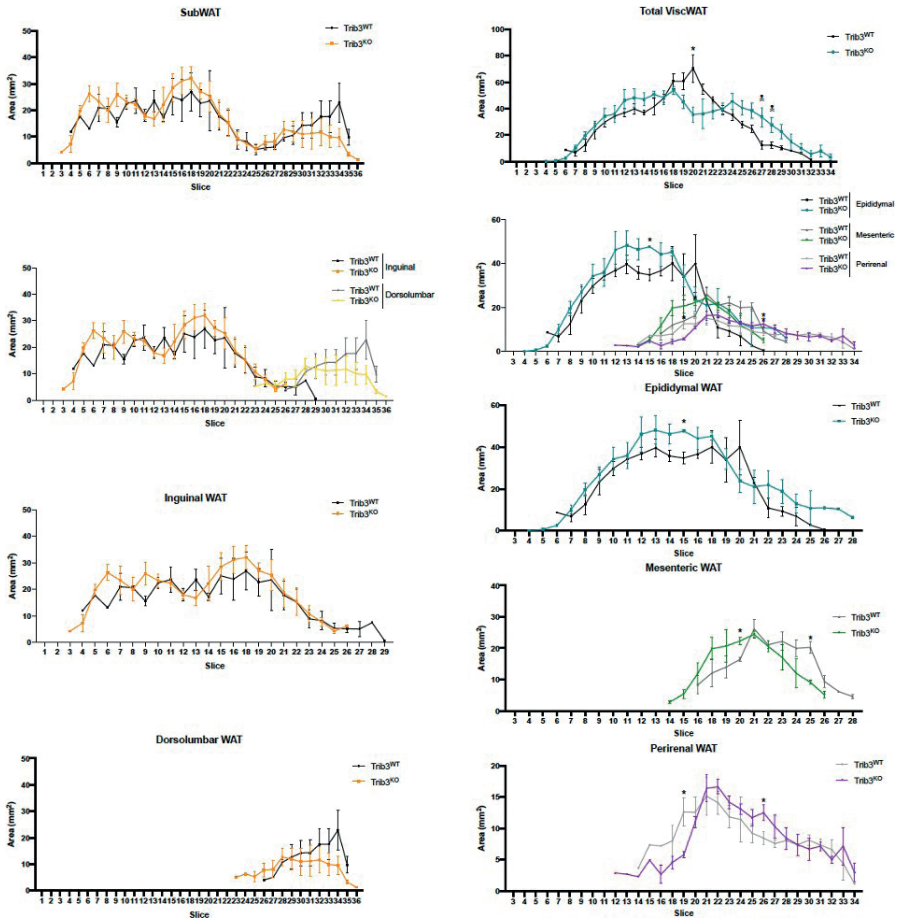

Suppl. Figure 3. MRI analysis of individual depots. Quantification of adipose area per slice within the different coronal regions, distinguishing between Subcutaneous (left, inguinal + dorsolumbar) and visceral (right, epidydimal + mesenteric + perirenal) depots.

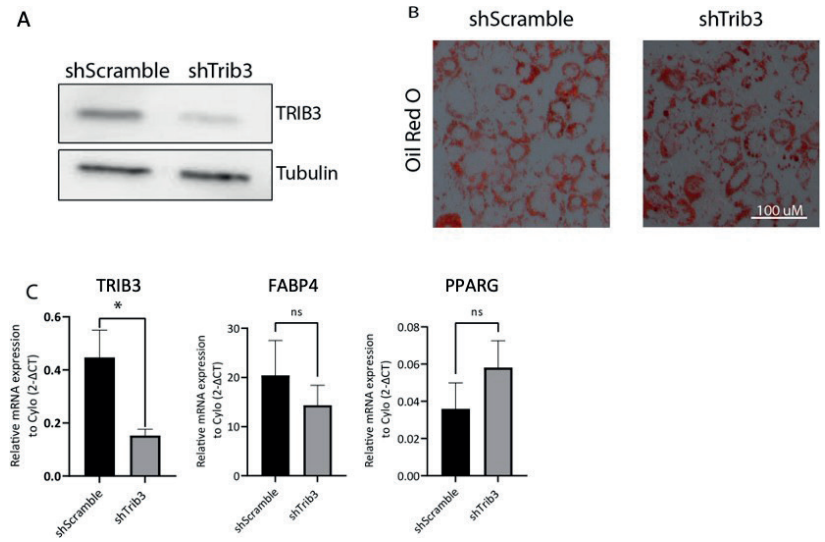

Suppl. Figure 4. *Trib3* KD in 3T3-L1. (A) Trib3 protein levels in 3T3-L1 cells scramble control and sh-*Trib3* cells. **(B)** Oil red O staining of sh-Scramble control and sh-*Trib3* cells. **(C)** mRNA expression of *Trib3*, *Fabp4* and *Pparg* in sh-Scramble and sh-*Trib3* 3T3-L1 cells.

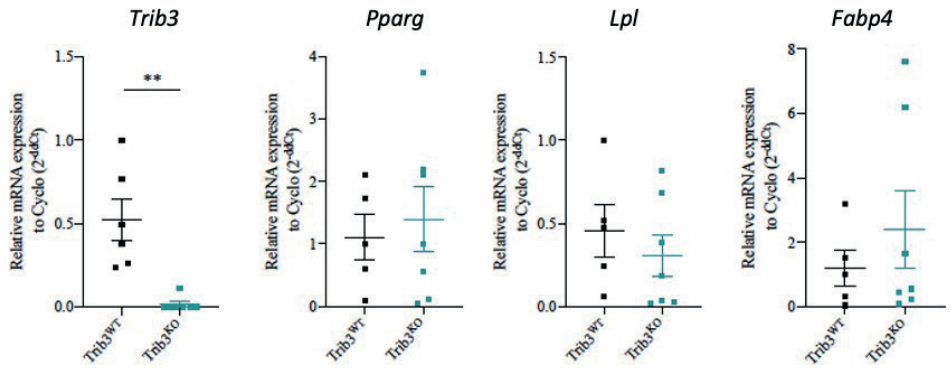

Suppl. Figure 5. mRNA levels of Trib3, Pparg, Lpl and Fabp4 in ex-vivo differentiated WAT from WT and Trib3^{KO} mice.

Suppl. Table 1. Top altered and significant canonical pathways identified by IPA.

Ingenuity Canonical Pathways	Ratio	z-score	Down-regulated	No change	Up-regulated	No overlap
Triacylglycerol Degradation	0.116	-2.236	22/43 (51%)	0/43 (0%)	10/43 (23%)	11/43 (26%)
Protein Kinase A Signaling	0.016	-1.633	177/374 (47%)	0/374 (0%)	175/374 (47%)	22/374 (6%)
Heparan Sulfate Biosynthesis (Late Stages)	0.0806	-1.342	16/62 (26%)	0/62 (0%)	30/62 (48%)	16/62 (26%)
Heparan Sulfate Biosynthesis	0.0725	-1.342	17/69 (25%)	0/69 (0%)	35/69 (51%)	17/69 (25%)
Gα12/13 Signaling	0.0787	-1	57/127 (45%)	0/127 (0%)	61/127 (48%)	9/127 (7%)
PPAR Signaling	0.049	-1	49/102 (48%)	1/102 (1%)	41/102 (40%)	11/102 (11%)
Natural Killer Cell Signaling	0.0298	-1	70/168 (42%)	0/168 (0%)	84/168 (50%)	14/168 (8%)
Estrogen Receptor Signaling	0.0125	-1	166/321 (52%)	1/321 (0%)	135/321 (42%)	19/321 (6%)
RhoGDI Signaling	0.0636	-0.632	81/173 (47%)	0/173 (0%)	82/173 (47%)	10/173 (6%)
LXR/RXR Activation	0.0455	-0.447	50/110 (45%)	1/110 (1%)	38/110 (35%)	21/110 (19%)
Corticotropin Releasing Hormone Signaling	0.0355	-0.447	50/141 (35%)	0/141 (0%)	74/141 (52%)	17/141 (12%)
Role of NFAT in Cardiac Hypertrophy	0.0287	-0.447	91/209 (44%)	0/209 (0%)	105/209 (50%)	13/209 (6%)
SPINK1 Pancreatic Cancer Pathway	0.0741	0	15/54 (28%)	0/54 (0%)	13/54 (24%)	26/54 (48%)
ERK/MAPK Signaling	0.0324	0	95/185 (51%)	0/185 (0%)	76/185 (41%)	14/185 (8%)
Calcium Signaling	0.0308	0	76/195 (39%)	0/195 (0%)	95/195 (49%)	24/195 (12%)
Wnt/β-catenin Signaling	0.0298	0	69/168 (41%)	1/168 (1%)	83/168 (49%)	15/168 (9%)
Systemic Lupus Erythematosus In B Cell Signaling Pathway	0.0163	0	83/246 (34%)	1/246 (0%)	122/246 (50%)	40/246 (16%)
Opioid Signaling Pathway	0.0336	0.378	101/238 (42%)	0/238 (0%)	115/238 (48%)	22/238 (9%)
Hepatic Fibrosis Signaling Pathway	0.0198	0.378	154/354 (44%)	1/354 (0%)	172/354 (49%)	27/354 (8%)
IL-6 Signaling	0.0492	0.447	58/122 (48%)	1/122 (1%)	55/122 (45%)	8/122 (7%)
Gαi Signaling	0.0488	0.447	52/123 (42%)	0/123 (0%)	53/123 (43%)	18/123 (15%)
Relaxin Signaling	0.0411	0.447	65/146 (45%)	0/146 (0%)	73/146 (50%)	8/146 (5%)
Endocannabinoid Neuronal Synapse Pathway	0.0394	0.447	47/127 (37%)	0/127 (0%)	66/127 (52%)	14/127 (11%)
Endothelin-1 Signaling	0.0331	0.447	81/181 (45%)	0/181 (0%)	84/181 (46%)	16/181 (9%)
Senescence Pathway	0.0192	0.447	126/260 (48%)	0/260 (0%)	126/260 (48%)	8/260 (3%)

Chapter 5

Early adipogenesis is repressed through the newly identified FHL2-NFAT5 signaling complex

Maria P. Clemente-Olivo*[1,2], Miguel Hernández-Quiles*[3], Rinske Sparrius[1], Miesje M. van der Stoel[6,1], Vera Janssen[1], Jayron Habibe[1,2], Janny van den Burg[1], Aldo Jongejan[4], Paula Sobrevals Alcaraz[5], Robert van Es[5], Harmjan Vos[5], Eric Kalkhoven[3,†] and Carlie J.M. de Vries[1,2,†,§]

[1] Amsterdam UMC location University of Amsterdam, Department of Medical Biochemistry, Amsterdam, the Netherlands.

[2] Amsterdam Cardiovascular Sciences, and Amsterdam Gastroenterology, Endocrinology and Metabolism, University of Amsterdam, Amsterdam, The Netherlands.

[3] Center for Molecular Medicine, University Medical Center Utrecht, Utrecht University, Utrecht, The Netherlands.

[4] Amsterdam UMC location University of Amsterdam, Department of Bioinformatics, Amsterdam, The Netherlands.

[5] Oncode Institute and Molecular Cancer Research, Center for Molecular Medicine, University Medical Center Utrecht, Utrecht University, Utrecht, The Netherlands.

[6] Present address: Department of Anatomy and Stem Cells and Metabolism Research Program, Faculty of Medicine, University of Helsinki, Helsinki, Finland.

*These authors have contributed equally to this work

[†] These authors have contributed equally to this work

[§] Corresponding author. Department of Medical Biochemistry Amsterdam University Medical Centers, Location AMC, Meibergdreef 15, 1105 AZ Amsterdam, the Netherlands.
c.j.devries@amsterdamumc.nl

Highlights

- FHL2 is expressed in pre-adipocytes and is downregulated during the early stages of adipocyte differentiation.
- FHL2 interacts with NFAT5 to refrain pre-adipocytes from differentiating towards mature adipocytes.
- FHL2 shows an important role at the intersection of mesenchymal stem cell differentiation, tilting this cellular process towards myoblast, osteoblast or adipocyte formation.

Abstract

The LIM-domain-only protein FHL2 is a modulator of signal transduction and has been shown to direct the differentiation of mesenchymal stem cells toward osteoblast and myocyte phenotypes. We hypothesized that FHL2 may simultaneously interfere with the induction of the adipocyte lineage. Therefore, we investigated the role of FHL2 in adipocyte differentiation. For these studies pre-adipocytes isolated from mouse adipose tissue and the 3T3-L1 (pre)adipocyte cell line were applied. We performed FHL2 gain of function and knockdown experiments followed by extensive RNAseq analyses and phenotypic characterization of the cells by oil-red O (ORO) lipid staining. Through affinity-purification mass spectrometry (AP-MS) novel FHL2 interacting proteins were identified. Here we report that FHL2 is expressed in pre-adipocytes and for accurate adipocyte differentiation, this protein needs to be downregulated during the early stages of adipogenesis. More specifically, constitutive overexpression of FHL2 drastically inhibits adipocyte differentiation in 3T3-L1 cells, which was demonstrated by suppressed activation of the adipogenic gene expression program as shown by RNAseq analyses, and diminished lipid accumulation. Analysis of the protein-protein interactions mediating this repressive activity of FHL2 on adipogenesis revealed the interaction of FHL2 with the Nuclear factor of activated T-cells 5 (NFAT5). NFAT5 is an established inhibitor of adipocyte differentiation and its knockdown rescued the inhibitory effect of FHL2 overexpression on 3T3-L1 differentiation, indicating that these proteins act cooperatively. We present a new regulatory function of FHL2 in early adipocyte differentiation and revealed that FHL2-mediated inhibition of pre-adipocyte differentiation is dependent on its interaction with NFAT5. FHL2 expression increases with aging, which may affect mesenchymal stem cell differentiation, more specifically inhibit adipocyte differentiation.

Keywords: mesenchymal stem cell, FHL2, NFAT5, adipogenesis, aging

Abbreviation list

ADIPOQ	adiponectin
CFD	Adipsin
AP-MS	Affinity-purification mass spectrometry
AMPK	AMP-Activated Protein Kinase
C/EBPβ-LIP	CCAAT Enhancer Binding Protein Beta
CCR4-NOT	Carbon catabolite repression 4 (Ccr4)-negative on TATA-less (Not) Complex
CHOP	C/EBP-Homologous Protein 10
CUGBP1	CUG triplet repeat, RNA binding protein 1
DLK1/Pref1	Delta Like Non-Canonical Notch Ligand 1
DMIX1	Differentiation mix
DMEM	Dulbecco's modified Eagle's medium
FABF4	Fatty acid-binding protein 4
GSEA	Gene set enrichment analysis
HIF1A	Hypoxia inducible factor 1A
logCPM	Log2-counts per million
NFAT5	Nuclear factor of activated T-cells 5
ORO	Oil Red O
Plin1	Perilipin 1
PPARγ	Peroxisome proliferating-activated receptor gamma
TCEP	Tris (2-carboxyethyl) phosphine hydrochloride
TGFB1	Transforming growth factor beta
Sh	Short hairpin
SVF	Stromal vascular fraction
WAT	White adipose tissue

1. Introduction

Mesenchymal stem cells can differentiate into distinct cell types such as adipocytes, myocytes, chondrocytes, and osteoblasts (1). The transition of precursor cells into cells with a mature cellular phenotype is orchestrated by the intricate expression pattern of cell-type-specific factors (2). Adipocyte differentiation occurs through two main phases: the commitment phase, when mesenchymal stem cells commit to the adipocyte lineage, and the terminal differentiation phase, which results in a unique adipocyte-specific gene expression profile and eventually the accumulation of lipid droplets in the cell (3). The adipocyte differentiation program involves a cascade of transcriptional events that regulate the expression of key proteins to establish the mature adipocyte phenotype. One of the key factors in adipocyte differentiation is the nuclear receptor peroxisome proliferating-activated receptor gamma (PPARγ) (4). Recently, it has been demonstrated that especially white adipose tissue (WAT) shows an extensive and relatively early differential gene expression pattern in aging mice (5). In addition, it has been proposed that peripheral fat loss with aging in humans involves defects in adipogenesis in the subcutaneous WAT depot (6). Overall, the differentiation capacity of pre-adipocytes gradually deteriorates with increasing age (7, 8). The impaired pre-adipocyte differentiation has been linked to reduced levels of adipogenic factors such as C/EBP family members and PPARγ, but also to enhanced expression of for example AMP-Activated Protein Kinase (AMPK) and Delta Like Non-Canonical Notch Ligand 1 (DLK1/Pref1) (9, 10). Given that pre-adipocyte (dys)function is a determinant of several human metabolic diseases (11), it is relevant that new factors and pathways that play a significant role in adipogenesis are still being discovered (12).

Four-and-a-Half LIM domains protein 2 (FHL2) is a member of the FHL subfamily of LIM-only proteins and is expressed in a wide variety of cells and tissues (13). FHL2 is a component of numerous signal transduction pathways acting through protein-protein interactions, thereby fine-tuning cellular processes (14). Recently, we demonstrated a novel function for FHL2 in energy metabolism, and more specifically in WAT (15). Using the mouse diet-induced obesity model, we observed that FHL2 deficiency in mice prevents weight gain, in part through enhanced browning of their WAT. FHL2 is also known to promote myoblast and osteoblast differentiation, through interaction with β-catenin and Wnt proteins, respectively (16-18). In the osteoblast study, it has been proposed that FHL2 deficiency may have an impact on adipocyte size, specifically in the bone marrow (16). However, a direct impact of FHL2 on adipogenesis has not been studied so far. Methylation of the human FHL2 gene is one of the strongest epigenetic DNA marks to identify the age of an individual, and FHL2 methylation is associated with an increased expression of this gene. Not only in blood but also in WAT, pancreatic β-cells, and skeletal muscle FHL2 methylation and expression is increased with aging (13). In the current study, we hypothesized that FHL2 plays a pivotal role in adipocyte differentiation. Therefore, the main aim of this study was to unveil a potential role for FHL2 in adipogenesis.

In two different models of adipogenesis *ex vivo* differentiated primary (pre) adipocytes and 3T3-L1 (pre)adipocyte cell line), we observed downregulation of FHL2 expression at the early stages of *in vitro* differentiation. Based on loss-of-function experiments (*ex vivo* differentiated FHL2-/- primary (pre)adipocytes) and overexpression experiments, we conclude that reducing FHL2 expression is essential for pre-adipocytes to undergo full differentiation into mature adipocytes. Considering that FHL2 exerts its biological functions through protein-protein interactions, we employed co-immunoprecipitation experiments followed by proteomics and identified the Nuclear factor of activated T-cells 5 (NFAT5) as a novel FHL2 interactor. NFAT5 has been reported to decrease adipocyte differentiation similarly to FHL2 (19, 20), and we show that FHL2 requires NFAT5 to exert its function. In conclusion, we demonstrated a crucial role of FHL2 in adipogenesis and propose that FHL2 is a determinant factor in early adipogenesis and cell lineage commitment.

2. Materials and methods

2.1 Animals and Stromal Vascular Fraction (SVF) isolation

All animal experiments were approved by the ethics committee of the Amsterdam University Medical Center, The Netherlands, and were performed following European directive 2010/63/EU guidelines (permit number DBC287). FHL2-deficient mice (FHL2-/-) were generated by R. Bassel-Duby (University of Texas Southwestern Medical Center, Dallas, TX) and were bred onto a C57BL/6 background for more than 11 generations. Male littermates of 11-week-old were used, and *n* refers to the number of single animals. Littermates from wild-type and FHL2-deficient genotype were randomly separated in ventilated cages with free access to water and food. The suffering of animals was minimized as much as possible. The isolation of pre-adipocytes from the mouse SVF was performed as described previously (15). In short, excision of subcutaneous white adipose tissue depots was performed in WT and FHL2-/- mice, and the SVF was isolated to obtain pre-adipocytes for differentiation *in vitro*. The tissue was minced and digested in collagenase solution (1.5 mg/ml; Sigma-Aldrich; #C6885). After filtering and centrifuging, the pre-adipocytes were purified using a red blood cell lysis buffer (Roche; # 11814389001) and neutralized with Dulbecco's modified Eagle's medium (DMEM) (Gibco, Thermo Fisher; #41965062)

supplemented with 10% FBS and 1% penicillin-streptomycin. Finally, cells were centrifuged again and seeded in cell culture plates for differentiation.

2.2 3T3-L1 cell culture and pre-adipocyte differentiation

The 3T3-L1 cell line (ATCC: CL-173) was cultured in DMEM supplemented with 10% FBS and 1% penicillin-streptomycin at 37ºC and 5% CO_2. The protocol for pre-adipocyte differentiation was performed as described elsewhere (21), and it was used for both 3T3-L1 and SVF pre-adipocyte differentiation. Cells were grown to confluency and after 2 days culture medium supplemented with differentiation mix 1 (DMIX1) was added to the cells for 2 days (DMIX1 contains: 500 µM of isobutyl-1-methylxanthine (IBMX), 1 µM of dexamethasone, and 170 nM of insulin). On day 4, DMIX1 was replaced by differentiation mix 2 (DMIX2; culture medium containing 170 nM of insulin) and this was replaced regularly until day 8 of differentiation.

2.3 Lentiviral transduction

Recombinant lentiviral particles encoding FHL2 with GFP tag (FHL2-GFP), only the GFP tag as control (CTRL-GFP), and two different constructs of shRNA targeting mouse NFAT5 (shNFAT5-1 target sequence is 5′- GCAGAACAACATCCCTGGAAT-3′ and, shNFAT5-2 target sequence is 5′- CCACCATGTTTCAGACACCAA-3′), as well as one without NFAT5 as control (shCTRL), were produced, concentrated, and titrated as described previously (22). Cells were seeded at 70-80% confluency and incubated with recombinant lentivirus for 24 hours. After 24 hours, the medium was refreshed, and cells were cultured using medium containing 1 µg/mL of the selection marker puromycin (for the GFP constructs) or 500 µg/mL of neomycin (for the shNFAT5 constructs). After 3-10 days resistant cells were further expanded for experiments.

2.4 RNA isolation and reverse transcription (RT)-qPCR

Total RNA isolation from cultured cells was performed using TRI Reagent® (Sigma Aldrich; #T9424). Then, cDNA was synthesized using iScript® cDNA Synthesis Kit (BioRad; #1708890). Quantitative PCR was carried out using a LightCycler 480 II PCR platform (Roche) with the correspondent pair of primers (sequences listed in Table S1) and SensiFAST SYBR No-ROX Kit (Bioline; #BIO-98050). Cycle quantification and amplification efficiency were calculated using the LinReg PCR software package (23) and Rplp0 and β-actin were used as housekeeping genes to normalize target gene expression.

2.5 RNA sequencing

Cells transduced with lentiviral particles and stably expressing CTRL-GFP or FHL2-GFP were differentiated for 2 days as described before. RNA isolation from these cultured cells was performed using TRI Reagent® according to the manufacturer's protocol.

Libraries were prepared using Truseq RNA stranded polyA (Illumina) and sequenced on an Illumina nextseq2000 in paired-end 50 bp reads. Reads were subjected to quality control (FastQC, dupRadar), trimmed using Trimmomatic v0.39, and aligned to the genome using HISAT2 (v2.2.1) (24-26). Counts were obtained using HTSeq (v0.11.0) using the corresponding GTF. Statistical analyses were performed using the edgeR and limma/voom R packages. Count data were transformed to log2-counts per million (logCPM), normalized by applying the trimmed mean of M-values method and precision weighted using voom. Differential expression was assessed using an empirical Bayes moderated t-test within limma's linear model framework including the precision weights estimated by voom. The resulting p values were corrected for multiple testing using the Benjamini-Hochberg false discovery rate. Genes were re-annotated using biomaRt using the Ensembl genome databases. Geneset enrichment is performed with MSigDB genesets using CAMERA approach as implemented in limma (27), and applying the Geneset Enrichment Analysis (GSEA) tool. The resulting DEGs, expression plots, and geneset enrichment results are shown in an in-house made Shiny-app. The raw and processed RNA-seq data have been deposited in the Gene Expression Omnibus (GEO) database under accession number GSE200920.

2.6 Western blotting

Proteins from cultured cells were obtained using RIPA lysis buffer (150 mM NaCl, 50 mM Tris pH 7.4, 1% IGEPAL-CA630, 0.5% sodium deoxycholate, 0.1% SDS and Roche cOmplete™ protease inhibitor cocktail). Concentration was calculated using the DC protein assay (BioRad; #5000111) to load equal amounts of sample into SDS-PAGE gels. After transferring to nitrocellulose membranes, these were blocked with 2% non-fat milk for 1 hour and incubated overnight at 4ºC with the corresponding primary antibody (Mouse anti-FHL2 - #MA1-40200 from ThermoFisher, Rabbit anti-NFAT5 - #ab3446 from Abcam, Rabbit anti-HA tag - #3724S from Cell Signaling, Mouse anti-c-Myc tag - #sc-40 from Santa Cruz and Mouse anti-alpha-tubulin - #CLT9002 from Cedarlane as loading control). After washing the membranes, they were incubated with the appropriate HRP-conjugated secondary antibody at room temperature for 1 hour. Visualization of protein bands was done in ImageQuant 800 imager using SuperSignal West Pico PLUS Chemiluminescent Substrate (ThermoScientific #34579), and quantification of band intensity was possible using the ImageJ Gel Analysis software.

2.7 Intracellular lipid staining and immunofluorescence staining

To stain lipid accumulation in 3T3-L1 cells, we used two different methods: Oil Red O (ORO) staining and HCS LipidTOX Deep Red Neutral Lipid Stain (Invitrogen; #H34477), both methods stain neutral lipids in cultured cells. For the ORO staining, cells were fixed for 20 minutes at room temperature using 4% formalin. Fixative was

removed and after washing again with PBS, the 0.2% ORO solution was added to the wells and incubated for 30 minutes at room temperature. After this, cells were washed several times with distilled water. For quantification, the dye was eluted using 100% 2-propanol, and absorbance was measured at 510 nm in triplicate. For LipidTOX staining, cells were grown on gelatin-coated glass coverslips and fixated as described before. Then, coverslips were incubated with LipidTOX (1:150 dilution) and DAPI nuclear staining (1:1000) for 30 minutes at room temperature. After washing, coverslips were mounted on slides and imaged. For immunofluorescence, cells were cultured on gelatin-coated glass coverslips for differentiation. On different days of differentiation, cells were fixed in 4% paraformaldehyde (Roth) for 20 minutes at room temperature. After the addition of 0.5% Triton X-100 for 5 minutes to permeabilize the nuclei, samples were blocked with 2% BSA and incubated with primary antibody (Rabbit anti-NFAT5 - #ab3446 from Abcam) and DAPI nuclear staining. Then, following washing and incubation with secondary (Alexa-488 goat anti-Rabbit) the samples were mounted in slides for imaging using a Nikon ECLIPSE Ti microscope with standard DAPI, GFP, and mCherry filter cubes. Images were processed using ImageJ Gel Analysis software.

2.8 Co-immunoprecipitation

HEK-293T cells were co-transfected with HA-tagged FHL2 and myc-tagged NFAT5 plasmids using the CalPhos Mammalian Transfection Kit (Takara; #631312) and incubated for 48 hours. For the LIM mutants, plasmids encoding different numbers of FHL2 LIM-domains (HA-tagged LIM0-1, LIM0-2, and LIM0-3) (28) were co-transfected together with myc-tagged NFAT5. Then, protein lysates were obtained using NP-40 lysis buffer (1% (v/v) Nonidet P-40, 50 mM Tris-HCl, 100 mM NaCl, 10% (v/v) glycerol) supplemented with protease and phosphatase inhibitors. After calculating protein concentration, lysates were incubated with pull-down antibody (Rabbit anti-HA tag - #3724S from Cell Signaling) overnight at 4ºC. The next day, the complex was incubated for 2 hours with magnetic Dynabeads® Protein G (ThermoFisher; #10003D). Immunoprecipitates were then washed and eluted from the beads and analyzed by western blotting.

2.9 Mass spectrometry

Precipitated proteins were denatured and alkylated in 50 µl 8 M Urea, 1 M ammonium bicarbonate (ABC) containing 10 mM TCEP (tris (2-carboxyethyl) phosphine hydrochloride) and 40 mM 2-chloro-acetamide. After 4-fold dilution with 1 M ABC and digestion with trypsin (250 ng/200 µl), peptides were separated from the beads and desalted with homemade C-18 stage tips (3 M, St Paul, MN), eluted with 80% Acetonitrile (ACN) and, after evaporation of the solvent in the speedvac, redissolved

in buffer A (0,1% formic acid). After separation on a 30 cm pico-tip column (75 µm ID, New Objective) in-house packed with C-18 material (1.9 µm aquapur gold, dr. Maisch) using a 140 minute gradient (7% to 80% ACN, 0.1% FA), delivered by an easy-nLC 1200 (Thermo), peptides were electro-sprayed directly into a Orbitrap Eclipse Tribrid Mass Spectrometer (Thermo Scientific), that was run in DDA mode with a cycle time of 1 second, with the FAIMS compensation voltage (CV) switching between -45V and -65V. The full scan (400-1400 mass range) was performed at a resolution of 240,000. Ions reaching an intensity threshold of 10E4, were isolated by the quadrupole with na 0.8 Da window, fragmented with a HCD collision energy of 30% and measured in de Iontrap on rapid mode.

After splitting of the raw files into the two CV channels with Freestyle Software (Thermo), analysis of the raw data was performed with MaxQuant (1.6.3.4), using the Uniprot fasta file (UP000000589) of Mus musculus (taxonomy ID: 10090) (2020 Jan 21). To determine proteins of interest, we performed a differential enrichment analysis. We filtered for proteins that were identified in at least two out of three of the replicates of one condition and background corrected and normalized the data by variance stabilizing transformation. We used a left-shifted Gaussian distribution to impute for missingness since our data presented a pattern of missingness not at random (MNAR). Finally, we performed a T-test with multiple testing correction using a Benjamini-Hochberg FDR approach set to 0.5%. The program used for the analyses was R [version 4.0.4] through R-Studio [version 1.5.64]. The mass spectrometry proteomics data have been deposited to the ProteomeXchange Consortium via the PRIDE partner repository with the dataset identifier PXD033974 (http://www.ebi.ac.uk/pride). Then, differential enrichment analysis was created to identify those proteins that were over-enriched and selected those with at least a 2.5-fold change and adjusted p-value ≤ 0.05.

2.10 Reporter assays

Transient transfection of HEK-293T cells with pcDNA3.1-Gal4DBD-NFAT5, pCMV-HA-FHL2, and pCMV-HA-LIM0-2 (28), pGL3 reporter, and TK-Renilla luciferase was performed using Xtreme gene 9 DNA transfection reagent (Roche; #XTG9-RO). Following incubation for 48 hours, cells were lysed and the Dual-Luciferase Reporter Assay System (Promega) was used to measure luciferase in a TriStar2 LB942 Multimode Reader. Independent experiments were performed three times.

2.11 BrdU proliferation assay

The proliferation of 3T3-L1 cells was determined using the BrdU cell proliferation ELISA (Roche; #11647229001) according to the manufacturer's protocol. An equal

number of cells stably overexpressing CTRL-GFP or FHL2-GFP were labeled with BrdU for 2 hours. After fixation, samples were incubated with a peroxidase-conjugated anti-BrdU antibody. Next, samples were washed and incubated with the substrate solution for color development. The reaction was stopped after 10-20 minutes, and absorbance was measured at 450 nm.

2.12 Statistical analysis

Statistical analyses were performed using GraphPad Prism software. Data are presented as mean ±SEM. P-values were calculated using Student's t-test, or two-way ANOVA with Tukey's posthoc correction if data were normally distributed. A p-value < 0.05 was considered statistically significant.

3. Results

3.1 FHL2 is expressed in WAT and expression is regulated during early differentiation of 3T3-L1 cells

To examine the expression of FHL2 in the different cell types in adipose tissue, subcutaneous WAT from wild-type C57BL/6 mice was separated into mature adipocytes and the stromal vascular fraction (SVF); the latter fraction contains immune cells, endothelial cells, and pre-adipocytes. FHL2 mRNA is expressed in both SVF (containing pre-adipocytes) and in the mature adipocyte fraction, with the highest expression in SVF (Fig. 1A). Therefore, we hypothesized that FHL2 expression might be regulated during adipocyte differentiation. To address this in an independent experimental model, we applied the 3T3-L1 cell line, a standard model to study adipogenesis (29, 30). Cells were differentiated for 8 days using standard hormonal cocktails and we confirmed a successful differentiation based on the expression of key adipogenic markers such as PPARγ and its target genes adiponectin (ADIPOQ) and fatty acid-binding protein 4 (FABP4) (Fig. 1B). During differentiation, FHL2 is transiently downregulated at day 2 of differentiation both at the mRNA and protein level (Fig. 1C-D), this being the moment that the adipogenic cocktail (here named differentiation mix or DMIX1) is added to trigger the initiation of adipocyte differentiation. Based on this observation, we decided to dissect which specific component of the DMIX1 causes this regulation of FHL2 expression. 3T3-L1 cells were incubated with separate components of the mix and we demonstrated that IBMX, which enhances intracellular cAMP levels, causes the decrease in FHL2 expression, whereas dexamethasone and insulin do not affect FHL2 expression (Fig. 1E). In conclusion, FHL2 is expressed in pre-adipocytes and is downregulated in the early stages of *in vitro* pre-adipocyte differentiation.

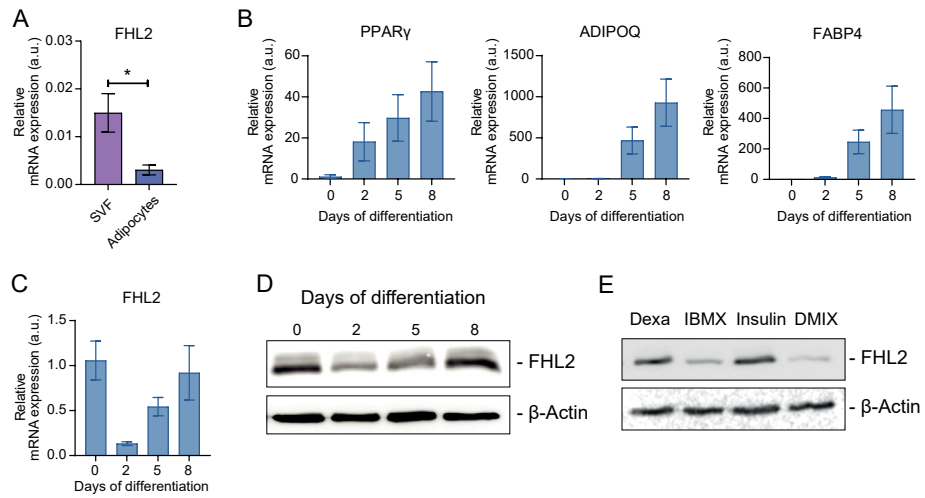

Figure 1. FHL2 expression in mouse adipose tissue fractions and 3T3-L1 adipocyte differentiation. **A)** Relative mRNA expression of FHL2 in pre-adipocytes from the SVF and in mature adipocytes. **B and C)** Relative mRNA expression of PPARγ, ADIPOQ, FABP4, and FHL2 during 8 days of differentiation of 3T3-L1 cells, where cells were cultured to confluency before receiving 2 days of treatment with DMIX1 and later maintained with DMIX2 until day 8 (section 2.2). **D)** Western blot to reveal FHL2 protein expression during 3T3-L1 differentiation (β-actin used as loading control). **E)** FHL2 protein expression in cells treated with Dexamethasone (1 μM), IBMX (500 μM), Insulin (170 nM), or full differentiation mix (DMIX1) for 2 days before protein harvest. Data are indicated as mean ± SEM (*p<0,05).

3.2 FHL2 overexpression inhibits adipocyte differentiation

To study the role of FHL2 in adipocyte differentiation in more detail, we used full-body FHL2-deficient mice and their wild-type littermates as control, FHL2-/- and WT mice; to isolate the pre-adipocytes from WAT and induce differentiation towards mature adipocytes. Similar to 3T3-L1 cells (Fig. 1 C and D), FHL2 expression is downregulated at day 2 in WT pre-adipocytes during differentiation (Fig. 2A), but we did not find any difference in adipocyte differentiation between WT and FHL2-/- pre-adipocytes based on the expression of the aforementioned adipocyte markers PPARγ, ADIPOQ, and FABP4 (Fig. 2B) nor lipid accumulation (data not shown). Therefore, we conclude that FHL2 deficiency does not alter the overall adipogenic capacity of mouse pre-adipocytes. However, given the transient and dramatic decline in FHL2 expression during early differentiation, we hypothesized that this reduction of FHL2 levels may present an essential step in adipogenesis. To investigate this, we constitutively overexpressed GFP-tagged FHL2 or GFP through stable lentiviral transduction in 3T3-L1 cells (Fig. 2C, Fig. S1A). Next, these cell lines were subjected to the differentiation protocol and we observed that cells constitutively expressing FHL2-GFP did not differentiate properly, based on reduced intracellular lipid accumulation using

LipidTOX staining after 5 days (Fig. 2D) and by Oil Red O lipid staining followed by quantification (Fig. S1B). Moreover, mRNA analyses showed that even though the early adipogenic marker CEBPβ is not different between groups, the expression of the late adipogenic markers PPARγ, ADIPOQ, and FABP4 is drastically inhibited in FHL2-GFP cells (Fig. 2E). Since cell differentiation often antagonizes cell proliferation (31), we evaluated whether FHL2 overexpression affects cell proliferation in these cells, but we did not observe any difference between GFP and FHL2-GFP cells (Fig. S1C). These experiments established that whereas lack of FHL2 has no apparent effect on adipocyte differentiation, constitutive expression of FHL2 prevents differentiation of pre-adipocytes into mature adipocytes. keeping them in an immature state.

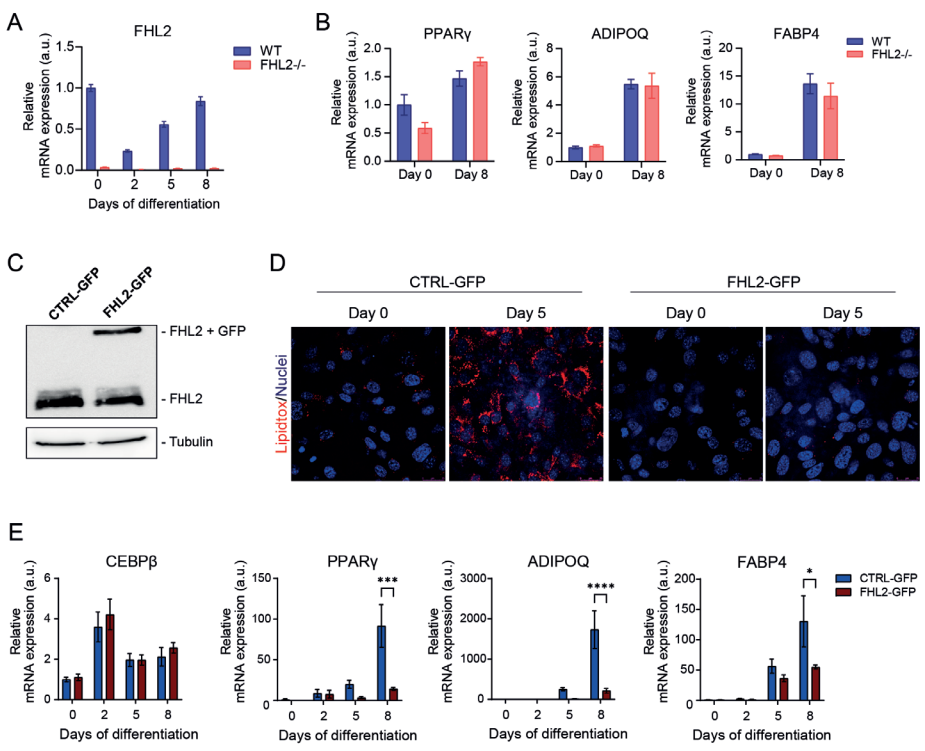

Figure 2. FHL2 overexpression inhibits the differentiation of pre-adipocytes. A) Relative mRNA expression of FHL2 during differentiation of pre-adipocytes derived from WT (n=3) and FHL2-/- (n=3) mice. **B)** Relative mRNA expression of PPARγ, ADIPOQ, and FABP4 at days 0 and 8 of differentiation of WT and FHL2-/- pre-adipocytes. **C)** Western blot to visualize protein expression of endogenous FHL2 and overexpressed FHL2-GFP in 3T3-L1 cells (tubulin used as loading control). **D)** Intracellular lipids (red) and nuclear DAPI (blue) staining of CTRL-GFP and FHL2-GFP 3T3-L1 cells at days 0 and 5 of differentiation. **E)** Relative mRNA expression of CEBPβ, PPARγ, ADIPOQ, and FABP4 during 8 days of differentiation of CTRL-GFP and FHL2-GFP cells. Data are indicated as mean ± SEM (*p<0,05).

3.3 FHL2 overexpression alters gene transcription in early differentiation

Given that FHL2 overexpression effectively represses differentiation, we next aimed to assess the effect of elevated FHL2 levels on the transcriptome of 3T3-L1 cells during the early stages of differentiation. We performed RNAseq transcriptomic analysis of confluent cell cultures before (day 0) and two days after the addition of the adipocyte differentiation cocktail necessary to start differentiation (DMIX1; Fig. 3A). The largest difference in terms of the number of differentially expressed genes between cells expressing FHL2-GFP and control cells (CTRL-GFP) was found on day 2 when 473 genes are significantly upregulated and 651 genes are downregulated. In contrast, 141 and 274 genes were found to be significantly up- and down-regulated at day 0, respectively (Fig. 3B), indicating that the main effect of FHL2 at the transcriptional level occurred after 2 days of differentiation. In Fig. 3C-D, volcano plots with several genes are indicated as the top differentially expressed genes in FHL2-GFP cells. At day 2, the top downregulated genes include well-established adipogenesis marker genes including the Pparγ target genes Adipoq, Perilipin 1 (Plin1), and Adipsin (Cfd), confirming the inhibition of adipogenesis upon FHL2 overexpression (Fig. 2). Extensive pathway analyses (Fig. 3E, Fig. S2A-B) revealed that adipogenic pathways, as well as other pathways that have been described to participate in adipocyte differentiation or lineage commitment, such as HIF1A targets and Response to TGFB1 (32, 33), are downregulated upon constitutive FHL2 expression during differentiation. A heatmap of genes involved in adipogenesis illustrates the repressive effect of FHL2 on the expression of these genes (Fig. 3F). Detailed gene set enrichment analysis (GSEA) of these data further illustrate these findings (Fig. 3G). These transcriptomic data strongly support our finding that constitutive FHL2 expression results in inhibition of early adipocyte differentiation.

3.4 FHL2 interacts with the nuclear factor of activated T-cells 5 (NFAT5) in 3T3-L1 cells

As FHL2 does not bind DNA by itself but modulates gene transcription through interaction with transcription factors (34), we wished to identify with which proteins FHL2 interacts to inhibit adipogenesis. We applied GFP-mediated affinity-purification mass spectrometry (AP-MS) to identify FHL2 interactors in 3T3-L1 cells, using an optimized technique (35), with GFP overexpressing cells as a control. Using this approach, we identified 51 significant interactors, some of which are shown in Table S2, for FHL2 in 3T3-L1 cells. In Fig. 4A the results are presented in a volcano plot with the most significant interactors indicated. The presence of FHL2 among this set of proteins confirms the specificity of this approach. Among the most significant interacting protein, we detected the nuclear factor of activated T-cells 5

(NFAT5), a transcription factor previously implicated in adipogenesis (19, 20, 36), and eight members of the carbon catabolite repression 4 (Ccr4)-negative on TATA-less (Not) complex, referred to as the CCR4-NOT or CNOT complex, a large, highly conserved, multifunctional assembly of proteins that is predominantly involved in the regulation of mRNA stability (37, 38). As NFAT5 has been shown to inhibit adipocyte differentiation and WAT browning (19, 20, 36), reminiscent of the function of FHL2 in adipocytes as presented in the current study and our previous study (15), we decided to focus on the interaction between FHL2 and NFAT5. First, we assessed the expression pattern of NFAT5 during adipocyte differentiation in more detail and examined whether its expression was altered upon overexpression of FHL2. NFAT5 shows a similar downregulation of expression at day 2 as FHL2, and overexpression of FHL2-GFP does not alter NFAT5 expression (Fig. 4B). To confirm the interaction observed in the AP-MS experiments between FHL2 and NFAT5, co-immunoprecipitation was performed for HA-tagged FHL2 and Myc-tagged NFAT5 (Fig. 4C). It is worth to mention that for this experiment same amount of DNA and cells was used across the different conditions, but the result shows enhanced expression levels of FHL2-HA and NFAT5-Myc when co-expressed, which suggests some degree of protein stabilization. Moreover, in this experiment three different mutants of FHL2 were included in which one or more LIM domains are missing; LIM0-1, LIM0-2, and LIM0-3. We observed that the LIM mutant lacking the last LIM domain (LIM0-3) was the only mutant, in addition to full-length FHL2, interacting with NFAT5 albeit to a lesser extent (Fig. 4D).

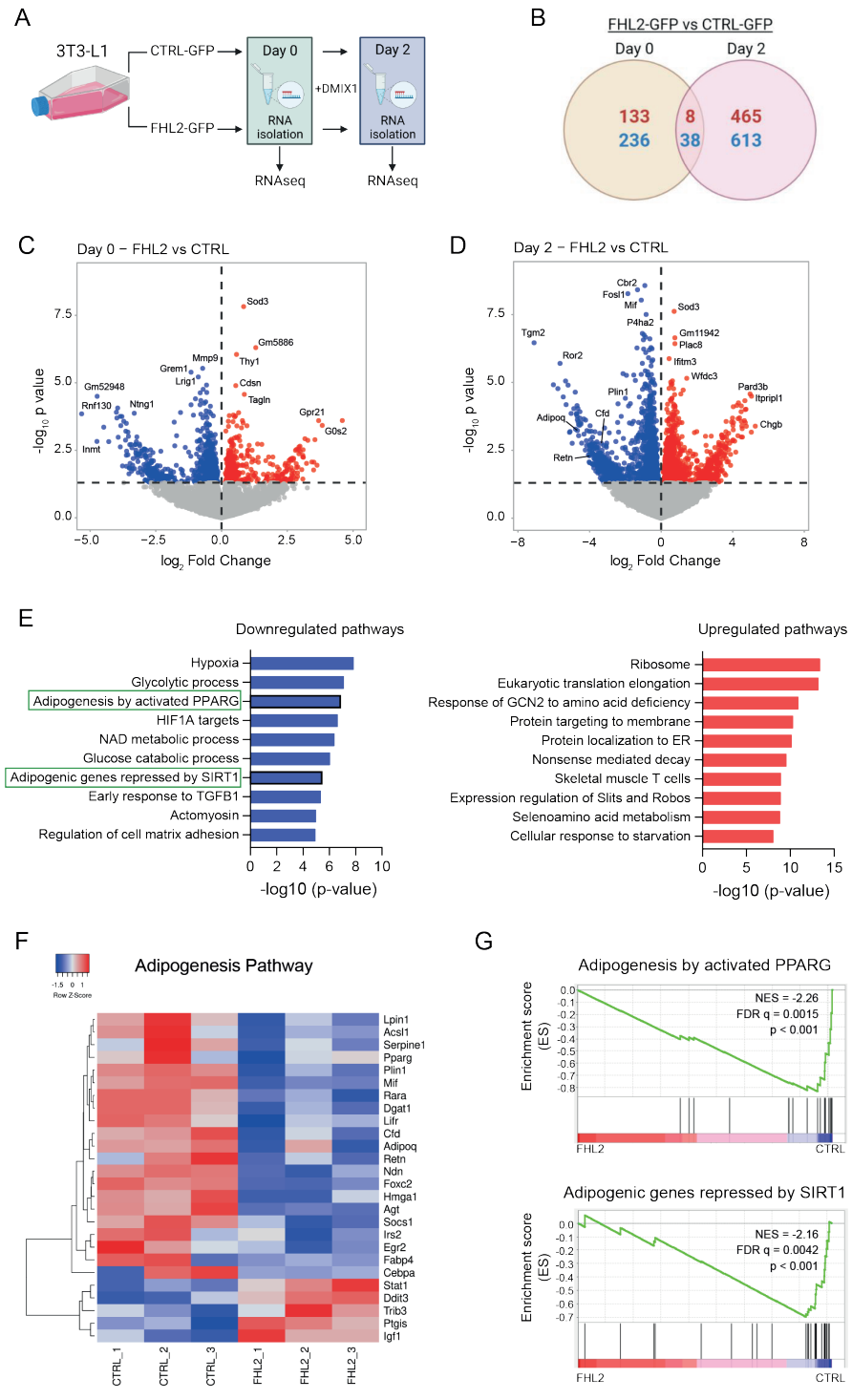

> **Figure 3. Transcriptional changes in FHL2-GFP and control 3T3-L1 cells. A)** Experimental setup scheme. **B)** Venn diagram of differentially expressed genes of FHL2-GFP vs CTRL-GFP comparison at days 0 and 2 of differentiation (p-value < 0.05). Upregulated genes in red and downregulated genes in blue. **C)** Volcano plot of RNAseq at day 0 and **D)** day 2 of differentiation (FHL2-GFP vs CTRL-GFP). **E)** Top up- and down-regulated pathways in FHL2-GFP cells at day 2 of differentiation. **F)** Heatmap depicting the gene expression pattern of the Adipogenesis pathway at day 2 in CTRL-GFP and FHL2-GFP cells. **G)** Significant GSEA Enrichment Score curves (in green) from two adipogenic pathways: Adipogenesis activated by PPARG (GSEA: C2_M1645) and Adipogenic genes repressed by SIRT1 (GSEA: C2_M2183). Genes on the far left (red) correlated with FHL2-GFP cells, and genes on the far right (blue) correlated with CTRL-GFP cells. The vertical black lines indicate the position of each gene in the studied gene set. The normalized enrichment score (NES), false discover rate (FDR), and nominal p-value are shown for each pathway.

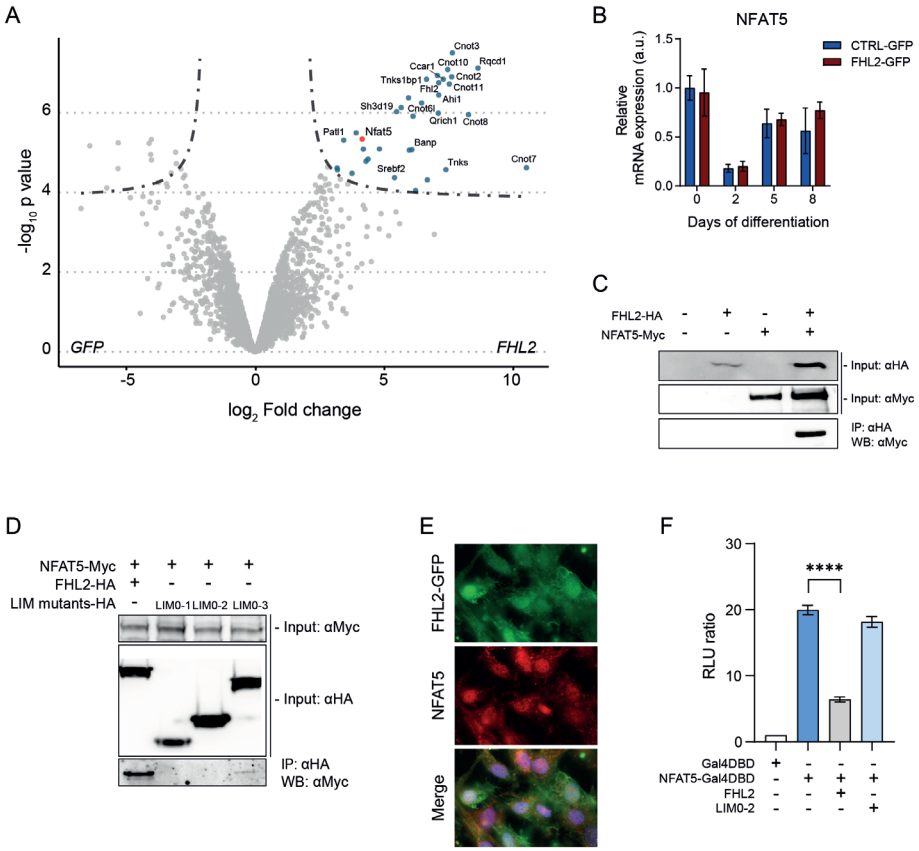

Figure 4. NFAT5 and FHL2 interact in 3T3-L1 cells. A) Volcano plot showing FHL2-GFP interacting proteins detected in the AP-MS experiment, compared to the GFP control results in 3T3-L1 cells. **B)** Relative mRNA expression of NFAT5 during 8 days of differentiation in CTRL-GFP and FHL2-GFP 3T3-L1 cells. **C)** Co-immunoprecipitation assay of FHL2-HA and NFAT5-myc in HEK-293T cells. Equal number of cells were transfected using the same amount of DNA through all conditions. **D)** Co-immunoprecipitation assay of LIM mutants (LIM0-1, LIM0-2, and LIM0-3) and NFAT5-Myc in HEK-293T cells. **E)** Fluorescence of FHL2-GFP (green), and immunofluorescence of NFAT5 (red), merged with nuclear DAPI (blue) in confluent 3T3-L1 cells. **F)** Gal4-reporter assay of NFAT5-Gal4DBD, FHL2, and LIM mutants LIM0-2. Data normalized using Renilla luciferase. Data are indicated as mean ± SEM (*p<0,05).

Given that NFAT5 is a transcription factor, we assessed whether the interaction between FHL2 and NFAT5 affects the transcriptional activity of NFAT5. First, we performed immunofluorescence staining for FHL2 and NFAT5 in 3T3-L1 cells and demonstrated that FHL2 is localized throughout the cell and that both proteins co-localize in the nucleus (Fig. 4E). As NFAT proteins are widely expressed (39), we next employed a Gal4-reporter assay to perform transcriptional activity assays, to avoid interference of endogenous NFAT proteins. Fusion of the Gal4 DNA-binding domain to NFAT5 resulted in a protein that activates a Gal4-luciferase reporter. The activity of Gal4-NFAT5 is reduced upon overexpression of FHL2, but not when the LIM0-2 variant of FHL2, which fails to interact with NFAT5 (Fig. 4D), was used (Fig. 4F). These data confirm that the interaction between NFAT5 and full-length FHL2 is functional.

3.5 FHL2 inhibition of adipocyte differentiation involves cooperation with NFAT5

Lee *et al*. (20) demonstrated that NFAT5 inhibits adipogenesis by blocking the expression of the PPARγ gene, similar to what FHL2 does after overexpression during differentiation. As both FHL2 (Fig. 2) and NFAT5 (19, 20) inhibit adipogenesis, and because these proteins functionally interact (Fig. 4), we considered that FHL2 and NFAT5 operate through a common cellular pathway. To examine this, we knocked down NFAT5 expression in CTRL-GFP and FHL2-GFP overexpressing cells using two different short-hairpin constructs (shNFAT5-1 and shNFAT5-2), resulting in approximately 40% knockdown of NFAT5 compared to the corresponding control (shCTRL) (Fig. 5A). We first confirmed that this level of inhibition of NFAT5 expression in 3T3-L1 cells leads to enhanced adipogenesis, as illustrated by the strong upregulation of FABP4 expression (Fig. 5B) (20). While FABP4 expression is inhibited in FHL2 overexpressing cells (Fig. 2E), simultaneous knockdown of NFAT5 resulted in a rescue of FABP4 expression for both short hairpins on both the mRNA and protein level (Fig. 5B-C and Fig. S4). Other differentiation markers (ADIPOQ and PPARγ) gave comparable results, with some variation between the two short hairpins used (Fig. S3A-B, Fig.S4 and Fig. 5C). To underscore the recovery of the FHL2-mediated inhibition of adipogenesis by reducing NFAT5 expression, we performed an intracellular lipid staining showing that FHL2 overexpression inhibits lipid loading of the cells unless NFAT5 expression is knocked down (Fig. 5D). Overall, these experiments support the conclusion that inhibition of adipogenesis in FHL2 overexpressing cells involves its interaction with NFAT5. In the absence of NFAT5, FHL2 can no longer inhibit PPARγ expression, and thus no longer affect the differentiation of 3T3-L1 cells. In conclusion, our data support a model where downregulation of the FHL2-NFAT5 pathway presents an essential step in early adipogenesis (Fig. 6).

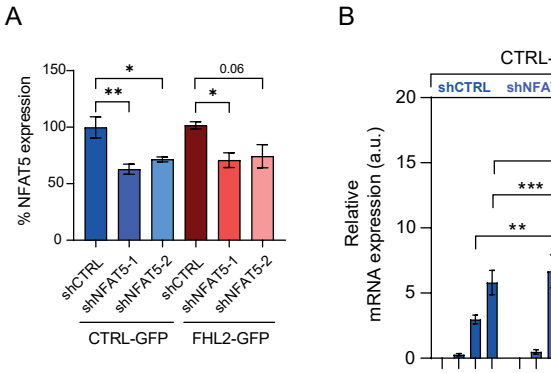

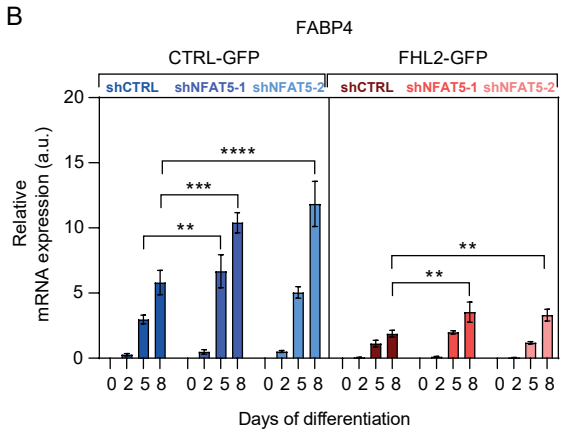

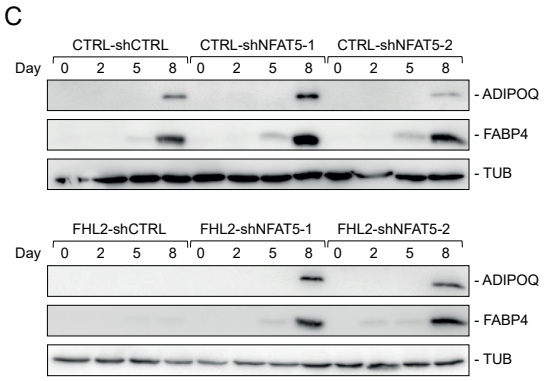

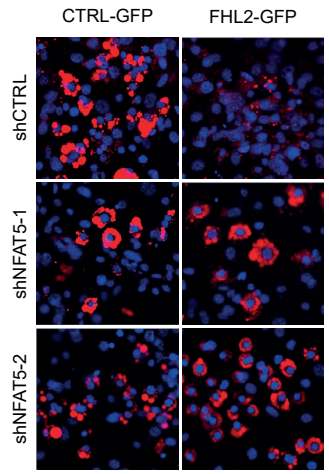

Figure 5. FHL2 overexpression inhibits adipogenesis through interaction with NFAT5. A) Relative mRNA expression of NFAT5 in CTRL-GFP and FHL2-GFP cells that were transduced with shCTRL or two different short hairpins for NFAT5 (shNFAT5-1 and shNFAT5-2). **B)** Relative mRNA expression of FABP4 in CTRL-GFP and FHL2-GFP transduced with shCTRL, shNFAT5-1, or shNFAT5-2. **C)** Western blot of FABP4, Adiponectin, and Tubulin in FHL2-GFP transduced with shCTRL, shNFAT5-1, or shNFAT5-2 cells during 8 days of differentiation. **D)** Immunofluorescence staining of intracellular lipids (red) and nuclear DAPI (blue) in differentiated cells. Data are indicated as mean ± SEM (*p<0,05).

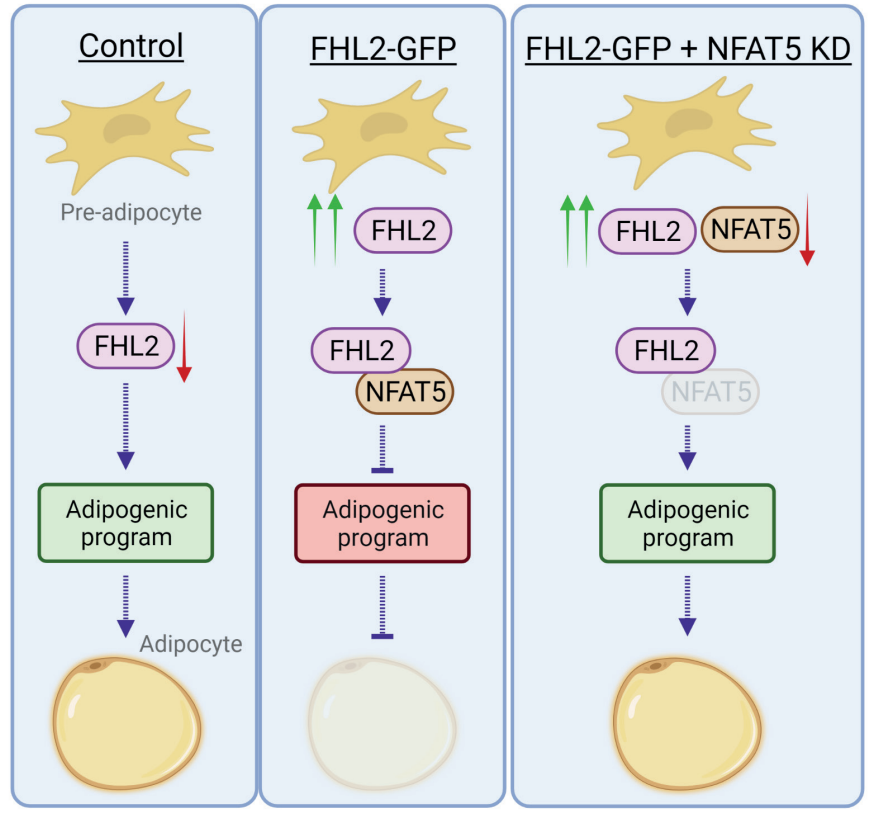

Figure 6. The FHL2-NFAT5 pathway in early adipocyte differentiation. Summary of the proposed mechanism by which FHL2 overexpression inhibits adipocyte differentiation through complex formation with NFAT5. Downregulation of FHL2 in early adipogenesis is an essential step in the differentiation process. Created with BioRender.com.

4. Discussion

Pre-adipocyte differentiation is a highly-regulated and complex process requiring the sequential expression of a considerable number of proteins, ultimately resulting in the generation of mature adipocytes. The expression of crucial proteins occurs in a specific chronological order during the distinct stages of adipogenesis with for example the transcription factor CEBPβ playing a crucial role during the early stages, while PPARγ is a key player at later stages (40). Furthermore, multiple proteins have been identified to inhibit adipogenesis, like AMPK, C/EBPβ-LIP, CHOP, and CUGBP1 (6, 9, 10). Any alteration in this intricately regulated gene expression profile affects the formation of mature adipocytes, either promoting or inhibiting appropriate differentiation (9, 10, 41, 42). In the current study, we discovered that the multifaceted protein FHL2 is transiently downregulated during the early stages of adipocyte differentiation, which is essential to achieving full differentiation. More specifically, we demonstrated that FHL2 expression is downregulated in two distinct adipocyte differentiation systems; in pre-adipocytes isolated from the SVF of mouse WAT, as well as in the 3T3-L1 cell line. The latter cell line is an extensively used model to study adipogenesis where cells are already committed to some extent to the adipocyte lineage (3).

We found that one of the components of the differentiation cocktail, IBMX, is sufficient to incite downregulation of FHL2 expression, indicating that increased intracellular cAMP inhibits the expression of FHL2 in pre-adipocytes. Further studies are required to identify the physiological stimulus triggering an intracellular cAMP increase in pre-adipocytes and to clarify which specific cAMP-dependent factor(s) or pathways trigger downregulation of FHL2 expression, both in cellular differentiation assays and *in vivo*. To substantiate that the decrease in FHL2 expression is essential for adipogenesis, we constitutively overexpressed FHL2, resulting in a complete block of the differentiation process. In line with the crucial downregulation of FHL2 expression to allow adipocyte differentiation, we demonstrated that the differentiation of pre-adipocytes derived from FHL2-deficient mice occurs normally. It is important to mention that FHL2 has a function in mature WAT, as we demonstrated recently (15). More specifically, in mice FHL2 regulates the 'browning' of WAT, thereby affecting the energy expenditure of this tissue, which may contribute to the extent of weight gain of the mice when exposed to a high-fat diet (15). Furthermore, also in humans, the expression level of FHL2 in WAT is associated with 'browning' genes.

Upon constitutive expression of FHL2, the adipogenic program involving the expression of PPARγ and its target genes ADIPOQ and FABP4 is blunted, as well as the final lipid loading of the cells. Taking into account that FHL2 acts through protein-protein interactions, we investigated the interactome of FHL2 in 3T3-L1 cells using a mass spectrometry method and identified NFAT5. This protein is part of the Rel family of transcription factors and is also known as a 'tonicity-responsive enhancer-binding protein' because it is involved in the cellular response to hypertonic stress (43). NFAT5 also has a function in the immune response, especially in T cells and macrophages (44). However, what made us particularly interested in this interaction partner, is its role in adipogenesis and adipose tissue (19, 20, 36). In 3T3-L1 cells, NFAT5 has been reported to bind to the PPARγ promoter and block PPARγ expression (20). In addition, the reduction of NFAT5 expression promotes a faster activation of the adipogenic program, whereas its overexpression inhibits adipogenesis (19, 20). This analogous behavior of NFAT5-overexpressing cells and FHL2-overexpressing cells is the main reason to hypothesize that FHL2 indeed inhibits adipocyte differentiation through its interaction with NFAT5. We confirmed the interaction of NFAT5 with FHL2 by co-immunoprecipitation and recovered adipocyte differentiation in overexpressing FHL2 cells by reducing NFAT5 expression. Previously, hypertonicity has been reported as a relevant process in lipid accumulation in 3T3-L1 cells, we may therefore speculate that the FHL2-NFAT5 complex modulates hypertonic stress in pre-adipocytes (45). Another finding that puts forward interesting aspects to be studied further, is our finding that the FHL2 pull-down in 3T3-L1 cells contains eight members of the CNOT complex, which strongly suggests that FHL2 participates in this complex. Given that FHL2 is known to interact with several nuclear receptors, among which ERα, it is of interest to mention that direct interaction of CNOT1 with the nuclear receptors ERα and RXR has been reported (46). Even more relevant for the current study, the CNOT complex is necessary for a correct adipocyte phenotype in mouse adipose tissue, as well as for appropriate differentiation of 3T3-L1 cells (47-49). We wish to propose that it is very likely that the binding of FHL2 with the CNOT complex, with NFAT5, and other factors identified in our pull-down screen, also occurs in other cellular systems undergoing differentiation (16, 18). Of note, the interaction between FHL2 and NFAT5, as well as with CNOT-elements has been reported before in the study by Huttlin *et al*, which concerns a protein interaction network study in T293 and HCT116 cells (50). The current study now demonstrates a functional interaction between FHL2 and NFAT5 in adipogenesis, and it will be of interest to assess the relative contribution of this specific protein-protein interaction in other cellular processes.

4.1 Conclusion

FHL2 is expressed in pre-adipocytes where it refrains the cells from differentiating towards mature adipocytes through its interaction with NFAT5. Our data indicate that the expression of both proteins needs to be reduced to initiate the

adipogenic program. Based on the present findings, we can firstly add FHL2 to the list of factors requiring timely regulation of expression to facilitate accurate adipocyte differentiation (3, 51, 52) and, secondly add adipocytes to the list of cells in which FHL2 plays an important role in differentiation (16, 18). Especially in elderly individuals, FHL2 expression in WAT is increased, which may interfere with appropriate adipogenesis and subsequent peripheral fat loss with aging. Finally, whereas FHL2 has been described to promote differentiation of myoblasts and osteoblasts (16, 18), we now demonstrated that FHL2 plays the opposite role in pre-adipocytes. Given that these cells are all derived from mesenchymal stem cells, this poses FHL2 at the intersection of these two distinct cellular processes, tilting the balance towards osteoblasts, whereas its downregulation facilitates pre-adipocyte formation (53).

Declarations

Supporting information

This article contains supporting information.

Data availability

The raw and processed RNA-seq data have been deposited in the Gene Expression Omnibus (GEO) database under accession number GSE200920. The mass spectrometry proteomics data have been deposited to the ProteomeXchange Consortium via the PRIDE partner repository with the dataset identifier PXD033974.

Funding and additional information

This research was supported by a grant from the Rembrandt Institute of Cardiovascular Sciences, and Research Institute Cardiovascular Sciences of Amsterdam UMC (C.J.dV.), and by a grant from the European Union's Horizon 2020 Marie Skłodowska-Curie Innovative Training Network, TRAIN (project no. 721532 – E.K.).

Acknowledgments

We thank Dr. Sebastiaan Winkler and members of the Kalkhoven and de Vries laboratories for helpful discussions. Graphical abstract, figure 3A and figure 6 were created with BioRender.com.

Author contribution

M.P. Clemente-Olivo, M. Hernandez-Quiles, E. Kalkhoven, and C.J.M. de Vries conceived the study and experiments. M.P. Clemente-Olivo, M. Hernandez-Quiles, R. Sparrius, M. van der Stoel, and V. Janssen performed the experiments. M.P. Clemente-Olivo, M. Hernandez-Quiles and A. Jongejan performed and analyzed the RNA sequencing experiment. M. Hernandez-Quiles, R. van Es, P. Sobrevals Alcaraz and H. Vos performed and analyzed the mass spectrometry data. M.P. Clemente-Olivo, M. Hernandez-Quiles, E. Kalkhoven, and C.J.M. de Vries wrote the manuscript.

Ethics approval

All animal experiments were approved by the ethics committee of the Amsterdam University Medical Center, The Netherlands, and were performed following European directive 2010/63/EU guidelines (permit number DBC287).

Consent for publication

This study is approved by all authors for publication.

Conflict of interest

The authors declare they have no conflicts of interest with the contents of this article.

References

1. Meirelles LD, Caplan AI, Nardi NB. In search of the in vivo identity of mesenchymal stem cells. Stem Cells. 2008;26(9):2287-99.
2. Lowe CE, O'Rahilly S, Rochford JJ. Adipogenesis at a glance. Journal of Cell Science. 2011;124(16):2681-6.
3. Farmer SR. Transcriptional control of adipocyte formation. Cell Metab. 2006;4(4):263-73.
4. Hernandez-Quiles M, Broekema MF, Kalkhoven E. PPARgamma in Metabolism, Immunity, and Cancer: Unified and Diverse Mechanisms of Action. Front Endocrinol (Lausanne). 2021;12:624112.
5. Schaum N, Lehallier B, Hahn O, Palovics R, Hosseinzadeh S, Lee SE, et al. Ageing hallmarks exhibit organ-specific temporal signatures. Nature. 2020;583(7817):596-602.
6. Ou MY, Zhang H, Tan PC, Zhou SB, Li QF. Adipose tissue aging: mechanisms and therapeutic implications. Cell Death Dis. 2022;13(4):300.
7. Kirkland JL, Tchkonia T, Pirtskhalava T, Han J, Karagiannides I. Adipogenesis and aging: does aging make fat go MAD? Exp Gerontol. 2002;37(6):757-67.
8. Schipper BM, Marra KG, Zhang W, Donnenberg AD, Rubin JP. Regional anatomic and age effects on cell function of human adipose-derived stem cells. Ann Plast Surg. 2008;60(5):538-44.
9. Ahmad B, Serpell CJ, Fong IL, Wong EH. Molecular Mechanisms of Adipogenesis: The Anti-adipogenic Role of AMP-Activated Protein Kinase. Front Mol Biosci. 2020;7.
10. Wang YH, Zhao L, Smas C, Sul HS. Pref-1 Interacts with Fibronectin To Inhibit Adipocyte Differentiation. Molecular and Cellular Biology. 2010;30(14):3480-92.
11. Hajer GR, van Haeften TW, Visseren FL. Adipose tissue dysfunction in obesity, diabetes, and vascular diseases. Eur Heart J. 2008;29(24):2959-71.
12. Ambele MA, Dhanraj P, Giles R, Pepper MS. Adipogenesis: A Complex Interplay of Multiple Molecular Determinants and Pathways. Int J Mol Sci. 2020;21(12):4283.
13. Habibe JJ, Clemente-Olivo MP, de Vries CJ. How (Epi)Genetic Regulation of the LIM-Domain Protein FHL2 Impacts Multifactorial Disease. Cells. 2021;10(10).
14. Johannessen M, Moller S, Hansen T, Moens U, Van Ghelue M. The multifunctional roles of the four-and-a-half-LIM only protein FHL2. Cell Mol Life Sci. 2006;63(3):268-84.
15. Clemente-Olivo PM, Habibe JJ, Vos M, Ottenhoff R, Jongejan A, Herrema H, et al. Four-and-a-half LIM domain protein 2 (FHL2) deficiency protects mice from diet-induced obesity and high FHL2 expression marks human obesity. Metabolism-Clinical and Experimental. 2021;121.
16. Brun J, Fromigue O, Dieudonne FX, Marty C, Chen J, Dahan J, et al. The LIM-only protein FHL2 controls mesenchymal cell osteogenic differentiation and bone formation through Wnt5a and Wnt10b. Bone. 2013;53(1):6-12.
17. Lai CF, Bai ST, Uthgenannt BA, Halstead LR, McLoughlin P, Schafer BW, et al. Four and half lim protein 2 (FHL2) stimulates osteoblast differentiation. J Bone Miner Res. 2006;21(1):17-28.

18. Martin B, Schneider R, Janetzky S, Waibler Z, Pandur P, Kuhl M, et al. The LIM-only protein FHL2 interacts with beta-catenin and promotes differentiation of mouse myoblasts. Journal of Cell Biology. 2002;159(1):113-22.
19. Kim SJ, Kim T, Choi HN, Cho EJ, Park JB, Jeon BH, et al. TonEBP suppresses adipocyte differentiation via modulation of early signaling in 3T3-L1 cells. Korean J Physiol Pharmacol. 2016;20(6):649-55.
20. Lee JH, Lee HH, Ye BJ, Lee-Kwon W, Choi SY, Kwon HM. TonEBP suppresses adipogenesis and insulin sensitivity by blocking epigenetic transition of PPARgamma2. Sci Rep. 2015;5:10937.
21. Rakhshandehroo M, Gijzel SM, Siersbaek R, Broekema MF, de Haar C, Schipper HS, et al. CD1d-mediated presentation of endogenous lipid antigens by adipocytes requires microsomal triglyceride transfer protein. J Biol Chem. 2014;289(32):22128-39.
22. Kurakula K, Vos M, Rubio IO, Marinkovic G, Buettner R, Heukamp LC, et al. The LIM-Only Protein FHL2 Reduces Vascular Lesion Formation Involving Inhibition of Proliferation and Migration of Smooth Muscle Cells. Plos One. 2014;9(4).
23. Ruijter JM, Ramakers C, Hoogaars WMH, Karlen Y, Bakker O, van den hoff MJB, et al. Amplification efficiency: Linking baseline and bias in the analysis of quantitative PCR data. Nucleic Acids Research. 2009;37(6).
24. Kim D, Langmead B, Salzberg SL. HISAT: a fast spliced aligner with low memory requirements. Nat Methods. 2015;12(4):357-60.
25. Robinson MD, McCarthy DJ, Smyth GK. edgeR: a Bioconductor package for differential expression analysis of digital gene expression data. Bioinformatics. 2010;26(1):139-40.
26. Bolger AM, Lohse M, Usadel B. Trimmomatic: a flexible trimmer for Illumina sequence data. Bioinformatics. 2014;30(15):2114-20.
27. Wu D, Smyth GK. Camera: a competitive gene set test accounting for inter-gene correlation. Nucleic Acids Res. 2012;40(17):e133.
28. Kurakula K, van der Wal E, Geerts D, van Tiel CM, de Vries CJM. FHL2 Protein Is a Novel Co-repressor of Nuclear Receptor Nur77. Journal of Biological Chemistry. 2011;286(52):44336-43.
29. Green H, Meuth M. An established pre-adipose cell line and its differentiation in culture. Cell. 1974;3(2):127-33.
30. Ruiz-Ojeda FJ, Ruperez AI, Gomez-Llorente C, Gil A, Aguilera CM. Cell Models and Their Application for Studying Adipogenic Differentiation in Relation to Obesity: A Review. Int J Mol Sci. 2016;17(7).
31. Ruijtenberg S, van den Heuvel S. Coordinating cell proliferation and differentiation: Antagonism between cell cycle regulators and cell type-specific gene expression. Cell Cycle. 2016;15(2):196-212.
32. Jiang C, Sun J, Dai Y, Cao P, Zhang L, Peng S, et al. HIF-1A and C/EBPs transcriptionally regulate adipogenic differentiation of bone marrow-derived MSCs in hypoxia. Stem Cell Res Ther. 2015;6:21.
33. Li SN, Wu JF. TGF-beta/SMAD signaling regulation of mesenchymal stem cells in adipocyte commitment. Stem Cell Res Ther. 2020;11(1):41.
34. Tran MK, Kurakula K, Koenis DS, de Vries CJM. Protein-protein interactions of the LIM-only protein FHL2 and functional implication of the interactions relevant in cardiovascular disease. Bba-Mol Cell Res. 2016;1863(2):219-28.

35. Hernandez-Quiles M, Baak R, Borgman A, den Haan S, Sobrevals Alcaraz P, van Es R, et al. Comprehensive Profiling of Mammalian Tribbles Interactomes Implicates TRIB3 in Gene Repression. Cancers (Basel). 2021;13(24).
36. Lee HH, An SM, Ye BJ, Lee JH, Yoo EJ, Jeong GW, et al. TonEBP/NFAT5 promotes obesity and insulin resistance by epigenetic suppression of white adipose tissue beiging. Nat Commun. 2019;10(1):3536.
37. Chalabi Hagkarim N, Grand RJ. The Regulatory Properties of the Ccr4-Not Complex. Cells. 2020;9(11).
38. Collart MA, Panasenko OO. The Ccr4-Not Complex: Architecture and Structural Insights. Subcell Biochem. 2017;83:349-79.
39. Mognol GP, Carneiro FRG, Robbs BK, Faget DV, Viola JPB. Cell cycle and apoptosis regulation by NFAT transcription factors: new roles for an old player. Cell Death Dis. 2016;7.
40. Sun WP, Yu ZJ, Yang SM, Jiang CY, Kou YB, Xiao LZ, et al. A Transcriptomic Analysis Reveals Novel Patterns of Gene Expression During 3T3-L1 Adipocyte Differentiation. Front Mol Biosci. 2020;7.
41. Fu YC, Luo NL, Klein RL, Garvey WT. Adiponectin promotes adipocyte differentiation, insulin sensitivity, and lipid accumulation. J Lipid Res. 2005;46(7):1369-79.
42. Christiaens V, Van Hul M, Lijnen HR, Scroyen I. CD36 promotes adipocyte differentiation and adipogenesis. Bba-Gen Subjects. 2012;1820(7):949-56.
43. Lee SD, Choi SY, Lim SW, Lamitina ST, Ho SN, Go WY, et al. TonEBP stimulates multiple cellular pathways for adaptation to hypertonic stress: organic osmolyte-dependent and -independent pathways. Am J Physiol Renal Physiol. 2011;300(3):F707-15.
44. Lee N, Kim D, Kim WU. Role of NFAT5 in the Immune System and Pathogenesis of Autoimmune Diseases. Frontiers in Immunology. 2019;10.
45. Ha EE, Bauer RC. Emerging Roles for Adipose Tissue in Cardiovascular Disease. Arterioscl Throm Vas. 2018;38(8):E137-E44.
46. Winkler GS, Mulder KW, Bardwell VJ, Kalkhoven E, Timmers HT. Human Ccr4-Not complex is a ligand-dependent repressor of nuclear receptor-mediated transcription. EMBO J. 2006;25(13):3089-99.
47. Li X, Morita M, Kikuguchi C, Takahashi A, Suzuki T, Yamamoto T. Adipocyte-specific disruption of mouse Cnot3 causes lipodystrophy. FEBS Lett. 2017;591(2):358-68.
48. Takahashi A, Takaoka S, Kobori S, Yamaguchi T, Ferwati S, Kuba K, et al. The CCR4-NOT Deadenylase Complex Maintains Adipocyte Identity. Int J Mol Sci. 2019;20(21).
49. Sohn EJ, Jung DB, Lee J, Yoon SW, Won GH, Ko HS, et al. CCR4-NOT2 Promotes the Differentiation and Lipogenesis of 3T3-L1 Adipocytes via Upregulation of PPARx03B3;, CEBPalpha and Inhibition of P-GSK3alpha/beta and beta-Catenin. Cell Physiol Biochem. 2015;37(5):1881-9.
50. Huttlin EL, Bruckner RJ, Navarrete-Perea J, Cannon JR, Baltier K, Gebreab F, et al. Dual proteome-scale networks reveal cell-specific remodeling of the human interactome. Cell. 2021;184(11):3022-+.
51. Audano M, Pedretti S, Caruso D, Crestani M, De Fabiani E, Mitro N. Regulatory mechanisms of the early phase of white adipocyte differentiation: an overview. Cell Mol Life Sci. 2022;79(3):139.

52. Mueller E. Understanding the variegation of fat: novel regulators of adipocyte differentiation and fat tissue biology. Biochim Biophys Acta. 2014;1842(3):352-7.
53. James AW. Review of Signaling Pathways Governing MSC Osteogenic and Adipogenic Differentiation. Scientifica. 2013;2013.

Supporting information

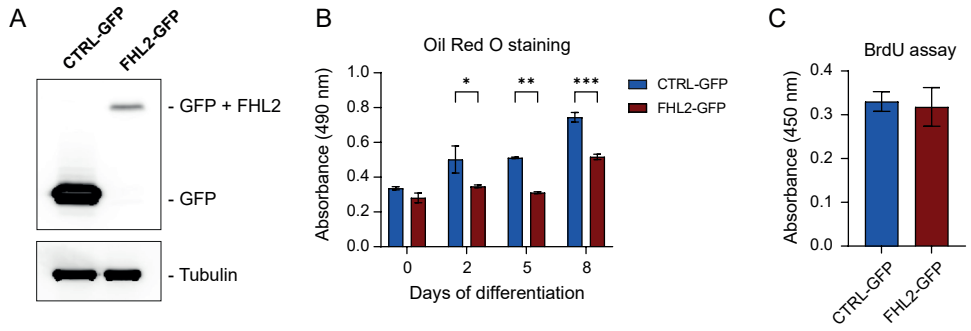

Figure S1. A) Western blot to visualize GFP in 3T3-L1 cells transduced with CTRL-GFP and FHL2-GFP (tubulin used as loading control). **B)** Oil Red O staining quantification of differentiated CTRL-GFP and FHL2-GFP 3T3-L1 cells. **C)** BrdU proliferation assay of CTRL-GFP and FHL2-GFP 3T3-L1 cells. Data are indicated as mean ± SEM (*p<0,05).

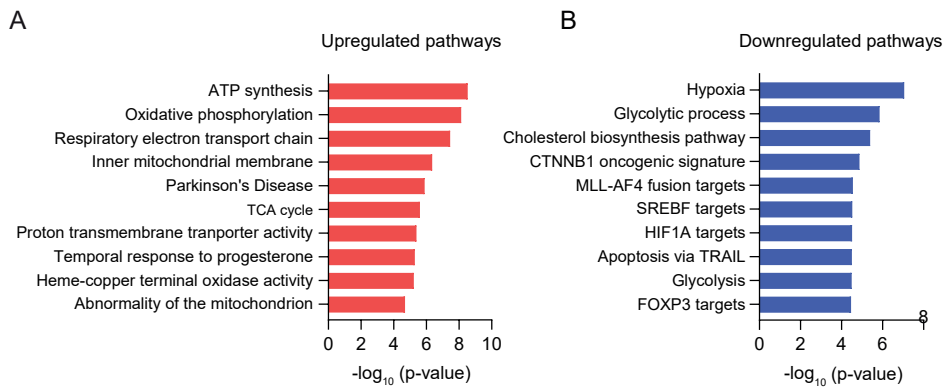

Figure S2. A) Top up- and **B)** down-regulated pathways in FHL2-GFP cells at day 0 of differentiation.

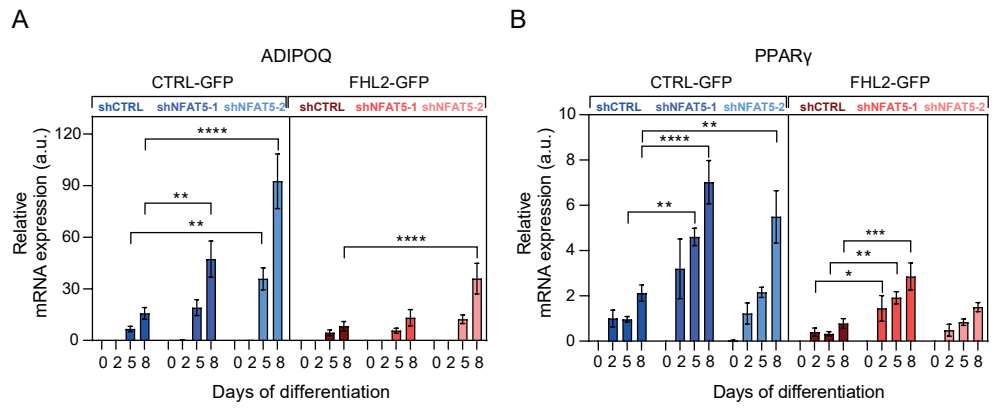

Figure S3. A-B) Relative mRNA expression of ADIPOQ and PPARγ in CTRL-GFP and FHL2-GFP transduced with shCTRL, shNFAT5-1, and shNFAT5-2. Data are indicated as mean ± SEM (*p<0,05).

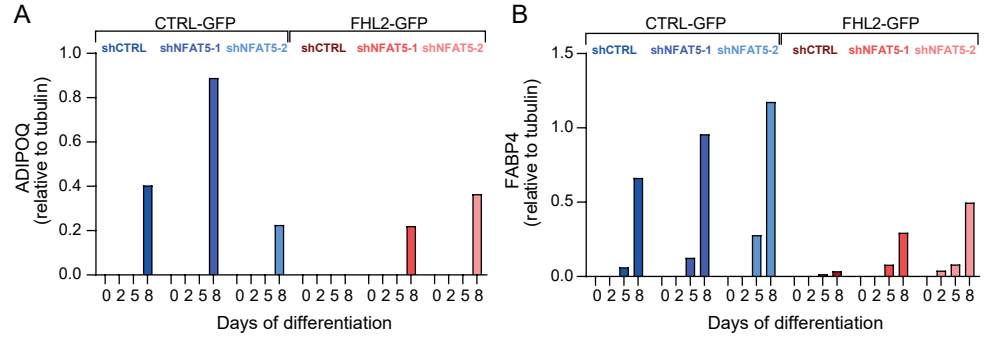

Figure S4. A-B) Protein expression of ADIPOQ and FABP4 relative to tubulin in CTRL-GFP and FHL2-GFP transduced with shCTRL, shNFAT5-1, and shNFAT5-2 (see Fig. 5C).

Table S1. List of primers used in RT-qPCR.

Mouse primers	Forward (5'-3')	Reverse (5'-3')
Actb (β-actin)	AGCCATGTACGTAGCCATCC	CTCTCAGCTGTGGTGGTGAA
Adipoq	ACTGCAACATTCCGGGACTC	GAGGCCTGGTCCACATTCTT
Cebpb	CAACCTGGAGACGCAGCACAAG	GCTTGAACAAGTTCCGCAGGGT
Fabp4	AACTGGGCGTGGAATTCGAT	CCACCAGCTTGTCACCATCT
Fhl2	TCACAGCACGGGATGAGTTTC	GTGCCACCCAGACCACTAATG
Nfat5	AAGCAGCCACCACCAAACATGA	AAATTGCATGGGCTGCTGCT
Pparg	CTCCTGTTGACCCAGAGCAT	AATGCGAGTGGTCTTCCATC
Rplp0	GGACCCGAGAAGACCTCCTT	GCACATCACTCAGAATTTCAATGG

Table S2. Top significant interactors from the AP-MS experiment (FHL2-GFP vs. CTRL-GFP 3T3-L1 cells).

Gene names	Protein names	-log10 (p-value)
Cnot3	CCR4-NOT transcription complex subunit 3	7,51
Rqcd1	Cell differentiation protein RCD1 homolog	7,12
Cnot10	CCR4-NOT transcription complex subunit 10	7,09
Btg3	Protein BTG3	6,94
Cnot2	CCR4-NOT transcription complex subunit 2	6,91
Ccar1	Cell division cycle and apoptosis regulator protein 1	6,85
Tnks1bp1	182 kDa tankyrase-1-binding protein	6,84
Fhl2	Four and a half LIM domains protein 2	6,75
Cnot11	CCR4-NOT transcription complex subunit 11	6,72
Ahi1	Jouberin	6,45
Rnf219	RING finger protein 219	6,38
Cnot6l	CCR4-NOT transcription complex subunit 6-like	6,25
Mkl2	Myocardin-like protein 2	6,13
Sh3d19	SH3 domain-containing protein 19	6,03
Qrich1	Glutamine-rich protein 1	5,99
Cnot8	CCR4-NOT transcription complex subunit 8	5,95
Tob2	Protein Tob2	5,91
Cyr61	Protein CYR61	5,50
Nfat5	Nuclear factor of activated T-cells 5	5,34
Patl1	Protein PAT1 homolog 1	5,31
Tax1bp1	Tax1-binding protein 1 homolog	5,09
Qser1	Glutamine And Serine Rich 1	5,09
Banp	Protein BANP	5,08
Eya3	Eyes absent homolog 3	5,06
Sp1	Transcription factor Sp1	4,84
Amotl1	Angiomotin-like protein 1	4,78
Cnot7	CCR4-NOT transcription complex subunit 7	4,62
Tnks	Tankyrase-1	4,57
Ggnbp2	Gametogenetin-binding protein 2	4,57
Hccs	Cytochrome c-type heme lyase	4,48
Srebf2	Sterol regulatory element-binding protein 2	4,37
Jmjd1c	Jumonji Domain Containing 1C	4,32
Ep400	E1A-binding protein p400	4,05

Chapter 6

Trib3 modulates PPARγ-mediated growth inhibition by interfering with the MLL complex in breast cancer cells

Miguel Hernández-Quiles[1], Rosalie Baak[1], Alba Orea-Soufi[2, 3], Anouska Borgman[1], Suzanne den Haan[1], Paula Sobrevals Alcaraz[4], Aldo Jongejan[5], Robert van Es[4], Guillermo Velasco[2, 3], Harmjan Vos[4] and Eric Kalkhoven[1#]

[1] Center for Molecular Medicine, University Medical Center Utrecht, Utrecht University, Utrecht, The Netherlands.

[2] Department of Biochemistry and Molecular Biology, School of Biology, Complutense University, Madrid, Spain.

[3] Instituto de Investigaciones Sanitarias San Carlos (IdISSC), Madrid, Spain.

[4] Oncode Institute and Molecular Cancer Research, Center for Molecular Medicine, University Medical Center Utrecht, Utrecht University, Utrecht, The Netherlands.

[5] Amsterdam UMC location University of Amsterdam, Department of Bioinformatics, Amsterdam, The Netherlands.

***** Correspondence: e.kalkhoven@umcutrecht.nl

Abstract

Aberrant expression or activity of proteins are amongst the best understood mechanisms that can drive cancer initiation and progression as well as therapy resistance. TRIB3, a member of the Tribbles family of pseudokinases, is often dysregulated in cancer and has been associated with breast cancer initiation and metastasis formation. However, the underlying mechanisms by which TRIB3 contributes to these events are unclear. In this study, we demonstrated that TRIB3 regulates expression of PPARγ, a transcription factor that has gained attention as a potential drug target in breast cancer for its antiproliferative actions. Proteomics and phosphoproteomics analyses together with classical biochemical assays indicate that TRIB3 interferes with the MLL complex and reduces MLL-mediated H3K4 trimethylation of the *PPARG* locus, thereby reducing PPARγ mRNA expression. Consequently, overexpression of TRIB3 blunts the antiproliferative effect of PPARγ ligands in breast cancer cells, while reduced TRIB3 expression gives the opposite effect. In conclusion, our data implicate TRIB3 in epigenetic gene regulation and suggest that expression levels of this pseudokinase may serve as a predictor of successful experimental treatments with PPARγ ligands in breast cancer.

Keywords: Tribbles; Breast cancer; PPARγ, Epigenetics; MLL-WRAD complex

Introduction

Tribbles are a family of serine/threonine pseudokinases that play a critical role in multiple cellular processes, such as metabolism, cell cycle, proteasomal degradation and cellular differentiation [1-4]. The family consist of three members, TRIB1, -2 and -3 and a more distantly related protein, serine/threonine kinase 40 (STK40)[5]. Tribbles have a well conserved structure consisting of a central pseudokinase domain that is flanked by an N- and C-Terminal domain [6]. In addition, while many structural features of canonical kinases including an N- and C- lobe structure and a DLK motif are conserved in Tribbles proteins, they are incapable of binding ATP and therefore incapable of catalyzing the transfer of a phospho group to their substrates because they lack the DFG motif [7]. Despite being pseudokinases, Tribbles have been shown to be able to regulate the phosphorylation status of certain proteins [8], they achieve this through binding to kinases or competing for substrates of active kinases [9]. Among the three members of the family, TRIB3 has drawn special attention in recent years for its ability to regulate gene transcription through binding of different transcription factors such as ATF4 and PPARγ [10, 11] or members of the FOXO family of transcription factors [12]. In fact, we and others have recently shown that TRIB3 localizes in the nucleus in breast cancer cells and that the N-terminal domain of TRIB3 interacts with a number of transcription complexes, including the WRAD complex [13]. The WRAD complex is formed by WDR5, RBBP5, ASH2L and DPY30, and they are the core subunits of the MLL-WRAD complex, the most prominent epigenetic writer of Histone H3 lysine 4 (H3K4) methyl mark in mammalian cells [14, 15]. The different levels of H3K4 methylation (mono-, di-, tri-) have different effects but it is generally associated with active transcription [16]. The MLL-WRAD complex is formed by one catalytic subunit (KMT2A/MLL1, KMT2B/MLL2, KMT2C/MLL3, KMT2F/SET1A or KMT2G/SET1B) and four core subunits (WRAD complex). The interaction with the core subunits is essential for the methyltransferase activity of the whole complex as it has been shown that inhibition of any of the core subunits results in depletion of H3K4 methylation [17, 18]. The WRAD complex is highly conserved from yeast to human, underpinning a fundamental role in eukaryotes cells. WRAD inhibitors are currently developed to treat cancers associated with MLL fusion proteins [19].

Finally, peroxisome proliferator activated receptor gamma (PPARγ) is a member of the nuclear receptor superfamily of ligand activated transcription factors. Is considered the master regulator of adipocyte differentiation and function [20] and plays a pivotal role in the regulation of lipid metabolism in immune cell [21]. Nuclear receptors have been the target of therapies for a number of diseases including cancer since more than 40 years ago [22]. Nuclear receptors, specially PPARγ, hold potential as key

factors for anti-cancer therapies as it functions as pro-differentiation factor reducing the proliferation capacity of tumorigenic cells [23, 24]. Previous studies have shown the capacity of PPARγ to inhibit epithelial to mesenchymal transition in breast cancer cells, having beneficial effects in reducing metastasis formation and reducing the proliferative capacity of tumor cells [25, 26].

Breast cancer is one the three most common malignancies and, although mortality has declined steadily during the last decades, breast cancer is still causing around half a million deaths per year worldwide [27]. Breast cancer is a complex multifactorial disease influenced by genetic alterations, including the well-known BRCA1 and BRCA2 mutations, epigenetic alterations [28] and altered cellular metabolism, including altered mitochondrial function [29, 30], and environmental factors [28]. Interestingly, some of these processes may be interconnected, as for example cellular metabolism is linked to epigenetic regulation through the rate limiting production of cellular metabolites that are the donors for histone and DNA modifications [31, 32]. In addition, obesity has been shown to play pivotal role in the development of the disease and in the prognosis of the patients [33, 34]. Because of this, incidence and mortality are expected to rise in the near future [35, 36]. In this context, developing new therapies that can prevent and tackle breast cancer remains of capital importance.

In this study we describe TRIB3 as a regulator of PPARγ expression in breast cancer cells, and we hypothesized that TRIB3 achieves this through binding to the WRAD complex and regulating H3K4me^3 mark around the PPARγ locus.

Materials & methods

Materials

Cell culture

Human embryonic kidney cell line (HEK293T, ATCC CRL-3216, Manassas, VA, USA) and human breast cancer cells (MCF7, ATCC HTB-22) were maintained in high glucose (d-glucose, 4.5 g/L) Dulbecco's Modified Eagle Medium (DMEM) supplemented with 10% fetal bovine serum and 1% penicillin and streptomycin. Inducible TRIB3-tGFP MCF7 cell line was generated using third-generation lentiviral constructs and described extensively previously [13]. TRIB3 knock down and control cell line in MCF7 cells were described previously [37].

Western blotting

Western blotting was performed as described previously [38]. In short, samples were treated accordingly and protein samples were extracted in RIPA lysis buffer. Protein concentration was measured and samples were supplemented with Laemmli Sample Buffer and loaded into 10-15% acrylamide gels. Samples were separated by SDS-PAGE and transfer to PVDF membranes. Finally, Samples were blocked in 5% milk in TBS-T for 45'. Primary antibody was incubated overnight at 4°C and secondary for 1h at RT. ECL solution was used to assess protein expression using a LAS4000 Image Quant.

RNA isolation and RT-qPCR

Total RNA form culturing cells was isolated using TRIzol reagent (Invitrogen). Then cDNA was generated using iSCRIPT cDNA synthesis kit (Biorad) following manufacture's protocol. SYBR-green was used in Quantitative PCR and was performed using the MyIq cycler (Biorad). Primers used are described in Supplementary table 1.

RNA sequencing

Sh-TRIB3 and control MCF7 cells were seeded in 10-cm dishes and RNA was isolated using as described previously. Libraries were generated using Truseq RNA stranded polyA (Illumina) and samples were sequenced on an Illumina nextseq2000 in paired-end 50 bp reads. Quality control was performed (FASTQC, dupRadar) and data was trimmed using Trimmomatic v0.39. Finally, samples were aligned to the genomes using HISAT2 (v.2.2.1) [39-41]. Using the appropriates GTFs counts were obtained using HTSeq (v0.11.0) and statistical analysis was performed using the edgeR and limma/voom R packages. Count data was transformed to log2-counts per million (logCPM) and the trimmed mean of M-values method was used for normalization of the data using voom. Differential expression was then assessed using limma's linear model framework including the precision weights estimated by voom [42]. Benjamini-Hochberg false discovery rate was used to adjust the p-values generated. The in-house Shiny-app was used for DEGs, expression plots, gene-set enrichment results. The raw and processed RNA-seq data have been deposited in the Gene Expression Omnibus (GEO) database under accession number GSE212489.

Immunoprecipitation

HEK293T cells were used for Co-IP experiments and protocol have been described previously [13]. In short, TRIB3-GFP and mutants, FLAG-ASHL2, FLAG-DPY30, FLAG-WDR5, MYC-WDR5 and mutants, MLL-FLAG and mutants were used for co-transfections using Xtreme-Gene 9 DNA Transfections Reagent (Roche) following manufacture's protocol. Protein lysates were obtained as described previously, and samples were incubated for 2h with either GFP-Trap agarose beads (Chromotek)

or anti-FlagM2 magnetic beads (Invitrogen) and IP was performed following manufactures instructions. Samples were then eluted from the beads and analyzed by western blotting.

Phosphoproteomics

Enrichment of phospho-peptides for SILAC labeling, MCF7 Trib3-KD cells or scramble control cells were cultured in high-glucose (10% dialyzed FBS (BioWest)) DMEM (Thermo) lacking lysine and arginine supplemented with Lys-0/Arg-0 or Lys-8/Arg-10 (Silantes). Cells were lysed in 8 M Urea, 1M Ammonium-BiCarbonate (ABC) containing 10 mM Tris(2-carboxyethyl)phosphine hydrochloride (TCEP) and 40mM 2-chloro-acetamide supplemented with protease inhibitors (Roche, complete EDTA-free) and 1% (v/v) phosphatase inhibitor cocktails 2 and 3 (Sigma, Cat. No. P5726 and Cat. No. P0044). After ultra-sonication, Heavy and light cell lysates were mixed 1:1 and proteins (20mg total) were over-night in solution digested with trypsin (1:50) (Worthington). Peptides were desalted using SepPack columns (Waters) and eluted in 80% acetonitrile (ACN). To enrich for phospho-peptides, 200 mg Calcium Titanium Oxide (CaTiO3) powder (Alfa Aesar, 325 mesh) was equilibrated 3 times with binding solution (6% Acetic acid in 50% ACN pH=1 with HCl) after which the phospho-peptides were allowed to bind at 40 ˚C for 10 minutes on a shaker. After 6 times centrifugation and washing, phospho-peptides were eluted twice with 200µl 5% NH3. The peptides were dried using a SpeedVac and the dissolved in buffer A (0.1% FA) before loading on in-house made C18 stage-tips and divided with high PH elution into three fractions (100mM NH3/FA PH=10 in 5%, 10% or 50% ACN).

LC-MS/MS analysis

After elution from the stage tips, acetonitrile was removed using a SpeedVac and the remaining peptide solution was diluted with buffer A (0.1% FA) before loading. Peptides were separated on a 30 cm pico-tip column (75µm ID, New Objective) in-house packed with 1.9 µm aquapur gold C-18 material (dr. Maisch) using a 140 minute gradient (7% to 80% ACN 0.1% FA), delivered by an easy-nLC 1200 (Thermo), and electro-sprayed directly into a Orbitrap Eclipse Tribrid Mass Spectrometer (Thermo Scientific). The latter was set in data dependent mode with a cycle time of 1 second, in which the full scan over the 400-1400 mass range was performed at a resolution of 240K. The most intense ions (intensity threshold of 10000 ions, charge state 2-7) were isolated by the quadrupole with a 0.4 Da window and fragmented with a HCD collision energy of 30%. The maximum injection time of the ion trap was set to 35 milliseconds. Dynamic exclusion of 10 ppm was set on 30 seconds, including isotopes.

Data analysis

Raw files were analyzed with the Maxquant software version 1.6.3.4 (Cox and Mann, 2008) with phosphorylation of serine threonine and tyrosine as well as oxidation of methionine set as variable modifications, and carbamidomethylation of cysteine set as fixed modification. The Human protein database of Uniprot (Jan. 2019) was searched with both the peptide as well as the protein false discovery rate set to 1%. The SILAC quantification algorithm was used in combination with the 'match between runs' tool (option set at two minutes). Peptides were filtered for reverse hits and standard contaminants. Forward and Reverse ratios were plotted in R (www.r-project.org). The mass spectrometry proteomics data have been deposited to the ProteomeXchange Consortium via the PRIDE partner repository (http://www.ebi.ac.uk/pride) (data identifier: PXD036341)

Cell proliferation assay

Cell proliferation was assessed by Cell titer Aqueous Cell Proliferation assay (MTS) kit (Promega). In short, 10.000 cells were seeded in 96-well plates and treated with Rosiglitazone for at different concentrations for 24-48h. Then cell proliferation was assessed following manufacturer's protocol.

H3K4me^3 ELISA

Histone H3 (tri-methyl K4) Quantification Kit (abcam) was used to assess the levels of H3k4me^3. Cells were culture and treated accordingly as described before, then acid extraction was performed following manufacturer's instructions to extract intact histones form cells, Histone concentrations was assessed by Coomassie blue. ELISA was performed according to manufacturer's protocol.

ChIP followed by RT-qPCR

Chromatin immuno-precipitation of H3K4me^3 was performed using EpiQuik-Chromatin Imunoprecipitation kit (Epigentek). Cells were lysed and DNA was shear using sonication as described previously [43]. RT-qPCR was performed as described before, primers used for quantitative PCR are described in supplementary table 2, HSBC and USMC genes were used as positive control for genes with high level of H3K4me^3 [44] and Negative control was also used.

Chromatin bond protein extraction

Chromatin extracts were generated as follow; cells were grown in 15-cm dishes and trypsin was used for harvesting the cells. Cells were washed with ice-cold PBS and spined down for 5 min at 400g, this was repeated twice. Cells were then resuspended in 5 times in volume Buffer A (10mM HEPES KOH pH 7.9, 1.5mM MgCl2,

10mM KCl) and incubate for 10' on ice. Then cells were centrifuged for 5' at 400g, followed by resuspension in 2 times volume of Buffer A+ (Buffer A + 0.5 mM DTT, EDTA-free protease inhibitor cocktail and NP-40 0.15% final volume). Then samples were homogenized using a dounce homogenizer (4x 10 strokes with type B pestle). Samples were centrifuged for 15' at 3200g at 4°C. Supernatant is the cytoplasmatic fraction, pellet was washed in PBS and centrifuged for 5' at 3200 g. Crude nuclei was resuspended in 2 times volume of Buffer C (420mM NaCl, 20mM HEPES KOH pH7.9, 20% Glycerol, 2mM MgCl2, 0.2 mM EDTA, 0.1% NP-40, 0.5mM DTT) and incubated in rotation for 1h at 4°C. Samples were then centrifuged for 30 min at 20.000g at 4°C. Supernatant is nuclear fraction, Pellet was washed in PBS and resuspended in 2 times volume RIPA buffer (150 mM NaCl, 50mM Tris pH 8.0, 1% NP-40, 5mM MgCl2, 10% glycerol), chromatin extract was stored at -80°C for further analysis.

Results

TRIB3 regulates PPARγ expression in breast cancer cells

TRIB3 levels have been shown to influence breast cancer tumorigenesis and metastasis formation but little is known about the mechanisms behind such associations [12, 45, 46]. In order to better understand the role of TRIB3 in breast cancer cells, we performed RNA sequencing of TRIB3 knock-down compared to scramble control in MCF7 cells [37] (Figure 1A). Depletion of TRIB3 results in the upregulation of 527 genes and downregulation of 245 genes (Fold change >1, Adjusted p-value >0.05) (Figure 1B). Signaling pathways involved in oxidative phosphorylation and MYC target genes were downregulated, whereas KRAS signaling and Apical junction signaling were upregulated (Supplementary Table 3). In addition, Cell differentiation index and white fat cell differentiation pathways were found upregulated in the knock down cells. In line with this, Among the top 10 most upregulated genes in TRIB3-KD cells we found PPARG (Log2 Fold change: 3.11, Adjusted p-value: 0.0003) (Figure 1C). This increase in PPARG mRNA levels was also observed on the protein level (Figure 1D). To further characterize the role of TRIB3 in MCF7 cells we used the previously described MCF7-TRIB3-tGFP inducible cell line [13] and assessed PPARG levels both at mRNA and protein level. We found that overexpression of TRIB3 results in reduced PPARγ protein levels (Figure 1E) and this reduction is also appreciated on the mRNA level (Figure 1F). Our data shows that TRIB3 levels influence PPARγ expression both at the protein and mRNA level, suggesting a transcriptional regulatory role for TRIB3 in these cells.

Figure 1. TRIB3 regulates PPARγ expression in MCF7 cells. (A) Schematic representation of RNA-seq experiment and volcano plot showing differentially expressed genes between Sh-TRIB3 and Sh-control cells. (B) Up and down regulated genes (p-adjusted value >0.05). (C) Counts per million of PPARG in Sh-control and Sh-TRIB3 cells. (D) Western blot of endogenous TRIB3 expression and PPARG in Sh-control and Sh-TRIB3 in MCF7 cells and Tubulin as loading control. (E) Western blot of TRIB3-tGFP using anti-tGFP antibody and endogenous PPARG in inducible TRIB3-tGFP MCF7 cells. (F) Relative mRNA expression of PPARG in inducible TRIB3-tGFP MCF7 cells treated with and without doxycycline.

Phospho-proteome of TRIB3-KD in MCF7 cells reveals its role as epigenetic regulator

To examine whether the potential role of TRIB3 as a transcriptional regulator may be linked to its ability to affect cellular phosphorylation events (see Introduction), we compared the phospho-proteomes of MCF7 TRIB3-KD cells to scramble control cells with stable isotope labeling of amino acids in cell culture (SILAC) quantitative proteomics. Pathway analysis revealed multiple proteins involved in chromatin organization, histone methylation and regulation of chromatin silencing, including the LARC complex, SWI/SNF and NCOR complexes. More specifically, we found differences in the phosphorylation status of SET1A, in particular at the tyrosine

in position 916 (Figure 2C). This phosphorylation is the most prominent post translational modification (PTM) found in MLL/SET1 family of proteins as it has been reported more than any other (Figure 2D). Previous studies have linked changes in PTM status of SET1A to changes in breast cancer development [47], but the kinase responsible has not been identified. In addition, pathway analysis confirmed previously reported roles for TRIB3 in cell-cell junction and focal adhesion, as well as regulation of receptor tyrosine kinase and insulin signaling [8, 37], supporting the validity of the experimental approach (Fig. 2B).

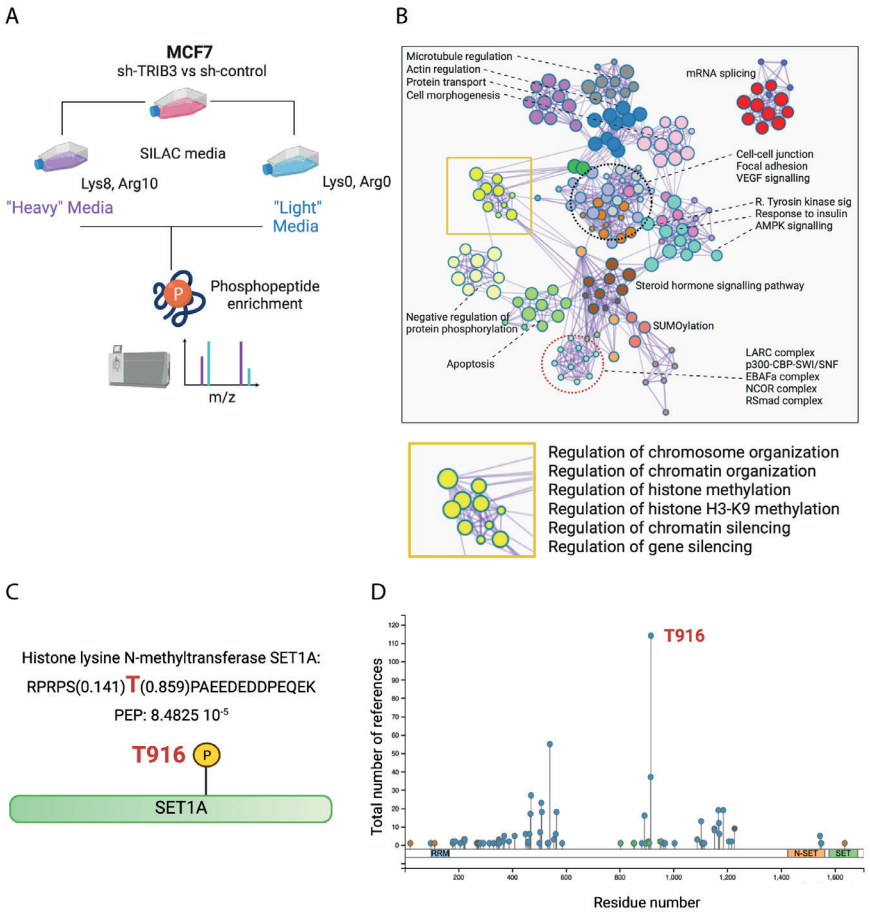

Figure 2. The phosphoproteome of TRIB3 knock down cells reveals downstream targets of TRIB3. (A) Schematic representation of Phosphoproteomics experiment using SILAC. (B) Pathways analysis of phosphor-peptides found differentially phosphorylated in Sh-TRIB3 compared to Sh-control in MCF7 cells. (C) Schematic representation of phosphorylation of T916 in SET1A. (D) Posttranslational modifications in SET1A according to Phosphositeplus [48].

TRIB3 interacts with WDR5 and ASHL2 subunits of the WRAD complex and with the SET domain of MLL/SET1 proteins:

The phospho-proteome results (Fig. 2), together with our previous TRIB3 interactome studies showing TRIB3 binding to components of the MLL-WRAD complex in MCF7 cells [13], point to the MLL-WRAD complex as a potential intermediate through which TRIB3 may regulate the expression of genes like PPARG (Fig. 1). To substantiate this hypothesis, we first analyzed interactions between TRIB3 and various subunits of the MLL-WRAD complex through co-immunoprecipitation analyses in HEK293T cells. Our results shows that TRIB3 is able to bind to the WDR5 and ASHL2 subunits (Figure 3A and Figure 3B) but not to RBBP5 and DPY30 (Figure 3B). To characterize these interactions further we made use of previously described point mutants of WDR5 and MLL. WDR5 is the subunit of the WRAD complex that coordinates the interaction with MLL/SET1 proteins, critically depending on residues in the WIN domain of WDR5 (S91 and F133) and the WD40 domain of MLL (R3765 in MLL1) [49-51]. The F133A mutation in WDR5 but not the S91K mutation disrupted the interaction with TRIB3 (Figure 3A). In addition, mutation of either the arginine at position 36 or 58 of TRIB3 – which potentially correspond to R3765 in MLL– did not affect the interaction with WDR5. (Fig. 3A) All together, our data indicate that the interaction between TRIB3 and WDR5 is mediated through the WIN domain of WDR5 and is similar to but not identical to the interaction between WDR5 and MLL/SET1 proteins.

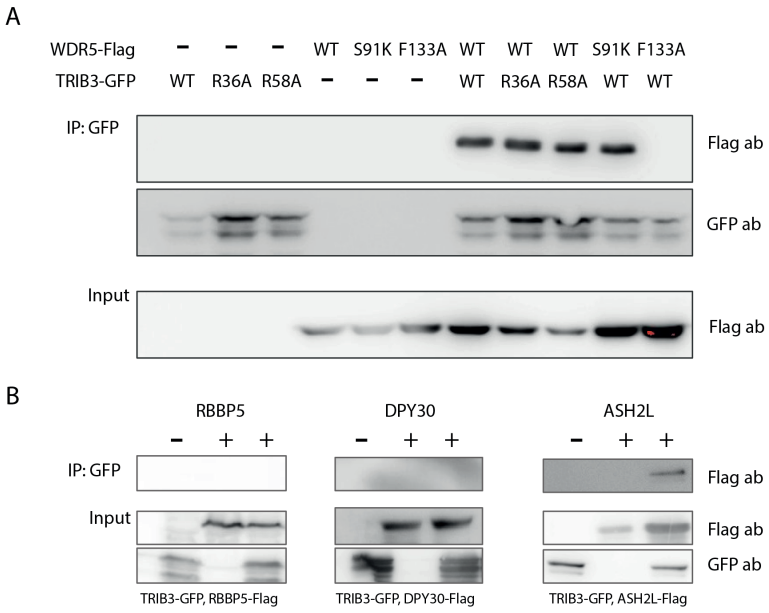

Figure 3. TRIB3 binds to WDR5 and ASHL2, subunits of the WRAD complex and to the SET domain of MLL/SET1 proteins. (A) Co-immunoprecipitation (IP) of TRIB3-GFP together with wild type Flag-WDR5 and Flag-WDR5-S91K and Flag-WDR5-F133A as well as TRIB3-R36A-GFP and TRIB3-R58A-GFP mutants. (B) co-IP of TRIB3-GFP with Flag-RBBP5, Flag-DPY30 and Flag-ASHL2. (C) Co-IP of TRIB3-GFP, MLL-Flag and WDR5-MYC. All co-IP were performed using HEK293T cells.

Furthermore, we assessed the interaction between TRIB3 and the SET domain of MLL/SET1 proteins. We found that TRIB3 is also able to interact together with the SET domain of MLL/SET1 proteins, independent of co-expression of WDR5 (Lanes 1 and 3 Figure 3C). Moreover, a WDR5 S91K mutant that is not able to bind MLL/SET1 [51] (Supplementary Figure 1) was still capable of binding TRIB3 (Lane 4 Figure 3C), indicating that the interaction between TRIB3 and MLL/SET1 is not mediated through WDR5. These findings suggest that TRIB3 could be competing with MLL for the WIN domain of WDR5. To test this, we performed Co-IP experiments between WDR5 and MLL/SET1 expressing increasing amounts of TRIB3 (Figure 4A). The results showed that WDR5 co-precipitates with MLL/SET1 when expressed together with MLL in the absence of TRIB3. When TRIB3 is co-expressed along them the amount of WDR5 that is precipitated decreases and when higher amounts of TRIB3 are expressed this reduction is even more pronounced (Figure 4A). To validate the assay, we showed that mutations in WDR5 (S91K and F133A) or mutations in MLL (R449A) as well as the use of an inhibitor of WDR5 completely disrupts the interaction between MLL and WDR5 as previously described (Supplementary Figure 1)[49, 50]. In addition, to characterize further the interaction between TRIB3 and MLL. We showed that the N-terminal domain of TRIB3 is not required for the interaction with MLL and that the arginine-449 of MLL, essential for the interaction with WDR5, is not required either for the interaction with TRIB3 (Figure 4B).

TRIB3 interferes with H3K4me^3 levels on a global and local level

As the ability of the MLL proteins to tri-methylate histones critically depends on the WRAD complex [17, 18] and as TRIB3 can compete for the MLL-WDR5 interaction (Fig. 4), we examined the effects of TRIB3 on MLL activity by assessing global H3K4me^3 levels. For this we first isolated the histones of MCF7 TRIB3-tGFP inducible cells treated with and without doxycycline for 48h. A significant reduction of global H3K4me^3 levels was observed upon induction of TRIB3 (Figure 4C). As a positive control, cells were treated with the WDR5 inhibitor OICR-9429 [52] (without induction of TRIB3 protein), showing an even more pronounced reduction (Figure 4C). To establish the link between epigenetic events and TRIB3 further, we examined whether TRIB3 was stably associated with chromatin. For this, chromatin bound protein extracts were generated and TRIB3 was readily detected in this fraction as well as in the nuclear and cytoplasmatic fractions (Figure 4D). Lamin B1 was used as a marker for chromatin bond proteins (Figure 4D).

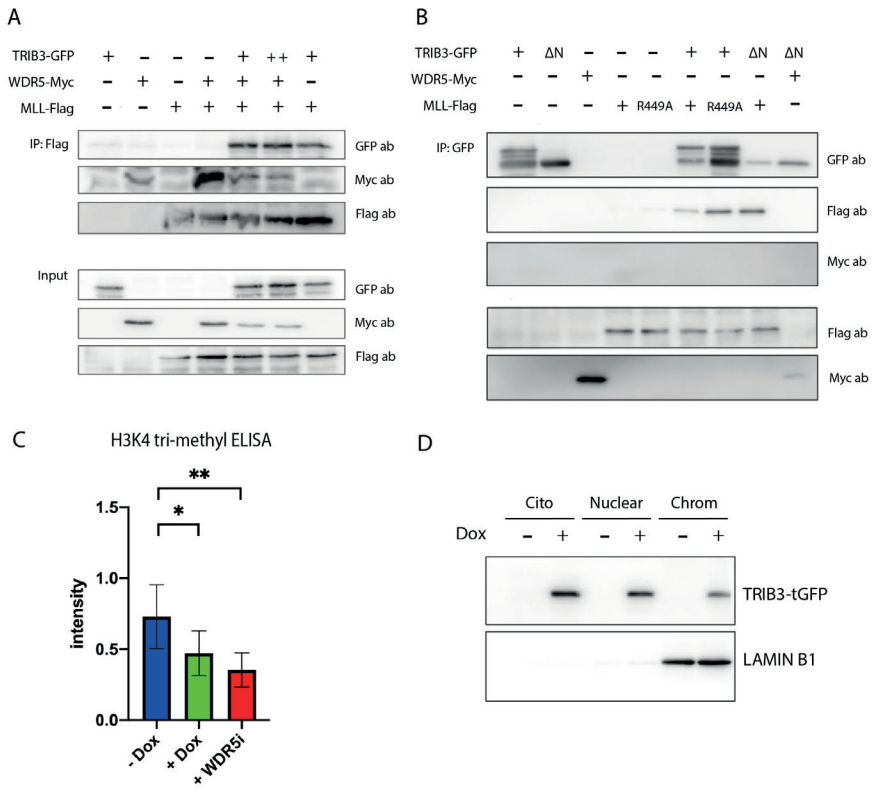

Figure 4. TRIB3 inhibits WDR5-MLL complex formation. (A) Co-IP of MLL-Flag together with WDR5-MYC and different concentrations of TRIB3-GFP in HEK293T cells. Different expression levels of TRIB3 were achieved by co-transfecting TRIB3, WDR5 and MLL in a 1:1:1 ratio (lane 5) or 2:1:1 (lane 6). GFP plasmid was used to compensate for the total amount of DNA transfected per condition (**B)** Co-IP of TRIB3-GFP and TRIB3-ΔN-terminal-GFP with MLL-Flag and MLL-R449A mutant in HEK293T cells. **(C)** H3K4me^3 ELISA in inducible TRIB3-tGFP MCF7 cells treated with and without doxycycline and inducible TRIB3-tGFP cells without doxycycline and treated with the WDR5 inhibitor OICR-9429. **(D)** western blot of TRIB3-tGFP in cytoplasmatic, nuclear and chromatin-bond fractions in inducible TRIB3-tGFP MCF7 cells with and without doxycycline.

To investigate whether the global inhibition of H3K4me^3 levels by TRIB3 observed may underly TRIB3-mediated inhibition of PPARG transcription (Fig. 1), the PPARG locus was investigated more specifically. We first examined publicly available datasets of chromatin immunoprecipitation followed by sequencing (ChIP-seq) experiments of subunits of the WRAD complex, MLL/SET1 proteins and H3K4me^3. In MCF7 cells the *PPARG* locus is marked with H3K4me^3 as seen in figure 5A and this is also the case in HEK293T cells. WDR5 and RBBP5, subunits of the WRAD complex, co-localized in the same region as well as MLL/SET1 proteins (KMT2A in HEK293T cells and KMT2C in MCF7 cells), suggesting that PPARG expression may be regulated

by the MLL-WRAD complex in MCF7 and HEK293T cells. Next, the H3K4me^3 levels in the PPARG locus in TRIB3-KD cells was compared to Sh-control cells by ChIP-RT-qPCR, results showed a trend of increased H3K4me^3 levels upon TRIB3 downregulation (Figure 5B). In addition, we used the HSCB gene as control since previously it has been shown that is heavily mark with H3K4me^3 in MCF7 cells [44] and we could not appreciate differences upon TRIB3 knockdown (Fig. 5D), suggesting that the effect of TRIB3 on H3K4me^3 is not completely genome wide but rather gene-specific. These results suggest that the TRIB3-driven differences in PPARG mRNA expression shown above (Figure 1) could be the result of changes in H3K4 tri-methylation and this be the consequence of the interaction between TRIB3 and the WRAD -MLL complex.

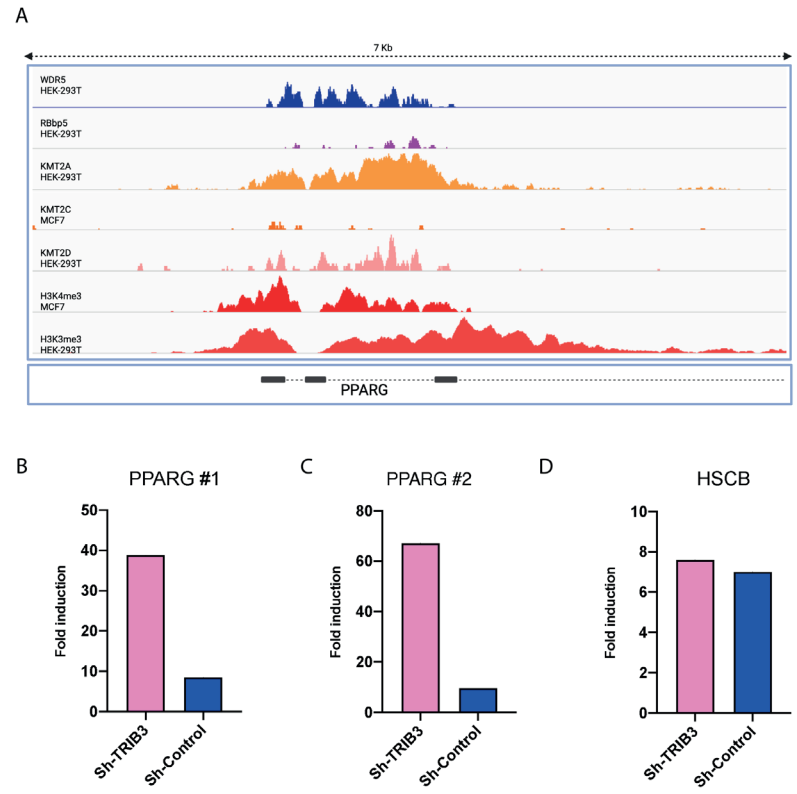

Figure 5. TRIB3 expression influences H3K4me^3 mark in the PPARG locus in MCF7 cells. (A) ChIP-seq data of WDR5 (GSM1493030), RBBP5 (GSM1037511), KMT2A (GSM2373702), KMT2D (GSM3444924) and H3K4me^3 (GSM3444908) in HEK293T cells as well as KMT2C (GSM3414777) and H3K4me^3 (GSM2813049) in MCF7 cells with 7 kilo-bases around PPARG locus shown. **(B)** ChIP-RT-qPCR of H3K4me^3 in Sh-TRIB3 and Sh-control cells in MCF7 using 2 different sets of primer pairs (**B and C)** designed around the PPARG transcription start site (TSS) showed in A. **(D)** ChIP-RT-qPCR of H3K4me^3 around TSS of HSCB gene.

TRIB3 modulates PPARγ-mediated growth inhibition in MCF7 cells

Our study situates TRIB3 as an epigenetic regulator that controls the expression of PPARG in breast cancer cells. To examine consequences on a cellular level, the effect of TRIB3 on PPARγ-mediated growth inhibition was examined, as proliferation of MCF7 cells has been shown to be sensitive to Rosiglitazone [53], a synthetic PPARγ agonist. We used an MTS assay to assess the proliferation capacity of cells treated with Rosiglitazone (40μM for 72h). Downregulation of TRIB3 resulted in lower proliferation compared to control cells (Figure 6A). In addition, Induction of TRIB3-tGFP in MCF7 cells showed increase proliferation rate compared to uninduced cells (Figure 6A). Taken together, our data suggest that TRIB3 modulates PPARγ-mediated growth inhibition by interfering with the MLL complex in MCF7 breast cancer cells, a schematic representation of our model can be found on Figure 6B.

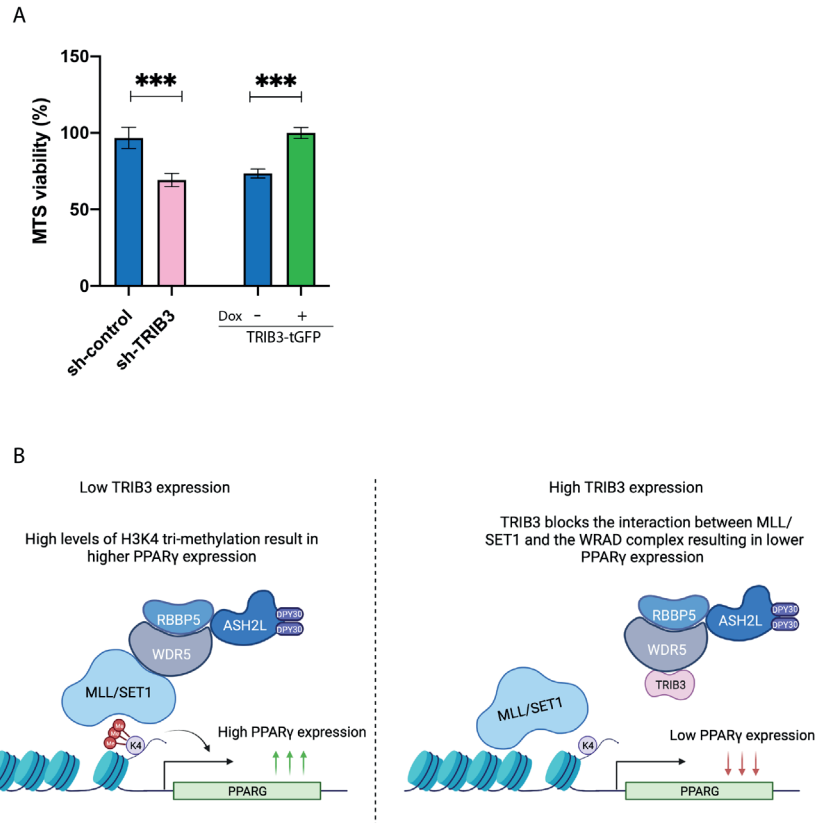

Figure 6. TRIB3 levels affects sensitivity of MCF7 cells to TZD treatment. (A) Sh-control, shTRIB3 and TRIB3-tGFP inducible MCF7 cells were treated for 72h with Rosiglitazone at 40μ. TRIB3-tGFP inducible cells were treated with or without doxycycline for 24h before cell viability was measured. **(B)** Schematic representation of the role of TRIB3 as epigenetic regulator.

Discussion

In this study we show that TRIB3 is able to regulate PPARγ expression in breast cancer cells. In addition, we show that TRIB3 binds to the WRAD complex and affect the MLL-WRAD complex formation and that the levels of $H3K4me^3$ around PPARG locus are influenced by TRIB3 expression. We present TRIB3 as a new epigenetic regulator that controls PPARγ expression through binding of the WRAD complex.

As we have shown previously TRIB3 is able to interact in MCF7 cells with a number of transcription factors including, ZBTB1, HIF1A or KDM3B, and other proteins such as FASN and p53 [13]. These interactions might also have an impact in gene expression or the phosphorylation status of certain proteins and we cannot discard that the changes we appreciated are only because of the interaction with the WRAD complex. In addition, we focus on TRIB3 in this study but given the redundancies in function found in the Tribbles family it might be possible that other Tribbles members exert similar functions.

Previous characterization of the interactome of the different subunits of the MLL-WRAD complex found that BAP18 was able to interact with TRIB3 in HEK293T cells [54]. Interestingly, in this study TRIB3 was not found as an interacting partner of other subunits of the WRAD complex, indicating that most likely TRIB3 interacts with a subfraction of MLL-WRAD complexes and is not a common subunit to be found on the complex. BAP18 is a member of the MLL-WRAD complex but also to the NURF complex [55], adding the possibility that TRIB3 influences other mayor transcriptional regulatory complexes. In addition, BAP18 has been also implicated in triple-negative breast cancer development through the activation of the oncogene S100A9 [56]. All in all, this only strengthens our conclusions as it shows TRIB3 as part of the interactome of MLL-WRAD proteins. However, the exact role of TRIB3 as a regulator of these complexes and under what circumstances it binds to these complexes remains to be fully elucidated and could represent a future area of research for the Tribbles scientific community. Furthermore, TRIB3 may represent a link between cellular metabolism and epigenetics, functioning as a nutrient sensor of glucose and aminoacids levels [57, 58] and regulating MLL-WRAD complex activity, the main epigenetic writer of histone H3 lysine 4 methylation in mammalian cells. Previously we have shown that TRIB3 interacts with a number of mitochondrial proteins [13], potentially indicating mitochondrial localization and action of TRIB3. Given the importance of mitochondrial amino acid metabolism for histone methylation [31, 32], by altering mitochondrial function TRIB3 may affect gene regulation in breast cancer through a second, more indirect mechanism. Future studies are required to investigate this hypothesis. In addition, it is worth mentioning that the present study

focused on *in vitro* systems only and *in vivo* studies are needed to complement our observations and fully comprehend the role of TRIB3 as epigenetic regulator.

PPARγ has been shown to function as tumor suppressor in colon, lung, pancreatic, prostate and breast cancer as increased PPARγ signaling in these diseases leads to reduced cellular growth and inhibition of tumor invasiveness [59-63]. In this context, upregulation of PPARγ expression via targeting the TRIB3-WRAD complex might represent a new possible therapy strategy. Nonetheless, activating PPARγ mutations have also been discovered and linked to cancer initiation in bladder and prostate cancer [64, 65] and PPARγ expression has been shown to be upregulated in certain breast cancer patients [66]. Noteworthy, PPARγ expression does not correlate with PPARγ activity as activation with PPARγ ligands have been shown to inhibit cancer growth in cancer cells [53]. PPARγ ligands have been shown to reduce epithelial to mesenchymal transition (EMT) in breast cancer and thus reduce metastasis capacity of the tumor cells [25]. PPARγ might be the target of a cancer therapy in the near future and finding new ways to regulate its expression could open the door to the treatment of a number of cancers for which currently options are limited.

Funding: This study was supported by grants from the European Union's Horizon 2020 Marie Skłodowska-Curie Innovative Training Network, TRAIN (project no. 721532) and a combined Diabetes Breakthrough grant from the Dutch Diabetes Research Foundation and the Netherlands Organisation for Health Research and Development (ZonMW; project no. 459001006).

Authors contribution: Conceptualization, MHQ, HV, EK; Methodology, MHQ, RB, AOS AB, SdH, PSA, RvE, HV; Validation, MHQ, RB, AB, SdH, PSA; Formal analysis, MHQ, RB, AB, SdH, PSA, AJ; Investigation, MHQ, RB, AB, SdH, PSA, RvE, AJ, GV, HV, EK; Data curation, PSA, HV; Writing –original draft preparation, MHQ; Writing –review and editing, MHQ, HV, EK; Supervision, HV, EK; Visualisation, MHQ, PSA; Funding acquisition EK. All authors have read and agreed to the published version of the manuscript.

Aknowlegments: We thank Dr. S.W.C van Mil for plasmids. We thank Prof. Dr. Michiel Vermeulen for helpful discussions and protocols. We also thank members of the Marie Skłodowska-Curie Innovative Training Network TRAIN (see Supplementary information) and Prof. Dr. Carlie de Vries and Maria P. Clemente (Amsterdam UMC) and members of the Kalkhoven and van Mil laboratories (both UMC Utrecht) for helpful discussions.

Conflict of interest: The authors declare no conflict of interest.

References

1. Kiss-Toth, E., G. Velasco, and W.S. Pear, *Tribbles at the cross-roads.* Biochem Soc Trans, 2015. **43**(5): p. 1049-50.
2. Dobens, L.L., et al., *Control of Cell Growth and Proliferation by the Tribbles Pseudokinase: Lessons from Drosophila.* Cancers (Basel), 2021. **13**(4).
3. Eyers, P.A., K. Keeshan, and N. Kannan, *Tribbles in the 21st Century: The Evolving Roles of Tribbles Pseudokinases in Biology and Disease.* Trends Cell Biol, 2017. **27**(4): p. 284-298.
4. Richmond, L. and K. Keeshan, *Pseudokinases: a tribble-edged sword.* FEBS J, 2020. **287**(19): p. 4170-4182.
5. Durzynska, I., et al., *STK40 Is a Pseudokinase that Binds the E3 Ubiquitin Ligase COP1.* Structure, 2017. **25**(2): p. 287-294.
6. Jamieson, S.A., et al., *Substrate binding allosterically relieves autoinhibition of the pseudokinase TRIB1.* Sci Signal, 2018. **11**(549).
7. Murphy, J.M., et al., *Molecular Mechanism of CCAAT-Enhancer Binding Protein Recruitment by the TRIB1 Pseudokinase.* Structure, 2015. **23**(11): p. 2111-21.
8. Salazar, M., et al., *Loss of Tribbles pseudokinase-3 promotes Akt-driven tumorigenesis via FOXO inactivation.* Cell Death Differ, 2015. **22**(1): p. 131-44.
9. Mace, P.D. and J.M. Murphy, *There's more to death than life: Noncatalytic functions in kinase and pseudokinase signaling.* J Biol Chem, 2021. **296**: p. 100705.
10. Jousse, C., et al., *TRB3 inhibits the transcriptional activation of stress-regulated genes by a negative feedback on the ATF4 pathway.* J Biol Chem, 2007. **282**(21): p. 15851-61.
11. Takahashi, Y., et al., *TRB3 suppresses adipocyte differentiation by negatively regulating PPARgamma transcriptional activity.* J Lipid Res, 2008. **49**(4): p. 880-92.
12. Yu, J.M., et al., *TRIB3 supports breast cancer stemness by suppressing FOXO1 degradation and enhancing SOX2 transcription.* Nat Commun, 2019. **10**(1): p. 5720.
13. Hernandez-Quiles, M., et al., *Comprehensive Profiling of Mammalian Tribbles Interactomes Implicates TRIB3 in Gene Repression.* Cancers (Basel), 2021. **13**(24).
14. Jiang, H., *The complex activities of the SET1/MLL complex core subunits in development and disease.* Biochim Biophys Acta Gene Regul Mech, 2020. **1863**(7): p. 194560.
15. Vedadi, M., et al., *Targeting human SET1/MLL family of proteins.* Protein Sci, 2017. **26**(4): p. 662-676.
16. Shilatifard, A., *Molecular implementation and physiological roles for histone H3 lysine 4 (H3K4) methylation.* Curr Opin Cell Biol, 2008. **20**(3): p. 341-8.
17. Ernst, P. and C.R. Vakoc, *WRAD: enabler of the SET1-family of H3K4 methyltransferases.* Brief Funct Genomics, 2012. **11**(3): p. 217-26.
18. Shilatifard, A., *The COMPASS family of histone H3K4 methylases: mechanisms of regulation in development and disease pathogenesis.* Annu Rev Biochem, 2012. **81**: p. 65-95.
19. Aho, E.R., et al., *Targeting WDR5: A WINning Anti-Cancer Strategy?* Epigenet Insights, 2019. **12**: p. 2516865719865282.

20. Rosen, E.D., et al., *PPAR gamma is required for the differentiation of adipose tissue in vivo and in vitro.* Mol Cell, 1999. **4**(4): p. 611-7.
21. Hernandez-Quiles, M., M.F. Broekema, and E. Kalkhoven, *PPARgamma in Metabolism, Immunity, and Cancer: Unified and Diverse Mechanisms of Action.* Front Endocrinol (Lausanne), 2021. **12**: p. 624112.
22. Yang, Z., et al., *Targeting Nuclear Receptors for Cancer Therapy: Premises, Promises, and Challenges.* Trends Cancer, 2021. **7**(6): p. 541-556.
23. Li, H., et al., *Morusin suppresses breast cancer cell growth in vitro and in vivo through C/EBPbeta and PPARgamma mediated lipoapoptosis.* J Exp Clin Cancer Res, 2015. **34**: p. 137.
24. Vella, V., et al., *PPAR-gamma Agonists As Antineoplastic Agents in Cancers with Dysregulated IGF Axis.* Front Endocrinol (Lausanne), 2017. **8**: p. 31.
25. Ishay-Ronen, D., et al., *Gain Fat-Lose Metastasis: Converting Invasive Breast Cancer Cells into Adipocytes Inhibits Cancer Metastasis.* Cancer Cell, 2019. **35**(1): p. 17-32 e6.
26. Dalamaga, M., G.S. Christodoulatos, and J. Liu, *Diverting epithelial-to-mesenchymal transition to transform cancer cells to adipocytes: A promising strategy to stop metastasis.* Metabol Open, 2019. **3**: p. 100012.
27. Harbeck, N. and M. Gnant, *Breast cancer.* Lancet, 2017. **389**(10074): p. 1134-1150.
28. Martin, A.M. and B.L. Weber, *Genetic and hormonal risk factors in breast cancer.* J Natl Cancer Inst, 2000. **92**(14): p. 1126-35.
29. Chen, K., et al., *Mitochondrial mutations and mitoepigenetics: Focus on regulation of oxidative stress-induced responses in breast cancers.* Semin Cancer Biol, 2022. **83**: p. 556-569.
30. Liu, Y.e., et al., *An Epigenetic Role of Mitochondria in Cancer.* Cells, 2022. **11**(16): p. 2518.
31. Bahat, A. and A. Gross, *Mitochondrial plasticity in cell fate regulation.* J Biol Chem, 2019. **294**(38): p. 13852-13863.
32. Reid, M.A., Z. Dai, and J.W. Locasale, *The impact of cellular metabolism on chromatin dynamics and epigenetics.* Nat Cell Biol, 2017. **19**(11): p. 1298-1306.
33. Chen, K., et al., *Advances in the Prevention and Treatment of Obesity-Driven Effects in Breast Cancers.* Front Oncol, 2022. **12**: p. 820968.
34. Calle, E.E. and R. Kaaks, *Overweight, obesity and cancer: epidemiological evidence and proposed mechanisms.* Nat Rev Cancer, 2004. **4**(8): p. 579-91.
35. Greaney, M.L., et al., *Study protocol for Young & Strong: a cluster randomized design to increase attention to unique issues faced by young women with newly diagnosed breast cancer.* BMC Public Health, 2015. **15**: p. 37.
36. Villarreal-Garza, C., et al., *Breast cancer in young women in Latin America: an unmet, growing burden.* Oncologist, 2013. **18**(12): p. 1298-306.
37. Orea-Soufi, A., et al., *The Pseudokinase TRIB3 Negatively Regulates the HER2 Receptor Pathway and Is a Biomarker of Good Prognosis in Luminal Breast Cancer.* Cancers (Basel), 2021. **13**(21).
38. Jeninga, E.H., et al., *Impaired peroxisome proliferator-activated receptor gamma function through mutation of a conserved salt bridge (R425C) in familial partial lipodystrophy.* Mol Endocrinol, 2007. **21**(5): p. 1049-65.

39. Kim, D., B. Langmead, and S.L. Salzberg, *HISAT: a fast spliced aligner with low memory requirements.* Nat Methods, 2015. **12**(4): p. 357-60.
40. Robinson, M.D., D.J. McCarthy, and G.K. Smyth, *edgeR: a Bioconductor package for differential expression analysis of digital gene expression data.* Bioinformatics, 2010. **26**(1): p. 139-40.
41. Bolger, A.M., M. Lohse, and B. Usadel, *Trimmomatic: a flexible trimmer for Illumina sequence data.* Bioinformatics, 2014. **30**(15): p. 2114-20.
42. Wu, D. and G.K. Smyth, *Camera: a competitive gene set test accounting for inter-gene correlation.* Nucleic Acids Res, 2012. **40**(17): p. e133.
43. Ramos Pittol, J.M., et al., *FXR Isoforms Control Different Metabolic Functions in Liver Cells via Binding to Specific DNA Motifs.* Gastroenterology, 2020. **159**(5): p. 1853-1865 e10.
44. Lee, S., et al., *ChIP-seq analysis reveals alteration of H3K4 trimethylation occupancy in cancer-related genes by cold atmospheric plasma.* Free Radic Biol Med, 2018. **126**: p. 133-141.
45. Wennemers, M., et al., *Tribbles homolog 3 denotes a poor prognosis in breast cancer and is involved in hypoxia response.* Breast Cancer Res, 2011. **13**(4): p. R82.
46. Wennemers, M., et al., *Regulation of TRIB3 mRNA and protein in breast cancer.* PLoS One, 2012. **7**(11): p. e49439.
47. Carrier, M., et al., *Phosphoproteome and Transcriptome of RA-Responsive and RA-Resistant Breast Cancer Cell Lines.* PLoS One, 2016. **11**(6): p. e0157290.
48. Hornbeck, P.V., et al., *PhosphoSitePlus, 2014: mutations, PTMs and recalibrations.* Nucleic Acids Res, 2015. **43**(Database issue): p. D512-20.
49. Guarnaccia, A.D., et al., *Impact of WIN site inhibitor on the WDR5 interactome.* Cell Rep, 2021. **34**(3): p. 108636.
50. Song, J.J. and R.E. Kingston, *WDR5 interacts with mixed lineage leukemia (MLL) protein via the histone H3-binding pocket.* J Biol Chem, 2008. **283**(50): p. 35258-64.
51. Bailey, J.K., et al., *WD repeat-containing protein 5 (WDR5) localizes to the midbody and regulates abscission.* J Biol Chem, 2015. **290**(14): p. 8987-9001.
52. Grebien, F., et al., *Pharmacological targeting of the Wdr5-MLL interaction in C/EBPalpha N-terminal leukemia.* Nat Chem Biol, 2015. **11**(8): p. 571-578.
53. Kim, K.Y., S.S. Kim, and H.G. Cheon, *Differential anti-proliferative actions of peroxisome proliferator-activated receptor-gamma agonists in MCF-7 breast cancer cells.* Biochem Pharmacol, 2006. **72**(5): p. 530-40.
54. van Nuland, R., et al., *Quantitative dissection and stoichiometry determination of the human SET1/MLL histone methyltransferase complexes.* Mol Cell Biol, 2013. **33**(10): p. 2067-77.
55. Badenhorst, P., et al., *Biological functions of the ISWI chromatin remodeling complex NURF.* Genes Dev, 2002. **16**(24): p. 3186-98.
56. Zhang, Y.L., et al., *Chromatin complexes subunit BAP18 promotes triple-negative breast cancer progression through transcriptional activation of oncogene S100A9.* Cell Death Dis, 2022. **13**(4): p. 408.
57. Ord, T., et al., *TRIB3 enhances cell viability during glucose deprivation in HEK293-derived cells by upregulating IGFBP2, a novel nutrient deficiency survival factor.* Biochim Biophys Acta, 2015. **1853**(10 Pt A): p. 2492-505.

58. Carraro, V., et al., *Amino acid availability controls TRB3 transcription in liver through the GCN2/eIF2alpha/ATF4 pathway.* PLoS One, 2010. **5**(12): p. e15716.
59. Kubota, T., et al., *Ligand for peroxisome proliferator-activated receptor gamma (troglitazone) has potent antitumor effect against human prostate cancer both in vitro and in vivo.* Cancer Res, 1998. **58**(15): p. 3344-52.
60. Sarraf, P., et al., *Differentiation and reversal of malignant changes in colon cancer through PPARgamma.* Nat Med, 1998. **4**(9): p. 1046-52.
61. Motomura, W., et al., *Activation of peroxisome proliferator-activated receptor gamma by troglitazone inhibits cell growth through the increase of p27KiP1 in human. Pancreatic carcinoma cells.* Cancer Res, 2000. **60**(19): p. 5558-64.
62. Tsubouchi, Y., et al., *Inhibition of human lung cancer cell growth by the peroxisome proliferator-activated receptor-gamma agonists through induction of apoptosis.* Biochem Biophys Res Commun, 2000. **270**(2): p. 400-5.
63. Bonofiglio, D., et al., *Combined low doses of PPARgamma and RXR ligands trigger an intrinsic apoptotic pathway in human breast cancer cells.* Am J Pathol, 2009. **175**(3): p. 1270-80.
64. Saez, E., et al., *Activators of the nuclear receptor PPARgamma enhance colon polyp formation.* Nat Med, 1998. **4**(9): p. 1058-61.
65. Lefebvre, A.M., et al., *Activation of the peroxisome proliferator-activated receptor gamma promotes the development of colon tumors in C57BL/6J-APCMin/+ mice.* Nat Med, 1998. **4**(9): p. 1053-7.
66. Wang, X., R.C. Southard, and M.W. Kilgore, *The increased expression of peroxisome proliferator-activated receptor-gamma1 in human breast cancer is mediated by selective promoter usage.* Cancer Res, 2004. **64**(16): p. 5592-6.

SUPPLEMENTARY INFORMATION

TRAIN Consortium Authorship:

Surname	First Name	Institution
Bhutia	Kunzangla	Instituto de Investigacion Santaria, Hospital Clinico SanCarlos
Brouard	Sophie	University of Nantes
Barril	Xavier	University of Barcelona
Carracedo	Arkaitz	Asociación Centro de Investigación Cooperativa en Biociencias
Castillo Lluva	Sonia	Instituto de Investigacion Santaria, Hospital Clinico SanCarlos
Danger	Richard A.E.D	University of Nantes
Day	Jack	Instituto de Investigacion Santaria, Hospital Clinico SanCarlos
Deshmukh	Sumeet R	The University of Sheffield
Feseha	Yodit	University of Nantes
Francis	Sheila	The University of Sheffield
Grzesik	Dominika J	William Harvey Research Institute, Queen Mary University, London
Hernandez Quiles	Miguel	Universitair Medisch Centrum Utrecht
Kalkhoven	Eric	Universitair Medisch Centrum Utrecht
Kiss-Toth	Endre	The University of Sheffield
Linford	Adam J	Institute for Diabetes and Cancer (IDC), Helmholtz Zentrum München
Martinez Campesino	Laura	The University of Sheffield
Metherall	Louise A	William Harvey Research Institute, Queen Mary University, London
Morris	Imogen	Universitair Medisch Centrum Utrecht
Niespolo	Chiara	The University of Sheffield
Pellegata	Natalia S	Institute for Diabetes and Cancer (IDC), Helmholtz Zentrum München
Ruiz Cantos	Miriam	William Harvey Research Institute, Queen Mary University, London
Salamanca Viloria	Juan	University of Barcelona

Surname	First Name	Institution
Satam	Swapna S	Institute for Diabetes and Cancer (IDC), Helmholtz Zentrum München
Scheideler	Marcel J.C.	Institute for Diabetes and Cancer (IDC), Helmholtz Zentrum München
Shahrouzi	Parastoo	Asociación Centro de Investigación Cooperativa en Biociencias
Shologu	Ziyanda	Universidade da Beira Interior
Shoulders	Carol C	William Harvey Research Institute, Queen Mary University, London
Sudbery	Ian	The University of Sheffield
Socorro	Silvia	Universidade da Beira Interior
Velasco	Guillermo	Instituto de Investigacion Santaria, Hospital Clinico SanCarlos
Villacanas Perez	Oscar	MindtheByte Ltd
Wilson	Heather	The University of Sheffield

Chapter 7

A C-terminal triple glutamic acid motif in TRIB3 protein contributes to the inhibition of AKT signaling

Miguel Hernández-Quiles*[1], Juan Salamanca Viloria*[2], Anouska Borgman[1], Endre Kiss-Toth[3] Boudewijn Burgering[1,4], Eric Kalkhoven[1#]

[1] Center for Molecular Medicine, University Medical Center Utrecht, Utrecht University, The Netherlands.

[2] Pharmacy faculty, University of Barcelona, Barcelona, Spain.

[3] Department of Infection, Immunity and Cardiovascular Disease, Medical School, University of Sheffield, Sheffield, UK.

[4] Oncode Institute and Molecular Cancer Research, Center for Molecular Medicine, University Medical Center Utrecht, Utrecht University, Utrecht, The Netherlands.

* Equal contributions

Abstract

The kinase AKT/PKB is a key intermediate in insulin and growth factor signal transduction. AKT activity is dysregulated in various human diseases: reduced activity is for example observed in insulin resistance and type 2 diabetes, while hyperactivation of AKT can drive tumorigenesis. The pseudokinase TRIB3 can interact with and inhibit AKT, representing an endogenous mechanism to regulate AKT activity that may offer an entry point for therapeutic intervention. However, disparate data on the TRIB3-AKT interaction and the effect on serine 473 (S473) phosphorylation in AKT have been published in recent years. In this study we used a combination of cell-based and computational approaches to investigate the interaction between TRIB3 and AKT in detail and found that the C-terminal domain of TRIB3 is able to interact with AKT. Moreover, we identified a triple glutamic acid (E) motif in this domain that is essential for this and propose that S473 phosphorylation is prevented or destabilized through an interaction between the triple E motif and a basic patch in AKT. This molecular interaction, which can potentially be regulated on multiple levels, may present a first step to elucidate the role of cellular context in AKT-TRIB3 interplay.

Introduction

The serine/threonine kinase AKT, also known as protein kinase B (PKB) [1, 2], was discovered more than 30 years ago and has been the focus of research ever since for its (dys)functions in many aspects of cellular biology, human physiology and pathology [3]. The overall view is that AKT activation promotes cell survival, cell growth, proliferation and regulates the metabolic state of the cell, with some cell type- and tissue-specific effects related to expression of AKT isoforms (AKT1 or PKBα, AKT2 or PKBβ and AKT3 or PKBγ) and/or specific regulatory mechanisms [3]. When receptor tyrosine kinase (RTK) or G protein coupled receptors become activated by extracellular stimuli such as insulin or growth factors, they activate PI3K, resulting in recruitment of inactive AKT to the plasma membrane [4]. Akt subsequently becomes phosphorylated on two key residues, T308 in the activation loop and S473 in the C-terminal hydrophobic motif [5, 6]. These residues are conserved in all AKT isoforms and their combined phosphorylation is required for full AKT activation. PDK1 is responsible of phosphorylation of T308 resulting in partial activation of AKT [7, 8]; phosphorylation of S473 by the mechanistic target of rapamycin complex 2 (mTORC2) is required for further activation of AKT and stabilization of the T308 phosphorylation [9]. DNA-dependent protein kinase (DNA-PK) has also been shown to co-localize and be able to phosphorylate S473 of AKT under certain conditions [10]. Fully active AKT is then released from the plasma membrane and can be found in multiple locations within the cell. AKT regulates a wide variety of cellular pathways through the phosphorylation of transcription factors, metabolic enzymes, E3 ubiquitin ligases and cell cycle regulators [11, 12]. Some of the best known AKT substrates include the forkhead box O (FoxO) family of transcription factors, AMP-regulated protein kinase (AMPK) and glycogen synthase kinase 3 (GSK3)[13-15].

Reduced AKT activation upon insulin stimulation in liver, skeletal muscle and adipose tissue is known as insulin resistance and is a hallmark in the development of the metabolic syndrome and type II diabetes. Moreover, AKT hyperactivation is among the most well studied mechanism that drives tumorigenesis, including activating mutations in genes upstream of AKT such as EGFR, HER2, RTKs, PDK1 and PIK2CA [16] and inactivating mutations in tumor suppressor genes such as PTEN and PHLPP [17]. For the past twenty years research has been focused on understanding AKT signaling cascade to identify cellular proteins and other biomolecules that can influence AKT activation, to either ameliorate insulin sensitivity in diabetic and obese patients or to treat a number of cancers.

The mammalian Tribbles pseudokinases have drawn a lot of attention as natural, cellular AKT inhibitors that can potentially be targeted in cancer and insulin

resistance patients. Originally discovered in Drosophila in a mutational screen for genes that control cell proliferation and migration [18-21], the human homologies TRIB1, -2 and -3 have been implicated in many different cellular processes such as differentiation and activation of immune cells, lipid metabolism and regulation of the cell cycle [22-26]. Tribbles are able to regulate such a large variety of pathways through their ability to interact with and modulate the activity of various cellular proteins, including transcription factors, kinases and components of the ubiquitin proteosome system [27, 28]. Human Tribbles have a well-defined structure that consist of a central pseudokinase domain (PKD) that is flanked by intrinsically disordered N- and C-terminal domains. The PKD lacks the DFG motif that is present is most bona-fide kinases and therefore they are incapable of binding ATP, this together with a modified glycine-rich loop makes Tribbles unable to catalyze the phosphorylation of their substrates. In contrast with the well conserved PKD that retains more than 50% sequence similarity among the Tribbles family members, the N- and C-terminal domains are more divergent and may therefore harbor unique functions of the different family members. The C-terminal domain contains two motifs that are well conserved among human Tribbles proteins and also across different species: the binding motifs of the E3 ubiquitin ligase COP1 and the MEK motif for the regulation of mitogen activated protein kinase cascade (MAPK) [28, 29],. The N-terminal domain has been traditionally associated with the protein stability of Tribbles but more recently we reported the N-terminal domain of TRIB3 to also acts as an interaction module that links TRIB3 with transcriptional regulatory proteins [30].

All 3 Tribbles family members have been linked to the different isoforms of AKT in different cellular settings, with the outcome being dependent on the identity of the TRIB protein and the cellular context [31, 32]. Human TRIB3 has been shown to be able to inhibit both phosphorylation sites of AKT, T308 and S473, in hepatocytes [25, 33] but not in muscle cells [31, 34] while in adipocytes downregulation of TRIB3 has been associated to a decrease in phospho-AKT (E. Kiss-Toth, personal communication). TRIB1 and especially TRIB2 have been shown to be activators of AKT, drawing attention to their role in cancer [35, 36]. These disparate findings prompted us to study the interaction between AKT and TRIB3 in more detail and try and elucidate how this may lead to altered phosphorylation of AKT. Here we combined cell-based studies with computational modelling approaches and found that the TRIB3-AKT interaction not only relies on the PKD of TRIB3 but also on its C-terminal domain. In addition, we identified a triple glutamic acid motif in the C-terminal domain of TRIB3 that we predict to bind to the basic patch in the AKT protein, thereby preventing or destabilizing the phosphorylation of S473.

Materials and methods

Materials

Cell culture

Human embryonic kidney cells (HEK293T, ATCC CRL-3216) were maintained in High glucose (d-glucose, 4.5g/L) Dulbecco's Modified Eagle Medium (DMEM). Media was supplemented with 10% fetal bovine serum (FBS) and 1% penicillin and streptomycin (P/S). Hep G2 (ATCC HB-8065) cells were maintained in low glucose DMEM, 10 % FBS, 1% P/S and 1% L-glutamine. Inducible pcw57.1 (EV, TRIB3-wt, TRIB3-3A and TRIB3-3K) cell lines were generated using third generation lentiviral constructs similarly as described previously [37].

Site-directed mutagenesis

All mutations introduced in this study were performed using Quickchange mutagenesis kit (Stratagene). In short, primers with the desired mutations were generated and PCR was carried out accordingly to primers annealing temperature and length of the plasmid. Samples were then incubated with *Dpn1* for 1h at 37°C. DH5-Alpha competent E. coli cells were used for bacterial transformation and successful mutagenesis was verified by Sanger sequencing analysis.

Western blotting

Western blotting was described in detail previously [38]. Briefly, protein samples were extracted using RIPA lysis buffer (150 mM NaCl, 50 mM Tris pH 8.0, 1% NP-40, 5mM $MgCl_2$, 10% glycerol). Protein concentration was measured and Laemmli sample buffer was added to the samples. Samples were then separated through SDS-PAGE and transfer to PVDF membranes. Blocking was performed during 45' with 5% milk in TBS-T and then membranes were incubated with Primary (4°C overnight) and secondary (1h RT) antibody before using ECL solution and LAS4000 Image Quant for visualization of the targeted protein.

Protein complementation assay

TRIB3-AKT complex formation was analyzed in live cells using the NanoBiT® PPI System (Promega). The large BiT (LgBiT, 18 kDa) and the small BiT (SmBiT, 1.3 kDa) were fused to the N- and C-terminus of TRIB3 and AKT constructs and all the combinations were tested to find the pair that displayed the most effective complementation of the split luciferase. The combination selected was the large BiT fused to the C-terminus of TRIB3 and the small BiT fused to the C-terminus of AKT.

HEK293T cells were seeded in 96-well plate (10.000 cells/well) and transfected with TRIB3-LgBiT (50 ng/well) and AKT-SmBiT (50 ng/well) using Xtreme gene (Sigma-Aldrich). After 48h cells were washed with PBS and diluted substrate was added according to manufacturer's protocol. Relative light Units (RLU) were measured by a Centro LB960 Luminometer (Berthold Technologies). The results are averages of at least three independent experiments assayed in triplicate.

Computational modeling

The interaction between TRIB3 C-tail and AKT Kinase Domain (KD) was built with Rosetta (release 2020.03) using the FlexPepDock ab-initio protocol [39]. Protein-peptide docking was carried out between the AKT KD (residues 144-450) and selected regions of the C-terminal tail of TRIB3 in ranges of 15 residues. AKT KD template PDB id 4GV1 was selected based on its high resolution. The C-terminal tail of AKT (residues 457-477) was removed to allow docking on the groove over the αC helix. The FlexPep-Dock ab-initio protocol was first evaluated over a linear C-terminal tail of AKT (res 463-477) to check the accuracy of predicting its binding mode.

A preliminary step of the FlexPepDock ab-initio protocol is the generation of fragment libraries for the peptide sequence. The fragment libraries of three and nine residues were generated with the Robetta server [40] using the peptide sequence of AKT and TRIB3 C-tail as reference for each case. We selected the last 28 residues from the C-tail of TRIB3 and split them in three fragments (residues 331-345, 338-352 and 344-358). The peptides were initially positioned approximately 10 Å away from the proposed binding pocket, the αC helix of AKT. Then, the input structures were prepacked to remove internal clashes in the protein and the linear peptide. We generated 100,000 models from each starting structure. The docking simulations were evaluated with the beta_nov16 score function. The top scoring 500 models were clustered using the Rosetta cluster application with a cluster radius cutoff of 3 Å peptide backbone atom RMSD. The models were ranked according to the reweighted score, in which interface residues are given double weight, and peptide residues are given triple weight. We considered the best model as the lowest structure with the biggest cluster in the top 10 lowest models.

Insulin stimulation

Hep G2 Cells (ATCC HB-8065) were cultured for 24h in low glucose (1.5 g/L D-glucose) Dulbecco's Modified Eagle Medium (DMEM) supplemented with 0.1% fetal bovine serum, 1% ampicillin and streptomycin and 1% L-glutamine. Cells were then incubated with insulin (1:10000) for 45 min to 1h and samples were harvested in RIPA lysis buffer. Phospho-AKT (Ser473) was checked as read-out of insulin stimulation by western blotting.

RESULTS

TRIB3-C-terminal domain interacts with AKT and is sensitive to S473 phosphorylation

To study the interaction between TRIB3 and AKT in detail, we developed a protein complementation assay (PCA) to measure the relative strength of the TRIB3-AKT interaction. In this system, luciferase is divided into two fragments (LgBiT and SmBiT) that are fused to C-terminal ends of TRIB3 and AKT respectively. When expressed in cells the individual proteins display no luminescence by themselves, while luciferase activity was detected when the 2 proteins were expressed together, as a result of the protein-protein interaction and subsequent reconstitution of a functional luciferase protein (Figure 1A and 1C). In this experimental setting a small yet non-significant increase in luciferase activity measured when the R84R variant of TRIB3 was tested (Fig. 1C), a genetic variant that has been shown to display increased *in vitro* binding to AKT and is associated with impaired insulin sensitivity [41].

Next, the contribution of the different domains of TRIB3 to the interaction with AKT was examined (Fig. 1B). TRIB3 proteins that lacked either de N- or C-terminus (ΔN- and ΔC-terminus), as well as the isolated PKD were able to interact with AKT (Figure 1C), supporting earlier studies showing that the PKD of TRIB3 can interact with AKT [42]. Surprisingly, the isolated C-terminal domain of TRIB3 was also able to interact with AKT (Figure 1C).

In addition, we wished to test if the interaction between TRIB3 and AKT was sensitive to the phosphorylation status of AKT. For this, we generated phosphomimic mutants of serine 473 and threonine 308 (S473D and T308D) as well as the corresponding phosphophobic mutants (S473A and T308A). The S473D but not the S473A mutation disrupted the interaction between the C-terminal domain of TRIB3 and AKT (Figure 1D). Both full length TRIB3 and the isolated PKD were not sensitive to the phosphorylation status of S473 of AKT (Fig. 1D). When testing the phosphorylation status of T308, no significant effects were detected for the AKT-TRIB3 interaction, either in the context of full length TRIB3 or with the isolated C-terminal domain (Fig. 1E and 1F).

Moreover, we tested if the phosphorylation of T308 may have an effect in the context of S473 phosphorylation, by combining the different mutations. The interaction between the un-phosphorylated form of AKT and TRIB3 (T308A/S473A) was significantly stronger compared to the bi-phosphorylated form of AKT (T308D/S473D), with the mono-phosphorylated forms of AKT (T308D/S473A and T308A/S473D) displaying a small decrease in binding (Figure 1G).

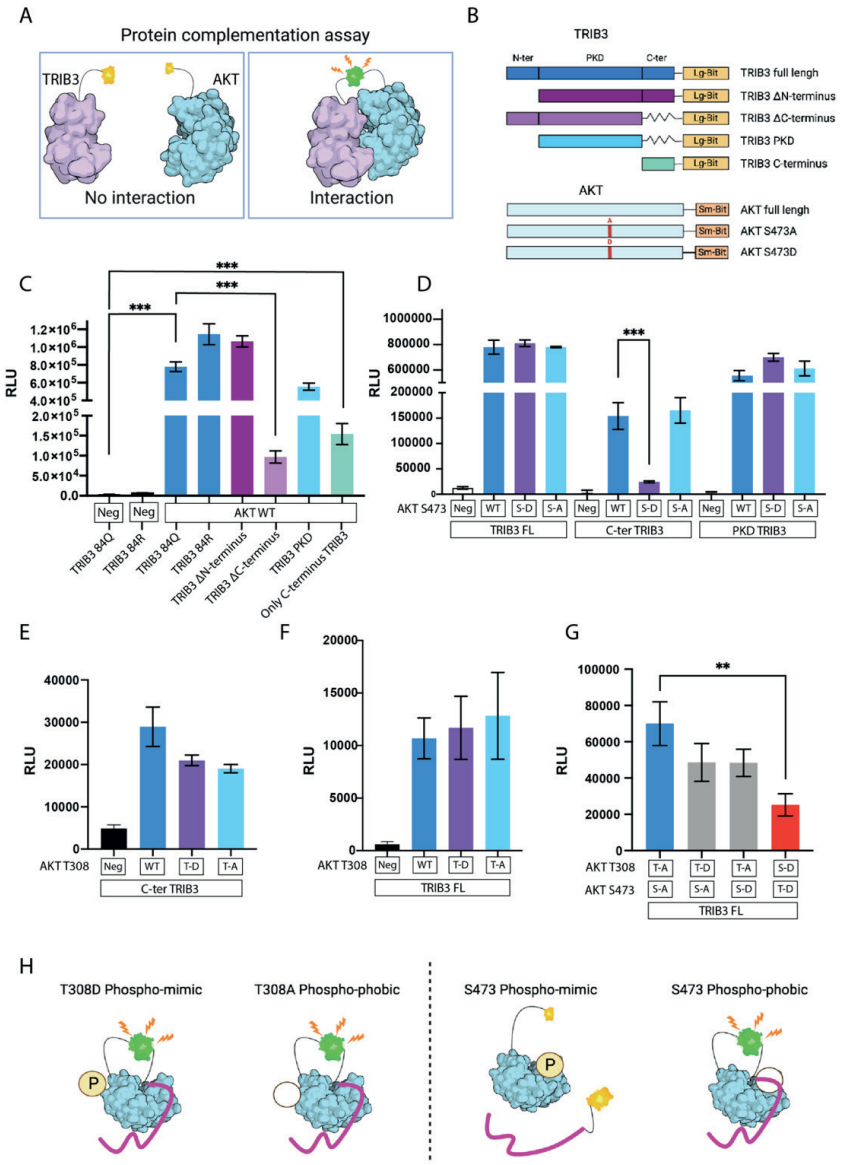

Figure 1. Protein complementation assay (PCA) to study TRIB3-AKT interaction. (A) Schematic representation of PCA. **(B)** Schematic representation of TRIB3 and AKT constructs used in the PCA. **(C)** PCA of TRIB3 WT (including natural polymorphism in position 84, R and Q), TRIB3 ΔN-terminal, TRIB3 ΔC-terminal, TRIB3 PKD and only the C-terminal domain of TRIB3 in combination with AKT WT. **(D)** PCA of full length TRIB3, C-terminal domain of TRIB3 or PKD TRIB3 in combination with AKT WT, AKT S473A and AKT S473D. **(E)** PCA of C-terminal domain of TRIB3 in combination with AKT WT, AKT T308A and AKT T308D. **(F)** PCA of full length TRIB3 in combination with AKT WT, AKT T308A and AKT T308D. **(G)** PCA result of full length TRIB3 in combination with AKT T308A+S473A, AKT T308D+S473A, AKT T308A+S473D and AKT T308D+S73D. **(H)** Schematic representation of the PCA results of the interaction between the C-terminal domain of TRIB3 and AKT phosphorylations.

Together these results support a bimodal interaction model where both the PKD and C-terminal domain of TRIB3 can interact with AKT, with the interaction between the PKD and AKT being insensitive and the interaction between the C-terminal domain of TRIB3 and AKT being sensitive to the phosphorylation status of AKT, with a dominant role for S473 phosphorylation.

Computational modeling of C-terminal domain of TRIB3 in complex with AKT1

To gain structural insights into the interaction of the C-terminal domain of TRIB3 and AKT we used the Rosetta FlexPepDock ab-initio peptide docking protocol to model AKT1 bound to a segment of the C-terminal domain of TRIB3. In all cases, we calculated 100.000 conformations starting from an extended peptide within 10 Å from the proposed binding site, the groove over the αC-helix of AKT. First, we used the Rosetta FlexPepDock an-initio protocol to model the binding of the C-tail of AKT (residues 463-477) to the AKT kinase domain (residues 144-450) (Supplementary Figure 1A) an already known structure (PDB 4GV1) that allow us to test the accuracy and precision of the protocol. For the analysis of the various protein-peptide docking screens, scattering plots were constructed for each model with the Rosetta score against the root mean square deviation (RMSD) with respect the native structure of AKT. We were able to generate models with high accuracy for the binding of the C-tail of AKT, with residues close to near-native as the predicted peptide conformation deviates by less than 2 Å RMSD. The best docking model corresponded to the representative model selected according to the best energy score of the biggest cluster in the top 10 ranked by energy. Six out of the ten best ranked models showed a RMSD lower than 2 Å (Supplementary Figure 1B). Next, protein-peptide dockings were carried out between the KD of AKT1 and the selected regions of C-terminal domain of TRIB3 in segments of 15 residues (Supplemented Figure 1C). The distance of the peptide was based on the maximum length of the benchmark peptides used to validate the FlexPepDock protocol. In all three segments the best model appeared docked in the groove over the αC-helix of AKT, the segment number three (residues 344-358) showed a more flexible structure and thus showed a larger RMSD distribution of the top 10 structures compared to the other two segments. Segments 1 (residues 331-345) (Figure 2A) and 2 (residues 338-353) (Figure 2A) showed a more converge solution and the best ten poses are shown in Figure 2B. Interestingly, a glutamic acid motif E347-E348-E349 in the C-terminal domain of TRIB3 –which is not conserved between the different TRIB proteins (Fig. 2E)– is present in two of the segments and docks to a region close to a basic patch (K142-H143-R144) in AKT, which has previously been implicated in stabilization of S473 phosphorylation (Figure 2C and D) [43]. By interacting with AKT, as proposed by these computational modeling approaches, the C-terminal tail of TRIB3 may prevent or destabilize S473 phosphorylation and inhibit AKT-mediated signal transduction.

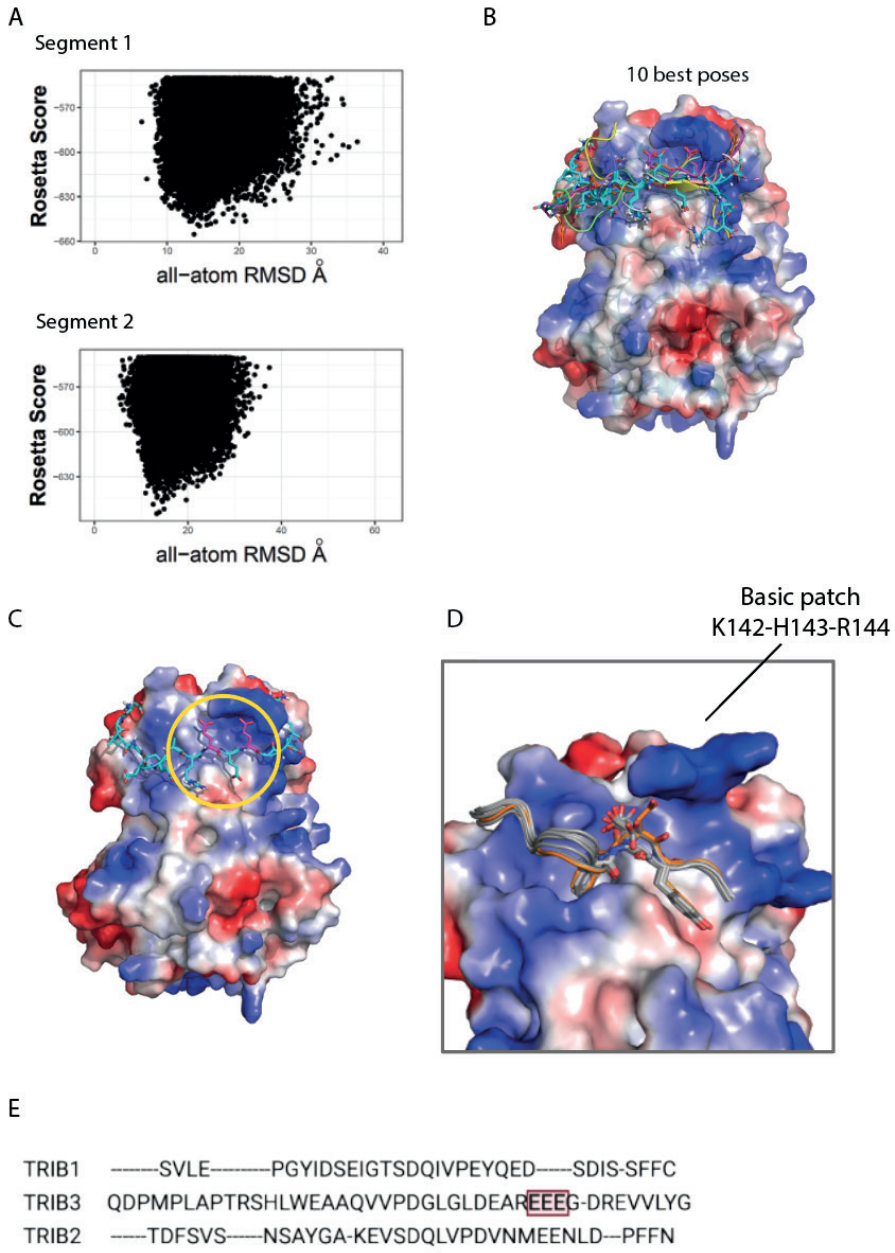

Figure 2. Modeling of C-terminal domain of TRIB3 in complex with AKT. (A) scattering plots of segment 1 and segment 2 of TRIB3 C-terminal domain, the Rosetta score is plotted against the root mean square deviation (RMSD) with respect the native structure of AKT. **(B)** Visualization of the best 10 poses of the C-terminal domain of TRIB3 in complex with AKT. **(C)** Best pose, under yellow circle the triple glutamic acid motif. **(D)** AKT in complex with its own C-terminal, basic patch stabilizes S473 phosphorylation. **(E)** Alignment of the C-terminal domains of TRIB1, TRIB2 and TRIB3.

The triple glutamic acid motif in the C-terminal domain of TRIB3 is important in the regulation of AKT S473 phosphorylation

Based on the computational modeling of the C-terminal tail of TRIB3 in complex with AKT (Fig. 2), we hypothesize that the triple E motif in the C-terminal tail of TRIB3 may impair the interaction between TRIB3 and AKT. It should be noted however that based on structural studies with the related pseudokinase TRIB1 by Jamieson *et al.* [44], TRIB3 may also adopt an auto-inhibited conformation where the C-terminal tail is folded onto the PKD. These authors showed that upon interaction with other proteins the conformation changes and the C-terminal tail is released, which would make the PKD more accessible for other protein-protein interactions (Supplementary figure 2). The E347A/E348A/E349A mutant may therefore display reduced or increased binding to AKT, depending on the relative importance of the different interaction interfaces (PKD and C-terminal tail) and/or the sequence of binding events. To distinguish between these possibilities, we generated a TRIB3 mutant where all three glutamic acids were mutated to alanine (E347A/E348A/E349A) and tested this in the PCA system. The triple mutant displayed increased binding compared to the wt TRIB3 protein (Fig. 3A), while no clear differences were observed when single glutamic acids or pairs were mutated. These findings support a model where the PKD of TRIB3 is less accessible for interaction with AKT when the C-terminal tail with its triple E motif is present and also that the interaction through the PKD precedes binding of the C-terminal tail (Fig 3B).

To investigate the role of S473 phosphorylation–which we showed above to be affect the AKT-TRIB3 interaction (Fig. 1)– in this conformational model, we combined mutants described earlier and tested the triple glutamic acid mutant (E347A/E348A/E349A) for its ability to interact with the S473A and S473E mutants of AKT. Our results showed that the interaction is reduced when the S473 is mutated into an alanine (S473A) and is not affected when the serine is mutated into aspartic acid (S473D) (Figure 3C). These results suggest that the triple E motif may be positioned closely to S473, since the outcome of mutating the triple E motif of TRIB3 is affected by mutation of S473 in AKT.

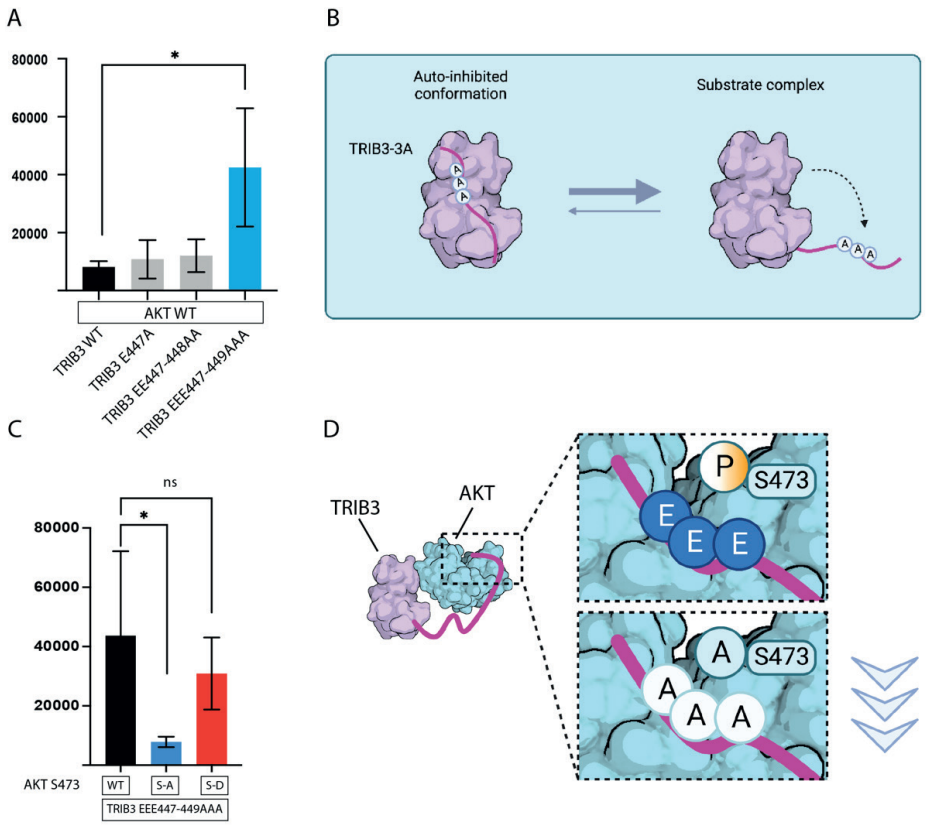

Figure 3. Triple E motif in C-terminal of TRIB3 and AKT S473 phosphorylation. (A) PCA results of TRIB3 WT, TRIB3 E347A, TRIB3 E347-348AA and TRIB3 EEE347-349AAA in combination with ATK WT. **(B)** Representation of autoinhibited and substrate complex conformation equilibrium of TRIB3 WT and TRIB3 EEE347-349AAA mutant. **(C)** PCA results of TRIB3 EEE347-349-AAA in combination of AKT WT, AKT S473A and AKT S473D. **(D)** Schematic representation of TRIB3 C-terminal domain interaction with AKT.

Insulin stimulated S473 phosphorylation of AKT is differentially regulated by TRIB3 mutants

To test the model in which the C-terminal tail of TRIB3 –and in particular the triple E motif– is important for the inhibition of S473 phosphorylation of AKT, we compared the effect of wt TRIB3 and the triple E motif mutant on insulin-stimulated S473 phosphorylation (Fig. 4A). We and others have previously used similar assays to test the capacity of insulin to induce the phosphorylation of AKT (S473) [45]. First, we generated HepG2 cells that overexpress GFP-tagged TRIB3 or the E347A/E348A/E349A mutant in a doxycycline inducible manner, as we reported before in other cell types [30, 37]. Insulin treatment resulted in a clear induction of S473 phosphorylation, as detected by phospho-specific antibodies (Fig. 4B). Upon doxycycline-induced

overexpression, wt TRIB3 was able to reduce the amount of phospho-AKT (Figure 4B) when compared to the uninduced cells. No reduction was observed in the cells expressing the TRIB3 mutant (Figure 4B). These data indicate that the triple E motif located in the C-terminal tail of TRIB3 contributes to inhibition of AKT activation.

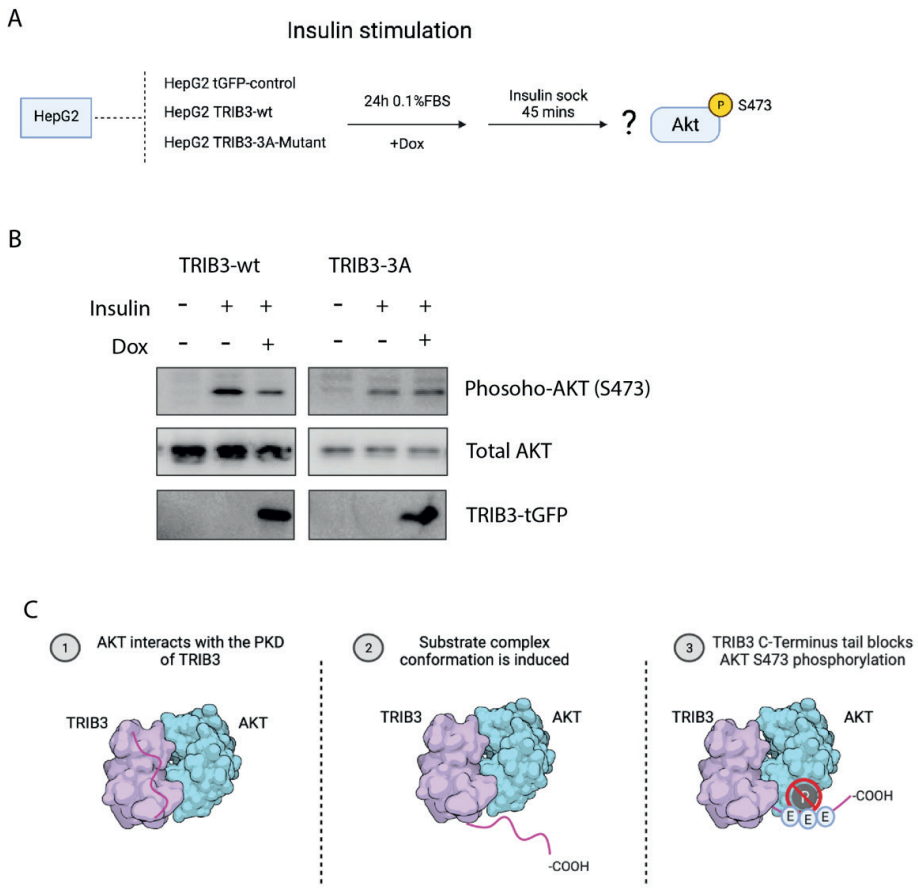

Figure 4. TRIB3 EEE347-349AAA mutant shows reduced ability to inhibit insulin-dependent AKT S473 phosphorylation in HepG2 cells. (A) Schematic representation of experimental set-up. **(B)** Western blots of total AKT, phospho AKT (S473) and GFP in inducible TRIB-WT and TRIB3 Triple A mutant (3A) in HepG2 cells. **(C)** Schematic model of AKT-TRIB3 interaction.

Discussion

In this study we have used a combination of cell-based and computational modelling approaches to investigate the interaction between TRIB3 and AKT. We have found that not only the PKD domain of TRIB3 interacts with AKT as previously shown, but also the C-terminal domain of TRIB3. Moreover, we have demonstrated that the C-terminal domain of TRIB3 is able to inhibit the phosphorylation of serine 473 of AKT. Our data indicate that this inhibition critically depends on a triple glutamic acid motif that might bind to the αc-helix of AKT. Based on our cell-based and computational modelling and structural studies on the related pseudokinase TRIB1 [44], we propose a multistep model for the AKT-TRIB3 interaction (Fig. 4C). Initially, TRIB3 is present in an auto-inhibited conformation, where the C-terminal tail (with its triple E motif) is folded over its PKD (Fig. 4C, 1). The PKD then interacts with AKT, where AKT may force TRIB3 into a different conformation where the C-terminal tail no longer shields the PKD and/or compete with the C-terminal tail for binding to the PKD (Fig 4C, 2). Finally, the C-terminal tail binds to AKT to a region close to the basic patch (K142/H143/R144) and prevents or destabilizes S473 phosphorylation (Fig. 4C, 3). Conversely, if S473 of AKT is phosphorylated, the interaction with TRIB3 is impaired. Interestingly, while the related pseudokinase TRIB2 can induce phosphorylation of S473 of AKT, and thereby play a role in the development of resistance to anti-cancer treatments, the C-terminal domain also plays a critical role in this case [35]. While the triple E motif is not strictly conserved, the C-terminal tail of TRIB2 contains an EENLD sequence (Fig. 2E) which may play a similar role. Together with the current study, these findings indicate that interfering only with the PKD-mediated TRIB3-AKT interaction, albeit effective is some experimental settings [42], may not always be sufficient to fully disrupt the complex between these two proteins.

While the model proposed above is partly based on experimental data, it should be noted that it also relies on the structure of TRIB1 that has been solved [27] and most of the current knowledge about Tribbles structure-function relationships comes from studies on TRIB1 [44]. Whether TRIB3 can indeed adopt the different conformations shown for TRIB1, an auto-inhibited conformation and a 'substrate complex conformation' [44], remains to be established. Nevertheless, conversion of one conformation into the next is potentially highly dependent on cellular context and extracellular signaling and may provide a molecular basis for the disparate findings on AKT-TRIB3 interplay reported so far (see Introduction). Post translational modifications (PTM) of TRIB3 may be an important regulatory mechanism in this context but are currently understudied. Therefore, additional structural studies of the individual AKT and TRIB3 proteins and in complex, together with detailed profiling of PTM on TRIB3 in different cellular settings and under different conditions, are required.

References

1. Coffer, P.J. and J.R. Woodgett, *Molecular cloning and characterisation of a novel putative protein-serine kinase related to the cAMP-dependent and protein kinase C families.* Eur J Biochem, 1991. **201**(2): p. 475-81.
2. Jones, P.F., et al., *Molecular cloning and identification of a serine/threonine protein kinase of the second-messenger subfamily.* Proc Natl Acad Sci U S A, 1991. **88**(10): p. 4171-5.
3. Manning, B.D. and A. Toker, *AKT/PKB Signaling: Navigating the Network.* Cell, 2017. **169**(3): p. 381-405.
4. Vanhaesebroeck, B., et al., *The emerging mechanisms of isoform-specific PI3K signalling.* Nat Rev Mol Cell Biol, 2010. **11**(5): p. 329-41.
5. Burgering, B.M. and P.J. Coffer, *Protein kinase B (c-Akt) in phosphatidylinositol-3-OH kinase signal transduction.* Nature, 1995. **376**(6541): p. 599-602.
6. Alessi, D.R., et al., *Mechanism of activation of protein kinase B by insulin and IGF-1.* EMBO J, 1996. **15**(23): p. 6541-51.
7. Alessi, D.R., et al., *Characterization of a 3-phosphoinositide-dependent protein kinase which phosphorylates and activates protein kinase Balpha.* Curr Biol, 1997. **7**(4): p. 261-9.
8. Stokoe, D., et al., *Dual role of phosphatidylinositol-3,4,5-trisphosphate in the activation of protein kinase B.* Science, 1997. **277**(5325): p. 567-70.
9. Yang, J., et al., *Crystal structure of an activated Akt/protein kinase B ternary complex with GSK3-peptide and AMP-PNP.* Nat Struct Biol, 2002. **9**(12): p. 940-4.
10. Feng, J., et al., *Identification of a PKB/Akt hydrophobic motif Ser-473 kinase as DNA-dependent protein kinase.* J Biol Chem, 2004. **279**(39): p. 41189-96.
11. Manning, B.D. and L.C. Cantley, *AKT/PKB signaling: navigating downstream.* Cell, 2007. **129**(7): p. 1261-74.
12. Berwick, D.C., et al., *The identification of ATP-citrate lyase as a protein kinase B (Akt) substrate in primary adipocytes.* J Biol Chem, 2002. **277**(37): p. 33895-900.
13. Horman, S., et al., *Insulin antagonizes ischemia-induced Thr172 phosphorylation of AMP-activated protein kinase alpha-subunits in heart via hierarchical phosphorylation of Ser485/491.* J Biol Chem, 2006. **281**(9): p. 5335-40.
14. Cross, D.A., et al., *Inhibition of glycogen synthase kinase-3 by insulin mediated by protein kinase B.* Nature, 1995. **378**(6559): p. 785-9.
15. Kops, G.J., et al., *Direct control of the Forkhead transcription factor AFX by protein kinase B.* Nature, 1999. **398**(6728): p. 630-4.
16. Altomare, D.A. and J.R. Testa, *Perturbations of the AKT signaling pathway in human cancer.* Oncogene, 2005. **24**(50): p. 7455-64.
17. Song, M., et al., *AKT as a Therapeutic Target for Cancer.* Cancer Res, 2019. **79**(6): p. 1019-1031.
18. Seher, T.C. and M. Leptin, *Tribbles, a cell-cycle brake that coordinates proliferation and morphogenesis during Drosophila gastrulation.* Curr Biol, 2000. **10**(11): p. 623-9.

19. Mata, J., et al., *Tribbles coordinates mitosis and morphogenesis in Drosophila by regulating string/CDC25 proteolysis.* Cell, 2000. **101**(5): p. 511-22.
20. Grosshans, J. and E. Wieschaus, *A genetic link between morphogenesis and cell division during formation of the ventral furrow in Drosophila.* Cell, 2000. **101**(5): p. 523-31.
21. Rorth, P., K. Szabo, and G. Texido, *The level of C/EBP protein is critical for cell migration during Drosophila oogenesis and is tightly controlled by regulated degradation.* Mol Cell, 2000. **6**(1): p. 23-30.
22. Richmond, L. and K. Keeshan, *Pseudokinases: a tribble-edged sword.* FEBS J, 2020. **287**(19): p. 4170-4182.
23. Kiss-Toth, E., G. Velasco, and W.S. Pear, *Tribbles at the cross-roads.* Biochem Soc Trans, 2015. **43**(5): p. 1049-50.
24. Jadhav, K.S. and R.C. Bauer, *Trouble With Tribbles-1.* Arterioscler Thromb Vasc Biol, 2019. **39**(6): p. 998-1005.
25. Mondal, D., A. Mathur, and P.K. Chandra, *Tripping on TRIB3 at the junction of health, metabolic dysfunction and cancer.* Biochimie, 2016. **124**: p. 34-52.
26. Dobens, L.L., et al., *Control of Cell Growth and Proliferation by the Tribbles Pseudokinase: Lessons from Drosophila.* Cancers (Basel), 2021. **13**(4).
27. Murphy, J.M., et al., *Molecular Mechanism of CCAAT-Enhancer Binding Protein Recruitment by the TRIB1 Pseudokinase.* Structure, 2015. **23**(11): p. 2111-21.
28. Qi, L., et al., *TRB3 links the E3 ubiquitin ligase COP1 to lipid metabolism.* Science, 2006. **312**(5781): p. 1763-6.
29. Yokoyama, T., et al., *Trib1 links the MEK1/ERK pathway in myeloid leukemogenesis.* Blood, 2010. **116**(15): p. 2768-75.
30. Hernandez-Quiles, M., et al., *Comprehensive Profiling of Mammalian Tribbles Interactomes Implicates TRIB3 in Gene Repression.* Cancers (Basel), 2021. **13**(24).
31. Kato, S. and K. Du, *TRB3 modulates C2C12 differentiation by interfering with Akt activation.* Biochem Biophys Res Commun, 2007. **353**(4): p. 933-8.
32. Naiki, T., et al., *TRB2, a mouse Tribbles ortholog, suppresses adipocyte differentiation by inhibiting AKT and C/EBPbeta.* J Biol Chem, 2007. **282**(33): p. 24075-82.
33. Du, K., et al., *TRB3: a tribbles homolog that inhibits Akt/PKB activation by insulin in liver.* Science, 2003. **300**(5625): p. 1574-7.
34. Kwon, M., et al., *Skeletal Muscle Tissue Trib3 Links Obesity with Insulin Resistance by Autophagic Degradation of AKT2.* Cell Physiol Biochem, 2018. **48**(4): p. 1543-1555.
35. Hill, R., et al., *TRIB2 confers resistance to anti-cancer therapy by activating the serine/threonine protein kinase AKT.* Nat Commun, 2017. **8**: p. 14687.
36. Hill, R., et al., *TRIB2 as a biomarker for diagnosis and progression of melanoma.* Carcinogenesis, 2015. **36**(4): p. 469-77.
37. Hernández-Quiles, M., et al., *TRIB3 Modulates PPARγ-Mediated Growth Inhibition by Interfering with the MLL Complex in Breast Cancer Cells.* International Journal of Molecular Sciences, 2022. **23**(18): p. 10535.

38. Jeninga, E.H., et al., *Impaired peroxisome proliferator-activated receptor gamma function through mutation of a conserved salt bridge (R425C) in familial partial lipodystrophy.* Mol Endocrinol, 2007. **21**(5): p. 1049-65.
39. Raveh, B., et al., *Rosetta FlexPepDock ab-initio: simultaneous folding, docking and refinement of peptides onto their receptors.* PLoS One, 2011. **6**(4): p. e18934.
40. Kim, D.E., D. Chivian, and D. Baker, *Protein structure prediction and analysis using the Robetta server.* Nucleic Acids Res, 2004. **32**(Web Server issue): p. W526-31.
41. Prudente, S., et al., *TRIB3 R84 variant affects glucose homeostasis by altering the interplay between insulin sensitivity and secretion.* Diabetologia, 2010. **53**(7): p. 1354-61.
42. Yu, J.M., et al., *TRIB3 supports breast cancer stemness by suppressing FOXO1 degradation and enhancing SOX2 transcription.* Nat Commun, 2019. **10**(1): p. 5720.
43. Chu, N., et al., *The structural determinants of PH domain-mediated regulation of Akt revealed by segmental labeling.* eLife, 2020. **9**.
44. Jamieson, S.A., et al., *Substrate binding allosterically relieves autoinhibition of the pseudokinase TRIB1.* Sci Signal, 2018. **11**(549).
45. van Eijkeren, R.J., et al., *Endogenous lipid antigens for invariant natural killer T cells hold the reins in adipose tissue homeostasis.* Immunology, 2018. **153**(2): p. 179-189.

Supplementary figures

A

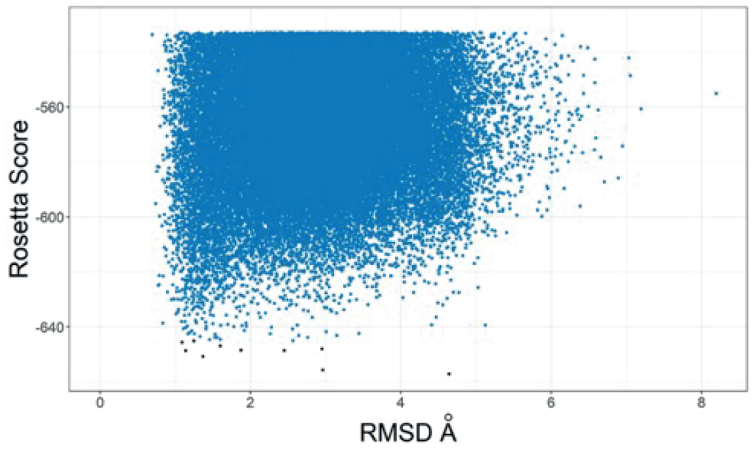

B

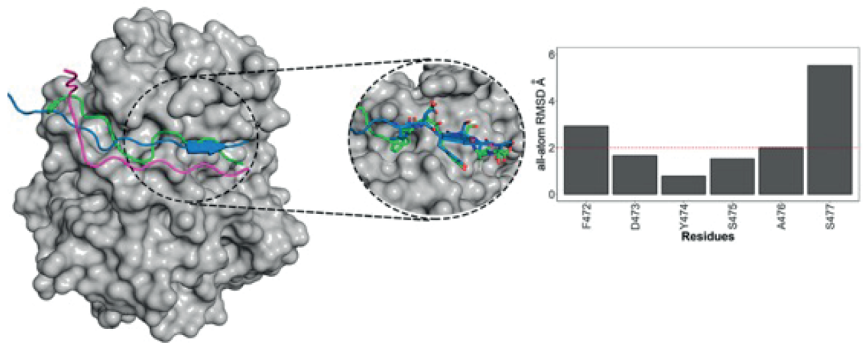

C

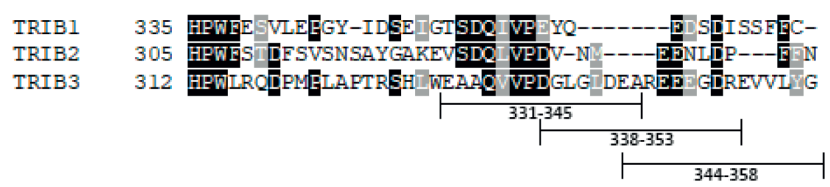

Supplementary Figure 1. Protein-peptide docking structure of AKT KD with its own C-tail (463-477). (A) Rosseta score energy landscape plots where each model is a blue circle according to its RMSD and its energy score. The top 10 lowest energy clusters created from the top 500 scoring models are shown as black circles. **(B)** The peptide starting orientation (magenta), the best model (blue), and the native peptide (green) are shown in complex with AKT KD (grey). A detailed view of the best result showing the peptide side chains compared with the crystallized region along with the RMSD of residues 472-477. **(C)** Alignment of the C-terminal domain of TRIB1, -2 and -3 and the three segments of TRIB3 C-terminal domain used for modeling.

A

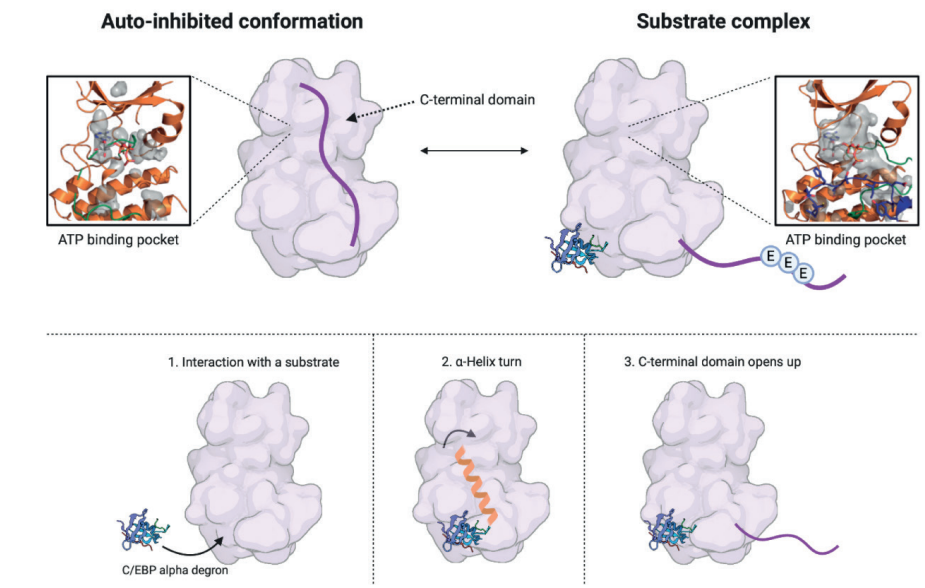

Supplementary Figure 2. Schematic representation of the transition between the auto-inhibited conformation of TRIB3 and the substrate complex conformation.

Chapter 8

General Discussion

Introduction

The connecting thread throughout this thesis is the use of MS-based proteomics approaches to study the role of non-enzymatic proteins in different contexts. We focused on the Tribbles family of pseudokinases and, more specifically, in TRIB3. This peculiar family of proteins was discovered twenty years ago in Drosophila in a screen for genes involved in cellular differentiation and growth [1-4]. Multiple groups simultaneously reported the findings of a kinase-like protein involved in oogenesis and gastrulation of the fly embryo, due to the tradition in the drosophila field to name genes based on the phenotype that mutations on them produce, the gene was named *Tribl*. Tribbles are Star Trek creatures that grow outstandingly quick as well as the *Trbl* mutant cells that exhibit premature mitosis. Trbl was found to be able to promote the degradation of *Slbo* [4] and *String* [3], the orthologs of the mammalian transcription factor C/EBPα and the phosphatase CDC25, involved in various cell cycle checkpoints [5, 6]. Shortly after, the human homolog TRIB3 was found able to inhibit AKT/PKB activation in the liver [7], this together with several associations with various cancers [8] increased the attention of the scientific community for this family of proteins. Despite the increasing number of publications since their discovery the knowledge about Tribbles molecular mechanism and exact function in different cellular settings is limited. Our way to contribute to this is by studying the interactome of Tribbles, as we hypothesized, the specific functions as well as the uniqueness and redundancies in Tribbles functions are dictated by their interactome in any given cellular setting. In Chapter 3, we used an unbiased MS-based proteomic approach to study the interacting partners of Tribbles in HEK293T and MCF7 cells. More important than the proteins that we found capable of interacting with TRIB1, -2 or -3 we used it as prove of concept. The function of a non-enzymatic proteins cannot be address only with the use of standard biochemical assays, as their role rely ultimately on the set of proteins its interacting at that particular moment. Analyzing their interactome in different cellular contexts allowed us to gain insights into different Tribbles functions, subcellular localization and their role in particular pathways as we showed in chapter 4 and chapter 6.

We used a similar AP-MS approach to study the role of FHL2 during adipogenesis, we discovered that FHL2 is able to interact with NFAT5, a known transcription factor that blocks the adipogenic transcriptional program and we showed in chapter 5 that they indeed cooperate to block adipocyte differentiation.

The study of the interactome of Tribbles and FHL2 have proven to be an insightful approach, however it has its limitations. The interactome is a snapshot of a specific

timepoint and its condition by the strength of the interactions as well as the abundance of the interacting proteins, which means that weak interactions or interactions with low-abundant proteins will be difficult to discover. This is why we complemented the AP-MS experiments with quantitative phospho-proteomics, this allowed us to have a more comprehensive view of the role of TRIB3 as well as reveal roles that would have very difficult to study only with the interactome. The main findings presented in this thesis as well as their impact and future perspective are discussed below:

1 Mass spectrometry-based proteomics for the study of pseudoenzymes function:

Pseudoenzymes are proteins that can be classified through sequence homology to a specific family of enzymes but they are predicted to be catalytically dead [9, 10]. They retain the structure and folding but they lack some of the key catalytic domains or motifs that have been shown to be critical for the enzymes function. Their origin is still controversial but the most accepted theory is that they emerged from gene duplication [11], the lack of selective pressure over their catalytic domains due to spatiotemporal co-expression with the catalytic active counterpart allowed them to drift away and lose these catalytic motifs. Pseudoenzymes were overlooked and described as dead enzymes until early 2000 when genomes started to be sequenced and the high number of predicted pseudoenzymes, around 10%, and how conserved they are across different species came to light [12]. These evidences underpinned an important role for this "dead" enzymes in cellular biology. To this day pseudoenzymes are still understudied when compared to their enzymatic active counterparts, but we understand much more than 20 years ago. These proteins function as interacting platforms; regulating the function of active enzymes, competing for substrates, assembling complexes and preventing the formation of others, our knowledge about the molecular mechanism of pseudoenzymes has been growing tremendously. All their different mechanisms come down to one thing, their interactome. The set of proteins a given pseudoenzyme is interacting defines the pseudoenzyme function and can be very cell specific or timepoint specific, adding another layer of complexity to the study of these proteins.

Mass spectrometry (MS) based proteomics approaches have become the most powerful technology to identify protein-protein interactions. Affinity purification mass spectrometry (AP-MS) is commonly used to determine the set of interactors of a particular protein, generally using antibodies against the endogenous protein or against epitope tags that allowed a highly efficient purification. The use of epitope tags is often required when working with pseudoenzymes as high-quality

antibodies are limited and often exhibit cross reactivity [13]. In our case we used nanobodies against GFP that reduced the number of peptides released during on-beads digestion and the background binding. We combined nanobodies with the use of inducible systems, this allowed us to expressed our protein of interest in a controlled manner, in regard of the amount and timepoint when it is expressed. Granting us the opportunity to generate valuable comparisons between conditions or mutants. We performed interactome analysis of TRIB1, -2 and -3 in HEK293T cells and TRIB1 and TRIB3 in MCF7 cells, by comparing these interactomes we not only learnt about specific TRIB functions but also about uniqueness and redundancies. We also compared the interactome of different TRIB3 mutants, allowing us to gain insights into the role of those motifs but also on how the protein localization is regulated. For instance, we found a mitochondrial localization of TIRB3 that has not been reported previously. In addition, we unraveled the role of TRIB3 in adipocytes using a combination of AP-MS experiments with phospho-proteomics. This combination of proteomics approaches is very powerful, interactions found in AP-MS experiments are restricted to strong interactions, interactions with relatively high abundant proteins and to the interactions happening at the moment the experiment is performed. The use of quantitative phospho-proteomics allowed two things; to have a more comprehensive view of all interactions, weak or strong, and to monitored the consequences of TRIB3 interactions in different signaling pathways. MS-based proteomics approaches represent the most powerful technology to study pseudoenzyme function and will continue to expand our knowledge on this superfamily of proteins.

2. TRIB3 regulates adipose tissue expandability and works as a signal integrator molecule:

The adipose tissue is highly dynamic metabolic organ that plays a pivotal role in the development of the metabolic syndrome and diabetes type 2 [14, 15]. As the obesity epidemic has not shown signs of declining discovering new ways of tackling the advance of the disease has become of mayor focus for the scientific community.

TRIB3 plays a key role in metabolism; regulates lipid metabolism by targeting for degradation acetyl Co-A carboxylase (ACC), the rate-limiting enzyme in fatty acid synthesis [16]. During fasting TRIB3 is upregulated and through its association with the E3 ligase COP1 inhibits the biosynthesis of fatty acids and thus promotes lipolysis. The role of TRIB3 in glucose metabolism has also been address by numerous studies, TRIB3 is upregulated in liver, pancreatic β-cells, skeletal muscle and adipose tissue in patients with insulin resistance or type 2 diabetes [17]. TRIB3 regulates glycogen synthesis by affecting AKT signaling in the liver and in muscle cells TRIB3 has been shown to regulate insulin sensitivity and glucose homeostasis [18, 19]. Furthermore, TRIB3 expression is also trigger by amino acid availability in the liver [20] suggesting a role in amino acid metabolism as well. TRIB3 seems to regulate many different aspects of cellular metabolism and whether is a potential target for patients with type 2 diabetes is still unclear and perhaps the answer relies on the specific tissue we look at.

Since AT dysfunction is the first step in the development of insulin resistance, we focused on understanding the role of TRIB3 on this tissue by using a combination of in-vivo and in-vitro approaches. We showed that ablation of TRIB3 in mice results in increase adiposity, this difference in AT mass was found 12 weeks old animals that had not been challenge with an obesogenic diet. Is important to highlight that these animals were not metabolically unhealthy as shown by the insulin and glucose tolerance tests. This suggests a very fundamental role of TRIB3 in adipocytes controlling proliferation and expandability of these cells. TRIB3 plays an important role in immune cells and AT-resident immune cells have been shown critical for AT function [21, 22], we could however show that the AT dysfunction that we appreciated was consequence of the role of TRIB3 in the adipocytes a not in the immune cells, as we showed that downregulation of TRIB3 in 3T3-L1 adipocytes led to impaired lipid profile in line with the altered lipid handling phenotype appreciated in the *in vivo* model. We used a combination of MS-based proteomics approaches discussed previously to show that adipose TRIB3 functions as a signal integrator molecule, modulating the response to external stimulus like insulin and growth factors. TRIB3 achieves this by interacting with serine/threonine kinases involved in signal transduction and with transcription factors such as ATF4 and ATF7.

Particularly interesting is the interactions between TRIB3 and ERK3/MAPK6, a non-previously reported interaction of TRIB3. This atypical mitogen activated protein kinase (MAPK) was found in the AP-MS experiments in IBA cells and also in the phosphoproteomics where ERK3 Serine-189 was differentially regulated upon TIRB3 overexpression. This phosphorylation has been linked to promote entry in the cell cycle but more importantly the association between ERK3 and MAPKAPK5 (responsible of such phosphorylation [23]) have been shown to regulate lipolysis in adipocytes [24]. ERK3$^{-/-}$ mice exhibit lower adiposity and improved insulin sensitivity and disruption of the ERK3-MAPKAPK5 complex in the adipose tissue specifically resulted in reduced adiposity and improved metabolic parameters [24, 25]. The exact nature of the interaction between ERK3 and TRIB3 remains to be fully elucidated as TRIB3 could be promoting degradation of ERK3 or promoting the assembling of the complex between ERK3 and MAPKAPK5.

In addition, multiple transcription factors were found interacting with TRIB3 in adipocytes, including ASH2L member of the WRAD complex and involve in H3K4 tri-methylation [26, 27]. In chapter 6 we investigated in detail the interaction between TRIB3 and the WRAD complex and is not a surprise that this role of TRIB3 is conserved in multiple cellular settings.

Moreover, the upregulation of TRIB3 in adipocytes resulted in big changes in the phosphoproteome of these cells. Several transcription factors including; ATF7, STAT3, ATF4 and ERF, a transcriptional repressor often associated with MAPK1 [28, 29], were found differentially phosphorylated upon TRIB3 expression. Our data suggest that TRIB3 function as a signal integrator molecule, interacting with different signaling cascades that are downstream of membrane receptors and with TF that are downstream those majors signaling cascades. Adipocytes sense the nutrient availability and different hormone levels of the body and are able to respond to that and regulate whole body metabolism, different membrane receptors that converge in mayor signaling cascades such as insulin signaling or ERK pathway are connected to TF that activate or inhibit transcriptional programs that trigger glucose uptake or lipid synthesis for example. TRIB3 seems to act as a facilitator of communication between the external stimuli and the transcriptional response.

3. TRIB3-AKT interaction: more than just an inhibition

The study of Tribbles function has always been linked to AKT is some way, perhaps because of the capital importance of AKT signaling in cancer and insulin resistance or perhaps because the role of TRIB3 as an inhibitor of AKT was one of the first mechanism of Tribbles that was discovered. In any case, the tag of TRIB3 as an inhibitor of AKT phosphorylation is always present in most Tribbles studies. Little matter contradictory data where studies have failed to find any link between TRIB3 and AKT phosphorylation or studies were the role of TRIB3 seems to be the opposite and is able to enhance AKT phosphorylation [30]. What all these different results suggest is that the exact nature of the interaction between TRIB3 and AKT remains to be fully elucidated. What is not often mention is that TRIB3 localization appeared to be nuclear in most cellular settings, and when AKT reaches the nucleus is already been phosphorylated by PDK1 and mTORC2. AKT is phosphorylated in the plasma membrane and although there are some indications that drosophila *Trbl* might have some membrane localization researches have failed to show any membrane localization for TRIB3 in mammalian cells. The need for better tools to study TRIB3 localization, for example with high-quality antibodies, is crucial in this regard. Commercially available TRIB3 antibodies seems to be very cell type specific, detecting a protein in some type of lysates and not others. This might be the result

of different post translational modification (PTM) status of TRIB3 between these conditions, PTM can mask the epitope that antibodies are able to recognize making them unable to bind the target protein. PTM have been shown to be cell type specific and our knowledge of Tribbles PTM status is very poor as so far there has not been described any.

One of the most well-known mechanisms among pseudokinases is the regulation of the substrate specificity of kinases through direct interaction. We have appreciated a glance of this in the phosphoproteomics data, were upregulation of TRIB3 led to changes in phosphorylation status of some AKT substrates, in particular PRAS40, one the first AKT substrates to be described [31]. There have been over 100 different substrates of AKT been described in literature and is only logical to think that the substrate specificity of AKT is somehow regulated, and TRIB3 could be part of this. AKT signaling has different outputs including, cellular proliferation, cell growth or changes in metabolism and the interaction between TRIB3 and AKT would skew AKT signaling into some of these directions. Our data is a clear step forward into elucidating the role of the interaction between TRIB3 and AKT, where we have showed that the interactions is a 2-point contact between the pseudokinase domain and C-terminal domain of TRIB3 and AKT and might help to clarify some of the discrepancies in the field. Anyhow, more research is needed to understand the nature of this interaction and if can be used as a therapeutic target in cancer or insulin resistance.

4. TRIB3 a new chromatin regulator

Tribbles plays an important role in a plethora of cellular processes and they able to do this by interacting with kinases, components of the ubiquitin proteasome system and transcription factors. Already one of the first discovered interacting partner of drosophila *Trbl* was the C/EBP homolog *Slbo* [4] a transcription factor involved in cellular differentiation [32]. The mechanism around the interaction between tribbles and C/EBP proteins is one of the most well understood, where Tribbles are able to promote the degradation of different C/EBP proteins depending on the cellular context through the interaction with the E3 ubiquitin ligase COP1 [33-35]. Among the different members of the Tribbles family TRIB3 is the one that have been associated more often with other transcription factors in recent studies. Recently, TRIB3 has been shown to promote breast cancer stemness through the association with FOXO1, preventing its degradation and enhancing FOXO1 transcriptional activity [36]. Is still unclear whether the interaction was maintained when FOXO1 is bound to the DNA or is only happening away from the DNA context. In addition, TRIB3 has been shown to be able to interact with β-catenin and TCF4 in colorectal cancer

cells and in this study TRIB3 was found bound to these transcription factors when they were in complex with the DNA [37]. Finally, the interaction between TRIB3 and ATF4, a transcription factor involved in the cellular response to stress, has also been the subject of intense research [38]. Very recently studies have shown that TRIB3 is able to inhibit ATF4 transcriptional activity and, more importantly, ChIP-sequencing data of endogenously tagged TRIB3 have shown the ability of the pseudokinase to be bound to the DNA [39]. TRIB3 does not contain any canonical DNA binding motif so most likely is able to achieve this by interacting with other transcription factors. Our results clearly demonstrated that indeed TRIB3 can be found bound to chromatin (Chapter 6), DNA pull downs followed by mass spectrometry could answer the question of what other proteins are in complex with TRIB3 when is bound to the DNA. We found that TRIB3 can bind to the WRAD complex and specifically to the win domain of WDR5. We found components of the WRAD complex as interactors of TRIB3 in HEK293T, MCF7, BT474 (data not shown) and IBA cells, indicating that this is a general mechanism of TRIB3 rather that a specific role in breast cancer cells. We found that previous interactome studies of different subunits of the MLL and NuRD complex have found TRIB3 as interactor of some subunits, particularly BAP18 [40], a subunit that can take part in both complexes. All together this suggest that TRIB3 is a subunit of these major transcriptional regulatory complexes and the reason as why is has not been discover previously might be because TRIB3 is only present on a relatively small fraction of these complexes. The exact role of TRIB3 as part of these complexes is still unclear but we have demonstrated that can influence H3K4me^3 in cells. ChIP sequencing experiments of TRIB3 could help answering some of these questions. If we speculate about the role of TRIB3 as transcription factors and we take into account some the findings presented above, that situate TRIB3 as a signal integrator between external stimulus and transcription factors responses, this role of TRIB3 might be part of the same process. Cells need to adapt very quickly to changes in their nutrient availability and specially adipocytes and liver cells, cell types in which it has been shown that TRIB3 is upregulated upon low levels of glucose or aminoacids [20, 41]. In this situation cells need to change their transcriptional programs to rely less on the low-abundant glucose and start using lipids as well as generate the appropriate endocrine response that will allow the body to keep functioning on this starvation conditions. In this case TRIB3 might facilitate the re-localization of MLL/NuRD complexes to gene loci that need to get quickly express or remove the complex from genes that need to get repressed. Cellular metabolism plays a critical role regulating chromatin dynamics, it has been shown how different metabolites are substrates needed for posttranslational modifications, for example acetylation of histones, that massively impact gene expression [42]. TRIB3 is a nutrient sensor that its expression and possibly its function its regulated by different

nutrients availability, TRIB3 through the newly discover interaction with the WRAD complex can then regulate the epigenome of the cells. This could represent a new mechanism on how cellular metabolism can impact epigenetics, however the exact role of TRIB3 as epigenetic regulator remains to be elucidated.

5. Tribbles in cancer: druggable or undruggable?

As already mentioned, the associations between Tribbles and cancer are strong and are present for all three TRIB family members [8]. Some of these associations are TRIB1 with prostate cancer [43], breast cancer [44] and acute myeloid leukemia [45]; TRIB2 has been associated with melanoma and leukemia [46, 47] and TRIB3 with breast, lung and renal cancer among others [36, 48, 49]. There is not a single mechanism that drives Tribbles tumorigenesis as their functions are tremendously cell type specific, depending on the cellular context Tribbles act as oncogenes or tumor suppressors [50].

Protein kinases are one of the most targeted groups of drug targets, since the first protein kinase inhibitor was developed 40 years ago the number of kinases targeted have grown rapidly [51]. Most of these small molecules target the ATP binding site of the kinase and few are allosteric regulators in both cases resulting in reduced activity of the enzyme. Protein kinase inhibitors have shown great results in cancer therapy and more than 150 new molecules are currently different stages of clinical trials [51]. In contrast, pseudokinases are currently not the direct drug target of any cancer therapy [52]. Nevertheless, there are some examples of pseudokinases that hold potential as drug target mainly due to their similarity to a well studies kinase or because it conserves a high affinity for ATP. Tribbles are none of the above, although some studies have some a very weak affinity of TRIB2 and TRIB3 for ATP [53] this remains to be formally validated. However, targeting Tribbles with allosteric regulators or with small molecules that enhance Tribbles degradation using a proteolysis targeting chimera (PROTAC)[54] are still an option that remains to be explored. In order to achieve this a number of problems will have to be overcome. First, the lack of crystal structures for TRIB2 and -3, without a detailed structure of these proteins would not be possible to design specific molecules to target them in any way. Secondly and perhaps more importantly, there is still a very limited understanding of the molecular mechanism behind Tribbles action as well as the cell type specificity. Further research is needed to understand Tribbles physiopathology and molecular links behind Tribbles associations in different cancers, the work presented in this thesis is a step on the right directions and might represent a stepping stone for the development of future therapies but the road ahead remains long.

References

1. Seher, T.C. and M. Leptin, *Tribbles, a cell-cycle brake that coordinates proliferation and morphogenesis during Drosophila gastrulation.* Curr Biol, 2000. **10**(11): p. 623-9.
2. Grosshans, J. and E. Wieschaus, *A genetic link between morphogenesis and cell division during formation of the ventral furrow in Drosophila.* Cell, 2000. **101**(5): p. 523-31.
3. Mata, J., et al., *Tribbles coordinates mitosis and morphogenesis in Drosophila by regulating string/CDC25 proteolysis.* Cell, 2000. **101**(5): p. 511-22.
4. Rorth, P., K. Szabo, and G. Texido, *The level of C/EBP protein is critical for cell migration during Drosophila oogenesis and is tightly controlled by regulated degradation.* Mol Cell, 2000. **6**(1): p. 23-30.
5. Johnson, P.F., *Molecular stop signs: regulation of cell-cycle arrest by C/EBP transcription factors.* J Cell Sci, 2005. **118**(Pt 12): p. 2545-55.
6. Boutros, R., C. Dozier, and B. Ducommun, *The when and wheres of CDC25 phosphatases.* Curr Opin Cell Biol, 2006. **18**(2): p. 185-91.
7. Du, K., et al., *TRB3: a tribbles homolog that inhibits Akt/PKB activation by insulin in liver.* Science, 2003. **300**(5625): p. 1574-7.
8. Dobens, L.L., et al., *Control of Cell Growth and Proliferation by the Tribbles Pseudokinase: Lessons from Drosophila.* Cancers (Basel), 2021. **13**(4).
9. Eyers, P.A. and J.M. Murphy, *Dawn of the dead: protein pseudokinases signal new adventures in cell biology.* Biochem Soc Trans, 2013. **41**(4): p. 969-74.
10. Eyers, P.A. and J.M. Murphy, *The evolving world of pseudoenzymes: proteins, prejudice and zombies.* BMC Biol, 2016. **14**(1): p. 98.
11. Jacobsen, A.V. and J.M. Murphy, *The secret life of kinases: insights into non-catalytic signalling functions from pseudokinases.* Biochem Soc Trans, 2017. **45**(3): p. 665-681.
12. Pils, B. and J. Schultz, *Inactive enzyme-homologues find new function in regulatory processes.* J Mol Biol, 2004. **340**(3): p. 399-404.
13. Smits, A.H. and M. Vermeulen, *Characterizing Protein-Protein Interactions Using Mass Spectrometry: Challenges and Opportunities.* Trends Biotechnol, 2016. **34**(10): p. 825-834.
14. Chouchani, E.T. and S. Kajimura, *Metabolic adaptation and maladaptation in adipose tissue.* Nat Metab, 2019. **1**(2): p. 189-200.
15. Guilherme, A., et al., *Adipocyte dysfunctions linking obesity to insulin resistance and type 2 diabetes.* Nat Rev Mol Cell Biol, 2008. **9**(5): p. 367-77.
16. Qi, L., et al., *TRB3 links the E3 ubiquitin ligase COP1 to lipid metabolism.* Science, 2006. **312**(5781): p. 1763-6.
17. Lee, S.K., et al., *TRIB3 Is Highly Expressed in the Adipose Tissue of Obese Patients and Is Associated With Insulin Resistance.* J Clin Endocrinol Metab, 2022. **107**(3): p. e1057-e1073.
18. Kwon, M., et al., *Skeletal Muscle Tissue Trib3 Links Obesity with Insulin Resistance by Autophagic Degradation of AKT2.* Cell Physiol Biochem, 2018. **48**(4): p. 1543-1555.
19. Zhang, W., et al., *Skeletal Muscle TRIB3 Mediates Glucose Toxicity in Diabetes and High- Fat Diet-Induced Insulin Resistance.* Diabetes, 2016. **65**(8): p. 2380-91.
20. Carraro, V., et al., *Amino acid availability controls TRB3 transcription in liver through the GCN2/eIF2alpha/ATF4 pathway.* PLoS One, 2010. **5**(12): p. e15716.
21. Schipper, H.S., et al., *Adipose tissue-resident immune cells: key players in immunometabolism.* Trends Endocrinol Metab, 2012. **23**(8): p. 407-15.
22. Lu, J., et al., *Adipose Tissue-Resident Immune Cells in Obesity and Type 2 Diabetes.* Front Immunol, 2019. **10**: p. 1173.
23. Seternes, O.M., et al., *Activation of MK5/PRAK by the atypical MAP kinase ERK3 defines a novel signal transduction pathway.* EMBO J, 2004. **23**(24): p. 4780-91.
24. El-Merahbi, R., et al., *The adrenergic-induced ERK3 pathway drives lipolysis and suppresses energy dissipation.* Genes Dev, 2020. **34**(7-8): p. 495-510.
25. Loza-Valdes, A., et al., *Targeting ERK3/MK5 complex for treatment of obesity and diabetes.* Biochem Biophys Res Commun, 2022. **612**: p. 119-125.
26. Ernst, P. and C.R. Vakoc, *WRAD: enabler of the SET1-family of H3K4 methyltransferases.* Brief Funct Genomics, 2012. **11**(3): p. 217-26.
27. Jiang, H., *The complex activities of the SET1/MLL complex core subunits in development and disease.* Biochim Biophys Acta Gene Regul Mech, 2020. **1863**(7): p. 194560.
28. Sgouras, D.N., et al., *ERF: an ETS domain protein with strong transcriptional repressor activity, can suppress ets-associated tumorigenesis and is regulated by phosphorylation during cell cycle and mitogenic stimulation.* EMBO J, 1995. **14**(19): p. 4781-93.
29. Le Gallic, L., et al., *Transcriptional repressor ERF is a Ras/mitogen-activated protein kinase target that regulates cellular proliferation.* Mol Cell Biol, 1999. **19**(6): p. 4121-33.
30. Kato, S. and K. Du, *TRB3 modulates C2C12 differentiation by interfering with Akt activation.* Biochem Biophys Res Commun, 2007. **353**(4): p. 933-8.
31. Wiza, C., E.B. Nascimento, and D.M. Ouwens, *Role of PRAS40 in Akt and mTOR signaling in health and disease.* Am J Physiol Endocrinol Metab, 2012. **302**(12): p. E1453-60.
32. Nerlov, C., *The C/EBP family of transcription factors: a paradigm for interaction between gene expression and proliferation control.* Trends Cell Biol, 2007. **17**(7): p. 318-24.
33. Dedhia, P.H., et al., *Differential ability of Tribbles family members to promote degradation of C/EBPalpha and induce acute myelogenous leukemia.* Blood, 2010. **116**(8): p. 1321-8.
34. Murphy, J.M., et al., *Molecular Mechanism of CCAAT-Enhancer Binding Protein Recruitment by the TRIB1 Pseudokinase.* Structure, 2015. **23**(11): p. 2111-21.
35. Jamieson, S.A., et al., *Substrate binding allosterically relieves autoinhibition of the pseudokinase TRIB1.* Sci Signal, 2018. **11**(549).
36. Yu, J.M., et al., *TRIB3 supports breast cancer stemness by suppressing FOXO1 degradation and enhancing SOX2 transcription.* Nat Commun, 2019. **10**(1): p. 5720.
37. Hua, F., et al., *TRIB3 Interacts With beta-Catenin and TCF4 to Increase Stem Cell Features of Colorectal Cancer Stem Cells and Tumorigenesis.* Gastroenterology, 2019. **156**(3): p. 708-721 e15.

38. Jousse, C., et al., *TRB3 inhibits the transcriptional activation of stress-regulated genes by a negative feedback on the ATF4 pathway.* J Biol Chem, 2007. **282**(21): p. 15851-61.
39. Ord, T., et al., *Pharmacological or TRIB3-Mediated Suppression of ATF4 Transcriptional Activity Promotes Hepatoma Cell Resistance to Proteasome Inhibitor Bortezomib.* Cancers (Basel), 2021. **13**(10).
40. van Nuland, R., et al., *Quantitative dissection and stoichiometry determination of the human SET1/MLL histone methyltransferase complexes.* Mol Cell Biol, 2013. **33**(10): p. 2067-77.
41. Ord, T., et al., *TRIB3 enhances cell viability during glucose deprivation in HEK293-derived cells by upregulating IGFBP2, a novel nutrient deficiency survival factor.* Biochim Biophys Acta, 2015. **1853**(10 Pt A): p. 2492-505.
42. Reid, M.A., Z. Dai, and J.W. Locasale, *The impact of cellular metabolism on chromatin dynamics and epigenetics.* Nat Cell Biol, 2017. **19**(11): p. 1298-1306.
43. Shahrouzi, P., et al., *Genomic and Functional Regulation of TRIB1 Contributes to Prostate Cancer Pathogenesis.* Cancers (Basel), 2020. **12**(9).
44. Kim, T., et al., *TRIB1 regulates tumor growth via controlling tumor-associated macrophage phenotypes and is associated with breast cancer survival and treatment response.* Theranostics, 2022. **12**(8): p. 3584-3600.
45. Yoshino, S., et al., *Trib1 promotes acute myeloid leukemia progression by modulating the transcriptional programs of Hoxa9.* Blood, 2021. **137**(1): p. 75-88.
46. Hill, R., et al., *TRIB2 as a biomarker for diagnosis and progression of melanoma.* Carcinogenesis, 2015. **36**(4): p. 469-77.
47. O'Connor, C., et al., *Trib2 expression in granulocyte-monocyte progenitors drives a highly drug resistant acute myeloid leukaemia linked to elevated Bcl2.* Oncotarget, 2018. **9**(19): p. 14977-14992.
48. Zhang, X., et al., *TRIB3 promotes lung cancer progression by activating beta-catenin signaling.* Eur J Pharmacol, 2019. **863**: p. 172697.
49. Hong, B., et al., *TRIB3 Promotes the Proliferation and Invasion of Renal Cell Carcinoma Cells via Activating MAPK Signaling Pathway.* Int J Biol Sci, 2019. **15**(3): p. 587-597.
50. Eyers, P.A., K. Keeshan, and N. Kannan, *Tribbles in the 21st Century: The Evolving Roles of Tribbles Pseudokinases in Biology and Disease.* Trends Cell Biol, 2017. **27**(4): p. 284-298.
51. Bhullar, K.S., et al., *Kinase-targeted cancer therapies: progress, challenges and future directions.* Mol Cancer, 2018. **17**(1): p. 48.
52. Byrne, D.P., D.M. Foulkes, and P.A. Eyers, *Pseudokinases: update on their functions and evaluation as new drug targets.* Future Med Chem, 2017. **9**(2): p. 245-265.
53. Bailey, F.P., et al., *The Tribbles 2 (TRB2) pseudokinase binds to ATP and autophosphorylates in a metal-independent manner.* Biochem J, 2015. **467**(1): p. 47-62.
54. Paiva, S.L. and C.M. Crews, *Targeted protein degradation: elements of PROTAC design.* Curr Opin Chem Biol, 2019. **50**: p. 111-119.

Appendices

Summary

Adipose tissue (AT) regulates whole-body metabolism and energy homeostasis through the production and secretion of adipose-specific factors, the so-called: adipokines. Dysregulation of adipose tissue due to excessive and prolonged exposure to an over-caloric diet is a hallmark in the development of obesity and obesity-associated diseases like Type II Diabetes and cancer. Since the global obesity epidemic has not shown signs of declining, understanding the factors and signals that regulate adipose tissue function remains of critical importance for the scientific community.

The three main players of this thesis are introduced in **Chapter 1**. Adipose tissue, pseudoenzymes and their role in biology, and finally, mass spectrometry-based proteomics which is the connecting thread throughout the rest of the thesis.

In **Chapter 2**, the role of peroxisome proliferator-activated receptor gamma (PPARg), a member of the nuclear receptor superfamily, is summarized. With special emphasis on the different molecular mechanisms behind its function in different cellular contexts, such as adipocytes and immune cells. In addition, the role PPARg in cancer is explained in detail.

Chapter 3 is focused on Tribbles and their interactome. Tribbles are highly conserved pseudokinases that play a role in many aspects of biology, from metabolism to immune cell differentiation. We hypothesized that the different set of proteins that interacts with specific Tribbles in a given biological context is what determines their role in that cellular context. We used a mass-spectrometry-based approach to study the interactome of these proteins and we discover and validate that TRIB3 functions as a transcriptional repressor.

In **Chapter 4** we use a multidisciplinary approach to study the role of TRIB3 in AT. We characterized the phenotype of the Trib3 knock-out mice, and we used a combination of -omics technologies (transcriptomics, proteomics, and lipidomics) to look at the molecular mechanism. Similarly, in **Chapter 5**, we combined in-vivo with in-vitro techniques to understand the role of FHL2 in adipocytes. We found that FHL2 interacts with NFAT5 in early adipogenesis and that this signaling complex represses the adipogenic transcriptional program.

Next, in **Chapter 6** we validated the interaction of TRIB3 with the WRAD complex. The WRAD complex is the catalytic subunit of the histone writer SET1/MLL complex. This complex is responsible for histone H3 lysine-4 three-methylation (H3K4me3), a histone mark found in active promoters and link of transcriptional activation. We found that TRIB3 can regulate PPARg expression through the interactions with the WRAD complex and this signaling pathway might open the door to future therapeutic interventions in breast cancer patients.

Finally, in **Chapter 7** we studied the long-known interaction between TRIB3 and AKT. We used a combination of in-silico computational modeling and an in-vitro approach to map this interaction. We found a motif in the C-Terminal tail of TRIB3 that is pivotal for the interaction with AKT and might explain some of the controversies described during previous years. Lastly, some of the conclusions and future directions of the work presented in this thesis are described in **Chapter 8**.

Samenvatting

Vetweefsel reguleert het algehele metabolisme en energie homeostase van het menselijk lichaam door middel van productie en uitscheiding van vetweefsel-specifieke factoren, zogenaamde 'adipokines'. Verstoring van het vetweefsel door aanhoudende overmatige consumptie is een kenmerk van de ontwikkeling van obesitas en aan obesitas gerelateerde ziekten zoals diabetes type II en kanker. Omdat obesitas een mondiaal probleem vormt is het van wetenschappelijk belang om de factoren en signalen die de functies van het vetweefsel reguleren te begrijpen.

De drie algemene componenten van deze thesis worden geïntroduceerd in **Hoofdstuk 1**. Vetweefsel, pseudo-enzymen en hun rol in biologie, en als laatste massa spectrometrie proteomics, wat de connectie vormt in de rest van de thesis. In **Hoofdstuk 2** wordt de rol van peroxisome proliferator-activated receptor gamma (PPARg), een familielid van de nucleaire receptoren super familie, samengevat. De focus ligt op verschillende moleculaire mechanismen van de functie van PPARg in verschillende cellulaire contexten zoals adipocyten en immuuncellen. Bovendien wordt de rol van PPARg in kanker in detail besproken. **Hoofdstuk 3** omvat de Tribbles psuedo-enzymen en hun interactoom. Tribbles zijn evolutionair geconserveerde pseudo-kinases die een rol spelen in vele aspecten van de biologie, waaronder metabolisme en immuun cel differentiatie. Wij hypothetiseren dat verschillende sets van eiwitten die met Tribbles interacteren in een gegeven biologische context, bepalend is voor wat de rol is in die cellulaire context. Met behulp van massa spectrometrie hebben wij het intreractoom van deze eiwitten bestudeerd en ontdekt dat TRIB3 functioneert als een remmer van transcriptie. **Hoofdstuk 4** beschrijft een multidisciplinaire aanpak om de rol van TRIB3 te bestuderen in vetweefsel. We karakteriseerden een fenotype van Trib3 knock-out muizen en gebruikten een combinatie van -omics technologieën (transcriptomics, proteomics, and lipidomics) om te kijken naar de moleculaire mechanismen. Op vergelijkbare wijze bespreekt **Hoofdstuk 5** een gecombineerd in *in-vivo* met *in-vitro* technieken om de rol van FHL2 in adipocyten te begrijpen. We ontdekten dat FHL2 vroeg in adipogenese interacteert met NFAT5 en dat dit complex de adipogenese-specifieke transcriptie programma remt. Vervolgens wordt in **Hoofdstuk 6** de interactie van TRIB3 met het WRAD complex gevalideerd. Het WRAD complex is de katalytische sub-eenheid van het histon schrijver SET1/MLL complex. Dit complex is verantwoordelijk voor histon H3 lysine-4 tri-methylatie (H3K4me3), een histon modificatie die wordt geassocieerd met actieve promotors en transriptionele activatie. We vonden dat TRIB3 PPARg expressie kan reguleren door middel van interacties met het WRAD complex en dat dit mogelijk een interessant aspect is voor toekomstige therapieën en interventies voor borst kanker patiënten. Als laatste wordt in **Hoofstuk 7** de al langer bekende interactie tussen TRIB3 en AKT bestudeerd. We gebruikten een combinatie van *in-silico* modeleren en een *in-vitro* aanpak om deze interactie te analyseren. We vonden een motief in de C-terminale staart van TRIB3 die cruciaal is voor de interactie met AKT en mogelijk bestaande beschreven controversies van de afgelopen jaren verklaart. Conclusies en toekomstige directies van deze thesis worden beschreven in het laatste **Hoofdstuk 8**.

Curriculum vitae

Miguel Hernández-Quiles was born in Madrid where he attended high school and graduated from "Colegio Bernadette" after which he started his bachelor's in Chemistry at Universidad Complutense de Madrid. He then graduated in 2014 in Biochemistry and Biotechnology at Universidad Europea de Madrid. During his bachelor studies, he did an internship in the lab of Prof. Dr. José Alcamí where he found his passion for research in molecular biology. In October 2016, Miguel obtained his master's degree from the University of Nottingham in Advanced genomic and proteomic sciences. During his final internship in the group of Prof. Dr. David Heery, Miguel worked on the role of nuclear receptors (NR) in cancer and the use of the then recently discovered technique, CRISPR-Cas9 genome editing tool, to introduce mutations in NR and study their effects. Shortly after, Miguel started as a PhD student in the lab of Dr. Eric Kalkhoven at the University Medical Center Utrecht to study the role of Tribbles in adipose tissue using mass spectrometry-based proteomic techniques. In September 2022, Miguel started as a postdoctoral research fellow in the lab of Prof. Dr. Michiel Vermeulen at Radboud University and NKI to develop further expertise in mass spectrometry-based technologies.

Acknowledgements

First, I would like to thank my supervisor and co-promoter **Dr. Eric Kalkhoven** for giving me the opportunity to develop as a scientist, for guiding me through it and always supporting me. Thank you for all your help, it's been a blast, I don't think I could have had a better mentor. I also want to thank my promoter **Prof. Dr. Boudewijn Burgering** for all the advice that has giving me during these years and for making the CMM a great place to do science.

I specially want to thank **Cristina** for helping me every time I had a problem and for making me feel a little bit closer to the south of Europe every time we had time to chat. I want to extend my gratitude to all the present a former member of the Kalkhoven and van Mil labs, to **Prof. Dr. Saskia, Ellen, Jose, Nicolle, Suzanne, Koos, Judith**, **Anna**, **Monique** and **Miranda** thanks for all the laughs in the lab, the small talk and the fun activities during these years. **Thibaud**, we miss you in Utrecht you will be forever our favorite post-drunk. **Marjoleine,** thank for all the things you showed me in the lab, I will always be impressed by your organization skill and incredible memory. **Anouska**, thanks for all the help inside and outside the lab and for making sure everybody pronounced properly my name. **Bob**, Thanks for being a great office mate, I am sorry that you lost so many times at office-basketball and at every other sport we played. Thanks for your help to find an apartment in Utrecht when I first moved here and for becoming a very good friend. **Imogen**, thanks for everything and good luck finishing up I am sure you will do great. **Denise,** thanks for the good time sharing lab I wish I would have worked longer time together with you.

Harmjan, Thank you for your help. I really enjoyed all the beers we had during this time and I am sure there will be many more in the future. Thanks to **Robert** and **Paula** for their fantastic work and contribution to this thesis. Thanks to all the friends I made in the department for making the borrels a great way to end the work week, **Tianshu, Jose, Enric, Marc, Jooske**, **Alba** and many more.

Thanks to **Diana** and **Marjolein** for all the moments shared in the office during these years, I wish the best and I know any other office is going to be as cool.

I want to thank all the members of the TRAIN consortium, specially **Endre**, **Graham**, **Juan** and **Laura**. To **Endre and Graham** thanks for organizing such an amazing events were we grew as scientist so much and thanks for always looking after us. **Juan**, nos conocimos en el primer evento de TRAIN y enseguida me di cuenta de

que ibamos a ser amigos, hablar por teléfono o por zoom contigo es una rutina que espero sigamos teniendo durante muchos años. **Laura**, trabajar contigo ha sido genial, y me alegro mucho del tiempo que pasamos juntos en Sheffield. El viaje que nos hicimos los tres a Porto es uno de los mejores recuerdos de estos años. Gracias por todo.

Thanks to all the students I had the luck to supervised, **Soufian, Mirjam, Suzanne, Nur**…

Specially to **Rosalie,** I am really glad I had the opportunity to meet you, you were my first student and you were great, it is incredible how much you have grown. I am happy to call you my friend now I am sure the lab is in good hands.

Thanks to all my buffoons, these years would not have been the same without you. You guys are the best friends someone can ask for I wish you all the best. **Iliana** I met you hiding in the seahorse room and I could not imagine you would become such a good friend of mine. You are kind, funny and probably the slowest(walking) person I have ever met, I miss you and I hope you come back. **Peggy**, you are sweet, smart and your conversations with clement are proably the funniest memories I have of these years. I hope you come back soon as well. **Clement**, I still cant believe I have a French friend (my father still doesn't believe me) but I am glad is you. Thanks for all the lagunitas you bought me, they really help me finish this thesis. **Jamie**, at first you were only Clement´s boyfriend, but quickly you became a really good friend and I am really glad I found you.

Alexandra, Thanks for everything. We started together and since the moment I met you I knew you would become my closet friend, we have drunk, partied, fought, laughed, talked countless nights, and there are many more to come. You are the most thoughtful, persistent, and good friend someone can ask for. It has been incredible watching you grow in science, and I will always be there for you.

Gracias a **Guillermo** y **Jorge** por ayudarme con el diseño de la tesis.

También quiero dar las gracias a todos mis amigos que no han dejado que la distancia se interponga en nuestra amistad. Os dedico esta tesis y os echo mucho de menos. Gracias a **Chur, Suco, Adri, Jaime, Javi, Angel, Gabi, Guille, Carlis**…

Gracias a toda mi familia de Alicante y Madrid todos mis tios, primos y primas y especialmente a mis abuelas; **Rosario** y **Rosalia** por cuidarme siempre. Y a mis abuelos por dármelo todo.

A mi hermana, Ana, que aún en la distancia siempre he sabido que cuida de mí, y para Dani, ojalá algún día esta tesis le inspire a perseguir sus metas. A mi madre, que me ha enseñado a poner el corazón en todo lo que hago y a mi padre; que ha sido mi ejemplo e inspiración. Os lo debo todo, espero que algún día estéis la mitad de orgullosos de mí de lo que yo estoy de vosotros. Os quiero.

A la persona más importante, **María del Pilar Clemente Olivo**. Es difícil poner en palabras todo lo que representas para mí, gracias por ayudarme cuando lo necesito, animarme cuando estoy decaído, por celebrar mis logros junto a mí y por empujarme a ser mejor siempre. Nada de esto tendría sentido sin ti.